

Rochester Institute of Technology

RIT Digital Institutional Repository

Theses

7-2020

A Patient-Specific Infrared Imaging Technique for Adjunctive Breast Cancer Screening: A Clinical and Simulation - Based Approach

Alyssa Owens
anr6832@rit.edu

Follow this and additional works at: <https://repository.rit.edu/theses>

Recommended Citation

Owens, Alyssa, "A Patient-Specific Infrared Imaging Technique for Adjunctive Breast Cancer Screening: A Clinical and Simulation - Based Approach" (2020). Thesis. Rochester Institute of Technology. Accessed from

This Dissertation is brought to you for free and open access by the RIT Libraries. For more information, please contact repository@rit.edu.

RIT

**A Patient-Specific Infrared Imaging Technique for
Adjunctive Breast Cancer Screening: A Clinical and
Simulation - Based Approach**

by

Alyssa Owens (née Recinella)

A dissertation submitted in partial fulfilment of the requirements for the
degree of Doctor of Philosophy in Engineering

Engineering (PhD Program)

Kate Gleason College of Engineering

Rochester Institute of Technology

Rochester, New York

July 2020

**A Patient-Specific Infrared Imaging Technique for Adjunctive Breast Cancer Screening: A
Clinical and Simulation - Based Approach**

by
Alyssa Owens

Committee Approval:

We, the undersigned committee members, certify that we have advised and/or supervised the candidate on the work described in this dissertation. We further certify that we have reviewed the dissertation manuscript and approve it in partial fulfillment of the requirements of the degree of Doctor of Philosophy in Engineering.

Satish Kandlikar	07/30/2020
<hr/>	
Dr. Satish G. Kandlikar (Advisor) James E. Gleason Professor, Mechanical Engineering	Date
Kathleen Lamkin-Kennard	07/30/2020
<hr/>	
Dr. Kathleen Lamkin-Kennard Associate Professor, Mechanical Engineering	Date
Ke Du	07/30/2020
<hr/>	
Dr. Ke Du Associate Professor, Mechanical Engineering	Date
PD Phatak	07/30/2020
<hr/>	
Dr. Pradyumna Phatak Chief of Medicine, Rochester General Hospital	Date

Certified by:

Dr. Edward Hensel, P.E.	07/30/2020
<hr/>	
Dr. Edward Hensel Director, PhD in Engineering	Date

Acknowledgements

Firstly, I would like to thank Dr. Satish Kandlikar for hiring me as a co-op student in 2014. Before joining the lab, my path as a mechanical engineer alluded me. Throughout my five years in the lab as a co-op, Masters student and then PhD student, I have learned and grown so much as a person and an engineer. Dr. K's support and constant guidance has gotten me where I am today, and I am incredibly thankful. Thank you for giving me a chance.

This thesis would not have been possible without the efforts and help of Rob Kraynik, Jan Maneti, Bill Finch, and countless others in the ME machine shop and department that have taught me how to machine and how to design. Their help and assistance have gone a long way. Another thank you to Diane Selleck, Jill Ehmann, Hillary McCormick, Brittany Pasquale, Christie Leone, and many others in the ME department for constantly brightening up my day and assisting in the advisement of my career. There are too many professors and faculty members in the department that have impacted my life in a positive way. Thank you for your constant encouragement.

Thank you to my committee members who have served not only to assist in the realization of this thesis but who have also given thoughtful and constructive feedback for this work. The insights provided by Dr. Lamkin-Kennard, Dr. Du and Dr. Phatak have helped this work greatly and I appreciate it. Additionally, thank you to the PhD Engineering program, particularly Dr. Hensel and Rebecca Ziebarth, for their constant support and communication.

Thank you to all the hospital staff and clinicians who have supported myself and this study. Dr. Donnette Dabydeen, Dr. Lori Medeiros, Dr. Prad Phatak, and Dr. Manasi Godbole have provided so much knowledge, expertise, and support. I have learned so much from you and it has truly changed my viewpoint on the world. Thank you to the Clinical Research Team, Tia Albro, Kayla Malchoff, Megan Littleton, Kellie Sharron, and many more for recruiting patients, answering my emails or phone calls, and providing so much laughter and joy.

Thank you to all my friends and support network at the Doctoral Student Association, Engineers for a Sustainable World and Northridge Church. My time in the DSA and ESW has provided more practical and team-based knowledge than I could have received at a normal job. And the ladies in my Northridge small group have provided a shoulder to cry on, lots of tasty

snacks, and hours of laughter. Namely, thank you to Jessica Paulino, Heather Roberts, Laura Sutherland, Melissa McCormick, and Rachel Ludwig.

I would also like to thank my fellow lab members, past and present, who have not only assisted in my engineering development but who have also selflessly given up time and resources to aide in my research. A big thank you to Ankit Kalani, Arvind Jaikumar, Pruthvik Raghupathi, Aniket Rishi, Aranya Chauhan, Poornima Kalyanram and Jose Luis Gonzalez Hernandez for their loving friendship in and outside of the lab. Thank you to my friends that have provided love and laughter; David Schwartz, Avaneil Brock, Rachel Adams, Rachael Socolof, Sophie Hopps-Weber, Nick Stokowski, Ego Egbe, Matt and Kate Tomford, Juliana Posato, Jasmine Phan, Nolan Deller, Emily Becker, Clay Benson, Kris and Art Martz, Bob and Peggy Hatch, and many more.

Thank you to all my extended family from aunts and uncles to cousins to grandparents. Thank you to my Grandpa George Nadzan, Grandma Judy and Grandma Marilyn for your constant love and encouragement, always sending me articles or tools. Thank you to my Grandpa Silvio, an engineer at Ford, I look up to you and your tenacity as an immigrant living the American Dream. Thank you to all of my extended family for the laughter and love.

And last but not least, thank you to my incredibly supportive and loving family. Thank you to all my extended family for providing love and laughter. Grace and Bobby, thank you for the constant encouragement, words of wisdom and excellent cocktails. Cara and Justin, thank you for believing in me and giving me the strength and humor to continue on. Thank you to my wonderful nephews Tommy, Sammy, and Hank for bringing so much joy. Thank you to my parents-in-law, Kelly, and Chris, for treating me as your own and providing constant love and support. Thank you to my beautiful parents who have supported and nurtured my engineering habits from a young age from jigsaw puzzles to Rubik's cubes to calculus books. Mom, thank you for passing down your creativity and optimism. Dad, thank you for the "engineering gene" and helping me with your own engineering experiences. You have all supported me mentally, religiously, emotionally, and financially my entire life and I cannot even begin to describe my gratitude.

Finally, thank you to my wonderful and supportive husband, Trevor Owens. From high school through nine years of engineering school, you have been my rock. I feel so honored to be married to you and cannot wait to start our adventure in the 'real world'.

This is for all of you.

Dedication

Surrounded by love and friendship, it is too difficult to dedicate my work to one person. This work is dedicated to the following.

To Diana Decker or “Mama D” – a dear friend and second mom who passed away from metastatic breast cancer during my university studies.

My parents, Sherry and Dan Recinella – your support and love has been essential during my nine years at RIT.

And finally, to my husband, Trevor Owens – you constantly surprise me and have boosted my confidence and joy. My best friend, my husband, my soulmate, under God.

Abstract

Breast cancer is currently the most prevalent form of cancer in women with over 266,000 new diagnoses every year. The various methods used for breast cancer screening range in accuracy and cost, however there is no easily reproducible, reliable, low-cost screening method currently available for detecting cancer in breasts, especially with dense tissue. Steady-state Infrared Imaging (IRI) is unaffected by tissue density and has the potential to detect tumors in the breast by measuring and capturing the thermal profile on the breast surface induced by increased blood perfusion and metabolic activity in a rapidly growing malignant tumor. The current work presents a better understanding of IRI as an accurate breast cancer detection modality. A detailed study utilizing IRI-MRI approach with clinical design and validation of an elaborate IRI-Mammo study are presented by considering patient population, clinical study design, image interpretation, and recommended future path. Clinical IRI images are obtained in this study and an ANSYS-based modeling process developed earlier at RIT is used to localize and detect tumor in seven patients without subjective human interpretation. Further, the unique thermal characteristics of tumors that make their signatures distinct from benign conditions are identified.

This work is part of an ongoing multidisciplinary collaboration between a team of thermal engineers and numerical modelers at the Rochester Institute of Technology and a team of clinicians at the Rochester General Hospital. The following components were developed to ensure valid experimentation while considering ethical considerations: IRB documentation, patient protocols, an image acquisition system (camera setup and screening table), and the necessary tools needed for image analysis without human interpretation. IRI images in the prone position were obtained and were used in accurately detecting the presence of a cancerous tumor in seven subjects. The size and location of tumor was also confirmed within 7 mm as compared to biopsy-proven pathology information. The study indicates that the IRI-Mammo approach has potential to be a highly effective adjunctive screening tool that can improve the breast cancer detection rates especially for subjects with dense breast tissue. This method is low cost, no-touch, radiation-free and highly portable, making it an attractive candidate as a breast cancer detection modality. Further, the developed method provided insight into infrared features corresponding to other biological images, pathology reports and patient history.

Table of Contents

Acknowledgements.....	3
Dedication.....	5
Abstract.....	6
Table of Contents.....	7
List of Figures.....	10
List of Tables.....	14
Chapter 1. Introduction.....	15
1.1 Motivation.....	15
1.2 Breast Cancer.....	16
1.3 Cancer Biology.....	19
1.3.1 Hallmarks of Cancer.....	19
1.3.2 Necrosis.....	22
1.3.3 Body Rhythms.....	23
1.4 Medical Diagnosis.....	23
1.4.1 Risk.....	24
1.4.2 Cancer Classification.....	25
1.5 Medical Imaging.....	30
1.5.1 Imaging Techniques.....	31
a. Mammography and Digital Breast Tomosynthesis (DBT).....	31
b. Ultrasound.....	33
c. Magnetic Resonance Imaging.....	34
d. Other detection methods.....	36
e. Thermography.....	36
1.5.2 Statistical Considerations.....	37
a. Sensitivity and Specificity.....	38
b. Positive Predictive Rate (PPV) and Negative Predictive Value (NPV).....	40
c. Patient Population Considerations.....	42
d. Determining Statistical Significance.....	42
1.6 Clinical Studies.....	43
1.7 Conclusion.....	45
1.8 Dissertation Overview.....	45
Chapter 2: Background.....	47
2.1 Bioheat.....	47
2.2 Thermography.....	50
2.2.1 Breast Cancer Detection Demonstration Project.....	50
2.2.2 Dynamic and Steady State Thermography.....	55
2.2.3 Numerical Studies.....	58
2.2.4 Experimental Studies.....	58
2.2.5 Clinical Studies.....	60

2.3	Research Needs	63
2.3.1	Imaging Protocol.....	65
2.3.2	Image Interpretation.....	73
a.	Empirical Observation	73
b.	Temperature Dependent.....	75
c.	Scoring Systems.....	77
d.	Computational and Mathematical Methods.....	80
2.3.3	Scientific Validation	82
2.3.4	Thermal Biomarker Classification.....	84
2.4	Objectives	86
Chapter 3: Approach.....		88
3.1	Overview.....	88
3.2	Clinical.....	88
3.2.1	Ethical Considerations	89
3.2.2	Clinical Study – IRI-MRI	89
i.	Patient Population	89
ii.	Patient Flow	90
iii.	Clinical Protocol	91
iv.	Patient Questionnaire.....	91
v.	Clinical Setup.....	92
vi.	Data Collection	97
3.2.3	Clinical Study – IRI-Mammo	98
i.	Patient Population and Patient Flow	98
ii.	Clinical Protocol	99
iii.	Patient Questionnaire.....	99
iv.	Clinical Setup.....	100
v.	Data Collection	103
3.2.4	Image Acquisition.....	104
3.3	Numerical.....	105
3.3.1	MRI Images	105
3.3.2	3D Modeling Process.....	106
3.4	Conclusions.....	107
Chapter 4: Results.....		108
4.1	Acclimation Time	108
4.2	IRI-MRI Study.....	111
4.3	IRI-Mammo Study.....	119
4.4	Detection and Localization.....	125
4.5	Conclusions.....	129
Chapter 5: Design of a Large-Scale Clinical Study		131
5.1	Patient Population.....	131
5.2	Clinical Setup.....	139
5.3	Numerical Modeling	143
5.4	Additional Changes.....	144

Chapter 6: Thermal Biomarkers	146
6.1 Gautherie’s Work.....	146
6.1.1 Effective Thermal Conductivity	147
6.1.2 Metabolic Activity	151
6.1.3 Internal Rhythms.....	153
6.2 Calculating Blood Perfusion.....	156
6.3 Thermal Biomarkers	159
6.4 Tumor Aggressivity	161
Chapter 7: Conclusions	165
7.1 Summary of Work Done.....	165
7.2 Conclusions.....	167
7.3 Research Contributions.....	171
7.3.1 Technical Contributions.....	171
7.3.2 Societal Contributions.....	173
Chapter 8: Recommendations for Future Study	175
8.1 Adjunctive Technique.....	175
8.2 Screening Setup	176
8.3 Clinical Study.....	177
8.4 Non-Human Studies.....	179
8.5 Model Generation and Modeling.....	181
8.6 Additional Detection Methods.....	182
8.7 Additional Disease Detection	187
Chapter 9: References	190
Appendix	200
IRI-MRI Data – 1.....	201
IRI-MRI Data – 2.....	202
IRI-MRI Data – 3.....	203
IRI-MRI Data – 4.....	204
IRI-MRI Patient Questionnaire.....	205
IRI-MRI Consent Form.....	206
IRI-MRI IRB Proposal.....	213
IRI-Mammo Patient Questionnaire.....	217
IRI-Mammo IRB Addendum.....	218
IRI-Mammo Data – 1	219
IRI-Mammo Data – 2.....	220
IRI-MRI Pathology Report – Patient 029a (identifying information removed)	221
IRI-Mammo Pathology Report – Patient 002b (identifying information removed).....	232

List of Figures

Figure 1. Estimated cancer statistics for 2017 presented by the American Cancer Society [2].....	15
Figure 2. Frontward and side view of the human breast [4].	17
Figure 3. The most prevalent forms of breast cancer found in women [9].	18
Figure 4. The ten factors that influence the growth and spread of malignant cells [17].	22
Figure 5. The significance of the BRCA1 and BRCA2 mutations on increasing the risk of developing breast cancer [21].	25
Figure 6. (a) Tumor location based on the positions on a clock and (b) tumor depth with three different classifications (interior, mid, posterior).	26
Figure 7. Slice of invasive ductal carcinoma with tubule formation in over 75% of the tumor [27].	29
Figure 8. The electromagnetic spectrum with detectable waves and their accompanying frequencies [28].	30
Figure 9. Mammogram of different breast densities [35].	32
Figure 10. (a) A benign cyst resting inside of the breast and (b) a malignant mass [38].	34
Figure 11. (a) MRI image of the breast prior to fat saturation and (b) fat saturation MRI image of the breast.	35
Figure 12. Relationship between metabolic generation and doubling time [19].	50
Figure 13. Numerical breast model to examine effects of parallel convection on the breast surface of a breast with tumor [81].	57
Figure 14. Number of publications related with breast thermography [78].	63
Figure 15. Breast models, elastically deformed by gravity, using thermography by Jiang et al. [100].	70
Figure 16. Breast in prone for imaging without gravitational or thermal deformation [102].	72
Figure 17. Screening and diagnostic imaging patient flow.	90
Figure 18. Portable massage table retrofitted for infrared imaging.	93
Figure 19. IRI screening table in the screening room with curtain.	93
Figure 20. (a) Camera table setup with turntable and (b) FLIR infrared camera used for imaging.	94
Figure 21. Camera positions for 8 views of breast in prone.	95

Figure 22. Image of table with 2-inch foam, prior to covering with fabric.	96
Figure 23. (a) Staircase with table, prior to addition of railing and (b) myself standing next to table to show examples of height.	96
Figure 24. Images of the imaging room with the table design, sturdy staircase, and black curtain along the edges of the table.	97
Figure 25. New patient flow for IRI-Mammo study.	99
Figure 26. (a) Camera observes the breast at an angle similar to IRI-MRI study, (b) camera tilted to observe the breast horizontal, and (c) camera tilted to look straight up at the breast.	101
Figure 27. (a) Modular camera stand and (b) ICI 8640 camera.	102
Figure 28. Positions of camera at a 45° angle and a horizontal view; allows for capture of 49 images around the circumference of the breast.	103
Figure 29. Medical illustration of subject in prone position with camera table underneath.	104
Figure 30. Patient-specific breast model generation process using MRI images [60].	105
Figure 31. Breast model of Patient 013a from two different angles, showing the intricacies of the geometry.	106
Figure 32. (a) Breast geometry with added mesh and boundary conditions and (b) breast model in ANSYS with imposed tumor in the right breast [60].	107
Figure 33. Breast cooling over a period of 10 minutes; first image is at 0 minutes, second image is at 5 minutes and third image is at 10 minutes.	109
Figure 34. Acclimation time of Patient 25 left breast, with malignant tumor. Breast cooling over a period of 10 minutes; first image is at 0 minutes, second image is at 5 minutes and third image is at 10 minutes. Tumor is suspected to be in the upper right quadrant.	109
Figure 35. MRI of Patient 25, tumor can be seen in upper right quadrant with biopsy spot.	110
Figure 36. Image sequence of Patient 6a’s left breast and right breast. This patient had bilateral breast cancer with a tumor in both breasts. A detailed analysis is presented below.	114
Figure 37. Image sequence of Patient 13’s left breast and right breast. The malignant tumor is in the right breast, right above the nipple.	114

Figure 38. Image sequence of Patient 18’s left breast and right breast. The malignant tumor is in the right breast.....	115
Figure 39. Image sequence of Patient 29’s left breast and right breast. The malignant tumor is in the left breast.....	115
Figure 40. Images of subject 6 with bilateral breast cancer, (a) the left breast with hot spot in area of known 0.7 cm tumor and (b) the right breast with hot spot in area of known 2.7 cm tumor.....	116
Figure 41. Temperature distribution of right breast of patient 6: (a) IR image with two profile lines along the breast and (b) temperature profile for A and B.	117
Figure 42. MRI, renderization from MRI, and IRI images for three subjects [126].....	118
Figure 43. (a) The hot spot created by a malignant tumor and (b) the hot, short lines created by vasculature in the breast.....	119
Figure 44. Glow around patient images due to poor image focus.	120
Figure 45. Image sequence of the left breast of Patient 003b from the horizontal and 45° angles.....	121
Figure 46. Image sequence of right breast of Patient 003b from the horizontal and 45° angles.....	122
Figure 47. Image sequence of the left breast of Patient 004b from the horizontal and 45° angles.....	123
Figure 48. Image sequence of right breast of Patient 004b from the horizontal and 45° angles.....	124
Figure 49. Horizontal (left) and angled (right) view of the right breast of Patient 005b.	125
Figure 50. Flowchart of detection and localization process from Gonzalez-Hernandez [125].....	126
Figure 51. Comparison between predicted and actual values for tumor size and location within each breast.	127
Figure 52. Comparison of clinical and computed temperature distributions for Patient 003a [126].	128
Figure 53. Comparison of clinical and computed temperature distributions for Patient 006a [126].	128
Figure 54. Comparison of clinical and computed temperature distributions for Patient 007a [126].	129
Figure 55. Upgraded camera setup with multiple cameras at varying heights.	141
Figure 56. New modular table setup with IRI camera system and patient in prone position.....	142
Figure 57. Close-up schematic (1st panel) the old imaging table with the subject lying on one breast, (2nd panel) the proposed imaging table with two holes and (3rd panel) the proposed table with one breast pulled aside with cloth.	143

Figure 58. Edge of the IRI image found and silhouette created for patient-specific digital breast model without the need of MRI images.....	144
Figure 59. (Left) Temperature vs depth and (right) Effective Thermal Conductivity vs depth for malignant and healthy tissue, redrawn from Gautherie [19].....	149
Figure 60. (a)Temperature vs. depth of probe and (b) effective thermal conductivity vs. depth of probe for three different breast cancer patients with varying tumor sizes, redrawn from Gautherie [19].....	151
Figure 61. Relationship between metabolic generation and doubling time.	152
Figure 62. (a) P-CT image of gastric cancer with indication of tumor and (b) Perfusion map of blood flow. An average blood flow of 49.8 ml/min/100 g was calculated [134]......	157
Figure 63. Malignant gastrointestinal stromal tumor. (left) Blood volume map, (center) maximum intensity projection image and (right) physical specimen. Authors believe that areas pointed out with arrows are suggestive of necrosis [132]......	158
Figure 64. (top left) A conventional CT image, (top right) CT parametric map of blood volume or BV, (bottom left) CT parametric map of permeability-surface area product or PS and (bottom right) CT parametric map of blood flow or BS [132].	158
Figure 65. A top view (left) and bottom view (right) of a clinical bed with two holes and modular pieces to fit each subject.	176
Figure 66. Entire experimental setup with rotating camera stand and breast model.....	180
Figure 67. Breast model with imposed heaters to simulate chest wall temperature and tumor.	181
Figure 68. Potential pathways to detect thermal features within the breast.....	183
Figure 69. (a) Breast with tumor hot spot and vein hot spot, (b) gridding system on breast, (c) refined mesh highlighting tumor hot spot and (d) refined mesh highlighting vein hot spot.....	185
Figure 70. Images created by Gonzalez-Hernandez [52]. a) Thermal grid composed of latitudinal and longitudinal lines on a breast thermogram, b) Statistical indicators in selected regions of the grid.....	186
Figure 71. IR image of breast with tumor showing two regions of interest.....	187

List of Tables

Table 1. Factors associated with high risk [21].	24
Table 2. Different factors used in tumor staging [22]......	27
Table 3. Histologic grading system reported by the AJCC [26].	29
Table 4. Diagnostic techniques with corresponding sensitivity specificity, and cost [57].	43
Table 5. Clinical thermography studies with reported sensitivity and specificity values [97].	64
Table 6. Table adapted from Fernandez-Cuevas et al. [98] showing recommended ambient temperature and acclimation time from various authors.....	67
Table 7. Temperature scale and assessments performed in the Rassiwala study [105].	76
Table 8. Table adapted from Keyserlingk et al. [101].	78
Table 9. Comparison of major factors impacting imaging with the IRI-MRI FLIR camera and the IRI-Mammo ICI camera.	102
Table 10. Parameters used in the simulations [60], [124], [125].	107
Table 11. List of subjects with age, tumor location (size/position/depth) for breasts with tumor (BWT) and additional details such as cancer type, breast density and subject classification.	112
Table 12. Average temperature values in the breast without tumor and breast with tumor, for each subject imaged with IRI and the maximum temperatures seen at the tumor hot spot.....	113
Table 13. Patient data from the IRI-Mammo study for the six recruited patients.....	120
Table 14. Overall sensitivity and specificity of select screening techniques for comparison.....	132
Table 15. Screening parameters and corresponding equations adapted from Buderer [128].....	132
Table 16. Data collected from Poplack et al. [130] from the New Hampshire Mammography Network.	134
Table 17. Estimated sample size for a variable sensitivity and specificity for prevalence of 10% in patients classified as BI-RADS 3, 4 or 5.....	136
Table 18. Estimated sample size for a variable prevalence.	136
Table 19. Estimated sample size for variable prevalence and sensitivity.	137
Table 20. Estimated sample size for variable prevalence and specificity.....	137
Table 21. Estimated sample size for a variable sensitivity and specificity for prevalence of 10% in patients classified as BI-RADS 3, 4 or 5.....	138
Table 22. Mammography data and BI-RADS classifications over a six-month period at the Rochester General Hospital.	139
Table 23. Structured regiment for patients in Gautherie’s study for circadian rhythm control.	153
Table 24. Values of the parameters used in the simulations.	160

Chapter 1. Introduction

1.1 Motivation

Cancer is a deadly disease found all over the world in many different forms. Cancer involves the rapid uncontrolled growth of diseased cells and can form anywhere in the body [1]. Positive prognosis from cancer is dependent upon early diagnosis of abnormal (malignant) masses. Delayed diagnosis can cause delayed treatment which can increase the necessary costs needed for tumor shrinkage or removal. Many forms of cancer involve the growth of solid tumors, made of a mass of tissue. However, some forms such as leukemia or bile duct cancer do not have a solid tumor.

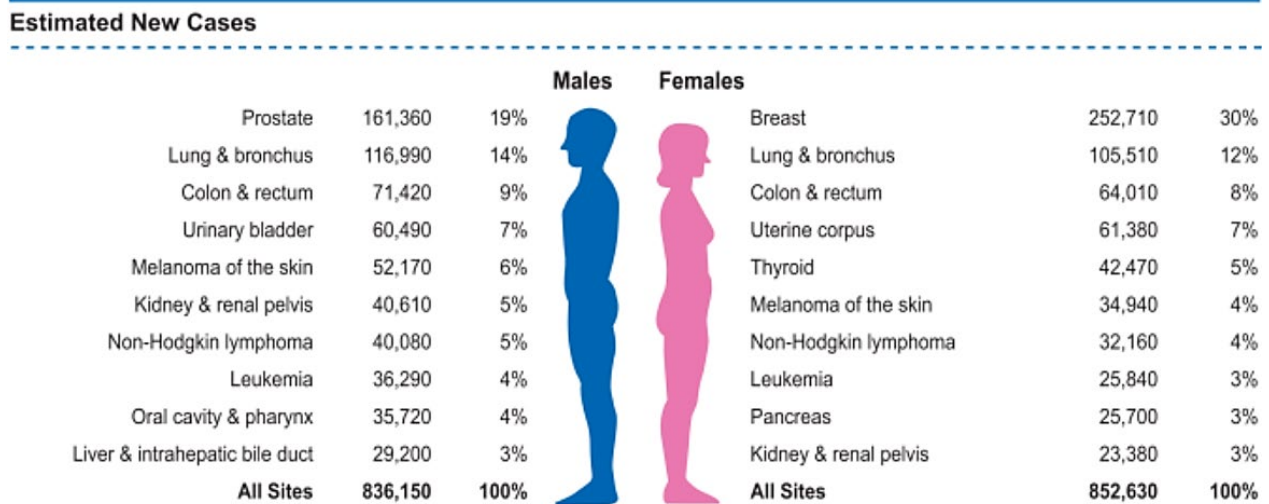


Figure 1. Estimated cancer statistics for 2017 presented by the American Cancer Society [2].

In any form, it is a destructive and widespread disease that affects millions of people throughout the world. A 2012 study estimated 14.1 million *new* cases of cancer were diagnosed with 8.2 million people killed from various forms of cancer [2]. In the United States alone, the American

Cancer Society estimates about 1.7 million new cancer cases with approximately 600,000 deaths. Lack of proper diagnostic techniques or treatment can lead to further loss of life and financial ruin. The Agency for Healthcare Research and Quality (AHRQ) estimates that in the US in 2015, a staggering \$80.2 billion accounted for all cancer-related medical costs [3]. This sum accounts for hospital visits, inpatient stays, treatments, and medicine. Many of the larger cancers present in the world include breast cancer, prostate cancer, and liver cancer. As seen in Figure 1, breast cancer remains as one of the highest occurring cancerous diseases in females. Figure 1 estimates the amount of breast cancer cases in 2017 at approximately 250,000.

1.2 Breast Cancer

The breast, as seen in Figure 2, is also known as a mammary gland and is present in both men and women. However, only women have functioning, lactating glands for infant nourishment. The breast consists of 15-25 lobes, separated by tissue, that contain lobules. Nonpregnant girls and men only have rudimentary ducts but when puberty is reached, the female breast experiences duct growth and increased fat deposition. Many major breast cancers form in the lobules and duct system. When detecting tumors in the breast, there are many factors to consider. Although all women develop ducts and fat with puberty, there are four different types of breast density: fatty, fibroglandular, heterogeneously dense and extremely dense. Extremely dense breasts have less fat and more fibrous and glandular tissue than fatty breasts. Fatty breast tissue is more common among younger females while extremely dense tissue is found in older women.

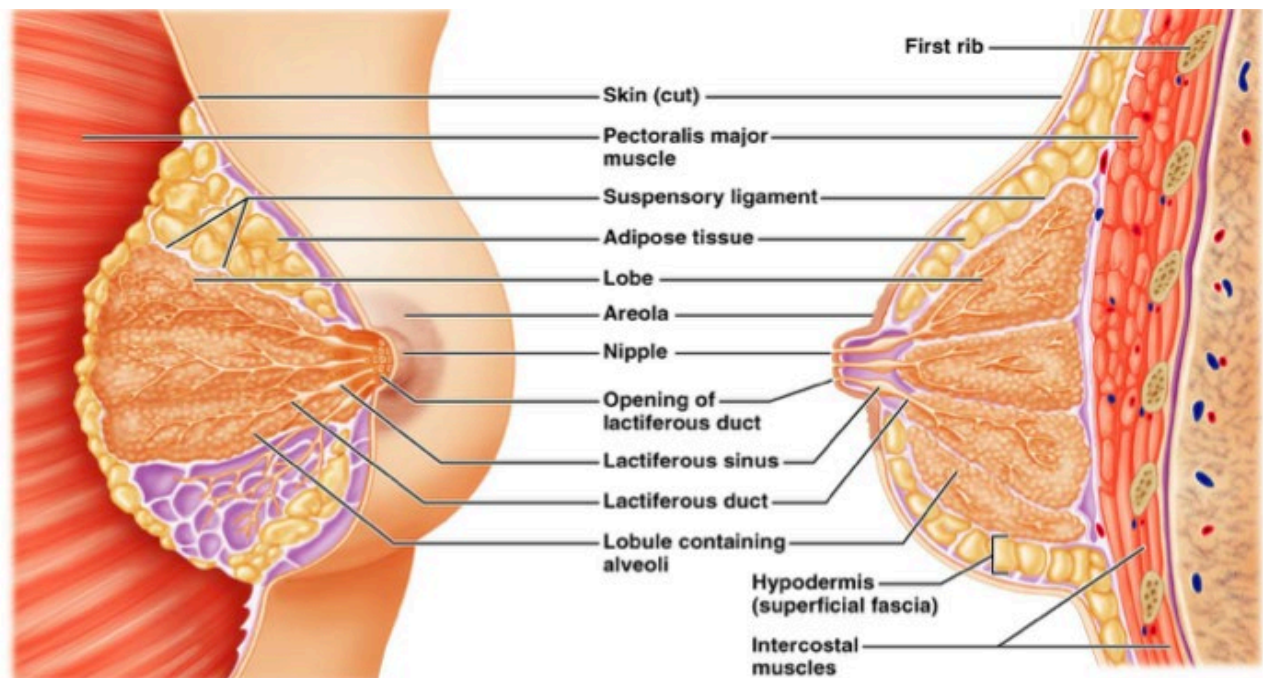


Figure 2. Frontward and side view of the human breast [4].

Breast cancer can be invasive, spreading to surrounding tissue, or remain in situ and stay within the breast. Rarer, inflammatory breast cancer only accounts for 1% of cancers [5]. The four more common breast cancers are ductal carcinoma in situ (DCIS), invasive ductal carcinoma (IDC), invasive lobular carcinoma (ILC) and lobular carcinoma in situ (LCIS). DCIS and LCIS, both in situ diseases, are non-invasive forms of breast cancer. Ductal carcinoma begins in the milk ducts of the breast but does not spread. Although DCIS can be treated, it can lead to a higher chance of developing an invasive form of breast cancer later in life [6]. The other in situ breast cancer, LCIS, differs in growth and later life effect. The term ‘lobular’ refers to the lobules or a milk producing gland, which can be seen in Figure 2 [7]. LCIS is not technically diagnosed as breast cancer but instead as lobular neoplasia or an abnormal cell growth [8]. Major types of breast cancer and the areas they afflict can be seen in Fig. 3.

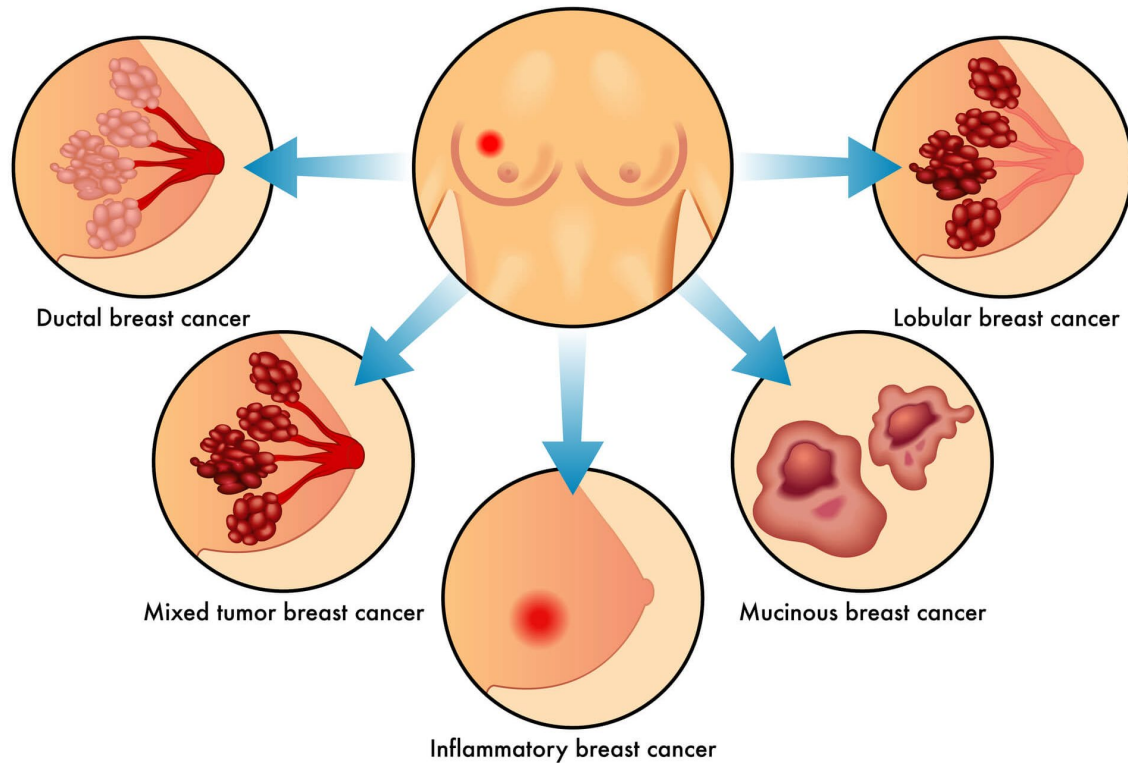


Figure 3. The most prevalent forms of breast cancer found in women [9].

Invasive breast cancers involve spreading diseases that begin in one spot in the breast but slowly metastasize to other parts of the body [10]. Invasive Ductal Carcinoma, similar to DCIS, begins in the milk ducts and is the most common form of breast cancer, accounting for 80% of all diagnosed cases [11]. Invasive Lobular Carcinoma, the second most common form of breast cancer, begins in the lobules and spreads to surrounding breast tissue. ILC can spread to the lymph nodes or other parts of the body and mostly affects older women [12]. The significance of these cancers for different diagnosis studies is tumor size, shape, and growth pattern. While many tumors grow in ball-like solid masses of cells, many tumors can form irregularly or in a stacked file. IDC tends to see abnormal, star-shaped tumors while tubular carcinomas have no palpable tumor but instead form in tube-like structures. Other rarer forms of breast cancer have softer tumors, sheet-like

tumors, or branching finger-like tumors [13] which can make it particularly difficult to use one diagnosis method for breast cancer detection. Having a comprehensive understanding of breast anatomy can lead to better detection methods for these rarer forms of cancer.

1.3 Cancer Biology

1.3.1 Hallmarks of Cancer

Cancer growth has been a widespread field of study for several decades. While the origin of the disease is still unknown, the mechanics behind cancer cell growth is slightly more understood. In 2000, Hanahan and Weinberg [14] discuss the various principles that encompass the complexity of cancer also known as the Hallmarks of Cancer. In 2011, Hanahan and Weinberg [15] added additional factors to this list. All ten principles are discussed in length below and can be seen in Figure 4.

1. *Sustaining Proliferative Signaling* – Unlike normal cells, cancer cells can sustain proliferation. Normal cells can maintain homeostasis by controlling the production and release of growth-promoting signals that cause the cell growth-and-division cycle. However, cancer cells can acquire this same ability and can control the growth of more cancer cells. They can do this through multiple methods, like producing the same signal, permanently activating the signal, or destroying ‘off switches’ to allow excessive growth.
2. *Evading Growth Suppressors* – Not only is the human body able to control signals to grow and divide cells, it is also able to regulate cell proliferation, halt cellular growth, and stop dividing once the space is filled. Cancer cells can alter these suppressor proteins and grow and divide into any surrounding space, whether it is full or not. Cancer cells want to

continue growing, uncontrollably, to take over the surrounding area and spread throughout the body.

3. *Resisting Cell Death* – Normal cells are programmed to have cell death or apoptosis in order to maintain homeostasis and prevent potential abnormal growth. Cancer cells can resist cell death and therefore become grossly abnormal.
4. *Enabling Replicative Immortality* – Similar to the point listed above, cells die after a certain number of divisions in order to prevent abnormality. Unlike normal cells, cancer cells are able to bypass this natural ability and can divide indefinitely. This causes the already abnormal cells to spread their mutations and create more abnormalities.
5. *Inducing Angiogenesis* – Angiogenesis is a normal process that occurs in the body to grow blood vessels for continued cell growth and production. Cells need oxygen and nutrients from blood vessels in order to survive. Cancer cells are also able to create new blood vessels in order to carry adequate oxygen and nutrients to the abnormal cells for continued growth and replication.
6. *Activating Invasion and Metastasis* – A primary cause of cancer-related deaths is cancer cell invasion and metastasis into surrounding tissues and organs. In order to metastasize to the rest of the body, the cells must first spread to localized tissue. This is a difficult process involving invading blood vessels and surviving in a harsh environment. Once the cancer cells have surpassed this barrier, they are able to metastasize and potentially become a larger concern.
7. *Genome Instability and Mutation* – For constant replication and growth, malignant or benign cancer cells must alter the genomes of neoplastic cells. Small genetic mutations are

often thought to be the beginning of tumor growth initially and begin to mutate at much faster rates as the cells grow and divide.

8. *Tumor-Promoting Inflammation* – There have been many studies showing that inflammation can lead to cancer development. More chronic inflammatory issues such as infections, obesity, smoking, alcohol consumption, etc. are all potential risk factors linked to cancer development through inflammation.
9. *Deregulating Cellular Energetics* – Cancer cells are able to generate energy in abnormal ways using metabolic pathways. First discussed by Otto Warburg [16], this process is now known as the Warburg effect. He hypothesized that tumors grow due to insufficient cellular respiration caused by manipulation of energy production. Instead of creating more energy (ATP), cancer cells convert acids into building blocks for more cancer cells.
10. *Avoiding Immune Destruction* – Similar to other hallmarks discussed above, cancer cells are able to avoid detection by the body's natural immune system. While most illnesses are sensed and destroyed, cancer cells can avoid destruction and continue to grow.

Although there are many factors that affect how cancer cells grow and replicate, few of these principles are hypothesized to contribute to hyperthermia. Two large factors that would allow for successful infrared imaging include inducing angiogenesis and tumor-promoting inflammation. Angiogenesis is a well-studied phenomenon within the body, both during normal cell growth and cancerous cell growth. The increase of vasculature to a growing tumor creates an area of hyperthermia. The increased metabolism in a tumor can also cause localized temperature increases.

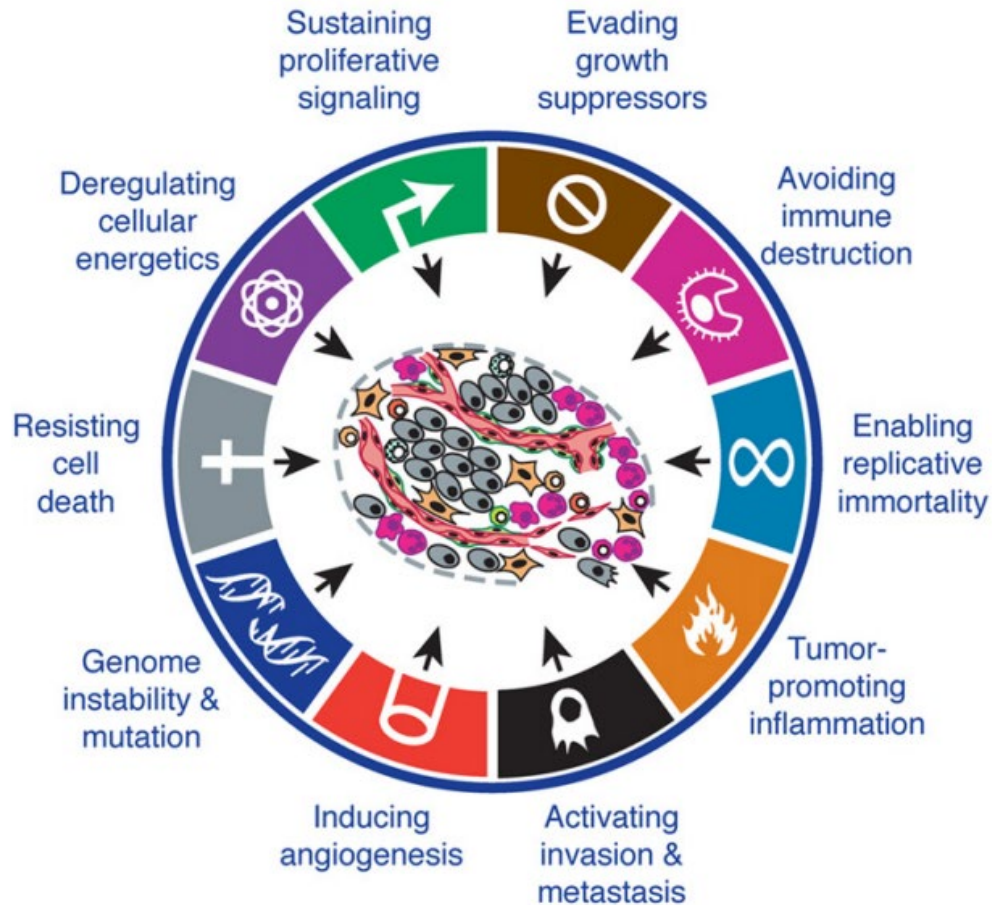


Figure 4. The ten factors that influence the growth and spread of malignant cells [17].

1.3.2 Necrosis

Necrosis involves cellular injury in which certain cells of living tissue are killed through autolysis. Apoptosis refers to a living cell receiving a signal to initiate controlled death whereas autolysis is cells dying in an uncontrolled manner, such as tumor necrosis. Additionally, cellular necrosis can cause further harm to surrounding cells [18]. As a tumor grows in an outward fashion, the middle of the tumor will be cut off from nutrients and oxygen, causing necrotic decay. This has been seen briefly in a study performed by Gautherie [19] to cause a dip in temperature. The study, discussed heavily in Chapter 6, presents the insertion of a temperature probe into the tumor of several patients. The temperature region within the center of the tumor is seen to dip, leading to the

assumption of necrotic tissue in more advanced, larger tumors. Gautherie concludes that a temperature change observed in his experiments are potential indicators of more aggressive, larger tumors with necrotic inner tissue.

1.3.3 Body Rhythms

There are many natural biological rhythms, affected by our body's chemicals or functions. Many often follow daily cycles or can be longer, depending on the type of rhythm. The four main biological rhythms are as follows [20]:

- Circadian rhythms: 24-hour cycle including physiological and behavioral rhythms
- Diurnal rhythms: circadian rhythm synced with day and night
- Ultradian rhythm: biological rhythms with a shorter period and higher frequency than circadian rhythms
- Infradian rhythms: biological rhythms that last more than 24 hours (such as menstrual cycle)

There are many potential disorders that can impact natural biological rhythms such as anxiety, sleep disorders, depression, etc. Some authors believe that natural biological rhythms can affect the temperature flow throughout the body, subsequently affecting resulting thermograms. Depending on the time of day or activities prior to imaging, the thermal results can change. Body rhythms are heavily discussed by Gautherie [19] as potential guidelines for imaging.

1.4 Medical Diagnosis

Prior to screening, a patient's risk level is identified based on many bodily factors and medical history. If someone is identified as breast cancer positive, the tumor is localized in terms of its

position on a clock, quadrant of the breast, distance from the nipple, and depth. Finally, they are diagnosed based on the tumor pathology.

1.4.1 Risk

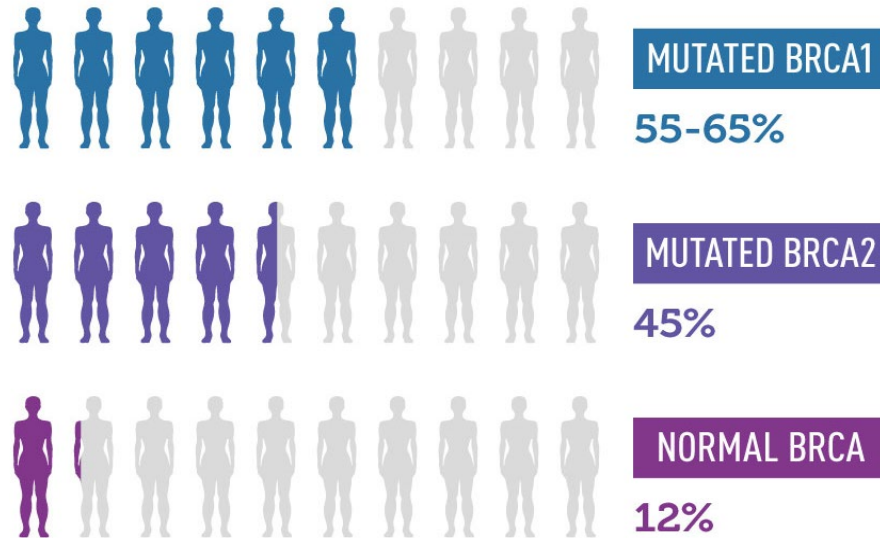
Patients are screened in different ways depending on their risk score. Risk is determined based on medical history, previous exposure (radiation, cancer, surgery) and genetic predisposition and family history. There are three main risk categories: high-risk, intermediate-risk and average-risk. The concept of ‘risk’ is measured based on various factors pertaining to the patient. They are as follows:

Table 1. Factors associated with high risk [21].

Unalterable Factors	Age
	Breast Density
	Genetic Mutation (BRCA1 or BRCA2)
	Family History
History	Pregnancy or Breastfeeding
	Previous history of cancer or breast disease
	Treatment with radiation therapy
Lifestyle-Related Factors	Physical Activity
	Weight
	Hormone altering substances such as oral contraceptives
	Alcohol and tobacco consumption

The image seen in Fig. 5 shows the National Cancer Institute’s statistical significance of the mutated BRCA1 and BRCA2 gene. Women with either gene are considered high-risk and must endure screening on a more regular basis, often with multiple modalities. Many women at high-risk will start receiving mammograms and MRIs every year, beginning at age 30.

NATIONAL CANCER INSTITUTE CHANCES OF DEVELOPING BREAST CANCER BY AGE 70



www.cancer.gov/brca-fact-sheet

Figure 5. The significance of the BRCA1 and BRCA2 mutations on increasing the risk of developing breast cancer [21].

While beginning breast cancer screening at a younger age can be beneficial and detect breast cancer at an earlier stage, many argue that inducing radiative screening techniques can have damaging effects. MRI is often used to screen for women younger than 30 with these mutations but has been shown to have a low specificity or increased false-positive rate.

1.4.2 Cancer Classification

Once someone is positively diagnosed with cancer, it is classified based on where the cancer is within the body. For example, if a tumor is found in the breast it is considered breast cancer. However, there are different areas within the breast where cancer can occur. If a mass is found within the epithelial tissue, it is considered a carcinoma whereas if cancerous cells are found within the connective tissue, it is considered a sarcoma.

Cancer is also identified by position and location. Characterizing a tumor or tumor location depends on several commonly known medical methods. Four different breast densities are used (as discussed above), three different depth parameters and several different locations. Figure 6 shows the tumor characterization widely used to localize location and position within the breast. For the tumor placement, a clockwise pattern is used including the center, seen in Fig. 6a while on the side view of the breast, there are anterior, mid, and posterior positions, seen in Fig. 6b. This information is important in localizing the tumor for further management such as biopsy or surgical resection and in correlating the findings with those of other imaging modalities.

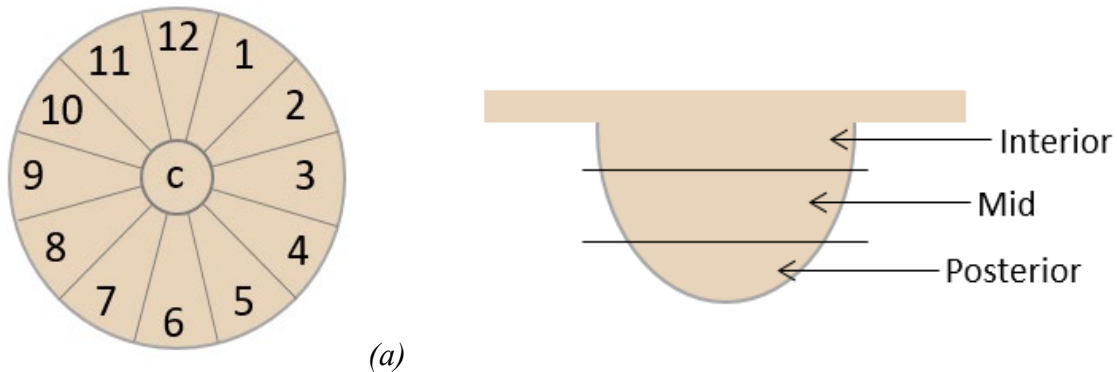


Figure 6. (a) Tumor location based on the positions on a clock and (b) tumor depth with three different classifications (interior, mid, posterior).

Once the tumor is examined and placed, it is assigned a grade. This grade is dependent on how the tumor is growing and spreading throughout the body [7]. Tumor grade is different than cancer staging, however. Cancer staging is dependent on three major factors: (1) Tumor (T), (2) Nodes (N), and (3) Metastases (M). For (T), a number is assigned dependent on how far the tumor has spread, how large it is, if it has begun to metastasize, etc. (N) involves the number of nodes affected by the disease. If the cancer has begun to spread into the lymph system, then a higher number will be assigned. Finally, (M) is dependent on whether cancer has started to spread to surrounding organs. The official system, presented by the National Cancer Institute, can be seen in Table 2.

Table 2. Different factors used in tumor staging [22].

Primary Tumor (T)		
	TX	Main tumor cannot be measured
	T0	Main tumor cannot be found
	T1- T4	Refers to size/extent of main tumor. Higher numbers indicate larger tumors that have grown more.
Regional Lymph Nodes (N)		
	NX	Cancer in nearby lymph nodes cannot be measured
	N0	There is no cancer in nearby lymph nodes
	N1- N3	Refers to number and location of nodes that contain cancer. Higher number indicates more nodes that contain cancer.
Distant Metastasis (M)		
	MX	Metastasis cannot be measured
	M0	Cancer has not spread to other parts of the body
	M1	Cancer has spread to other parts of the body

In 2018, the AJCC (American Joint Committee on Cancer) [23] announced an addition to the tumor grading system. Not only will the grade depend on TNM, but it will also include *prognostic staging*. Prognostic staging involves receptor status, genomic tests, and histologic grade.

Receptor Status – Receptor status refers to the hormones progesterone and estrogen that can drastically affect how cancer grows and spreads. When breast cancer is classified, proteins found in the cells are tested for estrogen or progesterone receptors. The following three are tested:

- ER (estrogen receptor) – Positive or Negative
- PR (progesterone receptor) – Positive or Negative
- HER2/neu – Positive or Negative

If a cancer is classified as receptor-positive, hormone therapy can be used to treat. The hormone therapy drugs block the hormone receptors that are helping the tumor grow and cut off the supply [24]. HER2 is a growth-promoting protein within the body that, if present within a tumor, can

cause cancer to grow and spread faster [41]. Similar to hormone-rich breast cancers, HER2 positive breast cancer can be treated with specified therapies. Breast cancers referred to as triple-negative are negative for ER, PR and HER2. These breast cancers are much more aggressive as the therapies and treatments normally used are not effective.

Genomic Tests – Genomic testing refers to the desired course of action following genetic testing to measure cancer risk. For breast cancer, this primarily refers to the BRCA1 and BRCA2 genes. As seen above in the discussion on risk, testing positive for one of these genes greatly increases chances of breast cancer and ovarian cancer. If someone tests positive for either gene, the Oncotype DX genomic test can predict aggressiveness of a tumor and what therapies will be most beneficial. Genomic testing can also be beneficial for patients with a family history. A patient diagnosed with cancer who also has a family history can participate in genomic testing to determine how the tumor will be influenced within the body and how it will grow and spread.

Histologic Grade – The grade is determined by observing various morphologic features such as tubule formation, nuclear pleomorphism and mitotic count [26].

- Tubule Formation – The amount of cancer cells that are in tubular formation (as seen in Fig. 7). The more tubules present in the cells gives a better score of 1 while a score of 3 is considered the worst.
- Mitotic Rate – This refers to the rate of multiplication and division of the cancer cells where 1 is the slowest and 3 is the fastest.
- Nuclear Pleomorphism – Finally, the nucleus is examined and given a score (1 to 3) dependent its appearance.

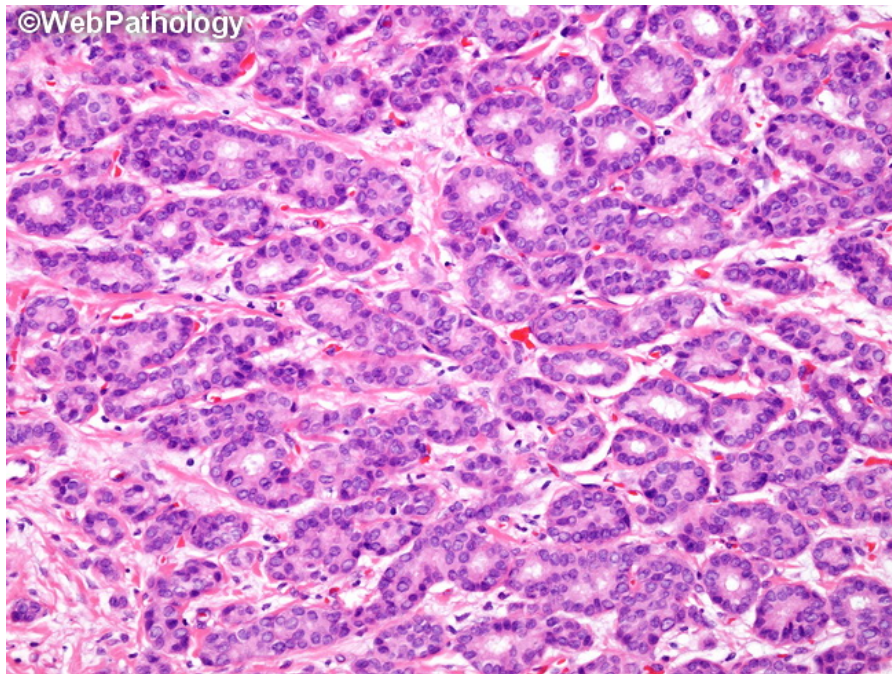


Figure 7. Slice of invasive ductal carcinoma with tubule formation in over 75% of the tumor [27].

The three features are given a score between 1-3 depending on intensity and prevalence. The sum of these scores designates the overall histologic score as seen below:

Table 3. Histologic grading system reported by the AJCC [26].

G	Grading Definition
GX	Grade cannot be assessed
G1	Low combined histologic grade (favorable), score of 3-5 points
G2	Intermediate combined histologic grade (moderately favorable), score of 6-7 points
G3	High combined histologic grade (unfavorable), score of 8-9 points

The currently classification of cancer primarily involves cellular and pathologic characteristics. Cancer and tumors are classified based on their growth and gene expression. However, there is no existing classification involving metabolic or thermal characteristics. There are many potential thermal biomarkers indicative of specific tumor growth. Many of these are discussed by Gautherie [19] and further presented below.

1.5 Medical Imaging

Most medical imaging techniques require a different type of wave to capture information in the body. Different forms of medical imaging simply manipulate different waves and frequencies on the spectrum in order to see into the body. The electromagnetic spectrum, seen in Fig. 8, shows all known detectable waves and their corresponding frequency range.

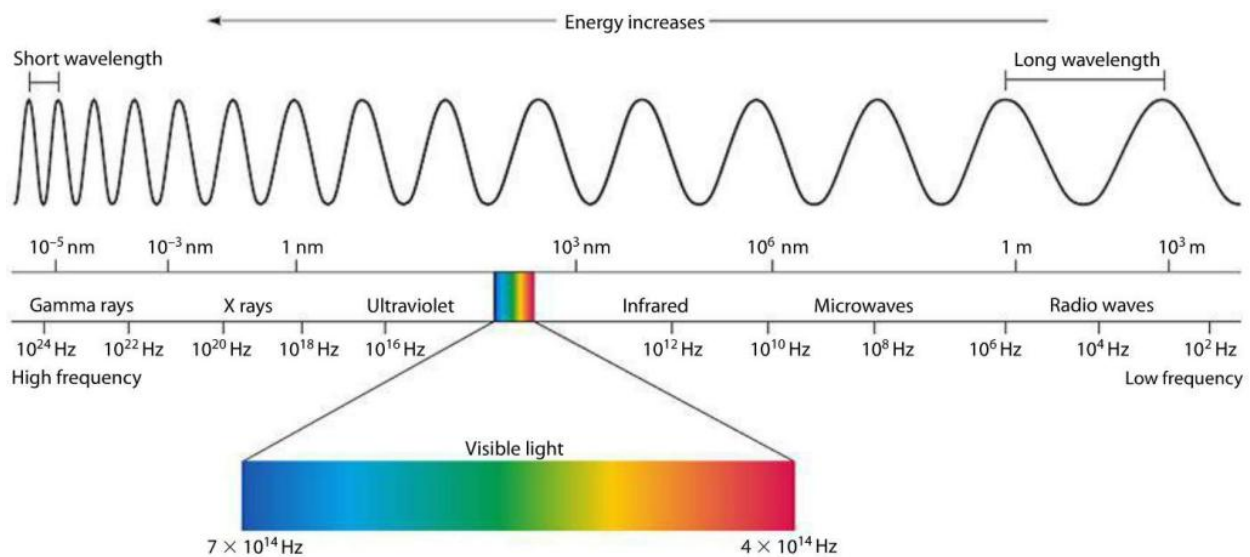


Figure 8. The electromagnetic spectrum with detectable waves and their accompanying frequencies [28].

Ultrasound uses acoustics and sound waves, MRI uses radio waves and mammography uses x-rays. Many medical systems utilize x-rays to visualize different parts of the body. X-rays are a type of electromagnetic radiation, similar to other waves seen on the electromagnetic spectrum. X-rays involve highly energetic photons that break up molecules and damage or destroy living cells. Some rays are absorbed into whatever material they are aimed at and others pass through. When the x-rays pass through the body, we can image or see inside. Utilizing x-rays, especially over a longer period, can cause radiation damage to the body and increase the risk of developing cancer.

Early detection of breast cancer is associated with improved chances of survival and options for curative treatment. The primary goal of cancer screening is to decrease cancer mortality through detecting asymptomatic cancers at an earlier curable stage before spreading to lymph nodes or distant organs, however overdiagnosis is a major concern in present screening techniques. Although there are many imaging techniques for breast cancer and other maladies found within the body, the three significant modalities (mammography, ultrasound, and MRI) are discussed here.

1.5.1 Imaging Techniques

a. Mammography and Digital Breast Tomosynthesis (DBT)

Mammography is currently the most widely used form of early breast cancer diagnosis. Mammography has been used since the 1970s for breast cancer screening in asymptomatic women. The screening in women aged 40-74 has been associated with relative reduction in breast cancer mortality of 15-20% [29]. Older methods involve 2D mammography while current techniques use 3D mammography or tomosynthesis. However, due to patient discomfort and radiation exposure, mammograms are only recommended for older women above the age of 50 [30]. A mammogram involves the compression of the breasts between an imaging plate and a clear plastic plate in order to x-ray the breast for screening and diagnostic purposes.

When a tumor is present, it will appear as a white mass on a mammogram. However, denser breast tissues also appear white. Women with scattered fibroglandular tissues, heterogeneously dense tissues or extremely dense tissues have a risk of a mammogram missing an existing tumor. Varying breast densities imaged mammographically are seen in Fig. 9. This is due to the white tumor mass blending in with the denser tissue. In 2D mammography, several images are taken at different angles to try and eliminate false positives or miss tumors behind dense tissues. Tomosynthesis,

which was approved by the FDA in 2011, is considered an adjunct to mammography, but is also expensive with a high radiation dose. Tomosynthesis is an imaging technique that utilizes x-rays, often used in women who are asymptomatic [31]. In digital breast tomosynthesis (DBT), also known as 3D mammography, the x-ray moves in an arc over the compressed breast, capturing many images to form a three-dimensional representation. The added enhancement allows for many views and therefore reduces any tissue overlap that could mask potential tumors [32]. The detection accuracy improves with DBT because multiple views are obtained, and the possibility of masked tumors decreases.

Breast density is an important consideration in all breast cancer screening. The four categories of breast density are fatty, scattered fibroglandular, heterogeneously dense and extremely dense. Heterogeneously dense and extremely dense breasts are considered “dense breasts” [33] (> 40% of women) and are at higher risk of developing cancer. However, mammography, currently the most widely used and available screening technique, is suboptimal in breasts with dense tissue; this results in ~38% of tumors to be missed or misdiagnosed [34].

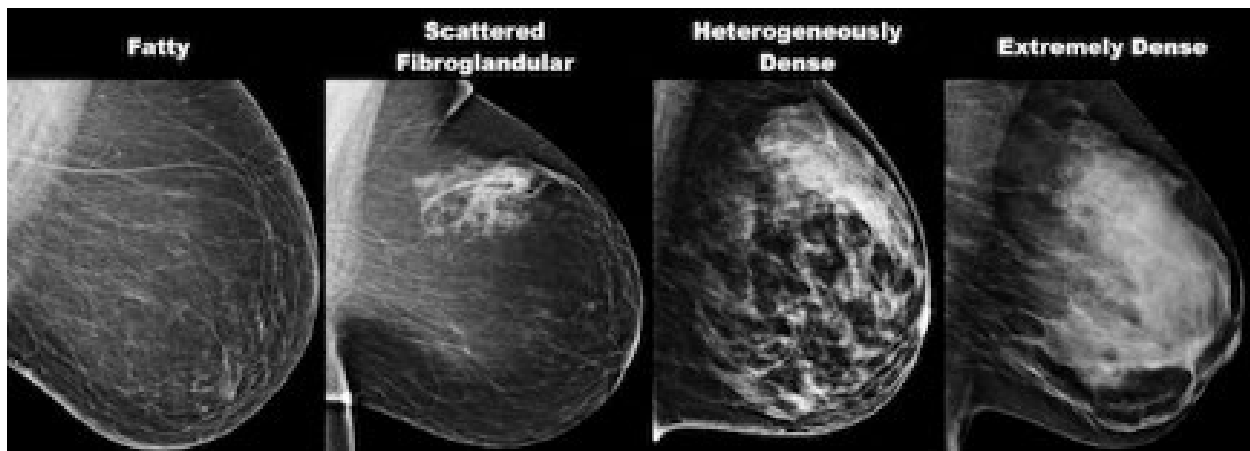


Figure 9. Mammogram of different breast densities [35].

b. Ultrasound

Ultrasound, a common adjunct diagnostic technique, and screening tool, is operator-dependent, and findings may be difficult to reproduce. Ultrasound imaging involves the manipulation of sound waves sent through the breast and converted into images. Although ultrasounds can be an insightful imaging technique, they are generally only used as a complement screening method to verify the presence of a tumor or for ultrasound-guided biopsy. The images are captured in real-time as well, which can allow for visualization of blood flow and any other movement occurring during imaging. The imaging process is completely noninvasive and, unlike mammography, there is no radiation involved in the process [36]. Although it is not generally used as a standalone screening method, it is highly beneficial for younger women. Younger women, who generally do not receive mammograms, are screened with ultrasound first if a lump is discovered before becoming exposed to other invasive methods such as mammography or MRI. It can also be beneficial for women with breast implants and women who are pregnant or breast-feeding [37].

Ultrasounds can be incredibly beneficial in differentiating solid masses (signifying malignant tumors) and fluid-filled benign cysts or fat lobules. Identifying the difference between a benign mass and a malignant tumor can spare emotional and financial burden and is therefore a crucial component of diagnosis. The images seen in Fig. 10 show a benign cyst and malignant tumor. Fig. 7a has distinct edges and is much more circular indicative of a fluid-filled cyst. Fig. 7b is clearly malformed, does not have clear, smooth edges and shows some potential branching patterns indicative of tumors.

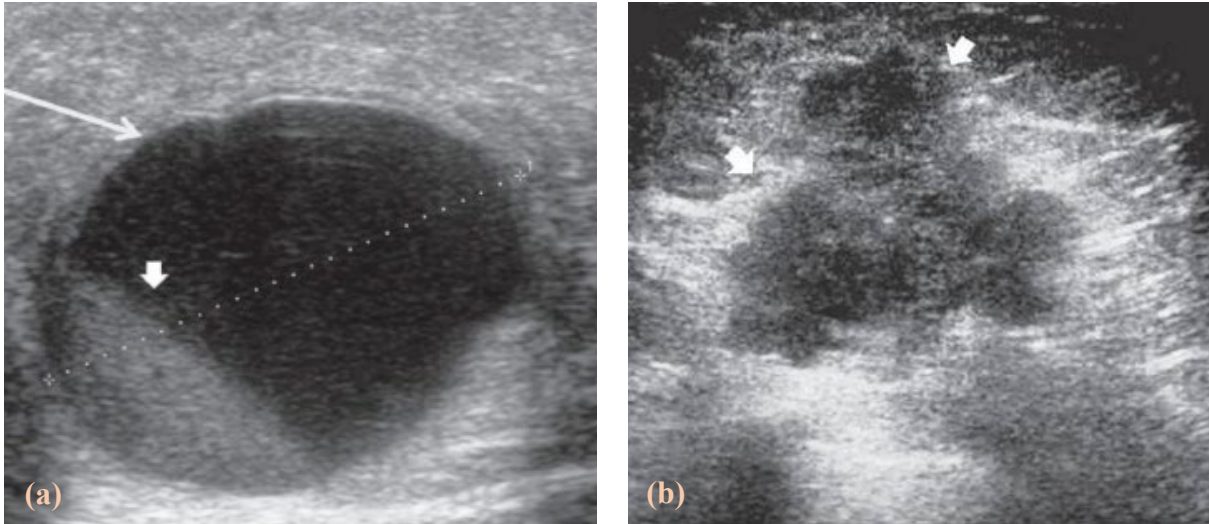


Figure 10. (a) A benign cyst resting inside of the breast and (b) a malignant mass [38].

c. Magnetic Resonance Imaging

Magnetic Resonance Imaging (MRI) uses magnetic fields and radio waves to reconstruct a three-dimensional, accurate representation of the breast. The images can also provide in-depth information on tumor characteristics and blood vessel networks. A breast MRI is generally used after a biopsy has been performed to examine the extent of the tumor for further treatment. A contrast dye is often used to enhance the images and make them easier to interpret. However, some women can have an allergic reaction to the contrast or it can cause further complications to those with kidney issues [39]. Fat saturation filters are used in post-processing to enhance certain portions of the breast for clarity. Magnetic Resonance Imaging (MRI) is an option but is time consuming and too expensive for general screening and as such is limited mainly to high risk populations (known or suspected mutation in a breast cancer causing gene or lifetime risk > 20%) by most insurers. In addition to its higher cost, MRI results in high number of false positives (low specificity); further increasing the cost of cancer treatment and diagnosis.

Women at high risk, such as women with >20% lifetime risk or known BRCA gene mutations, are screened using mammography and MRI annually. For this group, screening MRI has a higher sensitivity than mammography alone, the highest sensitivity occurs when both are combined [40]. In a study by Kriege et al. [41], 1,909 women at high risk were screened using mammography and MRI, the sensitivities were 33% and 79.5%, respectively. However, MRI led to twice as many unneeded additional examinations than did mammography (420 vs. 207) and three times as many unneeded biopsies (24 vs. 7). Gorechlad et al. [42] pointed out that annual MRI screening would incur significantly higher costs and is unlikely to improve overall survival.

An example of a breast MRI, before and after fat saturation can be seen in Fig. 11. The area with biopsy can be seen as a small black spot in the post-fat saturation image. The tumor can be seen either as dark gray (Fig. 8a) or bright white (Fig. 8b) with branching networks and vasculature visible in both.

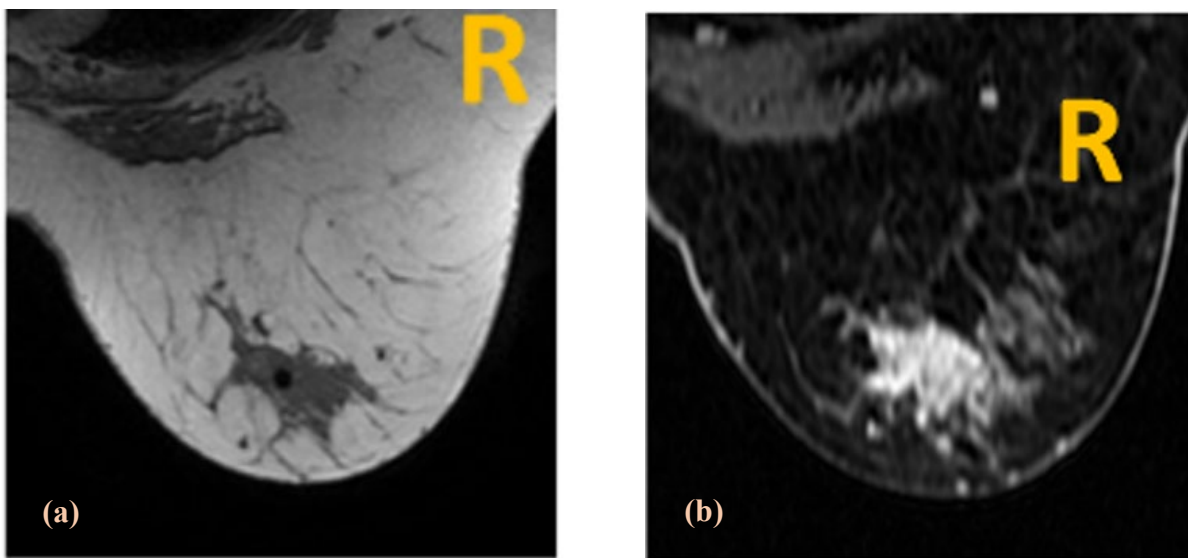


Figure 11. (a) MRI image of the breast prior to fat saturation and (b) fat saturation MRI image of the breast.

d. Other detection methods

Ultrasound, mammography/DBT and MRI are the most common methods used today for breast cancer detection and diagnosis. However, there are other methods currently being studied to improve imaging while reducing unnecessary protocol and invasive techniques.

Breast Specific Gamma Imaging – Breast Specific Gamma Imaging (BSGI) is a newer method of study that has high sensitivities as a screening method for breast cancer. The method is based on differences in metabolism, detecting how the injected radioactive agent accumulates in cancer cells over normal cells. It is beneficial for denser breast tissue and can take images from multiple angles. However, similar to MRI, it involves injection of a radiotracer and a longer exam of 40-45 minutes and similar to mammography, involves the compression of the breast between two plates [43]. The method is yielding good results, especially in women with dense breast tissue, but induces three- to four- times the amount of radiation used in a mammogram [44].

Positron Emission Mammography – Positron Emission Mammography (PEM) involves the measure of an increase of glucose to an area after an injection of a radiopharmaceutical that accumulates in a tumor. The materials injected are transformed into gamma rays and detected with gamma radiation detectors [45]. Although highly specific, PEM is not recommended as a screening technique due to higher levels of radiation. But the technique is valuable, especially for characterizing tumors.

e. Thermography

Infrared radiation, discovered by William Herschel in 1800, was found by studying the heat movement through different colored filters. Herschel measured the temperature outside of the visible spectrum of color and noticed an increase in temperature in what is known as the “invisible

spectrum of light” or infrared [46]. An IR camera uses a specific lens to detect temperature variation and heat emission from the object of focus. The captured light is translated into electrical impulses and, through signal processing, is translated into a color map with corresponding temperature gradients.

Thermography for breast screening was introduced in 1956 and was approved by the FDA in 1982. Infrared thermography fell out of favor due to poor sensitivity and nonstandardized clinical protocol. Throughout the past few decades, IR technology has improved dramatically with increasing sensitivity and better cameras. Companies such as FLIR boast thermal sensitivities as low as 20 mK with an accuracy of $\pm 1^\circ\text{C}$ or $\pm 1\%$ of the temperature reading [47]. A sensitivity and accuracy as low as this can be very beneficial for a variety of applications including leak detection, pipe blockage or biomedical imaging. With advances in infrared camera technology, there has been renewed interests on the use of infrared thermography as an adjunct to mammography for breast cancer screening with advantages such as lack of ionizing radiation, patient comfort (touchless and does not require compressing the breast), and portability. Because of the great promise for early breast cancer detection, many authors have studied thermography in different capacities. Theoretical studies, numerical models and experimental prototypes have all been studied to perfect thermography as a plausible tumorous detection method.

1.5.2 Statistical Considerations

In order to compare screening and diagnostic modalities more accurately, there are several statistical considerations needed. These include sensitivity, specificity, positive predictive value, and negative predictive value. Sensitivity and specificity are the statistical measures used to evaluate effectiveness of medical application. Sensitivity refers to the true positive detection rate whereas specificity refers to the true negative detection rate. High sensitivity is critical because it

measures how often the test generates positive results for subjects being tested that have the condition. Specificity measures how often the test generates negative results for subjects being test that do not have the condition. High specificity means the test correctly detect almost everyone without the condition. Positive Predictive Value (PPV) is the probability of a subject having a positive screening test who truly has the disease and Negative Predictive Value (NPV) is the probability of a subject having a negative screening test who truly does not have the disease. These factors are discussed at greater length below. The classifications presented from Rao [48] give a simplistic summary of the differences of these terms:

- Sensitivity: “I know my patient has the disease. What is the chance the test will show that my patient has it?”
- Specificity: “I know my patient doesn’t have the disease. What is the chance that the test will show that my patient doesn’t have it?”
- PPV: “I just got a positive test result back on my patient. What is the chance that my patient actually has the disease?”
- NPV: “I just got a negative test result back on my patient. What is the chance that my patient actually doesn’t have the disease?”

a. Sensitivity and Specificity

Sensitivity and specificity are two terms used widely throughout the biomedical field to evaluate different techniques. They refer to the detection of different diseases through different modalities in all areas of imaging and medicine. Sensitivity refers to the true positive detection rate and is calculated using Eq. (1) whereas specificity refers to the true negative detection rate and is calculated in Eq. (2).

$$\text{Sensitivity} = \frac{\text{True Positive}}{\text{True Positive} + \text{False Negative}} \quad (1)$$

$$\text{Specificity} = \frac{\text{True Negative}}{\text{True Negative} + \text{False Positive}} \quad (2)$$

Sensitivity and specificity depend not only on whether a patient is positively diagnosed with a disease but also whether or not the technology used for diagnosis is able to accurately diagnose.

An example of the calculations for sensitivity and specificity is seen below.

Example: 1000 patients are screened with NewModalityX to detect breast cancer. 730 test negative for breast cancer and the other 270 test positively.

	Positive for Disease	Negative for Disease
Test is Positive	230	30
Test is Negative	40	700

Out of the 270 that tested positively, 40 of them did not have breast cancer and were diagnosed incorrectly. The 230 that were correctly diagnosed are referred to as True Positive. To calculate sensitivity, we would do the following:

$$\frac{230}{230 + 40} = 0.85 * 100\% = 85\%$$

Out of that 730 that tested negatively, 30 of them actually did have breast cancer. The 700 that were correctly diagnosed are referred to as True Negative. To calculate the specificity, we would do the following:

$$\frac{700}{700 + 30} = 0.958 * 100\% = 96\%$$

This means that the NewModalityX will be able to correctly identify breast cancer 85% of the time and will be able to affirmatively state a patient does not have breast cancer 96% of the time.

b. Positive Predictive Rate (PPV) and Negative Predictive Value (NPV)

Although sensitivity and specificity are important factors in considering the accuracy of screening and diagnostic modalities, PPV and NPV are just as vital in determining the clinical relevance of the modality or test [49]. Sensitivity and specificity are fixed for a particular type of test while PPV and NPV are dependent on prevalence of disease in a population [48]. PPV is the probability that a positive test is truly positive (Eq. (3)) and NPV is the probability that a negative test is truly negative (Eq. (4)).

$$PPV = \frac{\textit{True Positive}}{\textit{True Positive+False Positive}} \quad (3)$$

$$NPV = \frac{\textit{True Negative}}{\textit{True Negative+False Negative}} \quad (4)$$

Prevalence involves the proportion of a given population who have specific characteristics. Equation (5) is used to determine prevalence:

$$\textit{Prevalence} = \frac{\textit{\# of people in sample with characteristic}}{\textit{Total \# of people in sample}} \quad (5)$$

An example of the calculations for PPV and NPV is seen below.

Example: 1000 patients are screened with NewModalityX to detect breast cancer. 730 test negative for breast cancer and the other 270 test positively. The same table as presented above is used here:

	Positive for Disease	Negative for Disease
Test is Positive	230	30
Test is Negative	40	700

$$Prevalence = \frac{270}{1000} = 27\%$$

$$PPV = \frac{230}{230 + 30} = 0.8846 * 100\% = 88\%$$

$$NPV = \frac{700}{40 + 700} = 0.9459 * 100\% = 95\%$$

Temporarily ignoring prevalence, this means that 88% of the individuals who test positive are truly positive for the disease and 95% who test negative are truly negative or disease free. However, in order to properly consider the population in which the disease is occurring, we must consider prevalence. The prevalence for this example is calculated as 27%. This means that 27% of our population is diseased and the remaining 73% are considered healthy.

Prevalence is particularly important in considering predictive values. Higher values for PPV and NPV suggest that the test is performing well. However, prevalence is directly proportional to PPV and inversely proportional to NPV. As the prevalence increases, NewModalityX has an increased probability of reading a true positive for a disease [50], [51]. Whereas if the prevalence is significantly lower, the probability of reading a true positive decreases. Considering our patient population is particularly important to the determination of accuracy of new methods.

c. Patient Population Considerations

Prevalence of disease is calculated dependent on the population being observed. For example, considering the number of women with breast cancer within the United States, there are several populations that are considered for statistical significance. There is the general population as a whole, those who are considered 'high risk' based on many different factors, those who have history of breast cancer, those who have a positive screen, etc. Determining what population is used to calculate prevalence can be vital in calculating accuracy of new screening modalities and therefore making comparisons against gold standard techniques.

If the selected observable population are those with suspicious mammograms who are receiving diagnostic mammograms, the prevalence of disease will most likely be higher than a general screening population of women getting an annual exam. This determination of prevalence will directly affect the probability of a positive or negative test being accurate. Careful considerations of patient population must be made for any new modalities being researched, especially as they are compared to gold standard. Additionally, the desired sample size may be dependent on the prevalence of disease within the population being considered. For this work, a new method is explored to screen and detect breast cancer. In order to determine the desired sample size for statistical significance, the observable patient population must first be selected. Depending on the selected patient population, the prevalence of disease may increase, requiring a smaller sample size. More considerations on patient protocol and statistical considerations are discussed in Chapter 3.

d. Determining Statistical Significance

Determining the sensitivity and specificity of a medical imaging technique is incredibly important not only for future clinical screening but also to quantify different modalities. Some methods are

highly sensitive and not very specific (such as MRI) while others are highly specific but not as sensitive (mammography). This leads to the conclusion that for some patients, a combination of methods may be the best way to screen for the most accurate results. Many authors have studied different modalities and calculated varying sensitivities and specificities than those listed below. However, the concluding statistics are dependent on the population studied, the number of patients screened and many other determining factors. For the purposes of this study, we are observing the sensitivity and specificity for various screening modalities for comparison. The values listed in Table 4 [52]–[56] give the relative sensitivity, specificity and the subsequent cost for various widely used screening and diagnostic methods.

Table 4. Diagnostic techniques with corresponding sensitivity specificity, and cost [57].

Technique	Mechanism of operation	Sensitivity	Specificity	Cost	Recommended for
Mammography	Low energy X-rays	84%	92%	Moderate	Screening and diagnostic evaluation
Magnetic Resonance Imaging (MRI)	Magnetic field and pulsating radio waves	90%	50%	High	Screening for women at high risk and diagnostic evaluation
Positron Emission Tomography (PET)	Gamma rays emitted by tracer substance	90%	86%	High	Determine spread of cancer
Ultrasound	High frequency sound waves	82%	84%	Low	Screening in women with dense breasts and diagnostic evaluation
Tomosynthesis (3D mammography)	Low energy X-rays	90%	92%	Moderate	Screening and diagnostic evaluation

1.6 Clinical Studies

A clinical study or clinical trial is identified as a specific intervention to medical care for willing and informed participants. Interventions can include medical products, drugs, procedures, or

changes to a participants' behavior (such as diet) [58]. They may involve the comparison of existing technology/pharmaceuticals or the introduction of brand-new products or approaches. When a new approach or product is introduced, it is unknown how harmful or helpful it may become. Prior to the implementation of a clinical trial, a clinical protocol is written discussing the purpose of the study, how the technology works, the potential risks and benefits, and the intended outcomes. Before recruitment can begin, the clinical protocol, clinical process, and informed consent forms must be approved by an Institutional Review Board (IRB). Additionally, whatever recruitment process and consent form will be used to recruit patients must also be IRB-approved. The IRB varies depending on the institution in which the clinical study is performed. Furthermore, some studies are also monitored by data monitoring committees to ensure the integrity and safety of the clinical trial.

Clinical studies can involve a small population of patients in one location or can be massive, involving thousands of patients and multiple locations. The standards set forth by the investigators illustrate who is eligible to participate and any exclusion criteria, if any. Patients are required to read and sign a consent form prior to participation. Informed consent is intended to protect participants and serves to inform them of the potential benefits or risks of the study. Additionally, participants can choose to withdraw from the study at any time throughout the process. For breast imaging studies, some methods pose the risk of radiation, contrast materials or discomfort. For example, the radiation risks associated with mammography or BSGI would be heavily discussed with the patient prior to consent.

Patient population is selected dependent on many factors including age, gender, risk of disease, type of disease, etc. For breast cancer studies, patients at higher risk may be selected over the general public, depending on the desired outcomes of the study. Women over the age of 18 are

generally selected because the risks of breast cancer are higher. Once the desired patient population and trial size are confirmed, the study can begin. More details on the patient flow and clinical process for this study are discussed in Chapter 3.

1.7 Conclusion

Breast cancer is currently the most prevalent form of cancer in women with over 266,000 new diagnoses every year [59]. There are many well-known modalities used to screen for breast cancer that range in accuracy and cost. However, many of these methods are invasive or inflict harm in order to screen and can still miss or misdiagnose cancer, especially in heterogeneously and extremely dense breast tissue. If someone is diagnosed with breast cancer, there are many classifications including type, grade, stage, and tumor biology. Steady-state Infrared Imaging (IRI) is unaffected by tissue density and has the potential to detect tumors in the breast by measuring and capturing the thermal profile on the breast surface induced by increased blood perfusion and metabolic activity in a growing malignant tumor. The details of the technology and scientific validation are discussed in the following sections.

1.8 Dissertation Overview

Chapter 1: This chapter involved basic introductions to many components crucial for this study including breast cancer, tumor pathology, medical imaging, statistical considerations, clinical protocol, and thermal imaging.

Chapter 2: An in-depth literature review is presented here including previous infrared imaging studies, research gaps, and objectives for this work.

Chapter 3: The approach is discussed including ethical considerations, clinical protocol, patient population, and experimental setup. The modeling work of Gonzalez-Hernandez [60] is discussed.

Chapter 4: The results of the study are presented showing patient data, IRI images, and methods for post-processing.

Chapter 5: Potential modifications are proposed for a suggested future large-scale clinical study. This includes recommendations on clinical updates and patient population sample size.

Chapter 6: Gautherie's work is presented and the thermal biomarkers are discussed as potential classifications. Additionally, angiograms are presented as an optional method to observe blood perfusion.

Chapter 7: Overall conclusions and major contributions (technical and societal) are presented.

Chapter 8: Finally, future considerations are presented including changes to clinical setup and infrastructure needed for a large-scale clinical study. The overall conclusions of this work are also given.

Chapter 2: Background

This chapter discusses the literature associated with bioheat transfer and thermography. These include studies on experimental representations, numerical simulation, and clinical investigations. The additional factors associated with thermography's positive attributes and fallbacks are also discussed.

2.1 Bioheat

The study of heat transfer throughout the body has been examined since the 1870s beginning with a Claude Bernard [61] who measured the heat transfer between arteries and adjacent veins. He focused on the measurements of arterial temperatures in animals. This pioneering work has been referenced and explored in many different bioheat studies, exploring the thermal relationships between different factors within the body.

In order to develop accurate mathematical models associated with the thermal transport within the body, a clear understanding of the underlying parameters such as metabolic heat generation, vascularity, and blood perfusion is needed. These factors greatly affect the thermal patterns that can be detected on the surface. Quantitatively calculating heat movement requires in-depth analysis allowing for blood flow and metabolic heat generation rate. The Pennes' bioheat equation, introduced by Henry Pennes in 1948 [62], is a widely recognized blood perfusion model based on the transient heat conduction equation. The equation, seen below, assumes the porous capillary beds are the only means of heat transfer and therefore a larger area is used for any heat exchange between the blood and tissue. Thermal equilibrium is added into the equation to compensate for

variations between the arterial blood temperature and the venous blood and tissue. Originally computed to measure heat in the resting forearm, the Pennes' bioheat equation is as follows:

$$\rho_t c_t \left(\frac{\partial T_t}{\partial t} \right) = \nabla \cdot (k_t \nabla T_t) + (1 - k') \omega_b c_b (T_a - T_t) + q'''_m \quad (6)$$

where ρ is tissue density, k is the thermal conductivity of tissue, c is the specific heat capacity, T is temperature, ω is the volumetric flow rate of blood, k' is thermal equilibration (either 0 for steady-state or 1 for transient conditions) and q'''_m is the metabolic heat generation rate. The subscripts b, t, and a stand for blood, tissue, and arteries, respectively. The Pennes' bioheat equation has been used extensively in the study of heat transfer within the body and living organisms for a wide array of application.

In 1980, Gautherie [19] used a fine-needle thermocouple (0.8 mm in diameter) to measure the internal temperature distribution of breasts, both healthy and with cancer. In his work, he reported that a tumor results in a peak of $\sim 3^\circ\text{C}$ in the region surrounding the tumor when compared to the internal temperature distribution of a healthy breast. Gautherie studied the natural progression of cancer on 128 subjects who refused to receive treatment. He measured the metabolic activity and blood perfusion in healthy and tumorous tissue (Figure 12). The following three categories of growth and relative metabolic heat production are shown below where DT is doubling time and q^* is metabolic heat production.

- Cancers with a fast growth rate ($DT \leq 150$ days) and intense metabolic heat production ($q^* \geq 20 \times 10^{-3} \text{ W/cm}^3$)
- Cancers with slow growth rate ($DT \geq 250$ days) and low metabolic heat production ($q^* \leq 10 \times 10^{-3} \text{ W/cm}^3$)

- Cancers with intermediary values of DT and q^* , classified into (1) or (2) if lymphatic spread is found or not.

Gautherie observed that fast growing tumors (doubling time < 100 days) have metabolic activities of up to $70,000 \text{ W/m}^3$. In contrast, slow growing tumors (doubling time > 250 days) had metabolic activities of about $10,000 \text{ W/m}^3$. He reported an exponential decaying relationship between tumor doubling time and metabolic activity. In his study, he reported that the metabolic activity of healthy breast tissues varies between 400 and 700 W/m^3 , demonstrating that tumors are at least 15 times more metabolically active than healthy tissue. All patients within the study group had consistent and identical sleep cycles and eating patterns. Gautherie also examined the natural thermal rhythms of each patient and identified patient's circadian, circaseptan, and circatrigintan rhythms. To determine the metabolic heat generation rate, Gautherie measured the temperature of the patient's breasts using fine-needle thermoelectric probes over the span of 700 days. He plotted the growth relationship between metabolic rate and double time of a tumor and this plot can be seen in Fig 12. Gautherie concluded in 1983 [63] that the resulting thermal increases from tumors was due to an increase in metabolism, localized or diffused increases in skin temperature due to convection and vascular changes.

Additionally, Gautherie delves into great detail on the effects of circadian rhythm and growing vasculature on the thermal relationships in the breast. Factors such as effective thermal conductivity, perfusion rate and metabolic activity must be taken into consideration when continuing any bioheat transfer study. Further details on the potential of Gautherie's work and the introduction of a thermal biomarker classification system are discussed in Chapter 5.

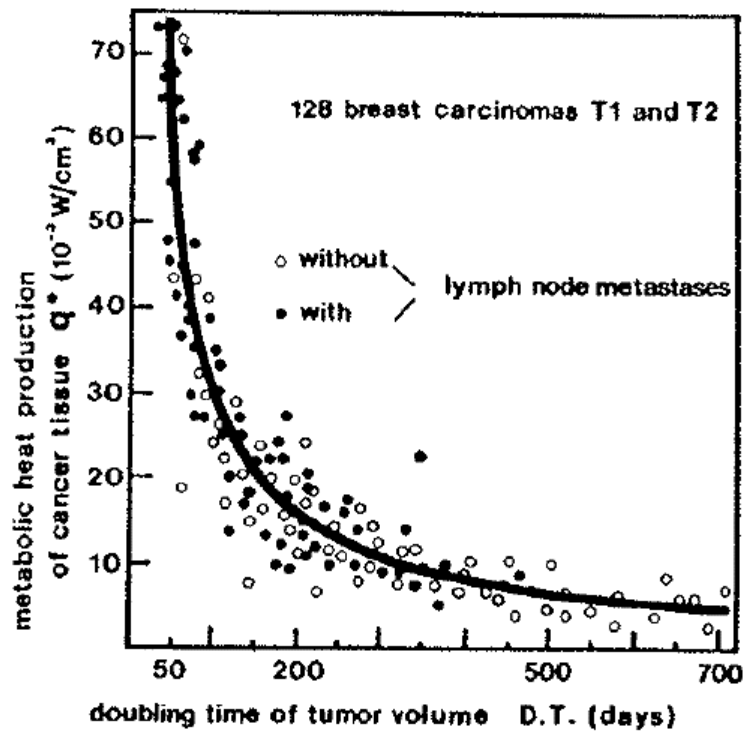


Figure 12. Relationship between metabolic generation and doubling time [19].

2.2 Thermography

2.2.1 Breast Cancer Detection Demonstration Project

The studies that have led to these conclusions have varied in technological advancement, post-processing techniques and scientific basis. The negative reputation of thermography begins with The Breast Cancer Detection Demonstration Project (BCDDP), starting in 1973. The BCDDP involved a large working group of biostatisticians, clinicians, and pathologists [64]–[72]. This study involved the participation of 27 centers throughout the United States. The project was meant to study early detection methods for breast cancer, among different populations and geographical locations. A collaborative act between the American Cancer Society and the National Cancer Institute, over 280,000 women participated. “Participants were screened for breast cancer on an annual basis using a combination of medical history, physical examination, mammography and

thermography to detect breast cancer in its earliest stages [73].” The majority of participants were between 35-74 years old and did not have a previous history of cancer. Throughout the duration of the project (1973-1981) 4,443 breast cancers were recorded, 80% of which were detected by the 29 centers.

At the beginning of an exam, every patient filled out a history form, received a physical examination, a mammogram and a thermogram. Thermography was introduced as a promising screening technique to replace mammography. The WG considered the use of thermography in this multi-year study due to the growing popularity of the time. Authors such as Lawson [40] and an increase in international use warranted further review, particularly because of the low-cost and non-radiative nature of the technology. The goal of the BCDDP was to study the efficacy of thermography as a pre-screening tool to reduce the number of women subjected to radiation from mammography. The WG also reference a study performed by Lilienfeld et al. [74] that showed a sensitivity and specificity for thermography similar to those from physical examination and mammography. At the time, thermography was an up-and-coming technology with poor camera sensitivity and unknown methods for image interpretation. The need for technological refinement and the readiness of thermography for large-scale detection were listed as major concerns.

Data reporting, image interpretation and diagnosis are discussed further in the report. “Positive physical examinations and mammographies were reported in various degrees of certainty about malignancy or as suspicious-benign; thermography was reported as ‘abnormal.’” Physical examinations were conducted by trained professionals and mammograms by trained technicians. Mammographic data was initially interpreted by both trained technicians and radiologists. The mammographic procedure, including radiation dosage, was consistently reviewed for quality and procedure issues. The thermogram procedure and image interpretation was “conducted by a

BCDDP's trained technician". Some sites utilized radiologists in addition to trained technicians for image interpretation. Similar to mammography, quality control checks were introduced by the project physicians. However, in several locations, the same technician reviewed and interpreted both the mammography and thermography data. Introducing obvious human bias from visual human interpretation could have contributed to the seemingly poor performance. Additionally, using the same technician for both mammogram interpretation and thermogram interpretation introduces further bias. Because mammography was considered the gold standard for screening, a positive or negative result from a mammogram (whether accurate or not) would automatically influence the technician's decision about the outcome of a thermogram. Although the WG called for batch reading separately of the images, any images interpreted by the same individual should not have been considered in the final results for thermography over the duration of this project. The WG also states "It is not known to what extent observations in one modality influenced the interpretation of another. [67]"

The WG reported 41% of the abnormal thermograms were breast cancers while the other 59% were interpreted as unknown or normal. Similar results are reported for the second screening. The WG also state that if routine mammography were not performed, many of the negative or unknown reports of thermography would have missed the cancer completely. They state, "Thermography was positive in 43% of the breast cancers detected during the first two screenings, but very few were negative in the initial interpretation of the mammography and physical examination findings."

The WG stress the importance of mammography has a routine screening method and determine that thermography is not an adequate replacement. However, the FDA, in 1982, approved thermography as an adjunctive technique, potentially due to the results of the BCDDP. While

several studies support the evidence of the lack in accuracy while using thermography as a standalone technique, the merits of the method as an adjunct to mammography and ability of thermography to view the breast in a different light should not go overlooked. In the report published in 1978, they conclude that thermography is not an adequate substitute for mammography.

The potential downfalls of thermography in the BCDDP are discussed: "...conclusions on the effectiveness of thermography in the BCDDP rest on available data, and these data do not reinforce the hopes that had been held out for the procedure. This finding should not be taken as a determination of the future of thermography. The procedure continues to be of interest because it does not entail the risk of radiation exposure and it is apparently more economical than is mammography." The authors state that they are unsure if the limitations from thermography are due to technologic limitations or procedure. The rest of the report continues to discuss pathology results and accuracy of physical examination and mammography and thermography is not discussed further. In the supplemental material [72], the WG state that "Analysis of the experience with thermography in individual projects of the BCDDP suggests that several projects had results that were more favorable than was the picture for the BCDDP as a whole. This finding encourages investment in the development and testing of thermography under carefully controlled study conditions, and the Working Group recommends that high priority be given to such studies." The WG does not discredit thermography as a technique but instead, recognize the potential and recommend further study is warranted.

However, some sites involved in the BCDDP saw varying results than the rest of the project. In 1984, two physicians who led centers during the BCDDP, Margaret Abernathy, MD and JoAnn Haberman, MD, spoke of the treatment of thermography during that time [75]. An interview

published by JAMA Medical News highlights the shortcomings of the BCDDP's handling of thermography. According to Dr. Abernathy, only five centers that participated had personnel experienced in obtaining or reading thermograms. "Expertise in mammography was a prerequisite for being awarded a contract to operate a center, she said, but previous knowledge of thermography was not required." Additionally, she adds that the quality of the collected thermograms were 'terrible.' Haberman expands on the mistreatment of thermography by radiologists stating "The radiologists who ran most of the BCDDP centers were quite uncomfortable with thermography. They were having to learn all the basics. Also, they were facing a huge task in evaluating thousands of women by mammography, and they just decided to cut down on their workload by tossing out thermography rather than learning to understand it." A third physician further expands on these thoughts, mentioning the complexity of breast cancer as a disease. Dr. Logan states that thermography offers an additional way to view the breast that would benefit patients. Furthermore, utilizing thermography, Logan has been able to detect small cancers often missed by other modalities. However, despite these assessments, Logan did not use thermography as a screening technique "because the method itself, regardless of the experience of those who use it, gives many more false-positive than true-positive results."

Several authors presented follow-up studies discussing survival rates and BCDDP process. Baker [73] wrote a five-year summary report of the BCDDP and their findings. They briefly discuss the removal of thermography as a screening technique and mention that restrictions on mammography were added for those under the age of 50. Smart [76] and Cunningham [77] both presented 25-year follow-up reports on the findings of the BCDDP. Both studies discuss follow-up of the diagnoses made during the BCDDP time-period. However, neither further discuss the usage of thermography and its removal from the study.

Although thermography was eventually FDA-approved as an adjunctive screening technique in 1982, the negative reputation surrounding thermography is ever abundant. The results from the BCDDP have led to a significant stigma against thermography within the medical community and additional factors have led to the propagation of thermography's bad reputation, despite technological progression. Predominantly, inconsistent imaging criteria dependent on empirical observation and little medical validation.

2.2.2 Dynamic and Steady State Thermography

An in-depth review paper published by Gonzalez et al. [78] discusses the nature of dynamic thermography and the many researchers that have employed this method. Dynamic thermography (DT) was introduced to reduce the false positives and false negatives present in pioneering studies using steady state thermography. The fundamental principles of DT involve the addition of a cold stress by (1) forced convection aimed at the breasts, (2) reduction in ambient temperature or (3) forced conduction by using ice packs on the breasts. In DT, sequential thermograms are captured after a cold stress is removed and the thermal response of the breasts is analyzed. The resulting thermal contrast between the tissue affected by a tumor and the 'healthy' or unaffected tissue becomes detectable by an infrared camera. The cold stress aims to reduce the overall temperature of the breasts in order to increase the thermal contrast in areas with abnormal vascularity and metabolism. Despite the innate patient discomfort induced by the addition of a cold stress, dynamic thermography has been widely studied by many in the field, for commercial use and for clinical trials. There are two main imaging protocols used in DT: (1) static image capture and (2) continuous imaging. Static image capture involves taking images at specified times, usually before, during and after cold stress is applied. Continuous imaging utilizes videos or constant image capture during the cold stress process to observe the cooling and rewarming of the breast. The goal

is to observe the changing thermal characteristics more vividly in the breast while the cold stress is applied. Kakileti et al. [79] state that continuous imaging is not as popular due the large processing time. However, more information is captured with this method, especially since “tumorous regions do not cool as fast as rest of the tissues.” Steady-state thermography is focused on maintaining a steady ambient temperature and allowing for proper acclimation for the breast temperature to reduce naturally prior to image collection.

The NoTouch BreastScan [80], developed by UE LifeSciences Inc., is an FDA cleared, noninvasive and radiation-free imager. The system blows air at the breasts from different positions to achieve an even air flow. Air is blown until the temperature on the breast surface decreases by 3-4°C. While air is blown, the IR cameras capture thermograms of each breast. Once the desired level of cooling is achieved, the airflow ceases, and the exam ends; the exam usually takes between 5 and 6 minutes. The NoTouch BreastScan uses Artificial Neural Networks to identify the salient features and compare them with known heat patterns typical for tumors.

Hu et al. [81], knowing that the majority of clinical thermography studies involved the use of dynamic cold air, studied the effects of colder air on the breast surface. Ignoring environmental factors such as perspiration or evaporation on the skin, they developed a 3D model of the breast using GAMBIT. They embedded a tumor into the breast and added the geometry into a constant, laminar air stream. Using Fluent, they tested five different tumor cases with air stream flowing horizontally across the breast. The authors state, “Thus the simulation demonstrates that the patterns of thermograms have strong dependence on the environmental cooling effect even in the presence of low velocity airflow.” Additionally, the authors discuss that normal clinical screening happens under looser controlled conditions, leading to inconsistent cooling, lack of repeatability and further issues in image interpretation. Ultimately, they conclude that using dynamic cold air

can greatly affect temperature distributions on the surface and create irregularities in tumor analysis. An example of the airflow analysis over a breast with tumor is seen in Fig. 13.

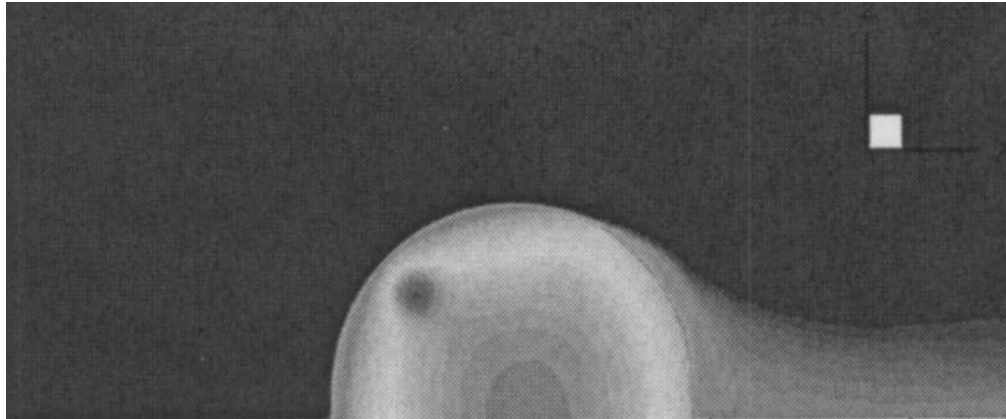


Figure 13. Numerical breast model to examine effects of parallel convection on the breast surface of a breast with tumor [81].

Ohashi and Uchida [82] performed a comparative study between dynamic and steady-state thermography on 728 subjects with biopsy-proven breast cancer. They utilized a fan blowing air over the breasts for a 2-minute duration. Infrared images were captured every 15 seconds over a 20-minute period. Although they saw improved accuracy with dynamic thermography (82%) over steady-state thermography (54%), they also had an increase in false positives with dynamic.

Wishart et al. [83] used the Sentinel BreastScan™ (discussed above) to image patients with breast cancer prior to breast biopsy. About 113 patients were recruited for this study and 106 core needle biopsies were performed. Patients were asked to disrobe from the waist up and place their arms at eye level on a support structure. Flowing air was directed at the breasts for 5 minutes while images were taken simultaneously. 65 biopsies ended up malignant and 41 were benign with an additional 13 patients excluded due to system malfunction. Of the 65 with malignancy, 30 patients were determined normal from the Sentinel Breast Scan™. The maximum sensitivity (78%) and specificity (75%) were seen in women who were under 50 years old.

2.2.3 Numerical Studies

Utilizing the basics of heat transfer and the Pennes' bioheat equation has resulted in many different studies for tumor detection. Creating a three-dimensional numerical model with programs such as COMSOL or ANSYS Fluent. Numerical simulations allow the user to create a model, impose a tumor or heat source, apply varying boundary conditions, and quickly calculate the resulting energy transfer and temperature profile through the system. Over the past few decades, computational software has increased in popularity and complexity making it simpler to perform in-depth simulations in a faster timeframe.

Many researchers have performed numerical simulations with varying breast models. Sudharsan et al. [84] used a 2D model with realistic layer densities and assigned values. They used FEMAP to generate their mesh and various other programs to calculate all PDEs and governing equations. They assumed a tumor growth at various sizes and ultimately concluded that adjusting values such as blood perfusion could assist in more accurate analysis or smaller/deeper tumor detection. A few years later, the same authors (Ng and Sudharsan [85]) performed a continuing study with a 3D model. Additional studies utilizing numerical methods for

2.2.4 Experimental Studies

Many authors discuss the reasoning for choosing thermography is improvement upon patient comfort during breast imaging. Utilizing an experimental model with material properties similar to those that are naturally occurring, such as agar-agar, can give an accurate depiction of resulting surface temperature profiles with the presence of a tumor. Using these models to experiment with different biological parameters can help characterize the effects of a cold stress on the breast and can assist in tumor detection methods without the need for breast cancer patients.

Feasey et al. [86] performed a theoretical and experimental study under steady state and dynamic conditions. Using a mixture of Perspex and paraffin wax, a phantom model was created and heated similar to the chest wall. A small resistor was used to replicate a tumor and the surface temperature distribution was captured with an IR camera. An electric fan induced cooling horizontally onto the model surface to simulate an added cold stress. The authors concluded that the addition of forced air reduced the temperature difference between the maximum temperature and surface temperature across the model “skin.” Due to promising results, a similar process was used on actual breast cancer patients. Nilsson and Gustafsson [87], [88] performed two separate experimental studies; one involved an embedded heat source underneath the skin of the rabbit and one involved the same embedded heat source under the skin of a man. The heat source encompassed a titanium cylinder wrapped in wire. The first study involved careful implantation to avoid any disruption to the localized tissue in six different rabbits. Corresponding theoretical calculations were performed to verify resulting temperature profiles. Maximum surface temperatures over the heat source were recorded based on implantation depth and heater capacity. The experiment was continued [87] further, and the heater was implanted into a human forearm. A constant ambient temperature was maintained while the heater capacity varied. For this study, the authors implemented three different ambient conditions of still air at 23°C and 17°C, and forced air convection at 23°C. The authors noticed a reduction in resulting surface temperature with the addition of forced convection. However, in a departure from more recent studies, the authors did not consider studying the resulting thermal recovery period used in dynamic breast thermography studies. They also noted that a change in ambient temperature did not have a significant effect on changing heater capacities although they noted a slight temperature increase with the lower ambient temperature.

Mital and Scott [89] utilized a cylindrical model with Difco Agar as the phantom tissue. A resistance heater was embedded into the center of the model and allowed to sit for several hours to ensure a steady state had been reached. Various wattage levels were tested to simulate changing metabolic activity, but no cold stress was applied. The goal of the experiment was to observe the relationship between heater location and power and the resulting surface temperature profiles. An algorithm was developed to estimate the location and power capacity from the collected IR images.

Wahab et al. [90] used an agar-agar mixture with an embedded mica heater. A larger heat capacity was used in order to accentuate the resulting surface temperature profile. An appropriate amount of time passed to ensure thermal equilibrium before taking images with an IR camera. The main objective for this study was the resulting image processing and the development of a hotspot detection algorithm to assist with post processing. The authors noticed variations in the temperature profile across the agar-agar model and concluded that a separate enclosure is needed in the future to reduce ambient temperature effects.

Despite the potential of these models, not many researchers have explored this option. For any future work, validating numerical or theoretical calculation with an experimental phantom model could be crucial to ensure that a future participant of an IR clinical study will remain comfortable and unharmed while still maintaining the efficacy of the technology.

2.2.5 Clinical Studies

Lawson [40] first introduced thermal imaging in 1956 using temperature probes on the breast surface. Out of 26 patients with proven breast cancer, the average temperature increase was 2.27°F. The largest temperature rise recorded was 3.5°C. Lawson speculated that examining temperature could have diagnostic possibilities for detecting breast cancer earlier. In 2000, Head and Elliot [91] published a long-term study involving multiple patient groups. The first portion of the study began

in 1973 and involved the following three categories of patients: (1) 126 patients who died of breast cancer and had IR imaging within a 1-year period after breast cancer diagnosis, (2) 100 randomly selected living breast cancer patients who also had IR imaging within a 1-year period before breast cancer diagnosis, and (3) 100 patients who had a variety of mastopathies but hadn't been diagnosed with breast cancer. Throughout the study, many statistical considerations were taken to determine the significance of the collected results.

Stark and Way [92] explored the use of thermography using 4,621 women, using mammography as an adjunctive technique for abnormal thermograms. They have termed their method as Aga Thermovision and identified three basic results: (1) the avascular (normal without veins), (2) the vascular (normal with visible veins), and (3) the mottled pattern. Their criteria for identifying malignancy are as follows: localized area of heat emission or hot spot, localized increased vascularity, generalized increase in temperature and increased heat of areolar area. They also noted that the correlation between temperature and tumors is less related to tumor size and more related to histologic activity. Similar to other authors, Stark and Way speculate that additional factors influence the resulting thermogram such as pregnancy, menstrual cycle, and contraceptives. Increased vascularity was seen during pregnancy and menstruation while varying results were seen for oral contraceptives. Out of all the patients imaged, all patterns were seen in all age groups with all different sized breasts. Ultimately, 628 women were identified as abnormal and given mammograms. However, similar temperatures were seen for benign diseases such as fibroadenoma and invasive ductal carcinoma. The authors conclude that thermography has great promise but may cause interpretation difficulties due to hyperthermia in both malignant masses and benign conditions.

Gutierrez-Delgado and Vazquez-Luna [93] used a similar image capture process including a room maintained between 18°-23°C and an acclimation period of 15 minutes. They imaged 911 women, 94% of which were diagnosed with cancer. In 1980, Gautherie and Gros [94] published a 12-year clinical study involving approximately 58,000 patients. They classified their subjects based on five separate stages (Th I – Th V) where Th 5 is the most suspicious. The first contact with each subject involved recorded history, physical examination, mammography, ultrasound, and thermography. If core needle biopsy was needed, a histologic report was obtained. 1,527 women were identified as Th III, meaning their thermograms were suspicious but inconclusive. Some of these patients were diagnosed with cancer at the initial visit but the remainder of the patients (1,245) were re-examined over the span of 12 years. Over the years, malignancy was eventually detected in 298 of these patients were diagnosed with malignancy. Gautherie and Gros hypothesized that irregular thermal patterns seen in healthy breasts could potentially signal cancer at an earlier, undetectable stage.

Haberman et al. [95] developed a mobile breast screening unit to examine women in primarily rural populations in South Dakota. Mobile clinics offered thermograms and physical examinations traveled throughout the state and recruited over 39,802 women. Each participant was cooled for 10 minutes in the supine position (on the back) with arms extended. A Spectrotherm 2000 camera was used to record three separate images of the breasts at different angles. Only 71 patients with cancer were identified and later confirmed with pathology. Of these 71, 15 were not detected using thermography leading to an overall sensitivity of 79%. Francis et al. [96] obtained thermograms of 24 individuals without breast cancer and 12 individuals with breast cancer. Individuals were imaged in prone position and 12 thermograms of each breast were obtained at both steady state and after an applied cold stress. First, thermograms were obtained at steady state and after the

temperature was reduced by 2 – 3°C and the breasts were re-imaged. The authors found an accuracy of 83.3% using the steady state thermograms and 70.8% when using the thermograms after cooling. However, the authors only obtained one thermogram at every position after cooling and did not track temperature evolution during recovery.

2.3 Research Needs

In a recent publication by Gonzalez-Hernandez et al. [78], the number of scientific publications related with breast thermography was reported to increase from 11 in the year 2000 to more than 55 in the year 2018 (Fig. 14).

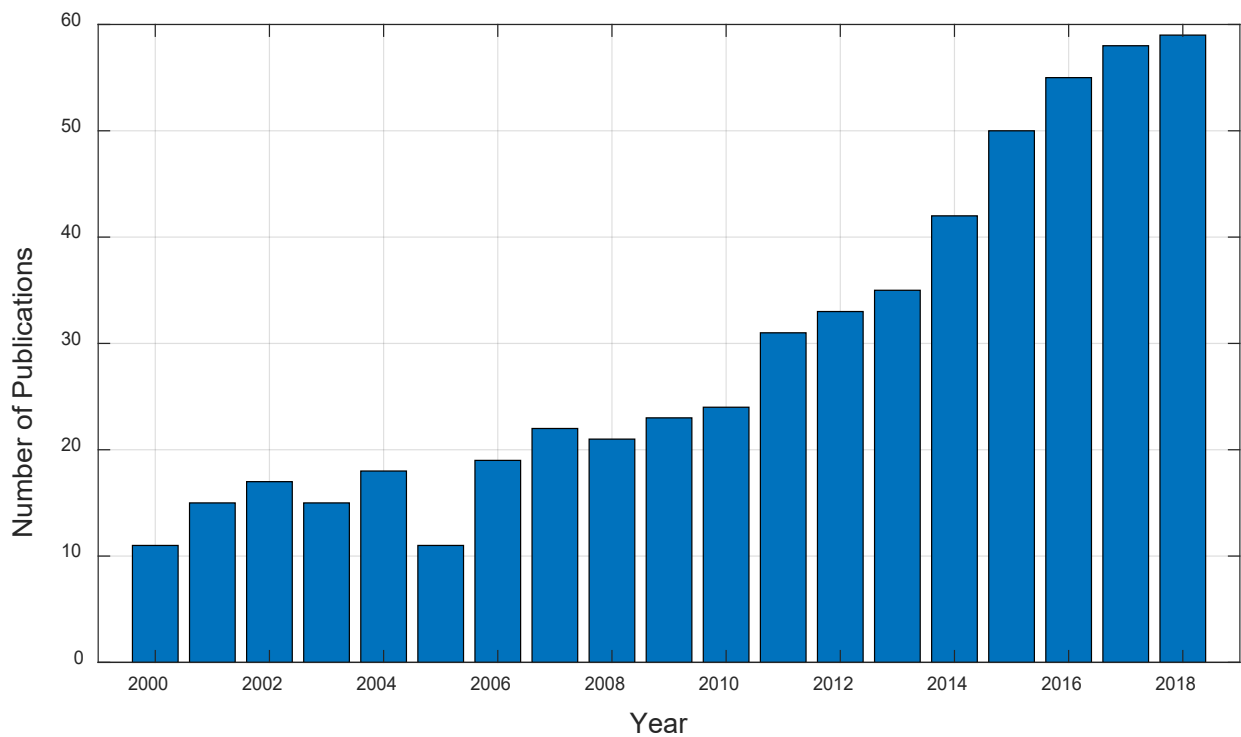


Figure 14. Number of publications related with breast thermography [78].

An extensive review paper written by Lozano and Hassanipour [97] discusses all clinical trials utilizing infrared imaging up to this point and the varied results achieved. The contradictory

sensitivity and specificity values achieved by many different studies examining the same technology provides evidence of non-standardized clinical procedure and detection methods. Table 5 below has a comprehensive list of various thermography studies and the achieved sensitivity and specificity values.

Table 5. Clinical thermography studies with reported sensitivity and specificity values [97].

Authors and Year	Reported Sensitivity	Reported Specificity
Moskowitz et al. (1976)	24%	56%
Stark (1985)	86%	98%
Williams et al. (1990)	61%	74%
Head et al. (1993)	65%	72%
Keyserlingk et al. (1998)	83%	81%
Parisky et al. (2003)	97%	14%
Arora et al. (2008)	97%	44%
Wang et al. (2010)	72%	77%
Kontos et al. (2011)	25%	85%
Rassiwala et al. (2014)	98%	99%

In all of these studies, many have explored different positions, different imaging durations, cameras, detection criteria, possible biological or hormonal interference, etc. There are many competing methodologies surrounding this technology that have created a negative stigma in the medical community. In order for this technology to advance, scientific validation and standardized clinical practice is needed.

The decrease in studies as well as the resurgence in thermography can be attributed to various factors influencing the imaging process. Many key factors, discussed in greater detail below,

include diagnostic criteria, image analysis, camera sensitivity, and imaging process. Researchers have tried to prove the usefulness of thermography as a successful screening technique and have arrived at the following contradictory conclusions:

1. Thermography is a useful tool with high accuracy and specificity.
2. Thermography is not a valid method for breast cancer screening.

Many of these aspects are discussed in the following subsections.

2.3.1 Imaging Protocol

The screening protocol involves several factors. These involve the process used by researchers to screen individuals, additional considerations of thermal influence and the position in which patients are screened. There is disagreement among researchers for proper protocol for thermographic screening, leading to inconsistencies in results. When screening individuals, especially when considering temperature-based diagnostic criteria, it is important to consider thermally altering factors. Environmental conditions, engaging in activities prior to imaging that cause thermal changes such as drinking coffee, exercising, wearing coats/scarves/warmer clothing, smoking tobacco, etc. or normal body cycle such as menstruation or menopause can significantly alter the temperature distribution throughout the body. Several studies have observed these changes and recommend managing controllable extrinsic factors, imaging at specific times of the day or month, or recording intrinsic factors that could influence the thermoregulation in the body.

Fernandez-Cuevas et al. [98] present a review paper that discusses many different environmental, individual and technical factors that potentially influence the outcome of thermograms and image interpretation. Environmental factors primarily focus on room conditions including humidity, temperature, and size. The size of the room, although not a significant factor, can influence the ambient temperature in the imaging space. Because thermography is highly dependent on

temperature, the ambient conditions in the room are a key factor for imaging. The ideal ambient conditions listed by the authors range from 18-25 °C, based on likelihood of shivering or sweating. In dynamic cases, the ambient temperatures could cause sweating or shivering, creating additional moisture on the skin surface. When an additional cold stress is applied, the increase in moisture could create further issues and thermal inconsistencies on the breast surface, leading to difficulties in image interpretation and an increase in false diagnosis. In steady-state thermography, the ambient temperature is vitally important, controlling the temperatures of the body and the breast. Letting the body to properly acclimate prior to imaging allows for steady state conditions and thermal equilibrium without subjecting the patient to discomfort from added cold stress. However, the ambient temperature and acclimation period are highly debated among researchers. The table below (Table 6), adapted from Fernandez-Cuevas et al. [98], shows the variation in external conditions for proper thermogram capture for a variety of medical conditions ranging from sports medicine and thermoregulation to diabetes and breast cancer. Finally, the authors discuss the additional room conditions such as humidity and atmospheric pressure affecting chances of perspiration or shivering of the patient.

Table 6. Table adapted from Fernandez-Cuevas et al. [98] showing recommended ambient temperature and acclimation time from various authors.

Authors	Year	Ambient Temperature (°C)	Acclimation Time (minutes)
Chudecka and Lubkowska	2015	25	20
Akimov and Son'kin	2011	21-22	10
Kolosovas-Machuca and Gonzalez	2011	22 ± 1	15
Bagavathiappan et al.	2010	25	5
Merla et al.	2010	23-24	20
Hildebrandt et al.	2010	21.5-22.3	20
Bouzida et al.	2009	24 ± 2	10
Savastano et al.	2009	23.1 ± 0.2	20
Zaproudina et al.	2006	23-25	15
IACT	2002	18-23	15
Ammer	2002	24	15
Ring and Ammer	2000	18-25	10-30
Gratt and Anbar	1998	21-23	15
Uematsu et al.	1988	23-26	20
Devereaux et al.	1985	20.5 ± 0.5	15
Nickoloff	1984	20	10
Gershon-Cohne and Haberman	1968	24	15
Brakemark et al.	1967	18-20	15-20

Individual factors such as age, anatomy, circadian rhythm and more can subtly influence thermal interactions within the body. Circadian rhythm has been explored by several different authors as a potential influencer into *when* a thermogram should be captured. Although there is variation in the outcome of circadian rhythm, the majority of authors agree that there is approved performance in the evenings due to the body's ability to better remove heat loads. Gautherie [19] discusses circadian rhythm in great detail, investigating the rhythms of mammary skin temperature on a group of 26 women. They controlled their eating patterns, sleep, and ambient conditions prior to thermal measurement of growing tumors. The most significant observation during this study is the changes in the breast with tumor. "In 15 cases, the circadian rhythm of skin temperature was

apparently desynchronized on the cancerous breast and replaced by components with periods that did not correspond to any known external or internal cyclic phenomena.” Additionally, they observed changing characteristics of the cancerous breast in the remaining patients although the 24-hour synchronized rhythm was maintained. Additional factors altering thermal imaging involve factors that cannot necessarily be controlled such as blood flow, metabolic rate, and genetics. However, there are controllable extrinsic factors that can be recorded or preempted before thermal examination. Some of these factors include drinking coffee, exercising, wearing coats/scarves/warmer clothing, smoking tobacco, etc. The authors discuss certain medications such as anti-inflammatory drugs or those related to hormonal changes (i.e. birth control) that can alter daily body temperatures, sometimes by as much as 0.6 °C. Additionally, alcohol intake can increase skin vasodilation and blood flow, leading to “an overall increased temperature and a more diffuse thermal pattern than normal” [99]. Other factors that should be monitored or avoided prior to imaging include tobacco, stimulants (caffeine), and food. Finally, the authors discuss other extrinsic factors that are applied to the skin. Ointments, cosmetics, or deodorant can alter the thermal emissivity of the skin, altering the way images appear. All of these factors can influence the thermoregulation of the body or alter the skin surface causing thermal maldistribution and altering collected thermal images. Additionally, not controlling these factors could potentially lead to improper image interpretation or poor accuracy.

There are two positions primarily used in breast cancer screening: prone (on the patient’s stomach) or upright. Methods such as MRI use prone, ultrasound primarily uses the supine position and mammography and thermography generally utilize the upright position. In most ‘traditional’ thermography studies, the patient is seated upright with their arms above their head. The camera or cameras are aimed at the chest and generally take several pictures from different angles.

However, when in this position, there is a significant risk of alterations. The gravitational deformation alters the shape of the breast, potentially changing areas of increased hyperthermia.

A study performed by Jiang et al. [100] explores the breast alterations due to gravity through a digital model. They considered the deformation due to gravity as well as the effects of dynamic thermography. The model considers a normal breast and a breast with an imposed tumor towards the surface. The initial breast geometry is assumed hemispherical and composed of glandular tissue, fatty tissue, and skin. An elastic FE model was used to induce gravitational deformation dependent on body posture. The authors also used elastic breast properties collected from MRI studies. Jiang et al. [100] focused predominantly on the effects of deformation in dynamic thermography studies where a cold stress is applied to the breasts while the patient is upright. The resulting images suggest a maldistribution in temperature, whether a tumor is present or not. The model, seen in Fig. 15, shows two different breasts; one is normal and the other has an imposed tumor on the top of the breast.

They concluded that malignant breast deformation has a major impact on surface temperature and their results will help in optimizing future dynamic thermography studies. This is a particularly important distinction, primarily because most thermography studies (both past and present) utilize an upright imaging position where the patient sits, upright, with arms locked above her head. Many of the thermography studies discussed previously that use scoring systems to determine abnormality may have been inadequate or inaccurate due to the imaging position. The thermal maldistribution through the breast due to the upright position could cause (1) abnormalities in the breast identified as “potential malignancies” or (2) warmer average temperatures in the breast used for comparison to identify abnormality.

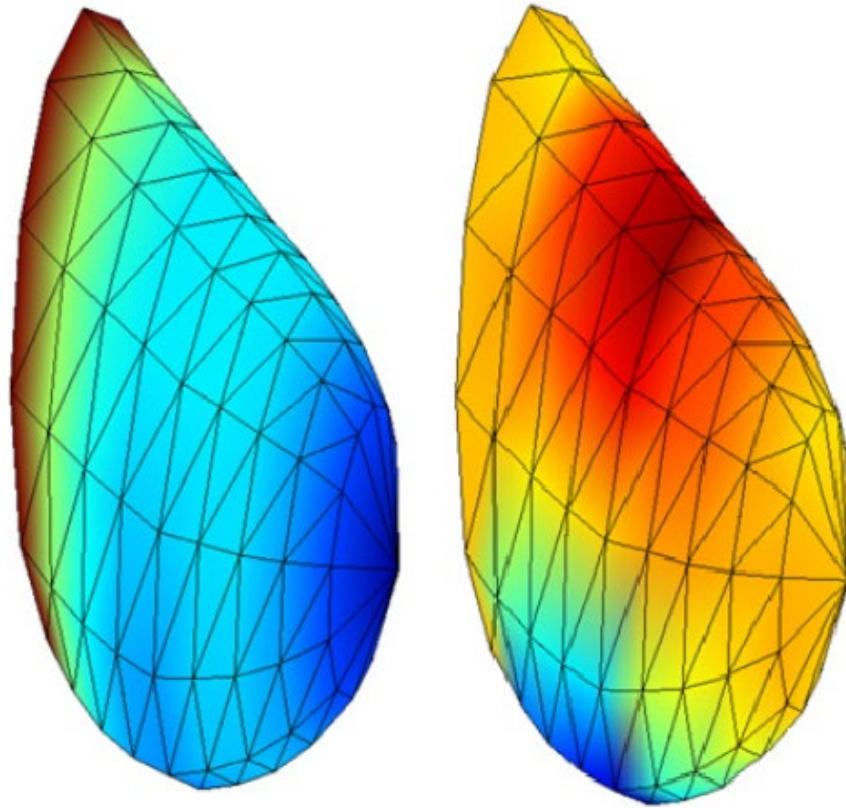


Figure 15. Breast models, elastically deformed by gravity, using thermography by Jiang et al. [100].

Keyserlingk et al. [101] utilized the upright position for IR imaging and captured four images of the patient's breasts for analysis. The use of only four images to ascertain abnormality presents several concerns. Mainly, the position in which images are captured is highly limiting, ignoring any thermal abnormality on the underside of the breast or the inframammary fold. The authors discuss obtaining one image of the 'undersurface' but do not discuss if they are simply capturing a picture at the bottom of the breasts or if the patient moves during imaging to obtain images of the inframammary fold. Any images taken of the 'undersurface' without proper acclimatization could result in increased hypothermia due to the breast touching the chest wall and could skew results greatly. Additionally, four images (anterior, undersurface and two lateral views) may not

be enough to adequately analyze areas of concern. A larger surface image of both breasts may not be able to capture smaller, intricate details indicative of slower growing or smaller tumors. Despite the positive results of this study, the position was a limiting factor in determining the accuracy and adequacy of thermography as an adjunctive screening modality.

Additionally, imaging in the upright position adds unwanted thermal distortions that can negatively impact diagnosis. The area in between the chest wall and the underside of the breast is referred to as the inframammary fold. When a patient is seated upright for imaging, the inframammary fold becomes a pocket of heat. If a tumor is located in the lower part of the breast, the upright position could cause a missed diagnosis leading to further cancer growth. Imaging in the prone position allows the breasts to hang relatively symmetrically, inhibited by gravitational deformation with no concerns of unwanted heat in the inframammary fold.

Despite the attraction of imaging in the prone position, very few researchers [102], [103] have employed this technique. Francis et al. [102] imaged 36 patients in the prone position using a specially made setup, referred to as Mammary Rotational Infrared Thermographic System (MAMRIT). The authors utilize dynamic thermography to cool the breasts and take advantage of the thermal recovery period once a cold stress is taken away. One breast is imaged at a time and hangs freely in an air-conditioned closed chamber. The unit cools the breast sufficiently through free convection to ensure a steady surface temperature. Due to the ease of access of the prone position, the entire breast is imaged in a series of 12 images. The researchers take two sets of pictures for each breast: a precooled series and a postcooled series. The precooled images were taken right when the patient's breast became exposed before any cooling took place whereas the postcooled images were taken after the chamber temperature was reduced by 2-3°. Choosing the prone position allowed for an unimpeded, 360° view of each breast. The authors also discuss that,

due to the imaging position, the warmer regions such as the neck carotid, armpits and inframammary folds do not affect the images, unlike normal thermograms. Because of the prone position, the authors reported higher accuracy. They state that the use of this position allowed for more overall coverage of the breast, leading to better post-processing and analysis. An example of the captured images in the prone position can be seen in Fig. 16.

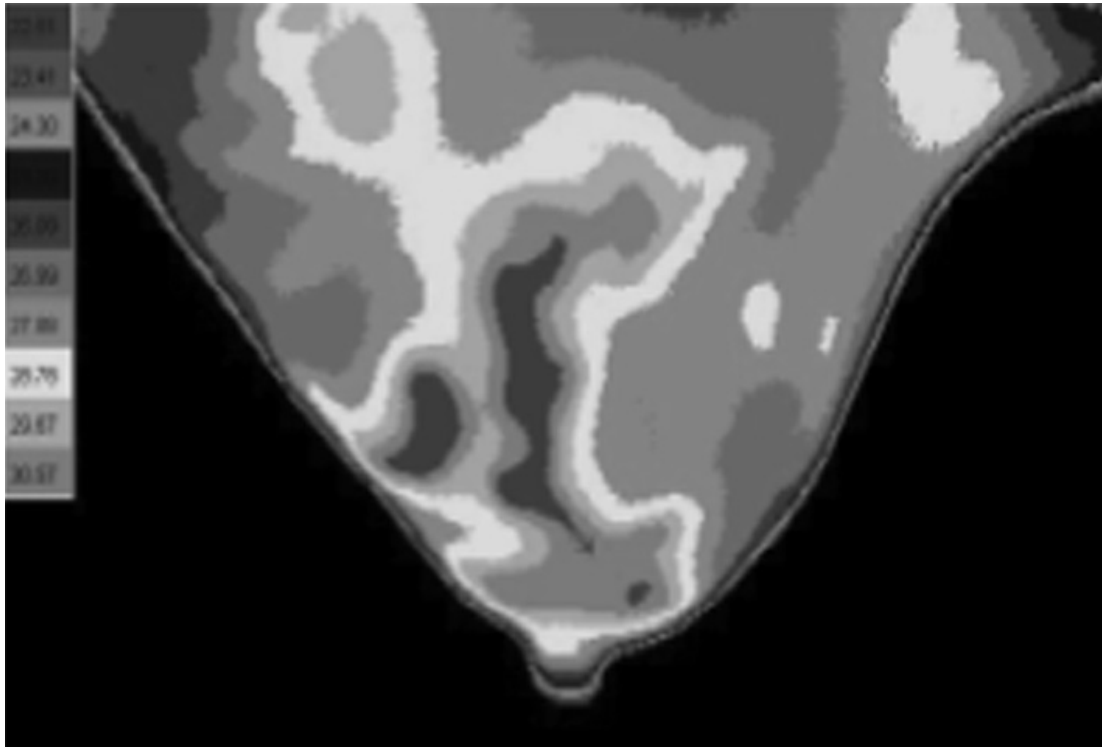


Figure 16. Breast in prone for imaging without gravitational or thermal deformation [102].

Parisky et al. [103] recruited 1,293 subjects, in five different institutions, who underwent breast biopsy due to abnormal mammograms, clinical findings or both. The subject lay prone on an imaging table with both breasts hanging through openings. Each breast was imaged individually while the contralateral breast was shielded from both the forced cool air and imaging using a protective gown. The authors utilized a refrigeration chamber with added cool air for the breast being imaged. They captured images before and during the cooling phase. They use the prone position in order to receive multiple views of each breast, primarily for post-imaging analysis.

Gonzalez et al. employed the prone position and steady-state infrared imaging to image several subjects with biopsy-proven breast cancer. They used the prone position to remove thermal artifacts in the inframammary fold and remove gravitational deformation of the breasts. Additionally, the utilized patient MRI images for validation and tumor characteristics. Because MRI also uses the prone position, direct comparison and validation were simpler to perform with the images in the same position.

2.3.2 Image Interpretation

The methods primarily used to determine malignancy are based in empirical observation or dependent on changes in temperature. The studies involving criteria based on shapes of heating patterns or dependent on the appearance of a hot spot lack scientific basis or validation. The studies that use scoring systems or gradients based on changing temperature do not discuss the involvement of vasculature, scar tissue, or other thermal abnormalities that could alter the detected temperature of the breast surface.

a. Empirical Observation

Several studies and commercial systems have depended on empirical observation for diagnosis. However, human bias can critically alter the accuracy of analysis. Areas they may be visually seen as abnormalities could simply be a part of the breast anatomy or vascularity. The following criteria have been suggested as signs of abnormality:

- Increased heat of areolar area
- Diffuse heat involving a quadrant of the breast, half of the breast or entire breast
- Localized regions of hyperthermia
- Visible vasculature in unusual or asymmetric locations
- An increase in vasculature to a certain area

Many authors have also used observational techniques to determine malignancy without considering quantifiable detection. Collett et al. [104] used a commercial system called the NoTouch BreastScan (NTBS) to screen 121 women with suspicious previous images. The NTBS uses an upright position and dynamic thermography in order to screen. Several images are taken and the NTBS software assigns a score between 0 and 10 dependent on various parameters seen in the resulting image. The software has several options for screening for increased accuracy such as high specificity and high sensitivity. Using both approaches on patient screening resulted in varying sensitivity and specificity results. The NTBS was developed in 2012 by UE LifeSciences Inc. and boasts the “latest advancement in the field of clinical infrared imaging.” However, the accuracy of the system itself is highly debated as many authors report sensitivities ranging from 45.5%-87% and specificities ranging from 48.6%-88.9%. This massive range in performance could account for negative or skewed results. The NTBS utilizes a scoring system, similar to other thermography studies, to calculate thermal gradients throughout the breast and determine suspicion. Similar to other scoring systems used by many authors studying thermography, the scoring systems do not discuss differentiation between tumors and other thermal abnormalities such as veins, scars, etc. Additionally, the system utilizes scoring factors from 1-10 and concludes those with a “green” score between 1-3 are healthy. An earlier stage tumor, slow growing tumor or very deep tumor could give a much smaller temperature profile during treatable stages before becoming much warmer and subsequently more aggressive. Twenty one patients were removed from the study due to inaccurate results such as (1) scan too blurry, (2) portion of image cut off, (3) artifact on breast, (4) poor initial positioning, (5) nonbreast primary malignancy, and (5) biopsy not performed. The authors acknowledge that the approach taken was potentially limiting as the ‘high specificity’ mode provided inaccurate sensitivity data and provided biased results. Due to

negative experience while using NTBS, the authors do not recommend the technology as a viable option for screening. Further, they agree with the Society of Breast Imaging's statement that thermography should not be used. However, the study only considered one commercial software and piece of equipment for study. The authors do not discuss the scientific methodology behind the technology, how malignancy is determined or how the 'thermography expert' operated or diagnosed patients using the technology.

Stark and Way [92] explored the use of thermography using 4,621 women, using mammography as an adjunctive technique for abnormal thermograms. They have termed their method as Aga Thermovision and identified three basic patterns: (1) the avascular (normal without veins), (2) the vascular (normal with visible veins), and (3) the mottled pattern. Their criteria for identifying malignancy are as follows: localized area of heat emission or hot spot, localized increased vascularity, generalized increase in temperature and increased heat of areolar area. They also noted that the correlation between temperature and tumors is less related to tumor size and more related to histologic activity. Out of all the patients imaged, all patterns were seen in all age groups with all different sized breasts. Ultimately, 628 women were identified as abnormal and given mammograms. However, similar temperatures were seen for benign diseases such as fibroadenoma and invasive ductal carcinoma.

b. Temperature Dependent

Rassiwala et al. [105] utilized infrared imaging involved 1,008 women for screening purposes. Initially, the results appear very promising with a high reported sensitivity of 97.6% and a high reported specificity of 99.17%. However, at closer review, the criterion used to determine if a patient tests positive for cancer is disconcerting. The initial patient pool of 1,008 women was drastically reduced to 41 through a process of elimination dependent on the temperature changes

between the contralateral breasts. The patients are screened in the upright position with arms above their head. Several images are taken in the frontal view and from the sides. Commercial software is used to detect the average temperatures throughout both breasts. The temperatures are compared, and suspicion is determined. The temperature scale used to determine suspicion is seen below.

Table 7. Temperature scale and assessments performed in the Rassiwala study [105].

No. of subjects	Thermography	Triple assessments	Remarks
959	$\Delta T < 2.5$	<ul style="list-style-type: none"> • Clinical examination normal 	Negative for malignancy
8	$\Delta T > 2.5$ but < 2.9	<ul style="list-style-type: none"> • 5 patients had suspicious lump on clinical examination. • All 8 mammograms were normal. • Biopsy confirmed fibrocystic disease in 5 patients.(fibroadenosis-4,fibroadenoma-1) 	Negative for malignancy
41	$\Delta T > 3$	<ul style="list-style-type: none"> • All patients had clinically palpable lump on examination. • 38 patients had abnormal mammography Biopsy:25 patients had Infiltrating Ductal Carcinoma • 14 patients had Ductal Carcinoma in situ • 1 patient had phylloides tumour • 1 patient had inflammatory carcinoma of breast 	3 patients had normal mammography but were found to be infiltrating ductal carcinoma.

The patients who were determined malignant were then tested for breast cancer using clinical, radiological, and histopathological examinations and malignancy was verified. However, there are several flaws with the process used to identify a region of interest. The authors discuss the temperature gradients above but do not explicitly state their method of analysis. The values do not appear as gradients but instead are fixed temperature differences. It appears that these temperature differences are calculated by identifying regions of interest on the suspicious breast and comparing the same region on the contralateral breast. However, the authors fail to mention how veins or other areas that could potentially influence thermal profiles are analyzed. Further, the authors do not discuss the process of temperature changes due to smaller or deeper tumors. A temperature change of 2°C could have signified a smaller tumor but instead, these patients were determined “healthy.” These patients received a clinical examination but did not have any other further testing or a mammogram. Therefore, the presented results used to calculate sensitivity and specificity are skewed towards those with large temperature differences. Larger temperature differences generally signify a larger tumor or a more advanced tumor. Ignoring any other smaller temperatures could

mean missing cancer at the earliest, most treatable stages. Further improvements are needed in processes used to identify and differentiate malignancy from other thermally altering factors. Additionally, more universal detection criterion is needed for accuracy and repeatability.

c. Scoring Systems

Some studies have looked at combinations of temperature variations and empirical observations to assign a “score” for classification and diagnosis. Several authors [101], [106], [107] have used the Ville Marie IR Grading System. The system uses several different parameters and corresponding descriptors. A comprehensive table of these factors can be seen in Table 8. The Ville Marie Grading System, used by Keyserlingk et al. [101], [108], identifies abnormal temperature signatures as well as various factors that identify cancer. Pertinent clinical information is examined, and both the breasts are observed for symmetry. For diagnosis, the Ville Marie IR Grading System was used to determine existence of abnormality. If significant asymmetry or temperature differences are present, the patient is assigned a number (IRI1 – IRI5). The resulting numbers are defined as the number of abnormal signs and the respective abnormality.

Keyserlingk et al. [101] examined 128 patients with an initial breast cancer diagnosis. Their scoring system relied on clinical information, comparison between both breasts and comparison of current images with previous images. In order to be considered abnormal, the presence of at least one abnormal sign was necessary. The authors discuss, at great detail, their results, and the statistical significance of their imaging technique. Overall, they achieved a sensitivity of 83% and compared all findings with mammography and clinical evaluation. The use of a scoring system provided an increase in suspicious areas deemed ‘abnormal’, especially in some patients with nonspecific mammograms. The authors had a limited screening population but produced adequate results for the technology, warranting further research. Further discussion on the imaging positions

they utilized are discussed in section 5. Keyserlingk et al. presented a well-rounded study with details of tumor pathology and in-depth comparison between infrared imaging, mammography, and clinical examination. Utilizing medical validation in determining the validity of a new method is crucial to understand impact and accuracy.

Table 8. Table adapted from Keyserlingk et al. [101].

Abnormal Signs	<ol style="list-style-type: none"> 1. Significant vascular asymmetry 2. Vascular anarchy consisting of unusual tortuous or serpiginous vessels that form clusters, loops, abnormal arborization or aberrant patterns. 3. A 1°C focal increase in temperature (ΔT) when compared to the contralateral site and when associated with the area of clinical abnormality. 4. A 2°C focal ΔT versus the contralateral site 5. A 3°C focal ΔT versus the rest of the ipsilateral breast when not present on the contralateral site 6. Global breast ΔT of 1.5°C versus the contralateral breast
Infrared Scale	<p>IR1 = Absence of any vascular pattern to mild vascular symmetry</p> <p>IR2 = Significant but symmetrical vascular pattern to moderate vascular asymmetry, particularly if stable</p> <p>IR3 = One abnormal sign</p> <p>IR4 = Two abnormal signs</p> <p>IR5 = Three abnormal signs</p>

In 1980, Gautherie and Gros [94] published a 12-year clinical study involving approximately 58,000 patients. The first contact with each subject involved recorded history, physical examination, mammography, ultrasound, and thermography. If core needle biopsy was needed, a histologic report was obtained. They classified their subjects based on five separate stages (Th I – Th V) where Th V is the most suspicious. This scoring system is dependent on varying temperature factors as well as probability of cancer. 1,527 women were identified as Th III, meaning their thermograms were suspicious but inconclusive. Out of these patients, 51% had no abnormal

findings, 30% had benign masses and the remaining 18% had biopsy-proven malignancy. This system is similar to BI-RADS (Breast Imaging Reporting and Data System) used primarily after ultrasound or mammogram to 'grade' someone based on identifying factors, histopathology, and patient history. However, similar to BI-RADS, the scoring system has many flaws. BI-RADS is subjective and dependent on the consulting radiologist. Similarly, the Th I – Th V system provides a subjective screening value for further diagnosis. This can clearly be seen in their definition of patients diagnosed as Th III. Firstly, the classifications of the scoring system are up to the thermographers interpreting the images. Similar to other diagnostic techniques, depending strictly on subjective observation will inevitably lead to misdiagnosis. The authors also state that the thermograms initially assumed as malignant but proved benign have no explainable basis. Although the authors were pioneers in this field, the analysis provided to determine diagnosis with a bias scoring system has proved faulty.

Wang et al. [107] utilized statistical factors to determine accuracy of a scoring method used to malignancy. They screened a population of 276 women with suspicious mammographic findings. Consulting radiologists were used to evaluate the corresponding images and assign a score ranging from IR1 – IR5. Although they utilized a scoring system for diagnostic purposes, they introduced biostatistical characteristics to further analyze the thermograms and diagnostic accuracy. Using statistical software to find the correlations of diagnostic IR (infrared) signs, they categorized lesions as malignant or benign. Additionally, they used a univariate logistic regression model and a multivariate regression model to compare the individual IR signs with the final disease status. The authors did see strong correlations between malignancy and higher IR score but discovered that the scoring system they used (IR1 – IR5) can be varied and highly dependent on the existence of vasculature. Utilizing biostatistics, Despite the issues with scoring systems for initial analysis,

they reach the conclusion that combining thermography with additional modalities will provide a more convincing diagnostic result. Similar to other studies, the consulting radiologists who interpreted the images were aware of the lesion site and size (discovered through conventional screening methods) prior to analyzing the infrared images.

Scoring systems could potentially be beneficial for screening purposes to determine whether more expensive techniques are needed for diagnosis, particularly as an adjunctive modality. However, using the observational process to provide the score delivers inconsistent results. If the scoring system is used in the future for screening, it should depend on computational methods rather than bias human interpretation.

d. Computational and Mathematical Methods

Francis et al. [102] utilized dynamic thermography in the prone position to image twenty-four healthy women and twelve women with cancer. Using their method, Mammary Rotational Infrared Thermographic System (MAMRIT), they extracted abnormal features and textures within the infrared image to determine abnormality. They extracted statistical features such as mean, variance, skewness, and kurtosis from each abnormal region of interest for further analysis. The authors captured images of the breast before the cold stress is applied and after in order to compare the statistical image features. While the authors are using statistical image features to determine abnormality, they are additionally focused on non-biased analysis. The system first crops the breast image and identifies a Region of Interest (ROI). It then utilizes an automatic detect system to extract features and determine abnormality. They report sensitivity and specificity for pre-cool and post-cool conditions using both statistical features and texture features. They calculate higher sensitivity and specificity for precooled conditions, using texture features as performance measures for analysis. The authors approach the post-processing and analysis of their images from

a scientific, computational, and mathematical standpoint. The accuracy achieved, with technology that has already been surpassed with new methods, shows the great potential of thermography without the bias of human interpretation.

Ng and Kee [109] analyzed thermograms using artificial neural networks (ANN) and different statistical methods for their study. Using a combination of computational and mathematical methods is meant to analyze large amounts of temperature data for more rapid diagnosis of malignancy. The authors collected data from 90 breast cancer subjects, selected at random, to test their diagnostic process. Specified thermal characteristics were compiled including mean, median and modal temperatures. First, linear regression (LR) correlates between observable variables in thermographic images and the actual health status of the patient (classified through mammogram and biopsy). A radial basis function network (RBFN) is then used to produce the desired outcome of 'positive' or 'negative'. Finally, receiver operating characteristics (ROC) is used to measure statistical significance of the produced results including sensitivity, specificity, and accuracy. To conclude the study, the authors state that combining ANNs with biostatistics and thermographic advancements could lead to a viable adjunctive screening technique. Determining precise tumor diameter and position is the next step to advancing this method further.

EtehadTavakol et al. [110] employed machine learning to train a program for thermogram image processing. They used 32 collected images (9 malignant, 12 benign, 11 normal) from various thermography centers around the United States and Australia. Using a Canny edge detector, they found the edges and boundaries of the breasts. The algorithm then defines regions of interest dependent on clusters of pixels correlating to hotter areas. The features are extracted and a fast Fourier transform (FFT) is used to differentiate bispectrum of the images. The defining features and compared with the pathology of the images for classification. Finally, the resulting images and

classifications are used to train an image processing system for abnormality detection and rapid diagnosis. Additionally, the authors discuss that the methodology can be mass employed for preliminary thermography screening.

2.3.3 Scientific Validation

A letter published by the Food and Drug Administration (FDA) in 2019 [111] warned against the risks of using thermography alone as a breast cancer screening technique. There are many thermography clinics around the country that screen for multiple afflictions without scientific proof of accuracy.

Although thermal imaging holds great promise, more research is needed in order to validate this modality as a specific and sensitive detection method. Despite the warnings of the FDA, there are individual boutiques that have popped up throughout the United States, offering full body thermal scans ranging from \$ and breast scans ranging from \$200 - \$350, screened by a Board Certified Clinical Thermologist. The breast exams involve a baseline thermogram with an additional screening at three months. If asymmetry is present, further screening is warranted. Otherwise, an annual thermogram is recommended. However, an asymmetrical baseline could be the result of maldistribution of heat or a change in hormones [112]. Some tumors that are more ‘slow-growing’ or do not have an extensive vascular network may be missed. The correlations developed could potentially be flawed but are ideally compared with other methods to ensure accuracy. Similar to previous studies, the patient is seated upright with their arms above their head. This causes gravitational deformation and an increase in hyperthermia in the inframammary fold. Additionally, any changes in heat from tumor closer to the underside of the breast will be inaccessible and more difficult to detect.

The warnings from the FDA against thermography as a valid screening technique lie within these centers. The core technology associated with Digital Infrared Thermal Imaging (DITI) is not approved as a standalone technology and not recommended for as a standalone screening method. While some women use DITI exclusively for their breast screening, this is not recommended by the American College of Clinical Thermology (ACCT). They additionally report that when used as an adjunct to mammography, sensitivity is increased. ACCT discusses the value of DITI or other thermographic tests and the comparisons of mammography and thermography as comparing tests of physiology and anatomy. Although the scientific basis used to analyze the breast are different for each screening modality, comparing the accuracy and statistical significance assists with medical choices.

The International Academy of Clinical Thermology (IACT), founded in 1983, is a non-profit organization dedicated to providing resources on thermography for both the healthcare community and general public. The IACT requires that all candidates looking to become Clinical Thermologists or Thermographic Technicians are qualified health care providers with a license to diagnose pathology [113]. The recommended education guidelines put forth by the IACT involve training courses, formal classroom hours and practical imaging experience. There are three qualified positions: (1) Certified Clinical Thermographic Technician, (2) Certified Clinical Thermologist and (3) Breast Thermologist. Recommended courses for certified clinical thermographic technicians involve basic thermal imaging principles, patient management, laboratory and imaging protocols and practical imaging experience. For clinical and breast thermologists, the list expands to include anatomy and physiology, pathophysiologic processes and image analysis and interpretation. The training required to work in a center does not account for the changes in technological improvement and screening process. In fact, the standards and

protocols in clinical thermographic imaging listed on their website were last updated in September 2002 [114].

Another organization, the Professional Academy of Clinical Thermology (PACT) have developed a training course for thermography training that involves a 12-hour online intro course, specialty training for \$399 (certified technician, neuromuscular thermologist, full body thermologist and breast thermologist), a 500-page manual, and a certification exam. PACT also offers interpretation services, analyzing images with three separate interpreters within seven days. For full body scans, they report on many bodily diseases that create thermal abnormalities. These include the following: breast cancer screening, fibrocystic breast ratings, cerebrovascular function, abdominal inflammation, thyroid function, nerve issues, localized inflammation, arthritis, and vascular conditions [115].

All three of these organizations, ACCT, IACT and PACT offer some form of certification to perform and interpret thermograms and guide thermologists in best practices. However, with constant changing technology, the importance of continuing education is vital. The ACCT programs require continuing education credits in order to maintain certification. The focus of these different organizations is to train thermologists on current thermography technology and interpretation. But if the previous methods of analysis are flawed, additional training will only propagate the problem. Scientific validation using techniques that are known to detect (such as mammography, ultrasound, or MRI) are key to refining thermography as an adjunctive technique.

2.3.4 Thermal Biomarker Classification

The Hallmarks of Cancer [14], [15], discussed above, involve factors that could potentially influence hyperthermia. Inducing Angiogenesis – Angiogenesis is a normal process that occurs in the body to grow blood vessels for continued cell growth and production. Cells need oxygen and

nutrients from blood vessels in order to survive. Cancer cells are also able to create new blood vessels in order to carry adequate oxygen and nutrients to the abnormal cells for continued growth and replication. Tumor-Promoting Inflammation – There have been many studies showing that inflammation can lead to cancer development. More chronic inflammatory issues such as infections, obesity, smoking, alcohol consumption, etc. are all potential risk factors linked to cancer development through inflammation.

Although there are many factors that affect how cancer cells grow and replicate, few of these principles are hypothesized to contribute to hyperthermia. Two large factors that would allow for successful infrared imaging include inducing angiogenesis and tumor-promoting inflammation. Angiogenesis is a well-studied phenomenon within the body, both during normal cell growth and cancerous cell growth. The increase of vasculature to a growing tumor creates an area of hyperthermia. The increased metabolism in a tumor can also cause localized temperature increases. Additionally, certain biological factors such as hormonal receptors or cancer type could potentially alter tumor growth within the system. Understanding the underlying cause of increased hyperthermia in tumors can assist with detection. Infrared imaging has the unique ability of capturing thermal activity in breast tissue resulting from a tumor. Thermal activity, characterized as thermal biomarkers, include cellular metabolism, increased vascularity due to angiogenesis, and increased blood perfusion which create areas of increased hyperthermia. Gautherie [19] initially presented a model, described above, to compare tumor doubling time with respective metabolic activity. He also explored the effect of vasculature on the heat transfer properties in the breast (effective thermal conductivity) when a tumor is present.

Developing these correlations cultivates a scientific basis in infrared imaging that could alter the negative reputation of the technology. Currently there are no studies comparing the metabolic

activity of growing tumors with the tumor biology. However, developing correlations is vitally important in order to understand the correlative nature between tumor diameter and metabolic activity. Some tumors may be smaller and grow more aggressively while others, considered “cold tumors” have low metabolic activities resulting in smaller temperature changes [26]. In the following sections, thermal biomarkers are discussed as potential factors for classification of different types of cancer.

2.4 Objectives

Based on the previous work performed and discussed in the literature review, many components were identified to determine the efficacy of steady-state infrared imaging (IRI) and address research needs. This dissertation addresses several key factors involving the study of IRI as an adequate adjunctive screening technique to detect breast cancer. In order to effectively evaluate this technology, many factors must be considered including bodily heat and mass transfer. The specific objectives of the proposed work are as follows:

1. Develop steady-state infrared imaging (IRI) as an effective breast cancer screening technique.

At present, there is no easily reproducible, reliable low cost screening method available for detecting cancer in breasts with dense tissue. The success of thermography in previous studies has been limited due to (i) lack of standard protocols during clinical screening [116] and (ii) lack of thermal sensitivity of IR detectors to capture subtle temperature variations [5]. The steady-state IRI method discussed below relies on the thermal characteristics (metabolic rate, neoangiogenesis) of a tumor, and thus is highly complementary to mammography

in cancer detection. Additionally, this project has identified the tumor in terms of its position on a clock, quadrant of the breast, distance from the nipple, and depth. This information is important in localizing the tumor for further management such as biopsy or surgical resection and in correlating the findings with those of other imaging modalities.

2. Establish clinical protocols and patient process for adequate screening using IRI.

Currently, there are no consistent methods or standards used for clinical thermography. One major goal of this study was to develop consistent protocols for patient observation and imaging. This includes imaging process, patient handling, informed consent, and data management. Additional factors needed to evaluate IRI include patient population, image interpretation, and scientific validation. The details of this study are presented below along with extensive future recommendations for the continuation of steady-state IRI.

3. Identify factors that influence heat production and develop thermal biomarker classifications.

While optimizing infrared cameras and patient protocols are vital in advancing thermography as a screening technology, studying heat movement from the tumor through the tissue will lead to a better understanding in the underlying heat transfer. An in-depth discussion on the thermal factors affecting heat movement in the body is presented. Additionally, a new classification system for thermal biomarkers present within the body, dependent on different forms of cancer is discussed.

Chapter 3: Approach

3.1 Overview

The work performed in this study involves two different aspects: clinical and numerical. Through a collaborative study with the Rochester General Hospital, patients have been recruited and imaged using steady-state infrared imaging. The collected images are then analyzed, and the regions of hyperthermia associated with malignant tumors are studied. The numerical portion, discussed heavily in Chapter 4, was the groundbreaking work of my research partner Jose Luis Gonzalez-Hernandez [60]. Together, the overall detection algorithm and the IRI images were used in validating the IRI steady-state algorithm for detecting breast cancer. The detailed approach is discussed below.

3.2 Clinical

Steady-state Infrared Imaging (IRI) is unaffected by tissue density and has the potential to detect tumors in the breast by measuring and capturing the thermal profile on the breast surface induced by increased blood perfusion and metabolic activity in a rapidly growing malignant tumor. In this new clinical approach, subjects with biopsy-proven breast cancer are imaged with steady-state IRI in the prone position and results are compared with preceding MRI images. The prone position is able to provide a thermal profile of the entire breast without any abnormalities from the inframammary folds.

The clinical protocol, design and process have changed throughout the duration of examination. The first is classified as IRI-MRI and the second is classified as IRI-Mammo. They are discussed at length below. All clinical work was conducted at the Rochester General Hospital (RGH) in

collaboration with the Rochester Institute of Technology (RIT). The study began in March 2018 and is ongoing.

3.2.1 Ethical Considerations

All personnel working on the project undergo human subjects training (Good Clinical Practice and Good Documentation Practice) and complete Collaborative Institutional Training Initiative certification. Additionally, all patient data is deidentified prior to transfer to RIT. The study is conducted in compliance with the protocol, 21 CFR 50 Protection of Human Subjects, 21 CFR 56 Institutional Review Board (IRB), Good Clinical Practice (GCP) as set forth in the International Conference on Harmonization Guidelines of GCP (ICH E6), and Health Insurance Portability and Accountability Act (HIPAA). Patients are assigned a number, starting with 001 and increasing incrementally. Because there were two separate protocols with two different patient populations, we have designated patient files as 001a and 001b.

3.2.2 Clinical Study – IRI-MRI

i. Patient Population

The first half of this study required MRI images that we could use for scientific validation and 3D model generation. Because of these qualifications, we recruited patients who have a breast cancer diagnosis and require an MRI in their clinical process. Although many women do not require an MRI prior to surgical resection, it was vital to participate in this study. An MRI is generally recommended if there is a possibility of cancer spread throughout the breasts that did not appear on a mammogram. Sometimes the MRI images would change a lumpectomy to a full mastectomy, depending on the type of cancer and amount of spread present.

ii. Patient Flow

MRI examination was recommended by the consulting breast surgeon on the project and the women were referred through her. Once a list of potential patients was generated, the clinical department contacted them for interest. On average, we screened 1-2 patients per month.



Figure 17. Screening and diagnostic imaging patient flow.

The patient imaging process generally looked like the one in Fig. 17. First, a mammogram is performed on an annual basis, after a suspicious physical examination or because of higher risk. Next, an additional mammogram is performed observing the area of suspicion for diagnosis. A core needle biopsy is then performed using ultrasound to find the area of suspicion. A report is generated detailing the extent of cancer and pathology of tumor. An MRI is performed in the prone position, recommended by the consulting breast surgeon. Images are stored on a disc and deidentified prior to transfer to RIT. Infrared imaging is conducted in the prone position, on the same day as MRI, capturing 8-24 images around the circumference of both breasts. Finally, the patient undergoes surgical resection by lumpectomy (removing the tumor and surrounding areas) or mastectomy (removing the entire breast).

Patients were recruited for IRI on the day of their MRI exam. The patient would arrive at the hospital for the MRI, proceed with the 45 minute – 1-hour long exam, and then receive IRI screening. Contrast material and inflammation from biopsy were considered problematic for this clinical study. However, given the ideal patient population, their potential effects were ignored. Prior to IRI, patients were given a few minutes for water and snacks to recover. Any tape markers

on the breast used for biopsy or surgical purposes were removed. After the patient was screened, they were brought back to the entrance of the hospital.

iii. Clinical Protocol

An Institutional Review Board (IRB) approved protocol has been developed for recruiting patients and acquiring IRI images. A copy of the IRB-approved protocol and consent form are seen in the appendix. As I am not a medical professional, the patients are consented by one of the RGH Research Coordinators in the clinical department. The protocol briefly describes the IRI technology and modeling process in layman's terms. This includes a step-by-step detailing of how their images and data are transferred to RIT and utilized. Additional details include study duration, study population and data collection techniques.

The risks and benefits are discussed with the patient prior to examination. The technology does not involve any contact with the patient and does not induce any radiation. Additionally, the treatment plan for each patient is not interrupted or influenced by this study. The only foreseeable risk involves the prone position; some patients are uncomfortable lying in this position for longer periods of time. In fact, we have had women complain of back pain or rib pain on the imaging table. Extra pillows and blankets are available to those who are experiencing discomfort. Furthermore, there are no direct benefits related with this examination. At the most, patients are participating in a study with a potentially beneficial future technology. Once the patient has asked any questions and feels satisfied with the terms and conditions, they sign and date the form.

iv. Patient Questionnaire

The first portion of the questionnaire involves a line of questioning corresponding to the patient's activity prior to the examination. The temperature of the room, the weather outside, hormonal

influences and factors such as coffee/alcohol consumption, smoking habits, exercise prior to examination, etc. [18–20] can potentially influence the surface temperature distribution. These include the following:

- Have you sunbathed within five days prior to the exam?
- Have you used lotion/cream, makeup, deodorant on the breasts on the day of the exam?
- Have you exercised today?
- Have you smoked or had alcohol today?
- Have you had coffee or tea today?
- Were you wearing tight-fitted clothing?

The latter portion of the questionnaire asks for details of the patient’s screening and diagnostic history including details of tumor size, stage, and location. This portion is filled in after biopsy and MRI are completed.

v. Clinical Setup

The initial imaging room was a small patient room in the hospital, approximately a 10-minute walk from the MRI imaging offices. The room had a small curtain for privacy and large windows. The windows posed a risk for reflection on the breast surface, potentially causing issues during imaging. Additionally, the fluorescent lights and lack of ambient control introduced additional concerns.

The table for capturing IRI images was a retrofitted massage table. Because the clinical screening room was actually a doctor/patient examination room, it was key for the table to be easily moved. The massage table could handle about 300 lb and was short enough for a simple step stool. The legs folded in and the table could fold in half, allowing for easy transport. Four 2-inch blocks were

purchased to raise the bed. A 9-inch hole was cut in the table for the breast to hang down and a pillow was provided for comfort. Several hospital sheets were donated, and a hole was cut in each to ensure the breast could hang in the hole, unimpeded. Finally, hygienic paper was placed on the bed and taped down. Images of the bed can be seen in Fig. 18 and Fig. 19 (a) and (b).



Figure 18. Portable massage table retrofitted for infrared imaging.

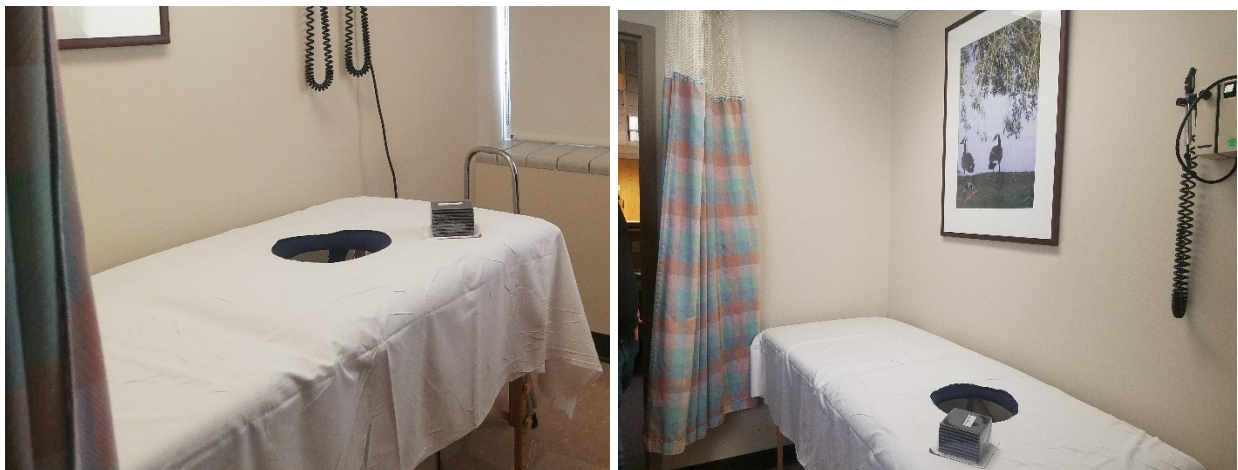


Figure 19. IRI screening table in the screening room with curtain.

However, the sturdiness of the table was a big concern. Unfortunately, the massage table was very thin and could only support a maximum of 300 lb. One patient who began to get on the bed almost tipped it over, and there were times when ‘cracking’ was heard when the bed was laid on. These are obviously major concerns, especially with patients in a delicate mental, emotional, and physical state. Additionally, the distance from the IRI camera and the bed was not enough to allow for sufficient focal distance. The bed needed to be stronger and needed more height. The table was redesigned to address these issues.

The details of the preliminary camera mount are shown in Fig. 20(a). The resolution of the IR camera is 640×512 pixels, with a thermal sensitivity of 0.02°C (FLIR SC6700). The camera rotates on a stand below the table and hole. Eight images are taken, beginning at the head, separated by 45° looking up at 25° angle to vertical. The angle and focus of the camera vary based on the breast size of the subject being tested. Larger breasts will hang lower in the hole requiring a different focal distant compared to smaller breasts. Eight images are taken for each breast, beginning at the head, separated by 45° looking up at 25° angle to vertical, as seen in Fig. 21.

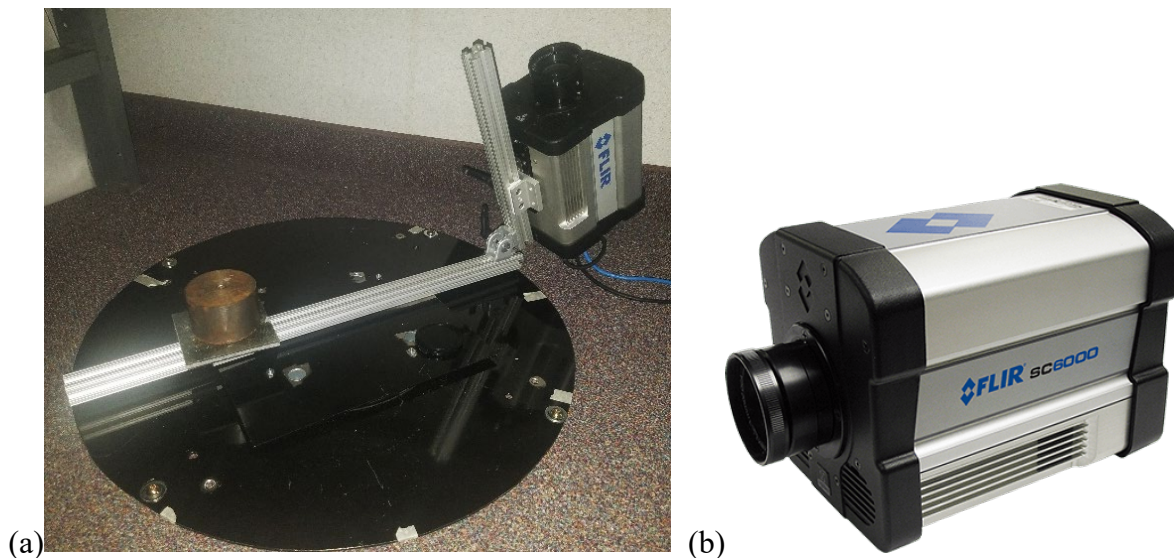


Figure 20. (a) Camera table setup with turntable and (b) FLIR infrared camera used for imaging.

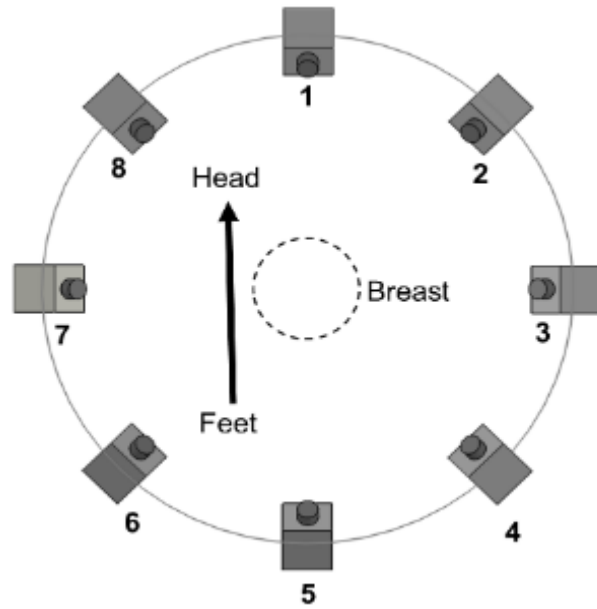


Figure 21. Camera positions for 8 views of breast in prone.

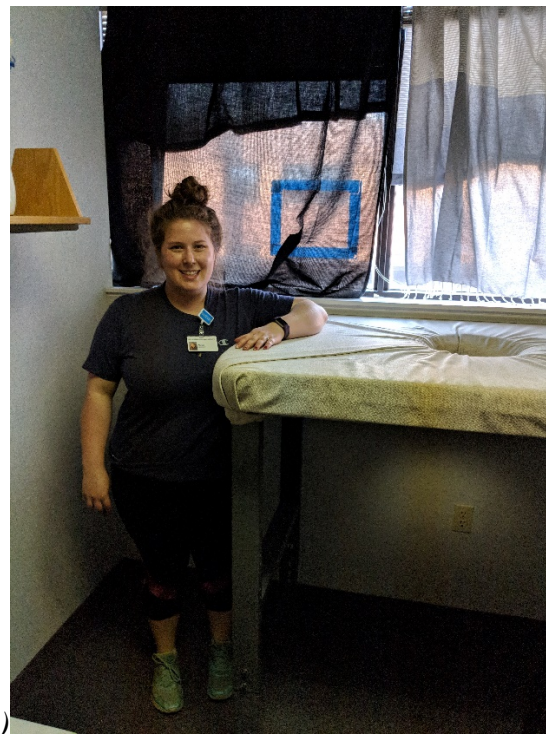
The new table for capturing IRI images is a sturdy retrofitted table (2' × 7') with a 9" hole for breast imaging. A 2-inch layer of foam is placed on top for comfort and fabric was added to hold the foam in place. An image of the lab table with added foam can be seen in Fig. 22. The bed was raised considerably, allowing for a 4-foot height between the camera and breast instead of a 2-foot height. Because of this adjustment, a larger stepstool was needed. A sturdy staircase with railing was added to help individuals get on top of the bed. The stool can handle 500-lb and the railing is welded together to ensure no movement during ascension. Images of the staircase prior to added handle and an example of the height of the bed (myself standing next to it) are seen in Fig. 23 (a) and (b). Finally, a black curtain was added around the edge of the table to hide the camera equipment and provide a consistent backdrop and ensure no reflection or stray thermal artifacts during imaging. The same sheets were added on the bed and a layer of disposable paper is used for hygienic purposes. The imaging table with staircase can be seen in Fig. 23(a) and Fig. 24.



Figure 22. Image of table with 2-inch foam, prior to covering with fabric.



(a)



(b)

Figure 23. (a) Staircase with table, prior to addition of railing and (b) myself standing next to table to show examples of height.



Figure 24. Images of the imaging room with the table design, sturdy staircase, and black curtain along the edges of the table.

vi. Data Collection

For this study, we collected the MRI images of all patients on a deidentified disc, a patient questionnaire with the questions above, infrared images and additional medical information. This involves the following information:

- Age
- Date of birth
- Initials
- Breast density

- Bra size
- Breast cancer details including size and location of tumor, type and stage of cancer, and reports from ultrasound, mammogram, and MRI

3.2.3 Clinical Study – IRI-Mammo

i. Patient Population and Patient Flow

The patient population for the second portion of the study is significantly different. After the process was scientifically validated (discussed further below), the population was adjusted for several reasons. Firstly, the addition of contrast material and screening after biopsy was cause for concern. Therefore, screening needed to occur prior to these activities. Second, we had already collected patients with biopsy-proven breast cancer and had proven that we could pinpoint the tumor. The obvious next step in determining the specificity of the technology was recruiting patients without known breast cancer. However, the technology is not yet at a stage to recruit from the general population. Finally, we still want to be able to scientifically validate the images we are collecting. This means we would need images of the breast from a source known for imaging success.

We therefore decided to collect patients classified as BI-RADS 3, 4, or 5 who were receiving a diagnostic mammogram. The results from the IRI studies are not used in clinical decision making. We did consider the ethical implications of this policy. All of our subjects will either be undergoing standard evaluations such as ultrasound or biopsy (BI-RADS 4 and 5) or monitoring (BI-RADS 3). It remains possible that some subjects will have a thermal profile suggestive of cancer but will be classified as BI-RADS 3 and therefore not undergo immediate intervention, though close follow-up will be planned. It is possible that IRI will find suspicious thermal profiles in subjects without cancer to avoid causing unnecessary distress. We believe this approach is acceptable since

all subjects will be getting the current standard of care and no clinical benefit or harm will ensue from the IRI based study. This is one of the reasons we have chosen not to pursue more “normal controls” with BI-RADS 1 and 2 mammogram readings. These would present a more challenging ethical dilemma on how we would handle the results since these subjects would not be followed as closely.

Using this population, we were able to collect patients with suspicious masses, many of which are later determined as benign, prior to biopsy. This reduced the risk of additional thermally altering factors from biopsy or contrast. Additionally, we can use the screening and diagnostic mammogram images for validation of our programs. The new patient flow can be seen in Fig. 25.



Figure 25. New patient flow for IRI-Mammo study.

ii. Clinical Protocol

No changes were made to the clinical protocol or process in which patients were consented.

iii. Patient Questionnaire

In addition to the questions from the IRI-MRI patient questionnaire, we added several questions about biological influence on bioheat. This includes the following:

- Is the patient menstruating or menopausal?
- Is the patient on any type of hormonal birth control?
 - If yes, what product?

- Has the patient had breast cancer before?
- Has the patient had breast surgery before?
 - If yes, which surgery: lumpectomy, mastectomy, breast reduction, breast implant, other

Based on other studies that show normal heat transfer throughout the body, especially during menstruation or menopause, these questions are vital to the further development of this technology. This could involve adapting the technology to account for hormonal changes or selectively imaging patients during more regular time periods.

iv. Clinical Setup

The clinical setup of the table has remained the same for the new study. However, the camera setup has been upgraded. More images were desired, especially from a horizontal and vertical view. Therefore, the camera setup needed much greater modularity. The three positions can be visualized in Fig. 26 (a), (b) and (c). The table can spin 360° for a full view of the entire breast circumference, the arm holding the camera can slide up and down and rotate a full 360° , and the camera can tilt 180° , if desired.

Additionally, in order to have a more modular setup, the camera needed to be significantly smaller and lighter. The updated camera is an ICI 8640, with similar properties to the FLIR camera. However, the size and weight are significantly smaller. A comparison of the FLIR camera (IRI-MRI) and ICI camera (IRI-Mammo) can be seen in Table 9. The actual camera and camera stand setup can be seen in Fig. 27 (a) and (b). Because the camera is moved to the table in position 2 (Fig. 26 (b)) to obtain a horizontal view, the camera stand has to match the height of the table. Further iterations of this clinical setup will involve lowering the table and camera stand to ensure

better patient safety and easy getting onto the bed. Finally, an increase in images are captured for smoother model generation. Twenty-four images are captured at each position with an additional image of the breast straight-on (a total of 29 images). A schematic of this can be seen in Figure 28.

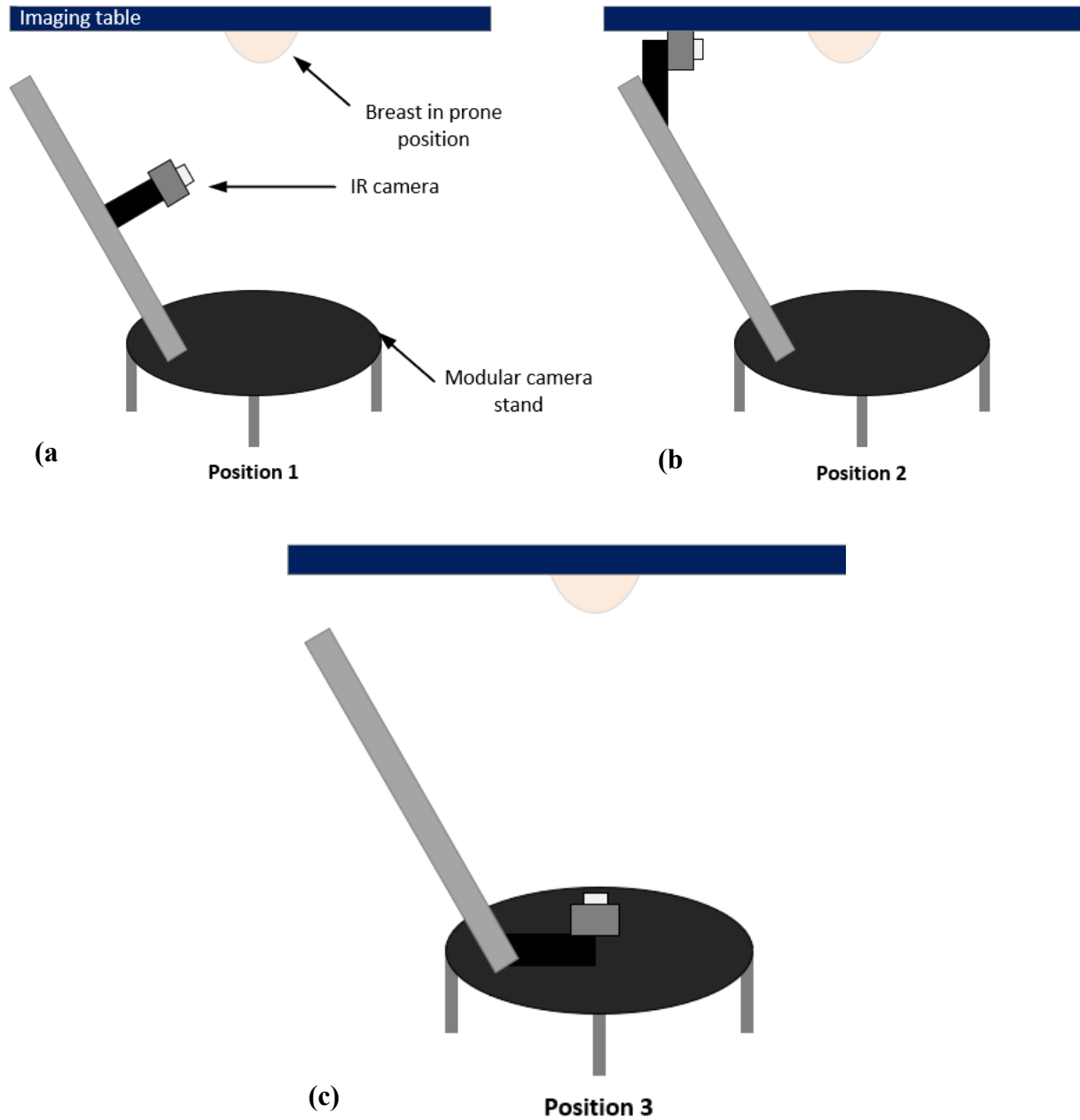


Figure 26. (a) Camera observes the breast at an angle similar to IRI-MRI study, (b) camera tilted to observe the breast horizontal, and (c) camera tilted to look straight up at the breast.

Table 9. Comparison of major factors impacting imaging with the IRI-MRI FLIR camera and the IRI-Mammo ICI camera.

	FLIR (old)	ICI 8640 (new)
Temperature Range	-20°C to 50°C	-20°C to 120°C
Pixel Resolution	640 x 512	640 x 512
Accuracy	±1°C	±1°C
Dimensions	8.6 × 5.64 × 6.21 inches	1.7 x 1.5 x 1.5 inches
Weight	10 pounds	74.5 grams
Pixel Pitch	15 μm	17 μm
Spectral Band	7.5 μm – 10.5 μm	7 μm – 14 μm



Figure 27. (a) Modular camera stand and (b) ICI 8640 camera.

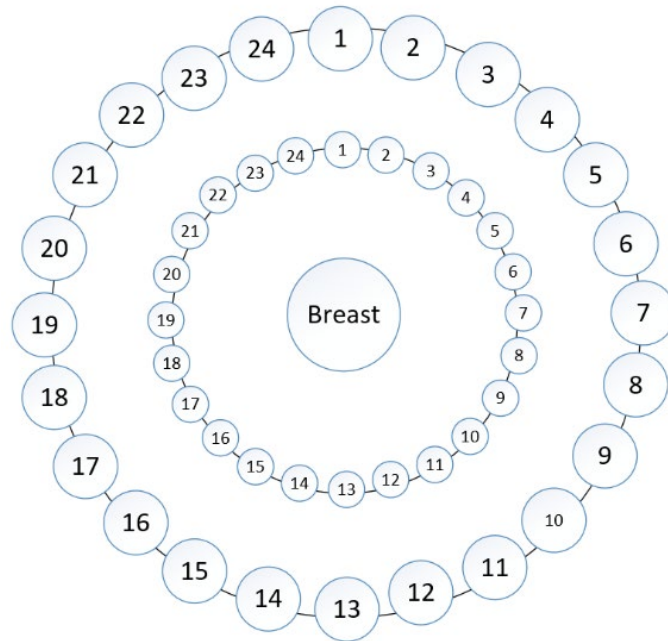


Figure 28. Positions of camera at a 45° angle and a horizontal view; allows for capture of 49 images around the circumference of the breast.

v. Data Collection

Unlike the IRI-MRI study, collecting MRI images is not necessary for this portion of the study. In addition to the patient questionnaire from both the IRI-MRI and IRI-Mammo studies, the following data is collected and deidentified:

- Age
- Date of birth
- Initials
- Breast density
- Bra size
- Mammography reports and eventual histopathology reports, if necessary
- If the patient gets an MRI due to a malignant diagnosis, the images will be provided

3.2.4 Image Acquisition

The ambient conditions in the room are held constant at 71°C and there is no active airflow during examination. After the patient has signed the informed consent form and filled out the patient questionnaire, she is then requested to disrobe from the waist up and wear a hospital gown that has an opening in the front. The patient lies down on the table in the prone position with one breast placed in the opening in the table. An example of this can be seen in Fig. 29.

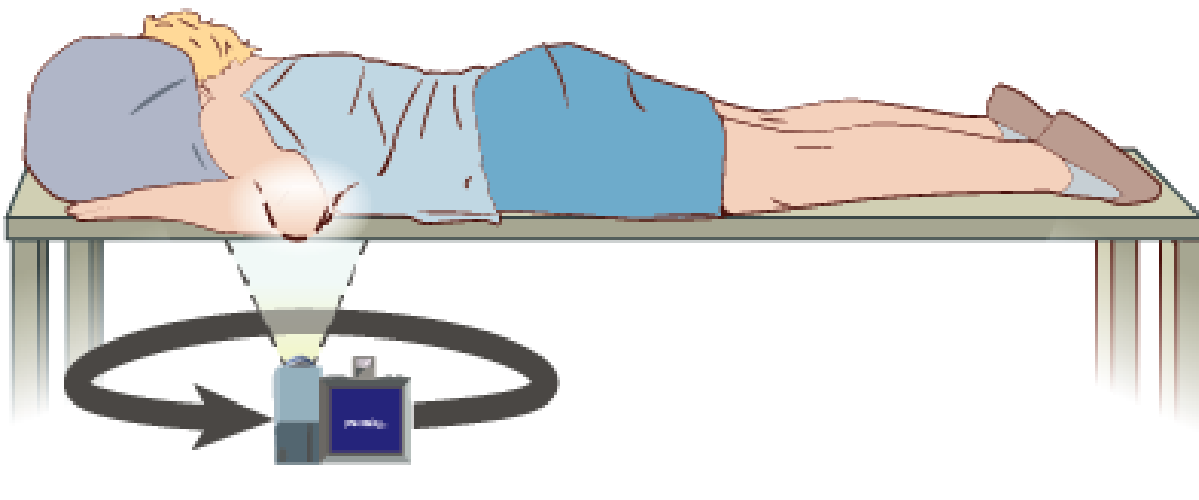


Figure 29. Medical illustration of subject in prone position with camera table underneath.

When the patient lies on the table, a timer is started. Based on data from previous studies [14–17], the acclimation time is approximately 10 minutes to reach proper steady state conditions. Images are taken during acclimation time to measure the changes in temperature throughout the ten minutes. However, it is possible that this amount of time is too lengthy or too short for steady state to be reached. The process of capturing all images only takes 90-120 seconds. When this process is complete, the patient is asked to switch to the contralateral breast and an identical process is completed. For each patient, the time to acclimate and the time taken for imaging is recorded.

3.3 Numerical

The numerical portion of this project was completed by Gonzalez-Hernandez [60]. The following images in this section are from his thesis work. Additional details can be found in two of his published papers [124], [125].

3.3.1 MRI Images

A digital breast model is created using the corresponding MRI images from the IRI-MRI study. Using a commercially available software called ImageJ, the inner breast architecture is removed (veins, tissue, etc.). A silhouette of all the MRI breast images in the series are created and stacked on top of each other. Finally, the breast geometry is smoothed using a mix of commercially available software (Autodesk Recap, MeshMixer, and ANSYS SpaceClaim). An example of this process can be seen in Figure 30.

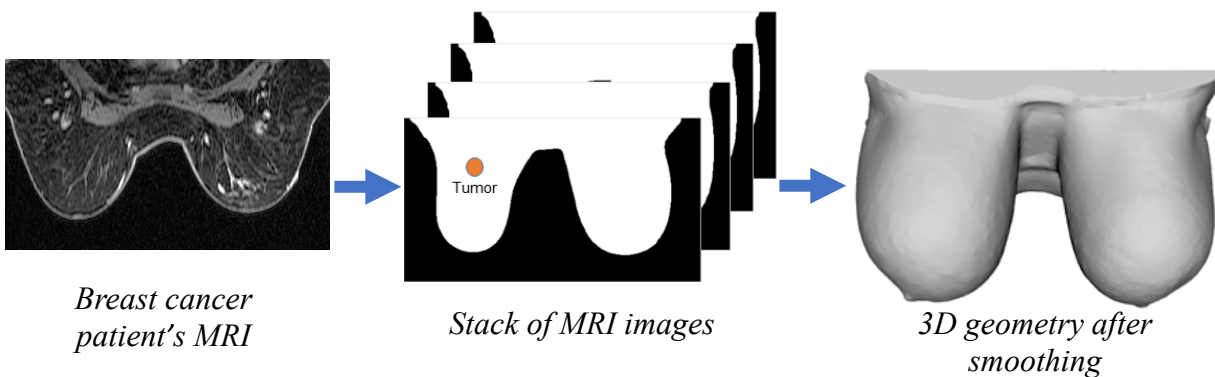


Figure 30. Patient-specific breast model generation process using MRI images [60].

This process creates a patient-specific digital breast model for each patient. This is important due to the intricate details on the breast surface that could potentially alter the resulting thermal profiles. Some of these intricacies can include concave surfaces, observable especially in the prone

position, as seen in Figure 31. After the geometry is generated using MRI images, the modeling process is started.

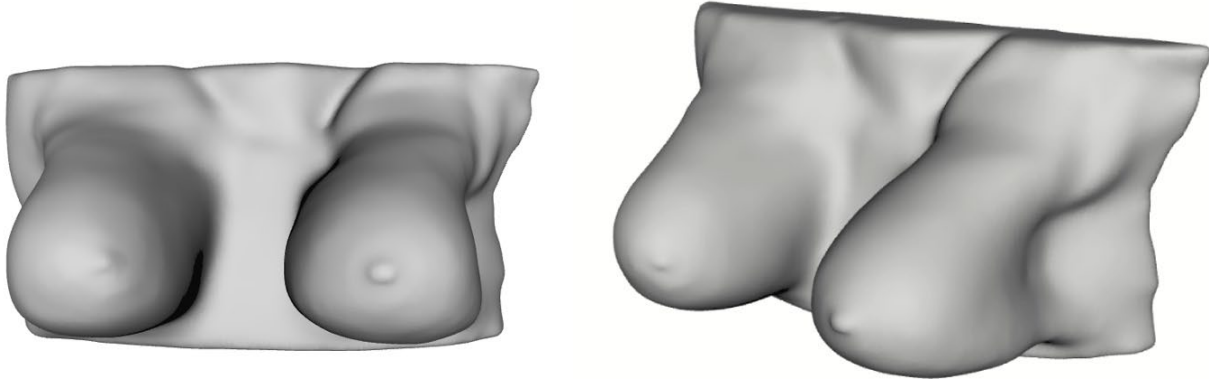


Figure 31. Breast model of Patient 013a from two different angles, showing the intricacies of the geometry.

3.3.2 3D Modeling Process

The modeling process involves importing the geometry into ANSYS and simulating the heat transfer effects of a tumor. A mesh is applied onto the model and boundary conditions are added (constant core temperature of 37°C , constant convection to the breasts through a steady ambient temperature). Initial parameters are used to develop a baseline CFD model with the patient-specific breast geometry. The values seen in Table 10 are generated from literature. Finally, a tumor is estimated and placed within the digital breast model to create a computed temperature distribution. From the simulations, computed temperature images are generated which are rearranged to match the same views as clinical IRI images. An example of this can be seen in Figure 32.

Table 10. Parameters used in the simulations [60], [124], [125].

Property	Value	Unit	Reference
Perfusion rate of healthy tissue	$1.8 \times 10^{-4} \text{ s}^{-1}$		7
Perfusion rate of tumor	$9 \times 10^{-3} \text{ s}^{-1}$		7
Metabolic activity of healthy tissue	450 W m^{-3}		7
Temperature of arteries	$37 \text{ }^\circ\text{C}$		8
Specific heat of blood	$3,840 \text{ J kg}^{-1} \text{ K}^{-1}$		8
Density of blood	$1,060 \text{ kg m}^{-3}$		8
Core Temperature	$37 \text{ }^\circ\text{C}$		9
Ambient temperature	$21 \text{ }^\circ\text{C}$		10
Heat transfer coefficient	$13.5 \text{ W m}^{-2} \text{ K}^{-1}$		11

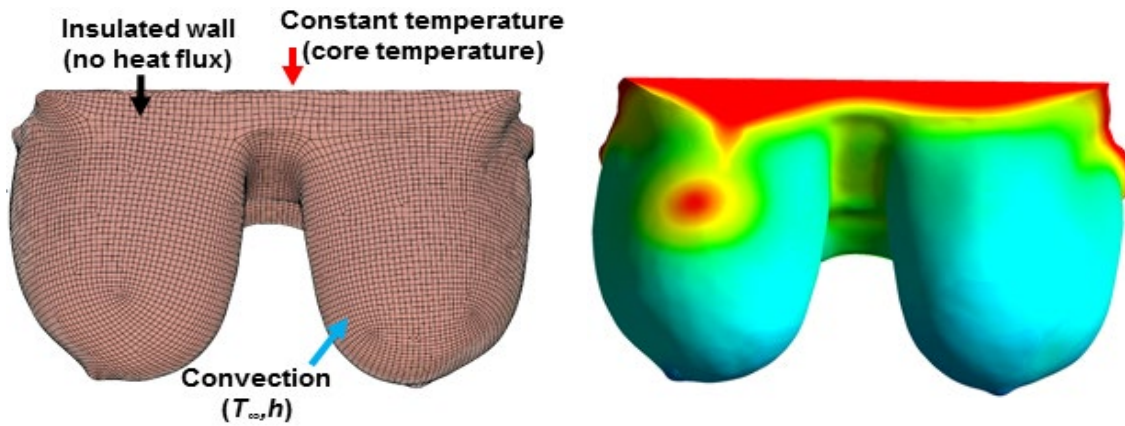


Figure 32. (a) Breast geometry with added mesh and boundary conditions and (b) breast model in ANSYS with imposed tumor in the right breast [60].

3.4 Conclusions

Through the clinical portions of this study, we were able to create a database of patient images for analysis and pathologic correlations. Additionally, we were able to study the patient protocol and potential adjustments for further optimization. The numerical study provided a patient-specific digital breast model capable of tumor detection and localization. Combining the clinical and numerical portions of this study, steady-state infrared imaging is seen as a more viable adjunctive technique to breast cancer detection. Further results are seen in Chapter 4.

Chapter 4: Results

4.1 Acclimation Time

As discussed in Chapter 3, IRI involves the acclimation of the body part to be imaged in order for steady state to be reached. Acclimation includes quasi-steady state conditions where temperatures are reasonably steady over a sufficient time. This period may be increased or decreased depending on the acclimation time needed for the breast surface to reach near thermal equilibrium state with the surroundings. Additional acclimation time may be given for the acclimation of the contralateral breast because the subject was lying on that breast on the table during the imaging of the first breast. This causes the breast to warm and takes longer for steady state to be reached.

The desired acclimation time to reach steady state is between 5 minutes and 20 minutes for efficient throughput with good imaging quality for accurate detection. A faster acclimation time may be reached by providing loosely fitting clothing or minimal clothing during wait period. The time used for the IRI-MRI and IRI-Mammo study was 10 minutes. The series of images in Fig. 33 shows the left breast, the breast without a tumor, of Patient 23 (further patient data found in Table 11). This patient had a lot of random vascular throughout the breast, some more striking or larger than other areas. The larger visible blood vessels running through the breast do not have a drastic temperature difference from the beginning of acclimation to the end. However, the smaller, deeper blood vessels do change over time and reflect differently on the surface.

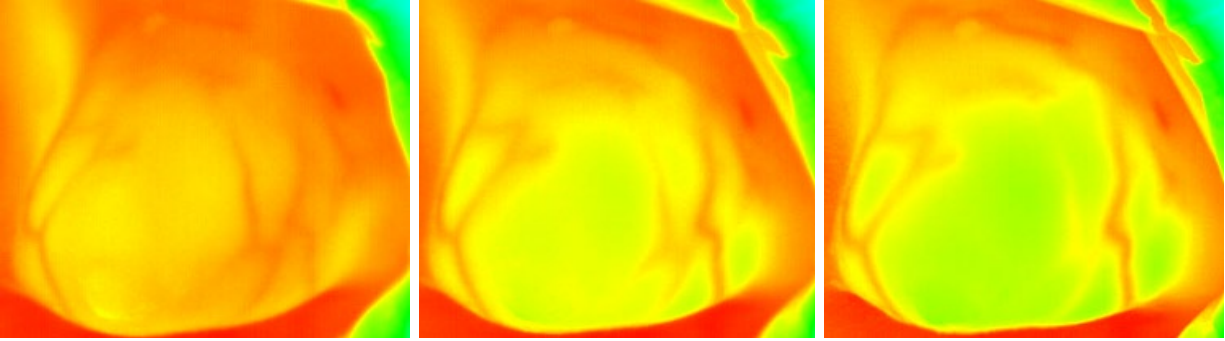


Figure 33. Breast cooling over a period of 10 minutes; first image is at 0 minutes, second image is at 5 minutes and third image is at 10 minutes.

The series of images in Fig. 34 show the acclimation period of 10-minutes for a breast with tumor. These images involve the left breast of Patient 25. The tumor is suspected to be in the upper right quadrant of the breast and is confirmed by the corresponding MRI seen in Fig. 35. The area surrounding the suspected malignancy is cooling throughout the period and the area of suspected malignancy is seen to stay red. The vascular system becomes more defined and the area of suspected malignancy becomes more defined throughout this time.

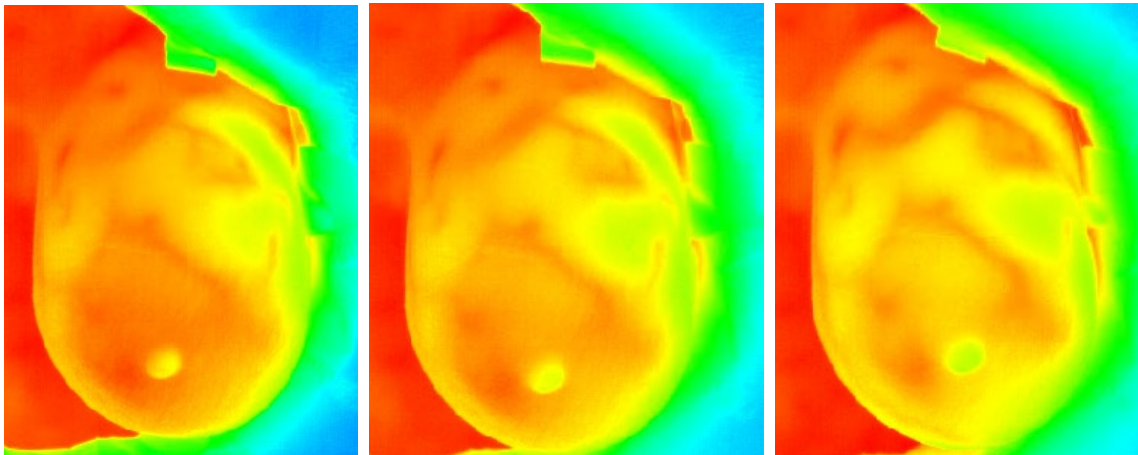


Figure 34. Acclimation time of Patient 25 left breast, with malignant tumor. Breast cooling over a period of 10 minutes; first image is at 0 minutes, second image is at 5 minutes and third image is at 10 minutes. Tumor is suspected to be in the upper right quadrant.



Figure 35. MRI of Patient 25, tumor can be seen in upper right quadrant with biopsy spot.

The change in acclimation time can change the visible thermal profiles on the breast surface, particularly where the blood vessels and tumor(s) effects are apparent. The resulting changes in thermal features related to vasculature can be observed over a period of time. The observable cooling period for the breast once exposed to the ambient temperature can help in differentiating hot spots due to tumors vs. hot spots due to vasculature. Hot spots are also referred to as an area of increased hyperthermia. As the breast cools, the lines of vasculature become more defined and linear while the thermal regions induced by the tumor remain more diffuse. Some changes are expected when the tumor is closer to the skin surface and the intensity of the thermal changes is considered.

4.2 IRI-MRI Study

For the first phase of this clinical trial, we needed to develop a system to localize and detect the tumor within the breast. The characteristics of the location of the tumor were essential for this portion of the study. The ultimate goal of the IRI-MRI study was to examine the position, size, and depth of the tumor within the breast. These factors were provided by pathology reports and confirmed with the corresponding MRI images. The additional data on the pathology reports that was collected include breast density, tumor grade and cancer type. These factors were collected primarily for future studies.

The IRI-MRI study recruited 30 adult women with biopsy-proven breast cancer who required a diagnostic MRI over the course of their clinical process. Table 11 shows the individual subject data for 30 individuals showing the tumor grade, type of cancer, breast density and tumor characteristics. IRI images were obtained with only 29 subjects as the images could not be obtained for Subject 5 due to camera malfunction. All women studied had tumor in one breast, except for Subject 6 and Subject 20 who had bilateral breast cancer.

As discussed in Chapter 3, the patients in the IRI-MRI study had eight images taken around the breast. Examples of the series of images are shown in Figure 36 - 39. One major issue with this clinical setup is the asymmetry of the breast. Although the camera setup may be centered, capturing the entire breast may be difficult. Additionally, with the weight and size of the camera the setup made it difficult to move and orient. This made getting consistent centered images difficult. The IRI-MRI study is still actively ongoing and recruiting patients, with the updated imaging system and ICI camera. The new modular camera setup is able to better capture the breast, despite how the table is setup or how the patient is positioned. This is primarily due to the high modularity in the system, allowing for more camera movement specific to each patient.

Table 11. List of subjects with age, tumor location (size/position/depth) for breasts with tumor (BWT) and additional details such as cancer type, breast density and subject classification.

Subject	Age	BWT	Breast Density*	Position	Size (cm)	Depth (cm)	Tumor Grade	Cancer Type**
001a	60	R	HD	10:00	1.6×1.0×1.1	Posterior	2	DCIS
002a	70	R	SF	11:00	0.8×0.7×1.1	Middle	2	IDC
003a	71	R	PF	10:00	0.9×0.6×0.9	Anterior	1	IDC
004a	62	L	SF	4:00	2.0×1.1×1.4	Middle	3	ILC
005a	<i>Data not collected due to technical computer malfunction</i>							
006a	68	R	SF	12:00	3.5×2.4×2.3	Middle	3	IDC
		L		2:00	0.8×0.6×0.4	Middle	1	ILC
007a	51	L	SF	5:00	2.6×1.1×1.2	Anterior	2	IDC
008a	67	L	SF	10:00	1.8×1.2×1.3	Posterior	1	IDC
009a	43	R	SF	12:00	1.2×0.8×0.8	Middle	1	IDC
010a	67	L	SF	12:00	1.0×0.8×0.8	Anterior	1	IDC
011a	46	R	HD	5:00	1.1×0.8×1.0	Middle	1	IDC
				5:00	1.0×0.8×0.7	Posterior	1	IDC
012a	48	R	SF	10:00	1.1×0.8	Posterior	2	IDC
013a	64	R	PF	11:00	1.5×0.9×1.2	Middle	1	IDC
014a	68	L	HD	2:00	MCs [□]	Middle	1	DCIS
015a	68	L	SF	3:00	1.7×1.1×1.3	Posterior	3	IDC
016a	56	L	SF	1:00	0.9×1.1	Middle	2	IDC
017a	70	L	SF	5:00	0.5×0.5×0.6	Posterior	3	IDC
018a	42	R	HD	10:00	0.4	Posterior	3	IDC
019a	49	R	SF	6:00	2.6×2.3×2.0	Middle	2	IDC
020a	70	L	SF	12:00	2.1×1.3×1.8	Anterior	2	ILC
		R		12:00	0.8×1.0×0.7	Posterior	1	LCIS
021a	65	L	HD	12:00	1.7×1.4×1.3	Middle	1	IDC
022a	67	L	ED	11:00	MCs [□]	Middle	2	LCIS
023a	72	R	SF	10:00	1.8×1.1×1.3	Middle	2	IDC
024a	72	L	SF	11:00	0.7×0.7×0.9	Anterior	3	IDC
025a	64	L	SF	2:00	1.9×1.7×2.4	Middle	1	IDC
026a	63	L	HD	11:30	MCs [□]	Posterior	1	IDC
027a	75	R	SF	10:00	1.0×0.8×0.7	Middle	1	IDC
028a	57	L	SF	10:00	1.4×1.0×0.7	Middle	2	IDC
029a	76	L	US	1:00	2.4	Anterior	1	IDC
030a	69	L	HD	2:00	0.7×0.6×0.3	Posterior	1	ILC

*SF = Scattered Fibroglandular, HD = Heterogeneously Dense, PF = Predominantly Fat

**DCIS = Ductal Carcinoma In-Situ, IDC = Invasive Ductal Carcinoma, LCIS = Lobular Carcinoma In Situ, ILC = Invasive Lobular Carcinoma

□MCs = Microcalcifications

For the first 20 patients of the IRI-MRI study, the average temperatures are calculated for the breast with tumor and the breast without tumor. The difference between the values are reported in Table 12. There is a temperature difference in nearly every case between the mean temperature of the BWT and the BWoT.

Table 12. Average temperature values in the breast without tumor and breast with tumor, for each subject imaged with IRI and the maximum temperatures seen at the tumor hot spot.

Subject	BWoT*	BWT**		Temp Difference	
	Average Temp. (°C)	Average Temp. (°C)	Maximum Temp at Hot Spot (°C)	Average BWT – Average BWoT	Hot Spot – BWT Average
1	31.1	31.2	31.8	0.1	0.6
2	30.9	31.0	31.7	0.1	0.7
3	27.5	27.8	31.5	0.3	3.7
4	28.7	29.1	30.3	0.4	1.2
5	Data for subject 5 has been omitted due to technical malfunctions resulting in unsaved images				
6	Bilateral Breast cancer, no BWoT	30.7, 30.8	32.2, 32.8	NA	1.5, 2.0
7	30.2	31.1	32.9	0.9	1.8
8	29.5	31.4	33.5	1.9	2.1
9	32.0	32.7	33.8	0.7	1.1
10	31.1	32.1	33.3	1.0	1.2
11	27.5	29.0	32.5	1.5	3.5
12	28.9	32.1	34.7	3.2	2.6
13	29.9	30.2	32.7	0.3	2.5
14	27.7	28.3	29.2	0.6	0.9
15	30.8	32.0	33.5	1.2	1.5
16	30.0	30.5	32.5	0.5	2.0
17	27.9	29.1	30.2	1.2	1.1
18	30.2	30.1	31.5	-0.1	1.4
19	29.5	29.7	33.4	0.2	3.7
20	29.9	31.2	32.8	1.3	1.6

*BWoT – Breast Without Tumor

**BWT – Breast With Tumor

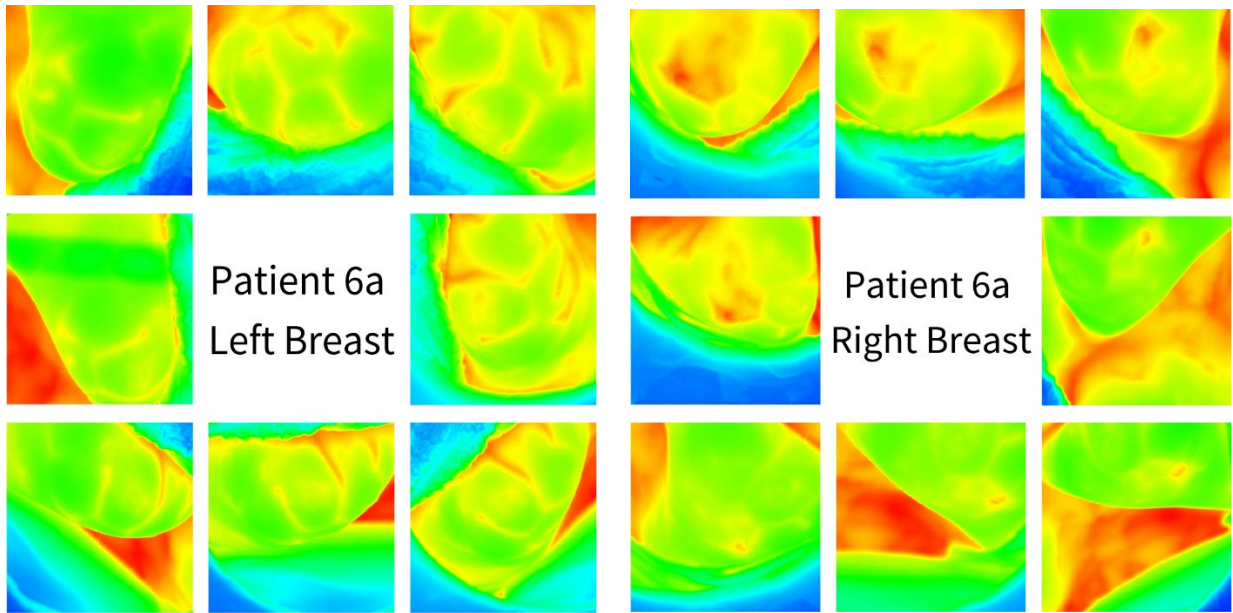


Figure 36. Image sequence of Patient 6a's left breast and right breast. This patient had bilateral breast cancer with a tumor in both breasts. A detailed analysis is presented below.

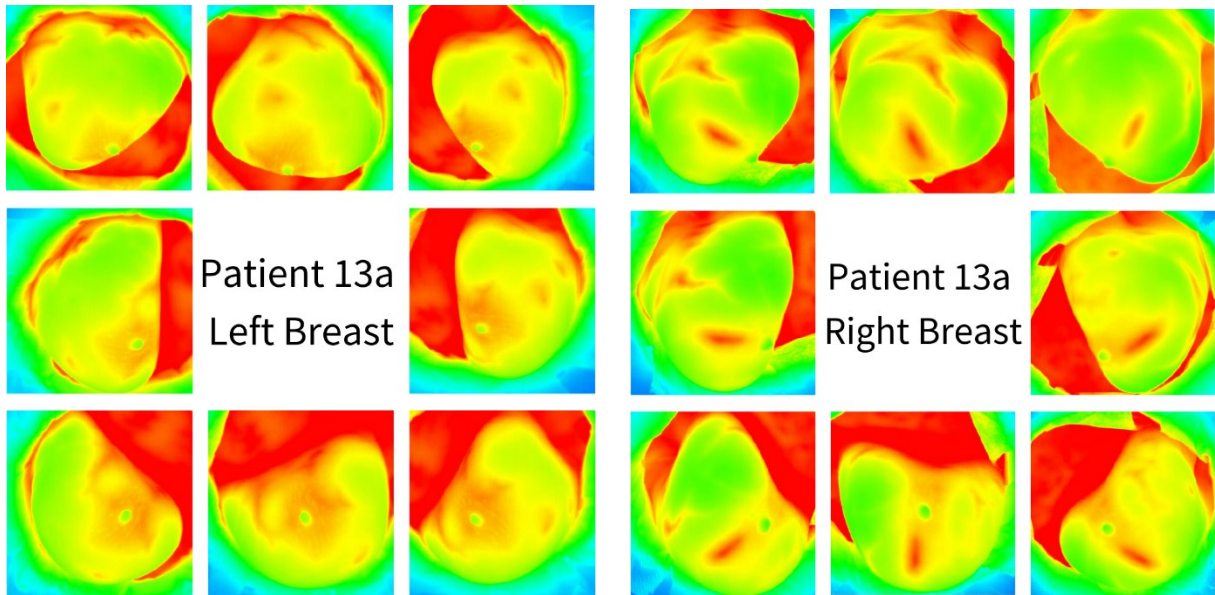


Figure 37. Image sequence of Patient 13's left breast and right breast. The malignant tumor is in the right breast, right above the nipple.

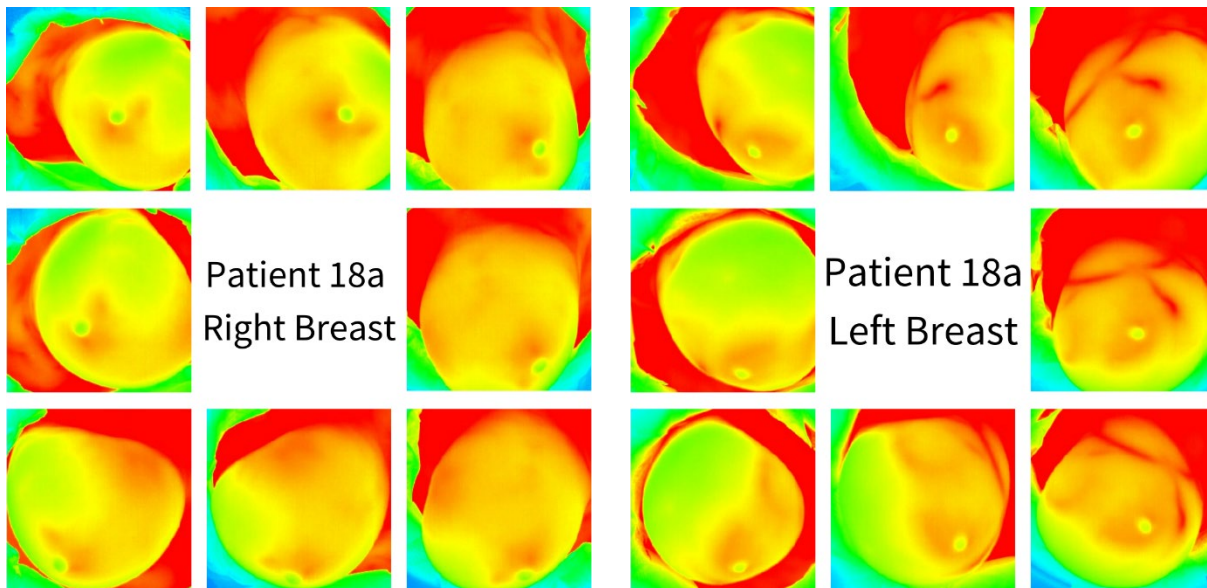


Figure 38. Image sequence of Patient 18's left breast and right breast. The malignant tumor is in the right breast.

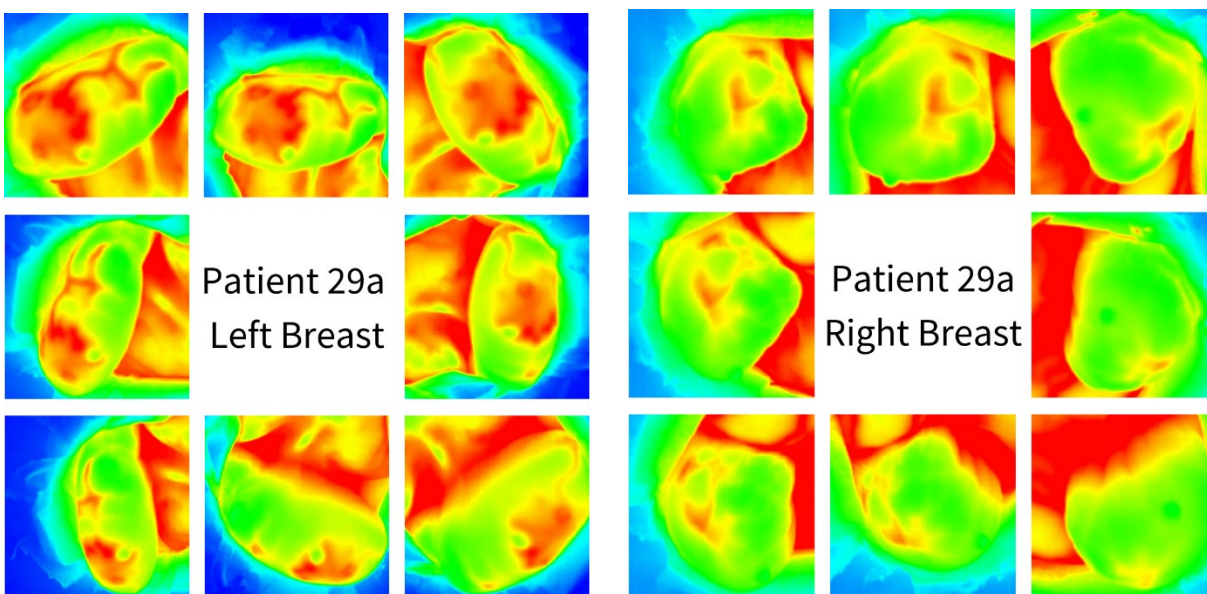


Figure 39. Image sequence of Patient 29's left breast and right breast. The malignant tumor is in the left breast.

Our preliminary results have shown visible hot spots by IR imaging, consistent with tumor, in each subject with known breast cancer. Patient 6 exemplifies the utility of infrared imaging as a potential adjunct to mammography in subjects with dense breast. Patient 6 is a 68-year-old woman who presented with a palpable abnormality in her right breast at 12:00. Bilateral breast tomosynthesis was performed which revealed a $3.5 \times 2.4 \times 2.3$ cm mass at 12:00 in the area of palpable concern. This mass was a biopsy proven invasive ductal carcinoma. In retrospect, this mass was present but was smaller in size on the mammogram a year prior. The mass was masked by overlapping fibroglandular tissue and not visible mammographically by the radiologist. An incidental $0.8 \times 0.6 \times 0.4$ cm invasive lobular carcinoma was also found in the left breast. This mass is not evident on the prior mammogram, even in retrospect. As both masses are seen on the IRI, we may have been able to detect the patient's breast cancer if thermography was used as an adjunct to screening mammography. The images of the left and right breast of Patient 6 can be seen in Fig. 40(a) and (b), respectively.

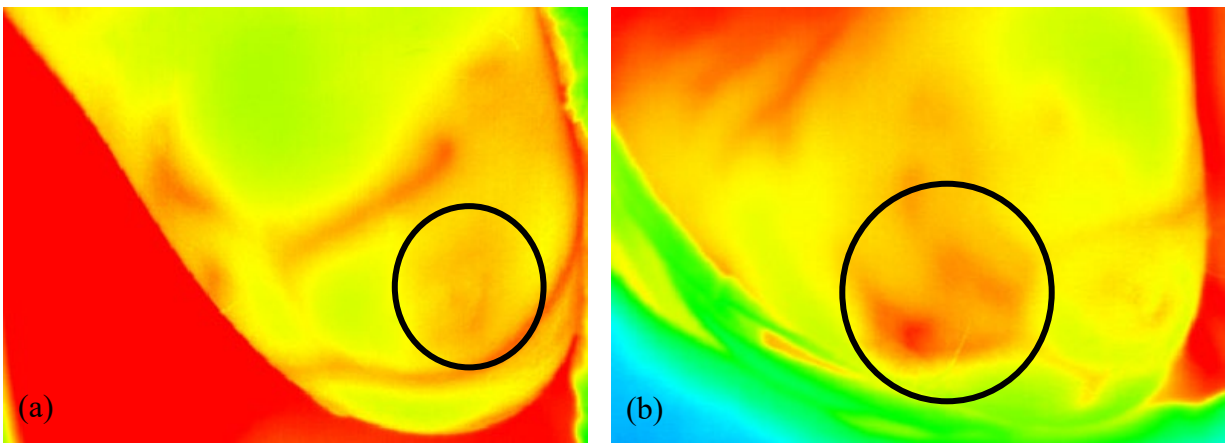


Figure 40. Images of subject 6 with bilateral breast cancer, (a) the left breast with hot spot in area of known 0.7 cm tumor and (b) the right breast with hot spot in area of known 2.7 cm tumor.

Further analysis of the thermal signature observed in the IRI images is performed to identify thermal features indicative of abnormalities associated with the presence of malignant tumors. Figure 40(a) shows an infrared image of the right breast for Patient 6 with a 2.7 cm tumor. Although the hot spot that correlates with the tumor is easily visible in the image, further quantification is performed by adding profile lines through the visible hot spot and through a cooler neighboring region of the breast.

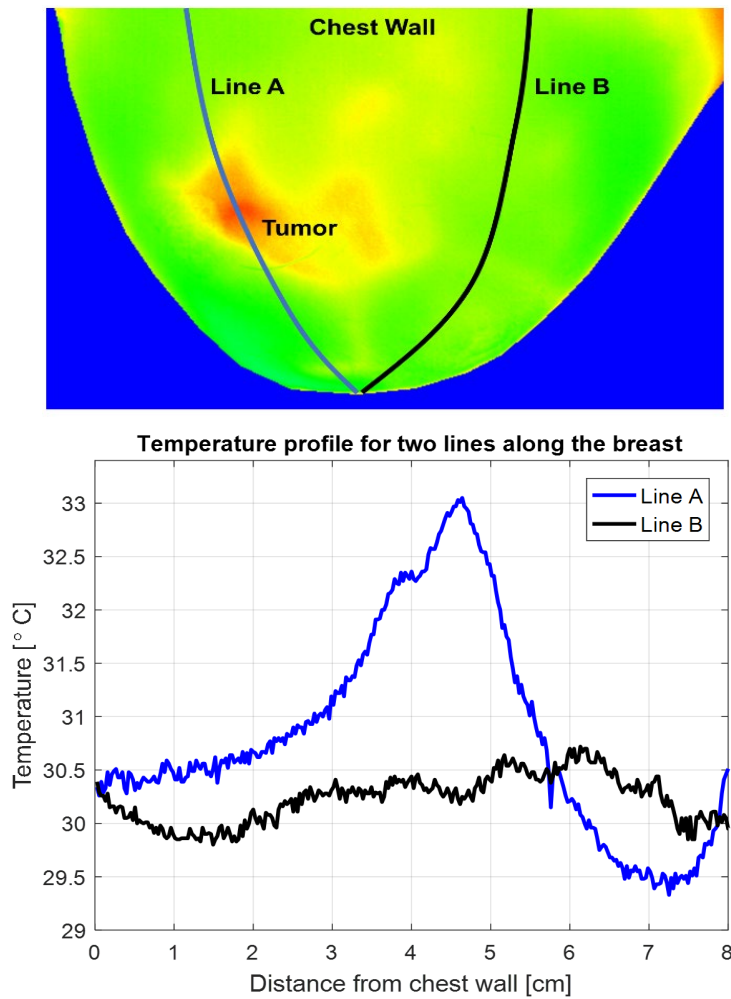


Figure 41. Temperature distribution of right breast of patient 6: (a) IR image with two profile lines along the breast and (b) temperature profile for A and B.

A temperature plot depicting the variations along these profile lines (Line A and Line B) are shown in Fig. 41(b). Line A passes through the hot spot correlating to a deep tumor and line B passes

through unaffected region. The temperature along Line B varies between 30-30.5 °C whereas the temperature at the hot spot corresponding to the tumor along Line A has a higher temperature of ~33 °C. The slope of the profile lines can further help in determining whether the thermal abnormality is associated to a malignant tumor or a superficial blood vessel. The hyperthermic lines seen faintly from the tip to the central region in Fig. 41(a) are indicative of blood vessels through the tissue in that region. The smaller temperature fluctuations seen between 4 cm and 8 cm distance observed in Line B of Fig. 41(b) correlate directly to the blood vessels clearly seen in the MRI rendering in Fig. 42. This approach enables differentiation between thermal signatures of a blood vessel from a malignant tumor.

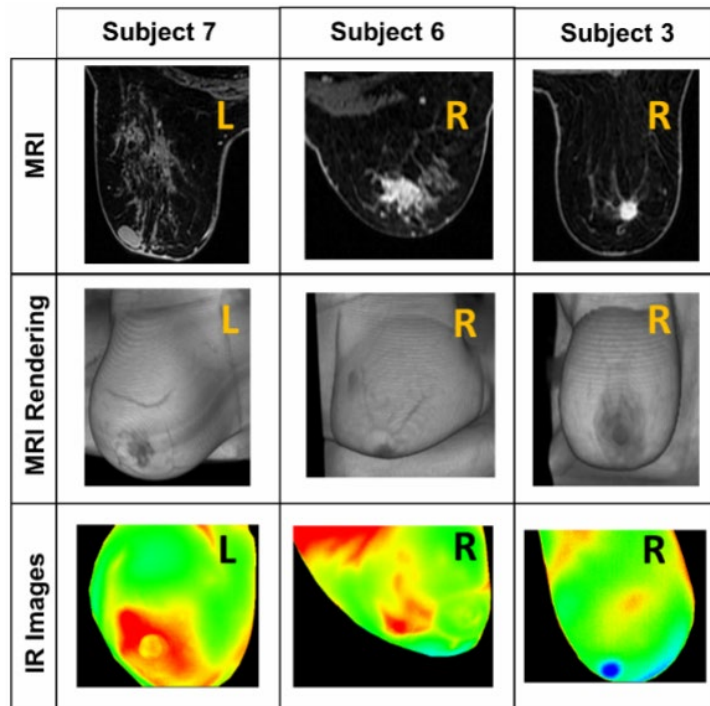


Figure 42. MRI, renderization from MRI, and IRI images for three subjects [126].

In this study, we determined that there are certain temperature profiles which establish whether a detected hot spot on the breast surface should be considered a malignant tumor or suspicious mass. In a given image, while there may be clear hot spots at the location of the tumor, there will also be

several hyperthermic lines present throughout the breast surface. These lines have been determined and correlated with MRI as superficial vasculature and the heating pattern they emit is different than those from the tumor. The images will be corrected for such thermal artifacts. Both tumors and blood vessels cause local temperature rises. Tumors generally have a larger area of diffusion from the center of the hot spot to the surrounding breast tissue. Other factors such as veins have a more secluded, well-defined hot spot. An example of this can be seen in Figure 43.

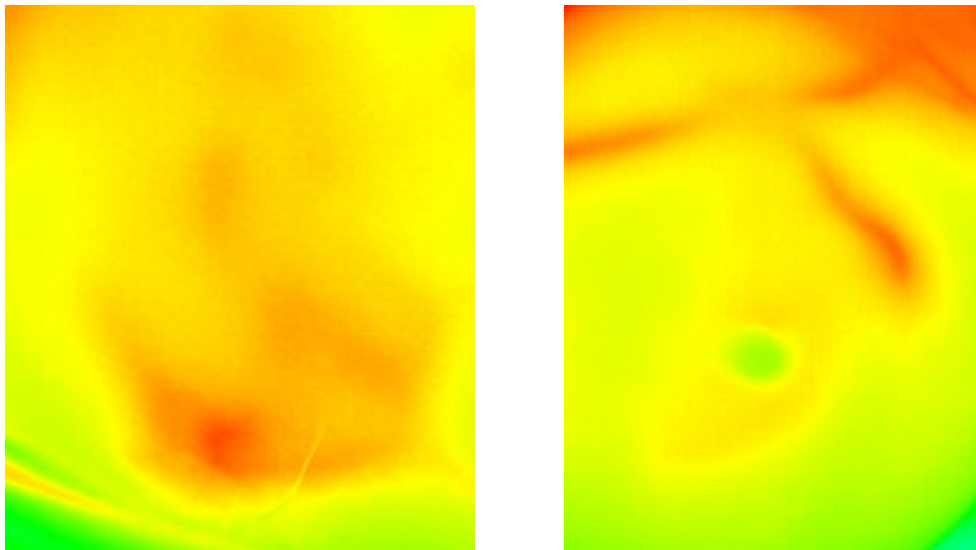


Figure 43. (a) The hot spot created by a malignant tumor and (b) the hot, short lines created by vasculature in the breast.

4.3 IRI-Mammo Study

For the second phase of this study, the focus shifted from tumor localization to determining specificity of the technology, understanding the bioheat transfer within the breast, and developing pathology correlations with the tumors and respective heat patterns. The patient population changed from those with biopsy-proven breast cancer to those with suspicious masses. The reports collected for this phase of the study mainly involve mammography reports and patient questionnaires. A pathology report was provided for any patient screened with an eventual malignant result. Additionally, the BI-RADS classifications seen in Table 13 are the classifications

given at the time of IRI screening. Two of the patients screened with a malignant result are Patient 005b and Patient 006b. However, the detection and localization process has not yet been performed on these patients. An example of some of the patient data collected in this part of the study is seen in Table 13.

Table 13. Patient data from the IRI-Mammo study for the six recruited patients.

Patient Number	Breast Density	Breast with Suspicion	BI-RADS Classification	Benign or Malignant?
001b	SF	Left	BI-RADS 3 – Probably Benign	Benign
002b	HD	Left	BI-RADS 1 – Negative	Benign
003b	HD	Right	BI-RADS 0 – Needs Additional Imaging	Benign
004b	SF	Left	BI-RADS 3 – Probably Benign	Benign
005b	HD	Left	BI-RADS 6 – Biopsy Proven Malignancy	Malignant
006b	SF	Left	BI-RADS 4 – Suspicious	Malignant

Additionally, the number of images captured at each angle for each breast increases. Images are taken in two different positions: horizontal, to receive and better outline of the breast, and at an angle, similar to the IRI-MRI study. Additionally, the new setup and camera introduced new challenges, primarily with image focus. The new camera requires a significant reduction in distance for accurate focus (FLIR required ~3 feet, ICI required ~1.5 feet). The focus of the camera was a challenge for the horizontal views. Examples of this can be seen in Patient 001b in Fig. 44.

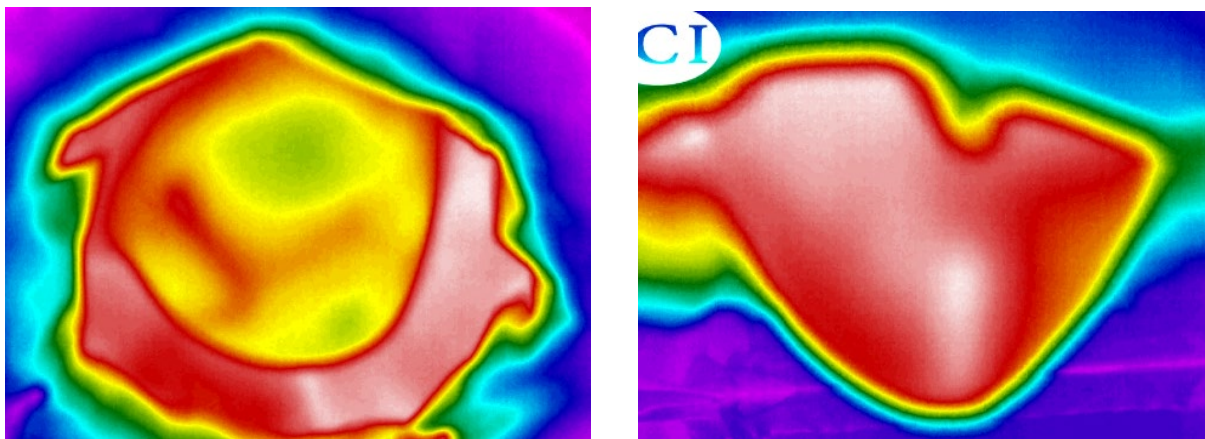


Figure 44. Glow around patient images due to poor image focus.

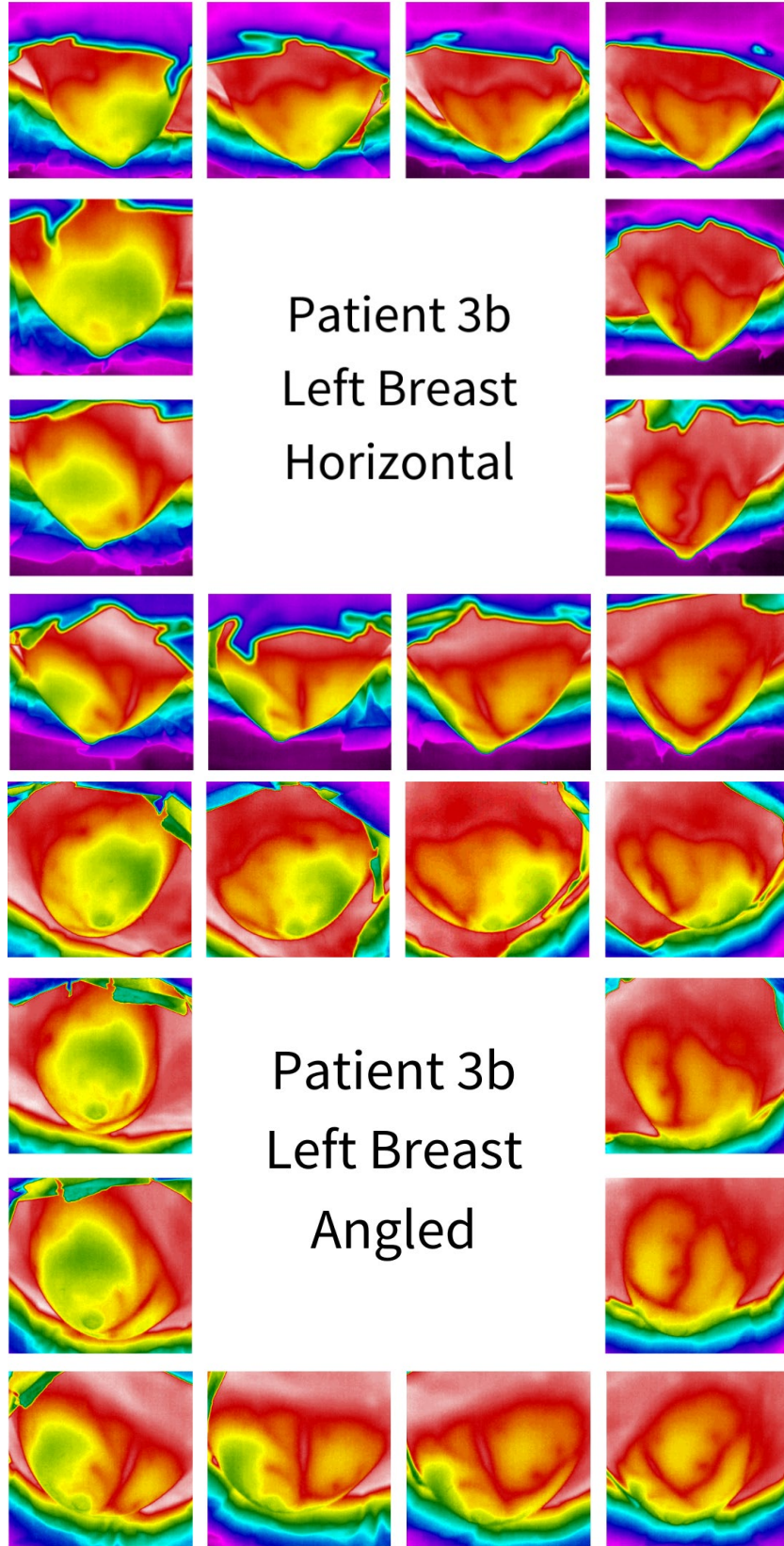


Figure 45. Image sequence of the left breast of Patient 003b from the horizontal and 45° angles

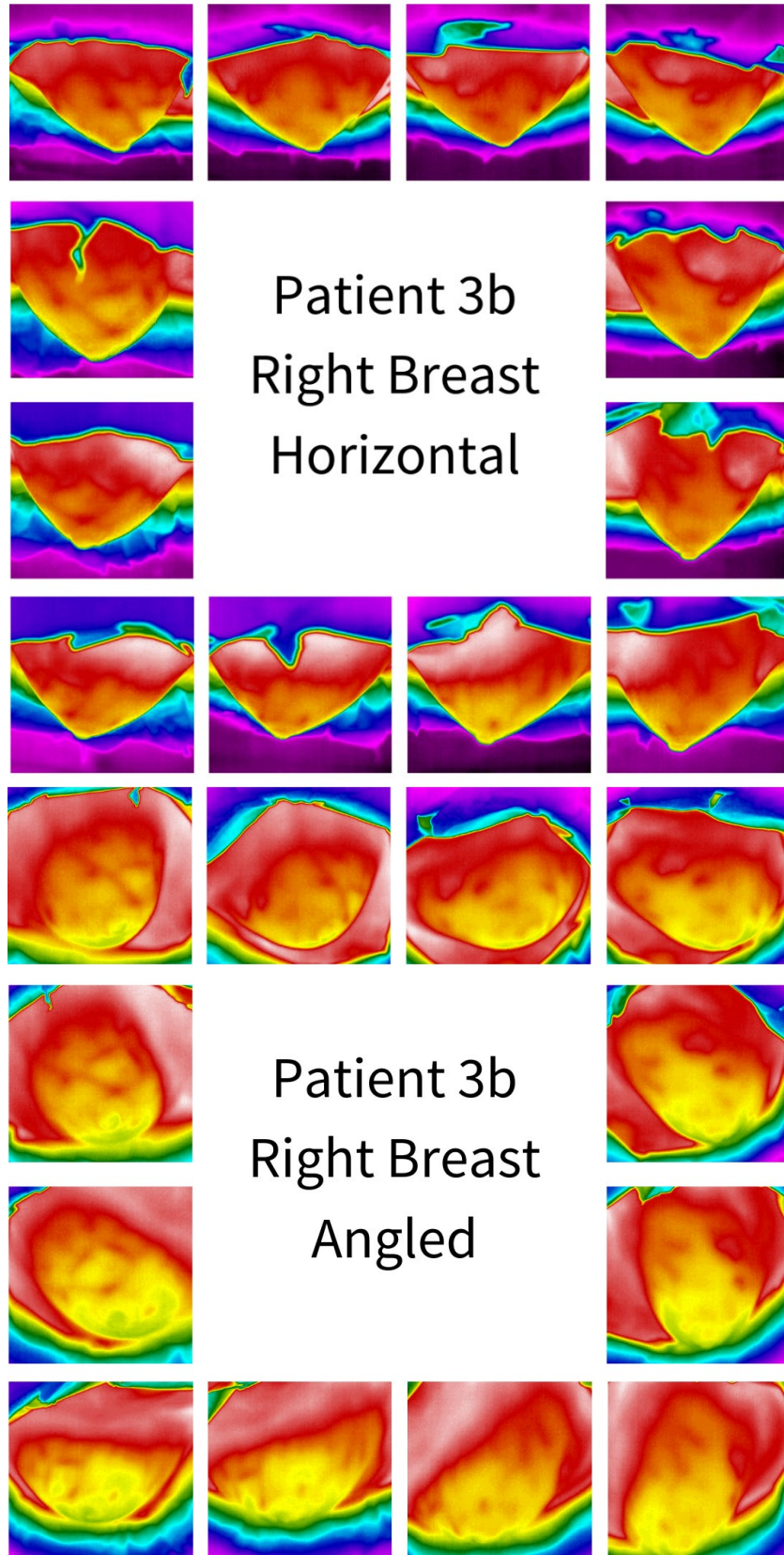


Figure 46. Image sequence of right breast of Patient 003b from the horizontal and 45° angles.

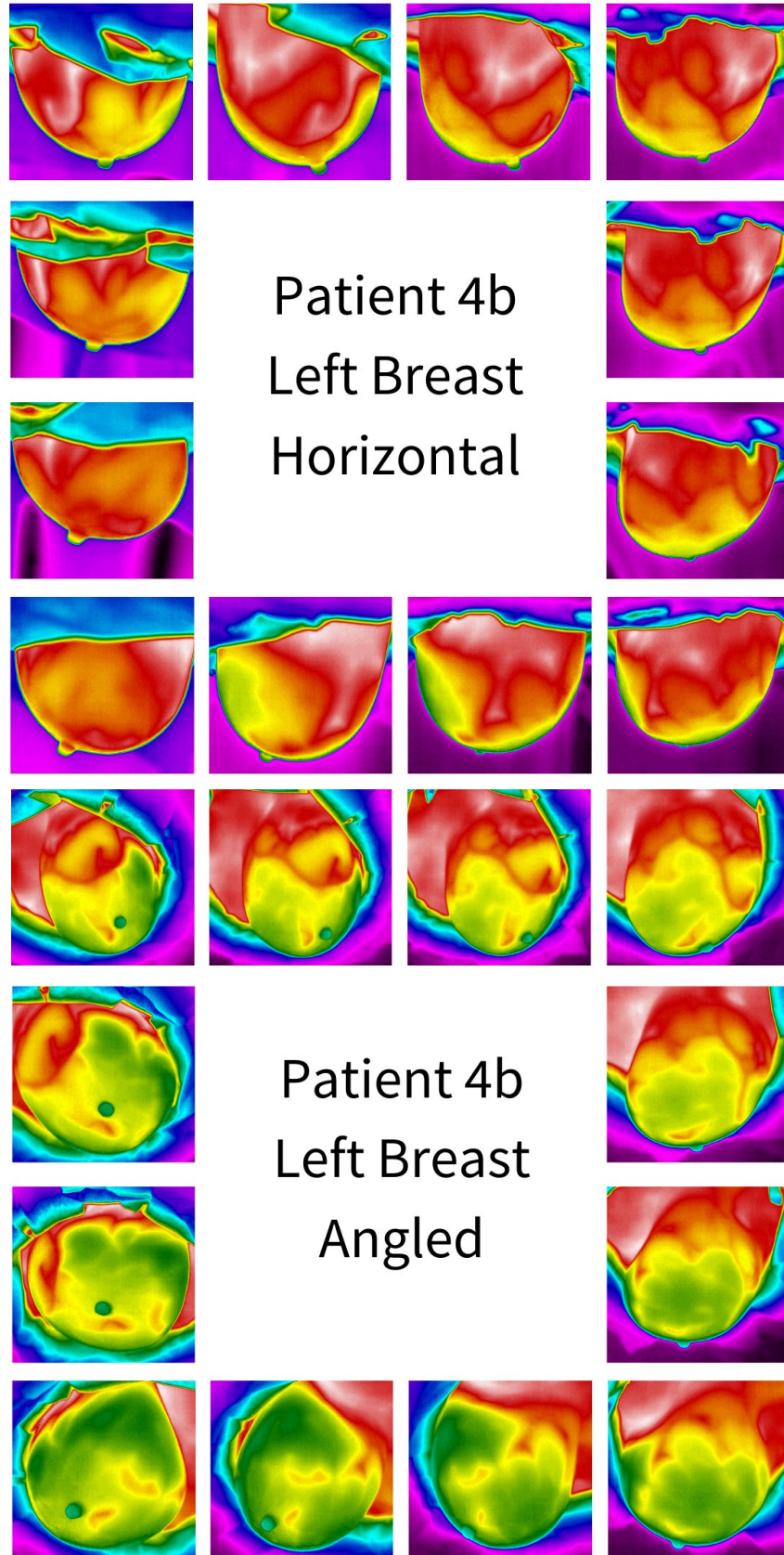


Figure 47. Image sequence of the left breast of Patient 004b from the horizontal and 45° angles.

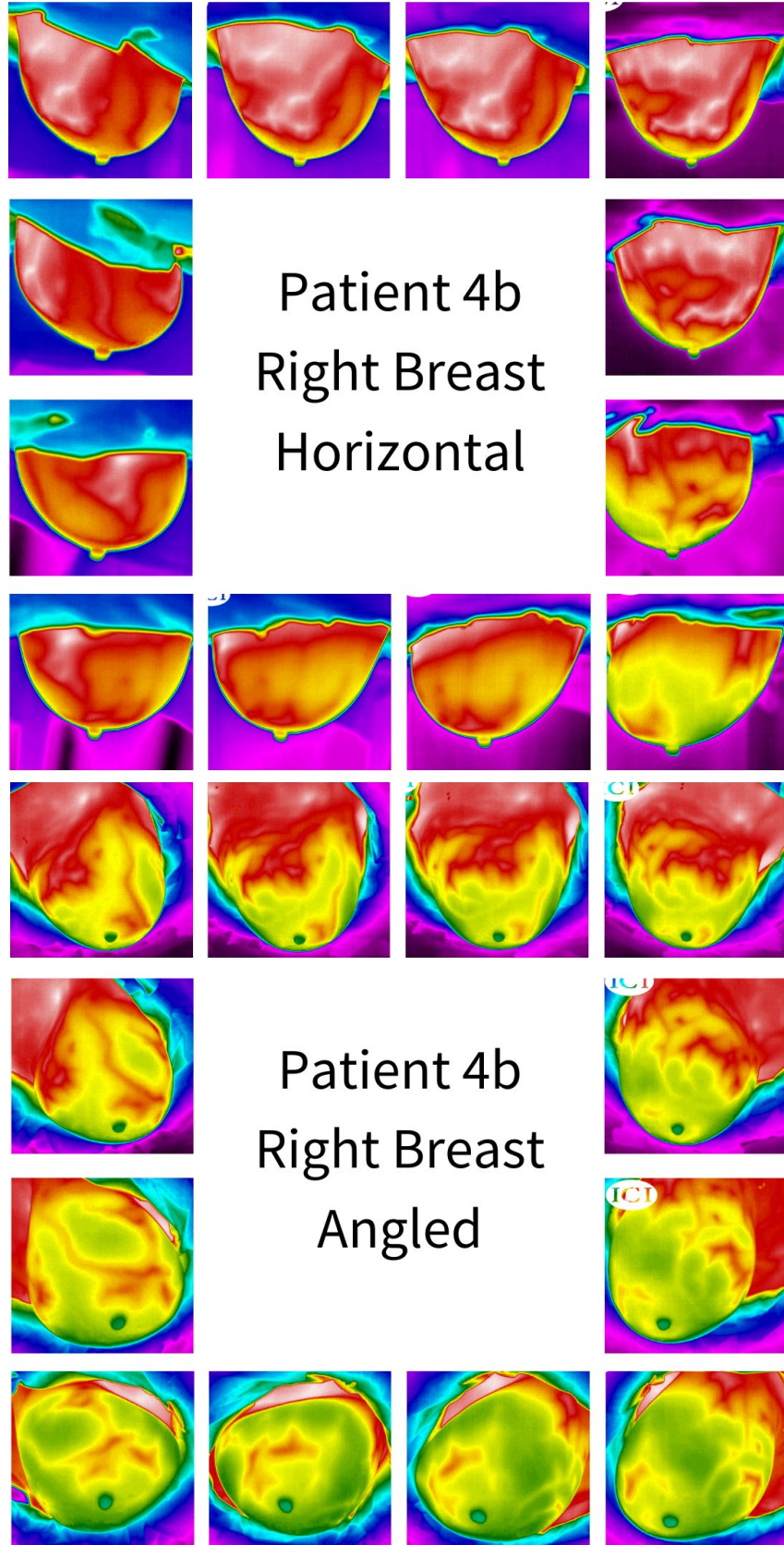


Figure 48. Image sequence of right breast of Patient 004b from the horizontal and 45° angles.

Similar to the IRI-MRI study, images (from all angles) are shown in Figures 45, 46, 47, and 48. The number of images has been reduced from 24 of each angle to 12 of each angle to show a comprehensive 360° view. A zoomed in view of the images of Patient 005b can be seen in Fig. 49.

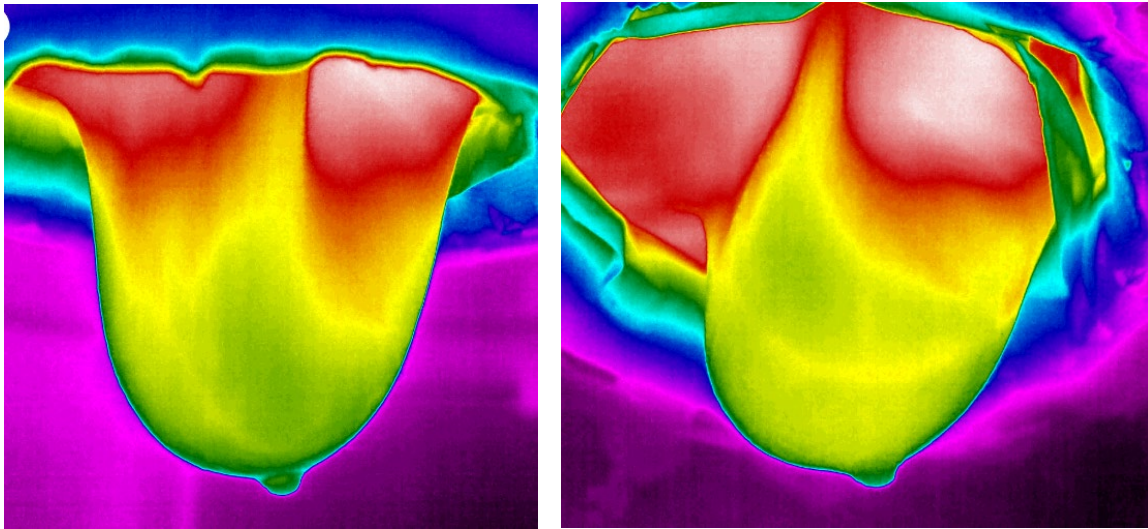


Figure 49. Horizontal (left) and angled (right) view of the right breast of Patient 005b.

4.4 Detection and Localization

Similar to Chapter 3, the detection and localization portion of this project was completed by Gonzalez-Hernandez [60]. The following images in this section are from his thesis work. Additional details can be found in two of his published papers [124], [125].

A tumor is estimated and placed within the digital breast model to create a computed temperature distribution. From the simulations, computed temperature images are generated which are rearranged to match the same views as clinical IRI images. The difference between the clinical and computed temperature distributions are further quantified by aligning the corresponding images in the same view in a process called image registration.

Once all digital model positions are identified to match the clinical IRI images, an iterative program is run in order to localize any tumor within the breast. The program identifies temperature variations on the clinical IRI images and compares them to the computed temperature distributions in the digital breast model. If a match is found, the program verifies that there is a tumor and computes its size and position. If a match is not found, the program continues to run until the match criterion ($0.1\text{ }^{\circ}\text{C}$ between actual and predicted values) is satisfied. Using this technique, we have been able to accurately detect a tumor and calculate its exact size and position within the breast. A flowchart of this process is shown in Fig. 50. Further study into this technology can potentially benefit subjects with dense breast tissue, which can mask tumor on mammography.

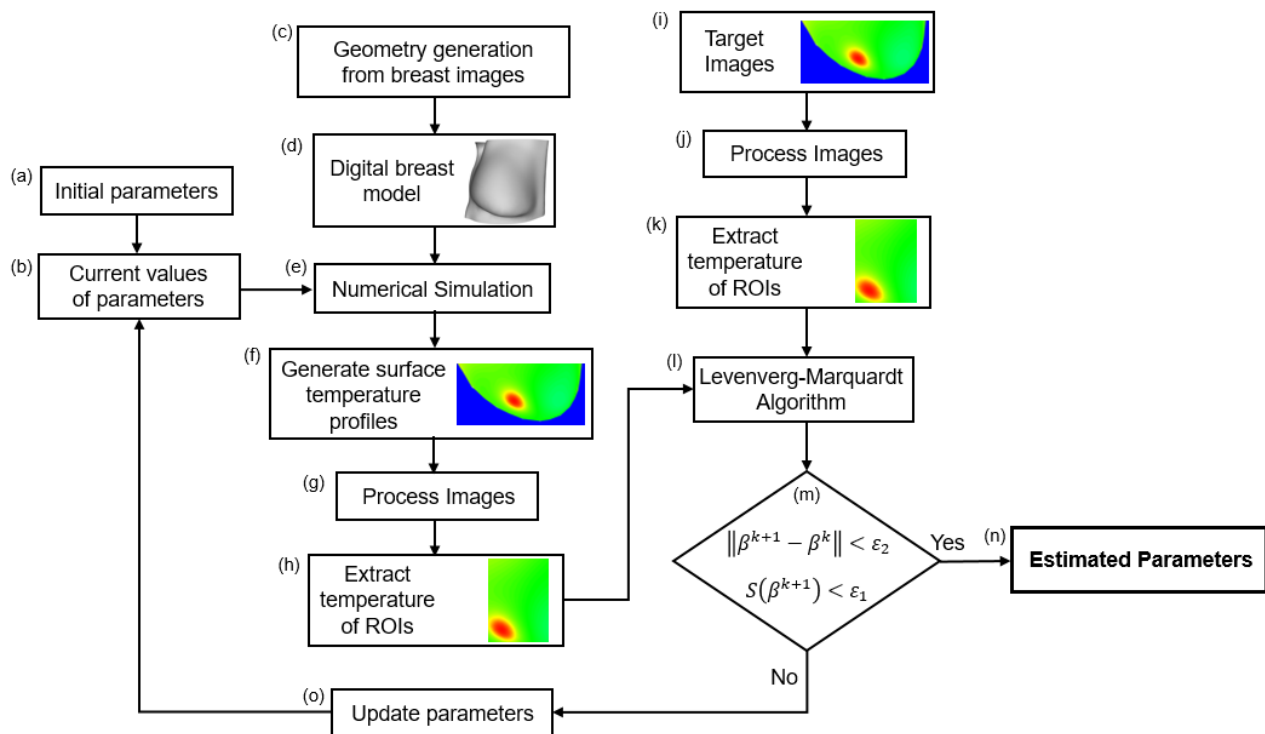


Figure 50. Flowchart of detection and localization process from Gonzalez-Hernandez [125].

The results for seven subjects are shown in Fig. 51(a) with the corresponding difference in predicted tumor diameter and actual tumor diameter in Fig. 51(b). It can be seen that the predictions were very accurate, within 2 mm for diameter and 2-7 mm for location.

Comparison Between Predicted & Actual Size and Location of Tumor				
Subject	Actual Diameter (cm)	Predicted Diameter (cm)	Actual (x, y, z) cm	Predicted (x, y, z) cm
1R	1.4	1.3	(7.6, 6.0, 11.8)	(7.4, 5.7, 12.1)
2R	0.8	1.0	(5.8, 6.8, 13.0)	(6.5, 7.1, 12.5)
3R	0.9	1.0	(5.2, 8.1, 11.8)	(5.2, 7.5, 11.2)
6R	2.7	2.7	(10.5, 14.5, 11.5)	(10.7, 13.9, 10.9)
6L	0.8	1.0	(4.5, 12.4, 10.3)	(3.9, 11.9, 9.6)
7L	1.9	1.9	(12.1, 12.8, 17.1)	(12.0, 13.2, 16.5)
8R	1.7	1.9	(4.7, 7.3, 12.3)	(5.1, 6.7, 11.6)
10R	1.1	1.2	(5.3, 4.8, 12.5)	(5.2, 5.2, 13.1)

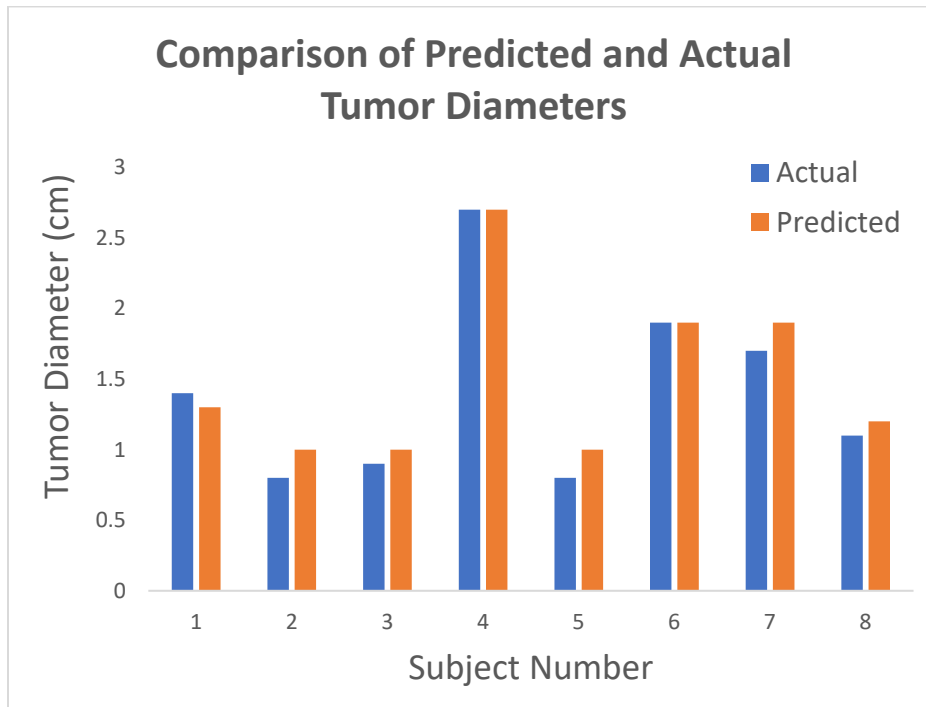


Figure 51. Comparison between predicted and actual values for tumor size and location within each breast.

The comparison between clinical IR and computer temperature distributions for Patients 003a, 006a and 007a are shown in Figs. 52-54, respectively. The two respective views shown in these figures correspond to the same views of the individual breasts. It is seen that the temperature distributions in the computer-generated thermal images accurately predict the trends.

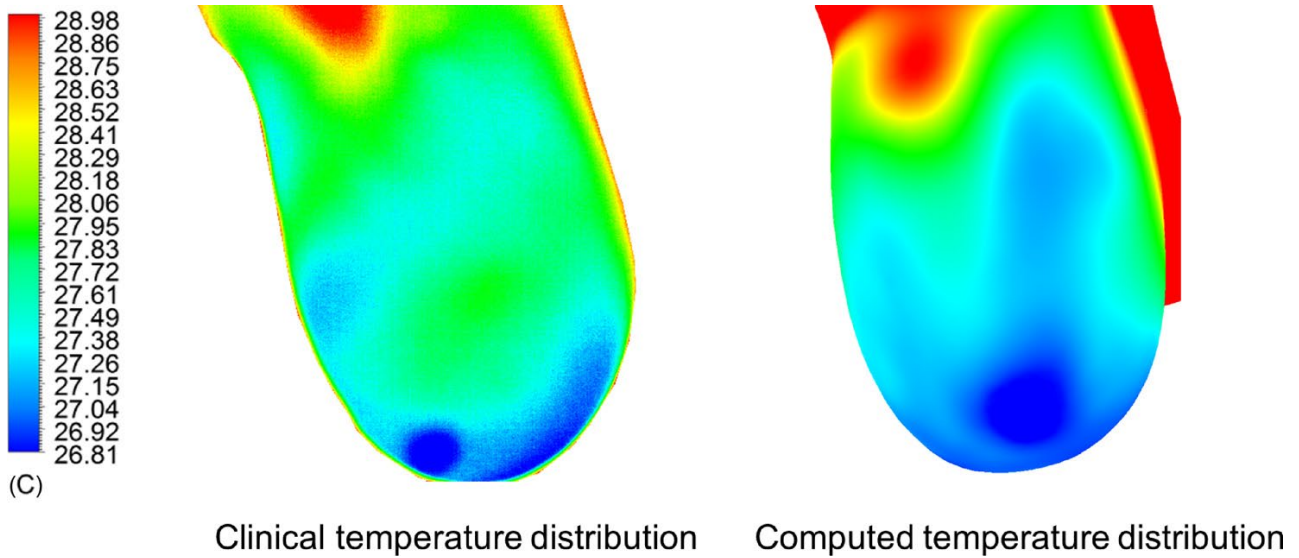


Figure 52. Comparison of clinical and computed temperature distributions for Patient 003a [126].

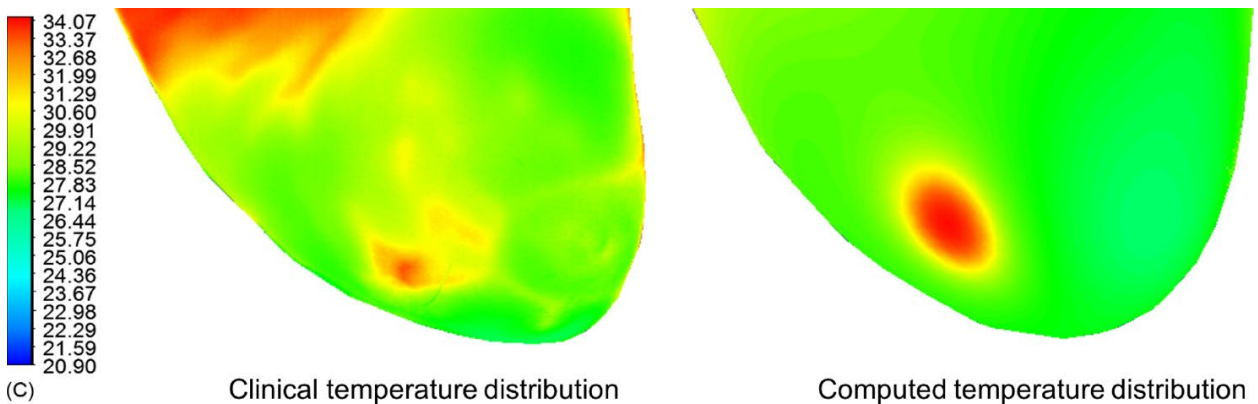


Figure 53. Comparison of clinical and computed temperature distributions for Patient 006a [126].

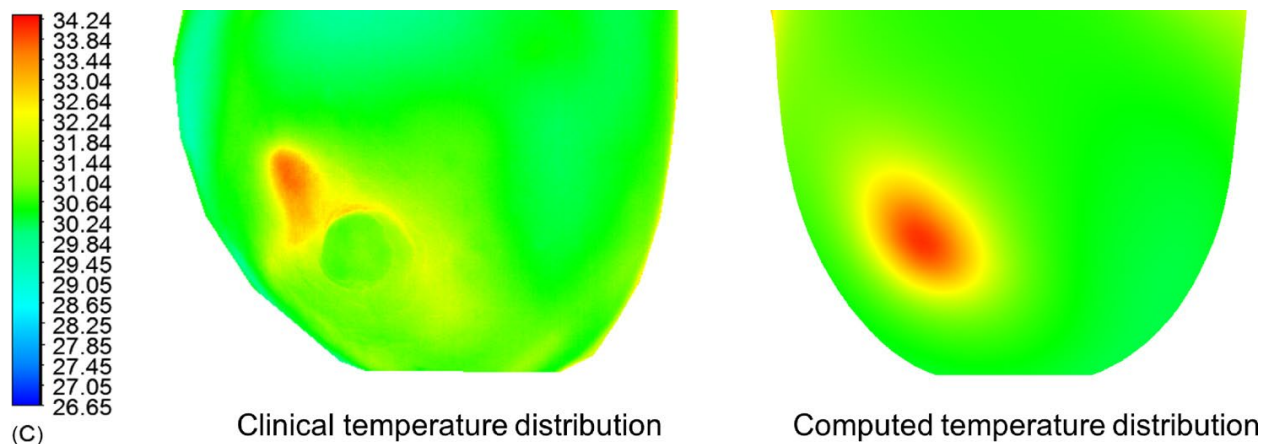


Figure 54. Comparison of clinical and computed temperature distributions for Patient 007a [126].

4.5 Conclusions

The IRI-MRI study has shown that IRI in prone has the capability of detecting malignant tumors irrespective of breast densities. Further, the numerical modeling process has shown great promise in localizing tumors in subjects with biopsy-proven breast cancer. For the first phase of this study, we were able to recruit and image thirty patients with biopsy-proven breast cancer. This allowed for the development and testing of the detection and localization process. We have shown the efficacy of the technology as an accurate detector of the method, particularly to find and localize a tumor within the breast.

The next phase of this study involves the specificity of this technology and determining the limits of detection. We have only recruited six patients to date but are eagerly recruiting to continue the clinical study. The new modular camera setup has shown great promise in obtaining more images from multiple angles and will undoubtedly prove beneficial in determining the specificity of this method. Slight modifications may be made in the future to further optimize the patient experience

and streamline the imaging process. The numerical process will be further refined to consider bioheat transfer within the breast, the effects of vasculature and breast architecture, internal and external influencers on the body, and more. The numerical modeling process can be automated to ensure faster diagnosis for each subject. While exact localization of the mass is important, the position will be translated into position on a clock, quadrant of the breast, depth, and distance from the nipple. These identifiers are used heavily in the medical realm for surgical resection and needed core-needle biopsy (CNB). Furthermore, the imaging process will be further refined for rapid diagnosis and wide-scale general population screening. Additional components will be considered for a potential future large-scale clinical study involving general population screening. Further details on the additions and modifications can be found in Chapter 5.

Chapter 5: Design of a Large-Scale Clinical Study

This chapter focuses on the potential of a large-scale clinical study in the Rochester General Hospital. The infrastructure needed has been designed and developed for this study and presented below. There are additional future recommendations that can be found in Chapter 8.

5.1 Patient Population

By recruiting patients with biopsy-proven breast cancer, the IRI-MRI method was tested and validated. Testing the simulation process using patients with a known, palpable mass allowed for validation against an MRI. As discussed in Chapter 3 and 4, the MRI images were used extensively to develop a patient-specific digital breast model, observe the actual shape of a tumor and compare the resulting thermal profile with the tumor placement in the breast [60], [124]–[126]. Now that the method has been proved and validated, further evaluation is needed to determine efficacy in a blind trial. The obvious next step includes patients that may or may not have breast cancer to ascertain the detectability limits of this technology and method.

When considering a sample size to determine the efficacy of this technology, there are many factors to consider. A study published by Bujang and Adnan [127] considers the reality that most researchers are not statisticians and also discuss the requirements needed for a minimum sample size in screening or diagnostic studies. Obviously two major factors used to compare various screening techniques lie in the sensitivity and specificity of the modality, discussed above. Bujang and Adnan [127] state the following for studies involving the value of a screening method over diagnostic tools: “If an objective of the research study is to determine whether (or not) a specific tool or instrument can be used as a screening tool; then researchers will have to ensure that it has

a sufficiently high degree of sensitivity but a lower degree of specificity can be tolerated.” However, once the method is considered for diagnostic purposes, both a high sensitivity and specificity are desirable. This following analysis first considers the sample size for infrared imaging as a base-level screening method and then as a diagnostic tool.

The primary factors used to determine sample size include prevalence of the disease (Prev), sensitivity and specificity. Observing the sensitivities and specificities reported for various screening techniques as seen in Table 14, relative values can be used to determine statistical significance. As thermography is often compared against mammography or used as an adjunctive technique with mammography, the sensitivity and specificity for mammography are used to determine screening sample size. The reported sensitivity is 84% and specificity is 92%.

Table 14. Overall sensitivity and specificity of select screening techniques for comparison.

Technique	Sensitivity	Specificity
Mammography	84%	92%
Magnetic Resonance Imaging (MRI)	90%	50%
Positron Emission Tomography (PET)	90%	86%
Ultrasound	82%	84%
Tomosynthesis (3D mammography)	90%	92%

A paper by Buderer [128] discusses the exact process of calculating sample size for sensitivity and specificity while incorporating prevalence. The author presents several steps accounting for set parameters, prevalence, true and false positives and negatives, and sensitivity and specificity. They also provide the required equations necessary. Table 15 is adapted from Buderer [128].

Table 15. Screening parameters and corresponding equations adapted from Buderer [128].

Screening Parameter	Estimate	Standard Error
Sensitivity (SN) the proportion of those who are diseased, who are labeled positive by the diagnostic test	$SN = \frac{TP}{TP + FN}$	$\sqrt{\left[\frac{SN(1 - SN)}{TP + FN} \right]}$
Specificity (SP): the proportion of those who are disease-free, who are labeled negative by the diagnostic test	$SP = \frac{TN}{TN + FP}$	$\sqrt{\left[\frac{SP(1 - SP)}{TN + FP} \right]}$
Positive predictive value (PPV); the proportion of subjects with positive diagnostic test results, who have the disease	$PPV = \frac{TP}{TP + FP}$	$\sqrt{\left[\frac{PPV(1 - PPV)}{TP + FP} \right]}$
Negative predictive value (NPV); the proportion of subjects with negative diagnostic test results, who do not have the disease	$NPV = \frac{TN}{TN + FN}$	$\sqrt{\left[\frac{NPV(1 - NPV)}{TN + FN} \right]}$

Where $TP = True\ Positive$, $TN = True\ Negative$, $FP = False\ Positive$, $FN = False\ Negative$

Prevalence involves the proportion of a given population who have specific characteristics. To get a general estimate of prevalence, data was taken from a study examining women from the New Hampshire Mammography Network [129], [130]. BI-RADS 0 are classified as ‘incomplete examinations’ and were removed from this dataset. Poplack et al. [130] provides the breakdown of BI-RADS classifications for the 47,112 patients, as seen in Table 16. Patients who were classified as BI-RADS 3, 4 and 5 were included in determining prevalence for screening.

Table 16. Data collected from Poplack et al. [130] from the New Hampshire Mammography Network.

BI-RADS		Screening	
1	Negative	37995	80.6%
2	Benign	4930	10.5%
3	Probably Benign	3345	7.1%
4	Suspicious	766	1.6%
5	Highly Suggestive of Malignancy	76	0.2%
TOTAL		47112	100%

The following equation is used to determine prevalence:

$$Prevalence = \frac{\# \text{ of people in sample with characteristic}}{\text{Total \# of people in sample}} \quad (7)$$

Based on the above numbers, the estimated prevalence [131] for this study is:

$$Prev. = \frac{BI - RADS \ 3, \ 4, \ \text{and} \ 5}{\text{Total \# of Patients}} = \frac{4187}{47112} = 8.8\%$$

For simplicity, the prevalence is rounded up to 10%. To determine sample size, the following parameters are needed:

- W – maximum clinically acceptable width of the 95% confidence interval (CI)
- P – estimate for prevalence of disease in the target population
- SN – value for expected sensitivity of new screening method
- SP – value for expected specificity of new screening method
- Confidence Intervals and coefficients
 - Assuming a 2-tailed, 95% CI
 - $\alpha = 0.05$
 - $Z_{\alpha/2} = 1.96$

Calculating the number of patients who have the disease (TP+FN)

$$TP + FN = Z_{\alpha/2}^2 * \frac{SN(1-SN)}{W^2} \quad (8)$$

$$TP + FN = (1.96)^2 * \frac{.84(1 - .84)}{0.1^2}$$

Calculating the number of patients who do not have the disease (FP + NP)

$$FP + TN = Z_{\alpha/2}^2 * \frac{SP(1-SP)}{W^2} \quad (9)$$

Calculating the sample size for required sensitivity, N1

$$N1 = \frac{TP+FN}{P} \quad (10)$$

Calculating the sample size for required specificity, N2

$$N2 = \frac{FP+TN}{1-P} \quad (11)$$

Calculating these equations with the assumed and estimated parameters leads to a desired sample size of N. However, if a higher sensitivity and specificity than mammography are desired, then a variable sample size is calculated. The following calculations and tables give different sample sizes depending on the desired parameters. Assuming a constant prevalence of 10% with a variable sensitivity and specificity, the following sample sizes are calculated:

Table 17. Estimated sample size for a variable sensitivity and specificity for prevalence of 10% in patients classified as BI-RADS 3, 4 or 5.

Variable Sensitivity	N1	Variable Specificity	N2
60%	922	60%	102
65%	874	65%	97
70%	807	70%	90
75%	720	75%	80
80%	615	80%	68
85%	490	85%	54
90%	346	90%	38
95%	182	95%	20
99%	38	99%	4

Assuming a constant sensitivity and specificity of 84% and 92%, respectively (from mammography) with a variable prevalence, the following sample sizes are calculated:

Table 18. Estimated sample size for a variable prevalence.

Variable Prevalence	N1	N2
1%	5163	2827
5%	1033	565
10%	516	283
20%	258	141
30%	172	94
40%	129	71
50%	103	57
60%	86	47
70%	74	40
80%	65	35
90%	57	31

Finally, assuming that both the prevalence and sensitivity/specificity are varying, the following sample sizes are calculated:

Table 19. Estimated sample size for variable prevalence and sensitivity.

Prevalence	Sensitivity							
	60%	65%	70%	75%	80%	85%	90%	99%
1%	9220	8740	8067	7203	6147	4898	3457	380
5%	1844	1844	1613	1441	1229	980	691	76
10%	922	922	807	720	615	490	346	38
20%	461	461	403	360	307	245	173	19
30%	307	307	269	240	205	163	115	13
40%	230	230	202	180	154	122	86	10
50%	184	184	161	144	123	98	69	8
60%	154	154	134	120	102	82	58	6
70%	132	132	115	103	88	70	49	5
80%	115	115	101	90	77	61	43	5
90%	102	102	90	80	68	54	38	4

Table 20. Estimated sample size for variable prevalence and specificity.

Prevalence	Specificity							
	60%	65%	70%	75%	80%	85%	90%	99%
1%	93	88	81	73	62	49	35	4
5%	97	92	85	76	65	52	36	4
10%	102	97	90	80	68	54	38	4
20%	115	109	101	90	77	61	43	5
30%	132	125	115	103	88	70	49	5
40%	154	146	134	120	102	82	58	6
50%	184	175	161	144	123	98	69	8
60%	230	218	202	180	154	122	86	10
70%	307	291	269	240	205	163	115	13
80%	461	437	403	360	307	245	173	19
90%	922	874	807	720	615	490	346	38

Ultimately, assuming similar sensitivity/specificity to mammography and the prevalence rate of 10% of patients diagnosed as BI-RADS 3, 4 or 5 after general population screening, we can observe Table 21 (seen again below) as the sample size estimation. The larger of the two sample sizes will be considered the sample size for the next study (516 patients).

Table 21. Estimated sample size for a variable sensitivity and specificity for prevalence of 10% in patients classified as BI-RADS 3, 4 or 5.

Variable Sensitivity	N1	Variable Specificity	N2
60%	922	60%	102
65%	874	65%	97
70%	807	70%	90
75%	720	75%	80
80%	615	80%	68
84%	516	85%	54
85%	490	90%	38
90%	346	92%	31
95%	182	95%	20
99%	38	99%	4

The capacity of the hospital and hired staff could handle a 500-patient study with BI-RADS 3, 4 or 5 patients. The numbers seen in Table 22 show the patients recruited over a 6-month timespan at the Rochester General Hospital (2,836 total patients). Assuming the clinical study would encompass three years, only 166 patients would need to be recruited every year (or 3 per week). The number of patients receiving mammograms classified as BI-RADS 3, 4 or 5 at RGH is 456 patients over a six-month period. Therefore, the current IRI-Mammo recruitment of approximately one patient per week would require a small increase to meet desired patient sample size. This would constitute hiring a separate individual to directly recruit patients, potentially creating an additional screening room, and redesigning the clinical equipment for more rapid screening and diagnosis.

Table 22. Mammography data and BI-RADS classifications over a six-month period at the Rochester General Hospital.

July 1, 2018 through December 31, 2018		RGH Mammography Data					
BI-RADS		Screening		Diagnostic		All	
	Not Applicable	0	0.0%	2	0.2%	2	0.1%
0	Need Additional Imaging	88	4.6%	2	0.2%	90	3.2%
1	Negative	1231	64.5%	208	22.4%	1439	50.7%
2	Benign	589	30.9%	244	26.3%	833	29.4%
3	Probably Benign	1	0.1%	131	14.1%	132	4.7%
3L	Probably Benign, Post Lumpectomy	0	0.0%	125	13.5%	125	4.4%
4	Suspicious	0	0.0%	135	14.6%	135	4.8%
5	Highly Suggestive of Malignancy	0	0.0%	65	7.0%	65	2.3%
6	Biopsy-Proven Malignancy	0	0.0%	15	1.6%	15	0.5%
	TOTAL	1909	100%	927	100%	2836	100%

5.2 Clinical Setup

Adding upgrades to the clinical setup will ensure more rapid screening and diagnosis. There are several components that cause patient discomfort that will be mitigated. These include the following and are discussed in greater detail below:

- **Acclimation Time:** Reducing the acclimation time will involve letting both breasts hang freely at the same time, while allowing for easy imaging access
- **Staircase:** Many patients have struggled with the stairs due to bad knees or joint pain
- **Imaging Position:** Those with back pain have complained about the position or struggle to lie in the position for more than 10 minutes
- **Automated Camera Setup:** Manual camera setup and image capture required the image taker to be underneath the table during screening, causing patient discomfort

- Cameras: Moving one camera into 49+ different positions takes a great amount of time, requiring a longer screening period

The proposed changes in the clinical setup will involve upgrades in both the camera setup and the screening bed. The camera setup will evolve to include at least two cameras (preferably twelve) located strategically around the breast, seen in Fig. 55. Six cameras will be located at an angle to the breast while the remaining six cameras will be pointed horizontally. Similar to the previous setup, the cameras will be located on a turntable. When the initial images are taken, the turntable will rotate four times to ensure up to 24 images from each angle or forty-eight images in total to ensure sufficient data for the modeling and analysis process. Additionally, the camera setup will be automated with motors to rotate the camera setup and cameras as opposed to manual manipulation. A computer program can be created to capture all the positions simultaneously, mitigating the need for manual capture. Automating the process will ensure more rapid screening and increased patient comfort. The cameras used for screening are the same as the IRI-Mammo study, with a resolution of 640×512 pixels and a thermal sensitivity of 0.02°C, the highest commercially available.

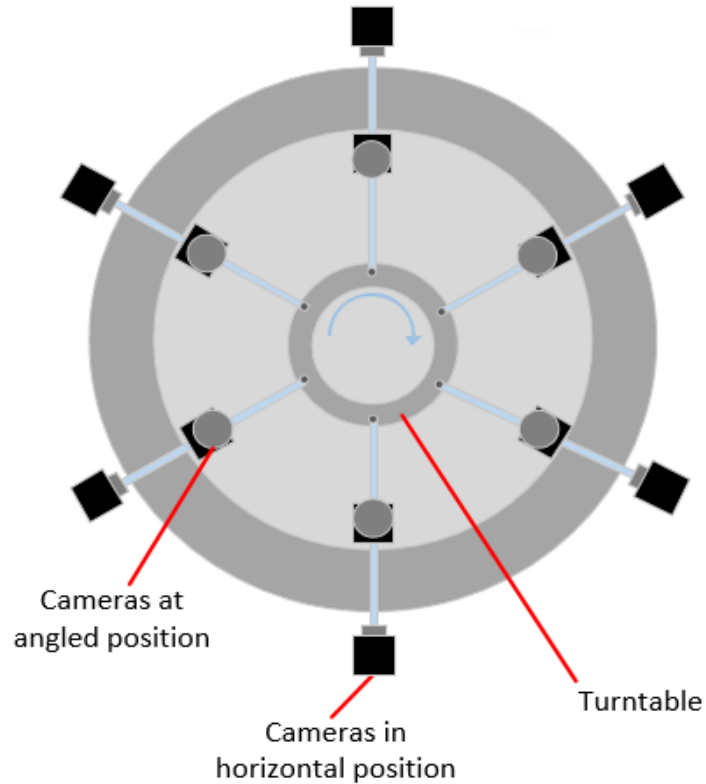


Figure 55. Upgraded camera setup with multiple cameras at varying heights.

The screening bed will be adjusted for subject comfort and optimized imaging views. The desired setup will involve a modular bed with rails on either side and a hole large enough for both breasts. The setup in both the IRI-MRI and IRI-Mammo studies involve a modified table with a staircase and handrail, several feet off the ground. For ease-of-use for subjects with disabilities, the new bed will not involve any staircase but will instead be modular, allowing for the subject to lay down before the bed is raised into position. An example of the new imaging setup with multi-camera system can be seen in Fig. 56.

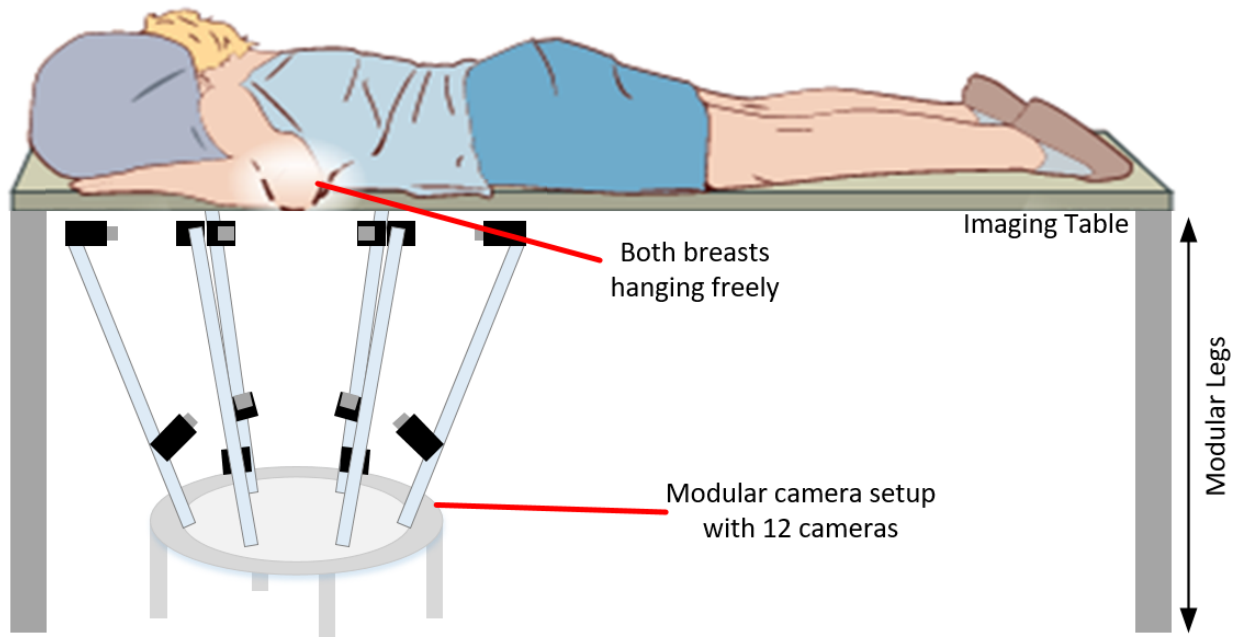


Figure 56. New modular table setup with IRI camera system and patient in prone position.

Additionally, removing any thermal alterations by utilizing the prone position and allowing both breasts to hang freely concurrently will aid in subject comfort and shorten the acclimation period, therefore shortening the imaging time. The future clinical table will be closer in design to a breast MRI table. One possible design includes two holes, one for each breast, with a perforated cloth lying between them. The cloth is added to move one breast out of the way so the other breast can be imaged in a 360° view. In Fig. 57, the first panel shows the compressed breast lying underneath the subject while the contralateral breast hangs freely through the opening in the table. This is found in the current clinical design, causing a longer acclimation and imaging period. The second panel shows the side view of a redesign with two holes cut in the table and the added perforated cloth in between the two. The final panel shows the perforated cloth swept to the side to move the second breast out of the way. Although one breast will be touching a perforated cloth, the perforations will prevent the breast from heating and will reduce acclimation time considerably.

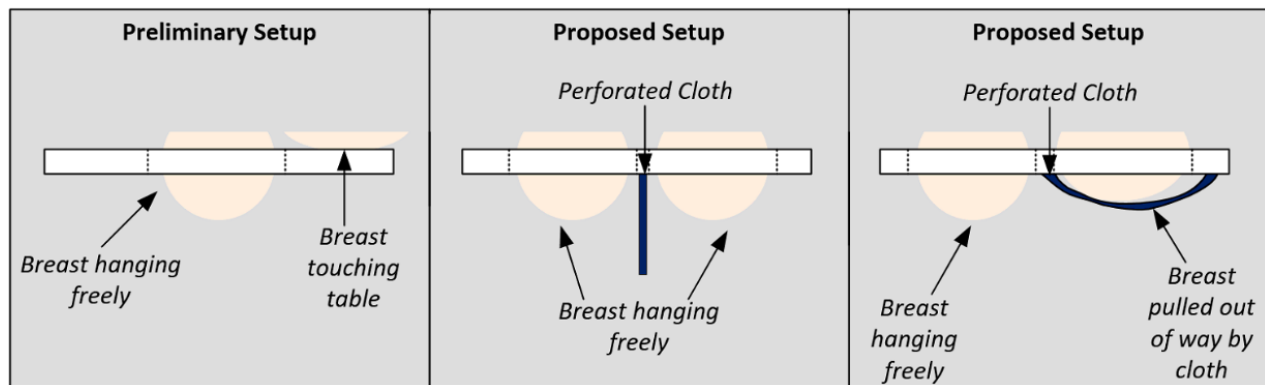


Figure 57. Close-up schematic (1st panel) the old imaging table with the subject lying on one breast, (2nd panel) the proposed imaging table with two holes and (3rd panel) the proposed table with one breast pulled aside with cloth.

5.3 Numerical Modeling

In addition to the proposed clinical changes, the numerical modeling process will also change. The numerical process discussed in Chapter 3 and Chapter 4 is highly dependent on the addition of MRI images. However, for the IRI-Mammo study and prospective large-scale clinical study, MRI images will not be available. This constitutes a different approach to create a patient-specific digital breast model. As discussed in Chapter 3, the intricacies associated with the breast can be difficult to capture without the use of MRI slices. The proposed additions include a mixture of IRI images and depth sensors to create the model.

Similar to the earlier approach, IRI images can be adapted to silhouettes and combined to create a rough model. However, because the IRI images are two-dimensional and cannot capture the intricate features, additional depth sensors will be added to find these geometries. The camera setup discussed above can be adapted to include two different depth sensors at different angles that capture the breast geometry prior to IRI image capture. A combination of the depth sensor data and IRI images will create the patient-specific breast model needed for numerical modeling and

tumor detection. The proposed digital breast model will go through a similar numerical modeling process as discussed in the current clinical study.

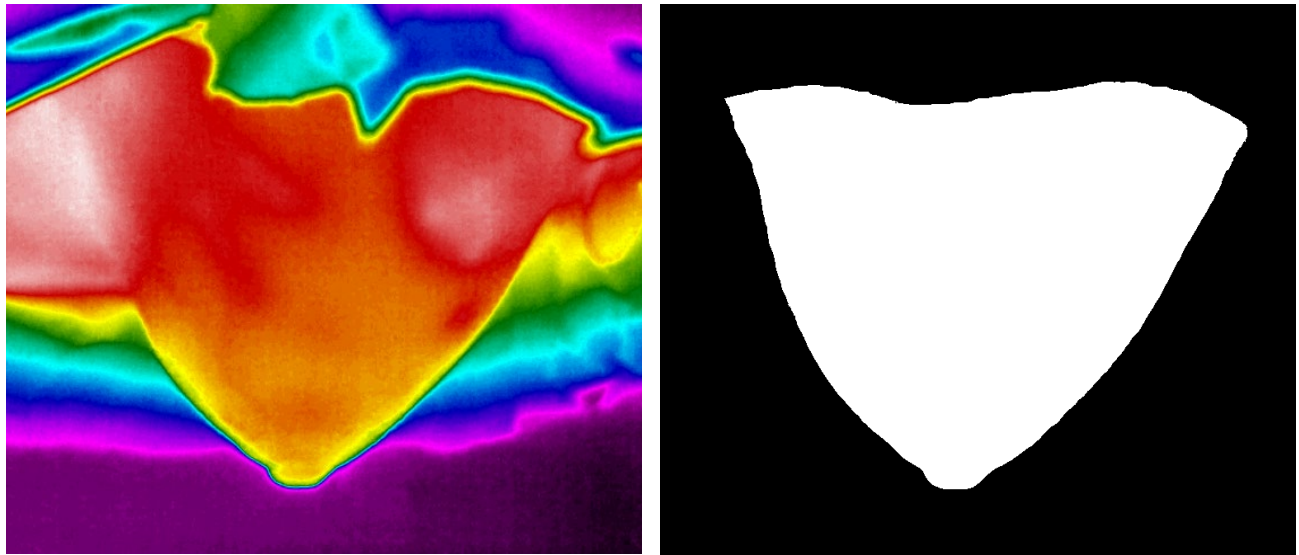


Figure 58. Edge of the IRI image found and silhouette created for patient-specific digital breast model without the need of MRI images.

5.4 Additional Changes

Additional modifications include clinical considerations and data management are presented here. In the current studies, the collected data primarily involve breast cancer and breast surgery history, hormonal changes, and screening reports (ultrasound, screening mammogram, diagnostic mammogram, and biopsy report, if applicable). While all of this is sufficient, future studies may want to add further medical history reports, especially factors that could thermally influence the body. This could include previous surgical history and alterations involving reproductive organs or hormonal changes. To truly determine the efficacy of the IRI method, a double-blind study should also be considered. This would mean the imaging personnel have no prior knowledge of the status of the patient being screened. Removing bias from the screening process would assist in a more accurate interpretation of the data and therefore a more accurate assessment of the sensitivity and specificity of the method.

Finally, for more rapid diagnosis and faster data sharing between all parties involved, a digital library could be employed to store relevant thermal and geometric data of the breasts. The library is where information or data is stored in electronic or other media forms. It may contain geometrical identifiers, thermal identifiers, and infrared images from different orientations and distances, patient details, tumor identifiers including size, shape and histology, details regarding how the information was obtained, computer generated thermal images and their geometrical, thermal identifiers and tumor identifiers. The tumor identifiers may include information regarding whether a tumor is present or not, its size, shape, pathology, and other tumor location details that enable location of the tumor in the breast. The thermal identifiers may include information on the tumor properties and how they affect the surface temperature profile. They will include information on maximum temperatures, minimum temperatures, and the gradient throughout the breast. The geometrical identifiers are identifiers that are related to the geometrical details of the breast. These could include size and shape of the breast and a detailed comparison to other patients already stored within the digital library. Data is currently stored in both hard copies and digital copies at RIT while the RGH staff has access to the medical reports for all patients. A more streamlined process should be created to share all data between all parties involved.

Chapter 6: Thermal Biomarkers

Breast cancer is not a uniform disease, and management is increasingly complex. Multiple factors need to be considered for optimal treatment and a trend is developing towards the practice of personalized medicine. With improvement in imaging technology, the hope is that we can detect cancer and differentiate aggressive tumors from the indolent tumors that can be safely monitored, sparing the subjects the potential risks of treatment. If optimized, the IRI approach discussed above has the potential to identify tumors at varying levels of aggression dependent on the pathological properties of the tumor.

Infrared imaging has the unique ability of capturing thermal activity in breast tissue resulting from a tumor. Thermal activity, characterized as thermal biomarkers, include cellular metabolism, increased vascularity due to angiogenesis, and increased blood perfusion which create areas of increased hyperthermia. Tumors have different levels of blood perfusion and metabolic activity. We therefore hypothesize that these different levels will result in varying thermal biomarkers that can be detected with IRI.

6.1 Gautherie's Work

Gautherie presented a model, described in Chapter 2, to compare tumor doubling time with respective metabolic activity. He also explored the effect of vasculature on the heat transfer properties in the breast (effective thermal conductivity) when a tumor is present. The fundamentals and key points of Gautherie's study are reiterated here.

In 1980, Gautherie [19] used a fine-needle thermocouple to measure the internal temperature distribution of breasts, both healthy and with cancer. Throughout his studies, approximately 58,000 patients were examined in the Department of Breast Diseases. However, because of the ethical nature of his study, only 147 patients were consenting and examined between 1969 and 1978. Due to the low technological advancements of the time, the only means of internal temperature measurement involved implanted probes into the breast tissue. Despite concerns of thermal and pathological alterations while the probes were implanted, no such evidence exists. Gautherie also reports that “this was confirmed by histologic studies following similar intratumoral investigations carried out on mice with breast carcinomas.” The probes (0.8 mm in diameter) were inserted in the breast tissue at varying depths in order to capture the evaluation of local temperatures and thermal conductivity. Two probes were inserted, one in the healthy breast and the other in the contralateral cancerous breast, in symmetrical locations. The probe in the cancerous breast was inserted into the tumor and verified to be in approximately the center of the tumor through a radiographic test. Thermal measurements were made at intervals of 5 mm.

6.1.1 Effective Thermal Conductivity

Although Gautherie performed many studies examining the efficacy of thermography, this study in particular investigates the “thermal phenomena associated with cancer growth, especially metabolic heat production, vascular changes, and circadian rhythms.” Perhaps most significant is Gautherie’s differentiation between thermal conductivity (k) and *effective* thermal conductivity (λ_e). The parameter λ_e was calculated in both the healthy and cancerous tissues through the use of the fine-needle probes, in *in vivo* conditions and after surgical resection. The effective thermal conductivity considers the convective heat transfer through the capillary vessels. To prove this, λ_e was measured in *in vivo* perfused tissue and *in vitro* excised tissue. Assuming a symmetrical

distribution of blood vessels and convective heat flow, the effective thermal conductivity was found to be significantly higher in perfused tissue. This conclusion makes logical sense as the convective heat transfer should be higher when blood vessels are actively present. Additionally, Gautherie mentions that the λ_e for cancerous tissues is much larger than that of healthy, alluding to the increasing presence of blood vessels due to angiogenesis. Overall, effective thermal conductivity combines the perfusion rate and the thermal conductivity of the breast tissue and tumor and provides a unique comprehensive thermal parameter that defines the heat transfer rate which can be employed in breast thermal models.

The graphs in Fig. 59, adapted and redrawn from Gautherie [19], show the effect of temperature and effective thermal conductivity as a result of a growing tumor. A probe was inserted into the breast, approximately 70 mm deep. It was placed into the breast with tumor, directly into the tumor, and into the same spot on the contralateral healthy breast. The first graph in Fig. 59(a) shows an increase in effective thermal conductivity (conductivity accounting for blood perfusion) in the breast with tumor, particularly where the tumor is within the breast. Additionally, in the areas surrounding the tumor, there is an increase in effective thermal conductivity. This could be due to the increase in vasculature and perfusion rate due to angiogenesis. The effective thermal conductivity of the healthy breast is seen to remain relatively steady. The second graph in Fig. 59(b) shows an increase in temperature vs the depth of the probe. In the healthy breast, the temperature steadily increases, as expected, as the depth moves deeper. The deeper the probe is in the breast, the closer to the chest wall and therefore closer to the internal body temperature of $\sim 37^\circ\text{C}$. However, in the cancerous breast, the increase in temperature is more striking and less gradual. The heat emanating from the tumor creates a sharper increase in temperature, closer to the internal body temperature, that steadily levels out further away from the tumor.

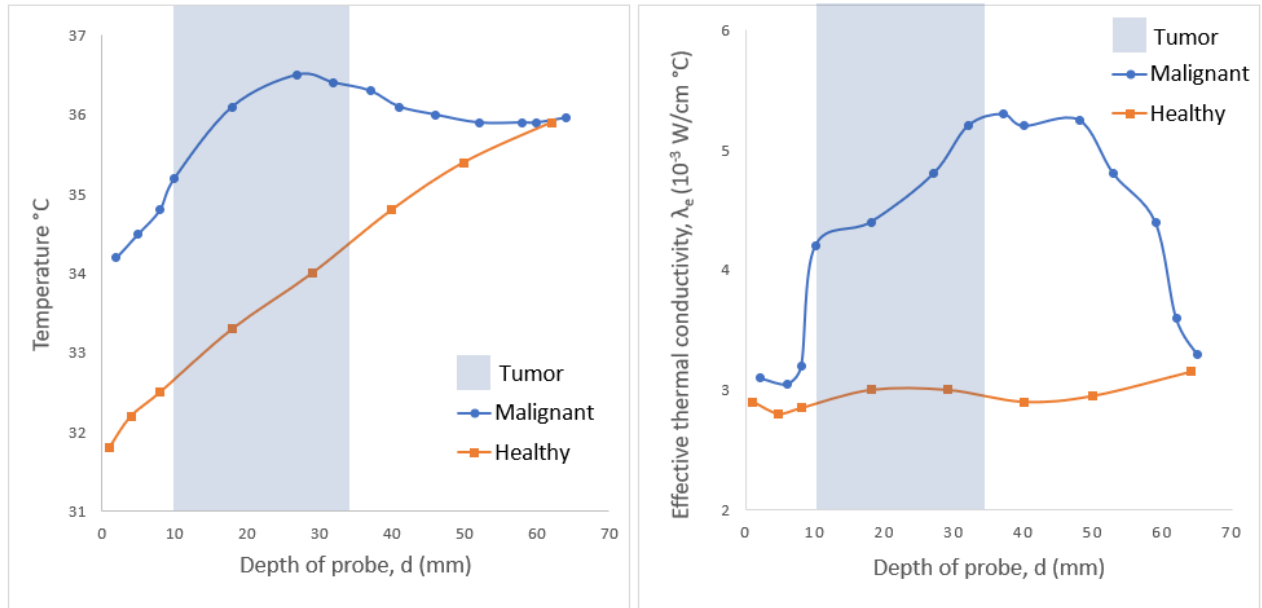


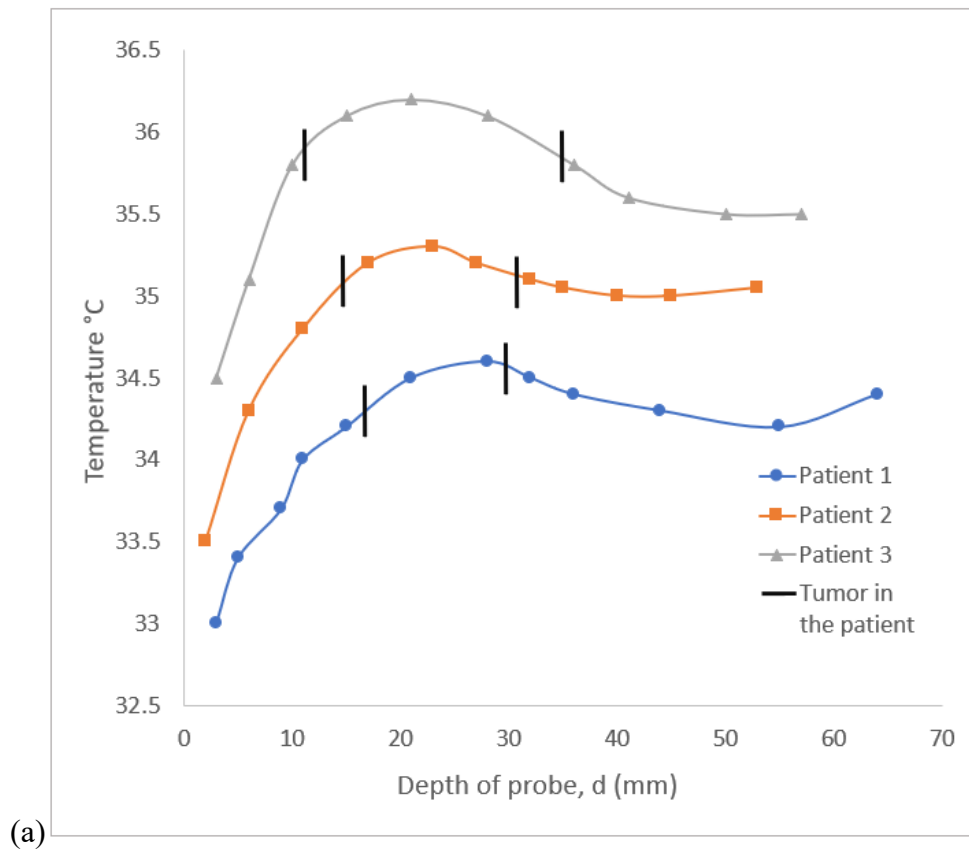
Figure 59. (Left) Temperature vs depth and (right) Effective Thermal Conductivity vs depth for malignant and healthy tissue, redrawn from Gautherie [19].

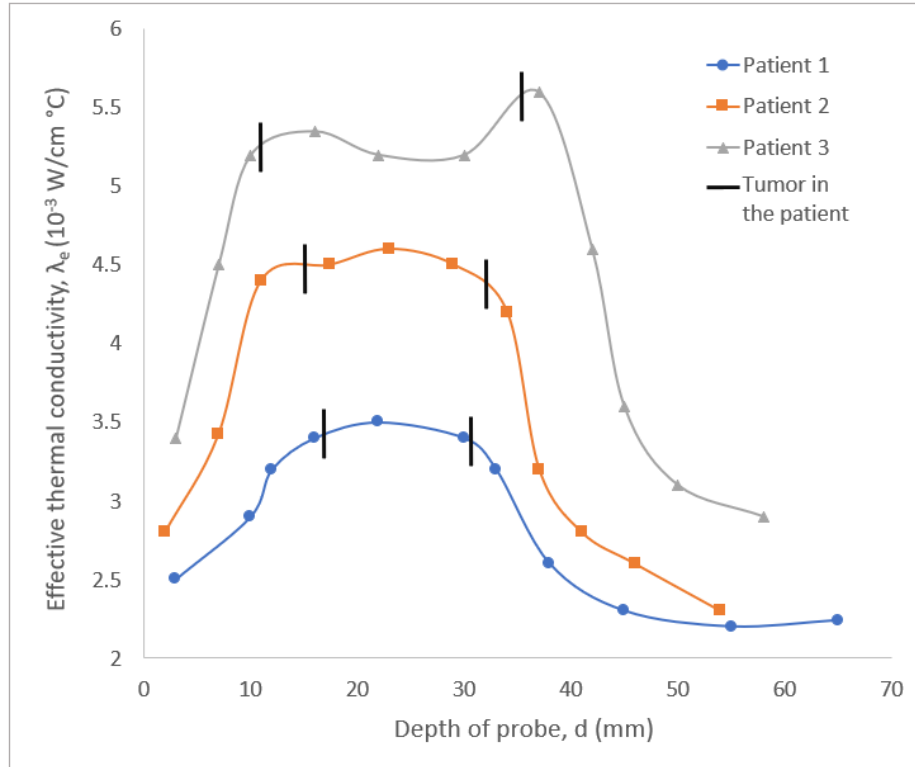
Gautherie used probes on 147 patients to differentiate thermal factors in cancerous and healthy breasts. He reports two major conclusions:

- Temperature and effective thermal conductivity higher in cancerous breast than in contralateral healthy breast. A ‘bell-shaped profile’ was seen in cancerous breasts. This could be due to the heat diffusing through the tissue from the tumor.
- Increases in temperature and blood flow around the tumor are well correlated. The greater the blood supply to a tissue, the greater the local metabolism and subsequently increased hyperthermia.

Gautherie postulated that the heat transfer in the breast occurs through ‘effective’ tissue conduction (conduction through the tissue and blood convection by capillary vessels) and convection through larger vessels. In Figure 60 (a) and (b), the progression of tumor growth and resulting thermal activity is examined until surgical resection. The graphs, redrawn from Gautherie [19], show the

natural growth of a tumor and the corresponding thermal influences. One notable difference is in Fig. 60(a) where there is a ‘dip’ in the effective thermal conductivity. This could be due to inner necrosis within the tumor where the center of the tumor, cut off from the needed blood and nutrients to favor growth and spread in the outer margins, begins to die off. If the necrosis within the tumor presents a ‘dead zone’ in terms of hyperthermia, this could potentially be indicative of more evolved tumors for future interpretation.





(b)

Figure 60. (a) Temperature vs. depth of probe and (b) effective thermal conductivity vs. depth of probe for three different breast cancer patients with varying tumor sizes, redrawn from Gautherie [19].

6.1.2 Metabolic Activity

Further evaluation of tumor effects on thermal activity is presented in an additional study focusing on 84 patients with tumors ranging from 0.9-3.8 cm. The tumor volume doubling time (DT) and metabolic heat production (q^*) were evaluated through the use of x-ray images recorded over an exponential timeframe. The following three categories of growth and relative metabolic heat production are discussed in Chapter 2 and reiterated here:

- Cancers with a fast growth rate ($DT \leq 150$ days) and intense metabolic heat production ($q^* \geq 20 \times 10^{-3} \text{ W/cm}^3$)

- Cancers with slow growth rate ($DT \geq 250$ days) and low metabolic heat production ($q^* \leq 10 \times 10^{-3} \text{ W/cm}^3$)
- Cancers with intermediary values of DT and q^* , classified into (1) or (2) if lymphatic spread is found or not.

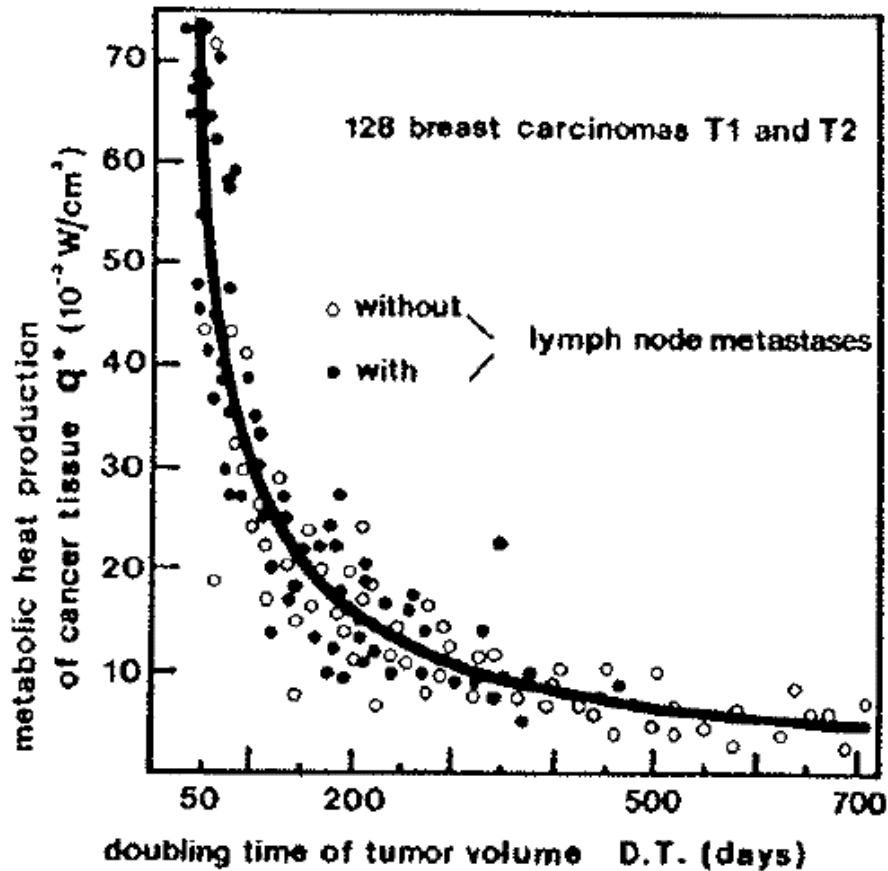


Figure 61. Relationship between metabolic generation and doubling time.

Ultimately, Gautherie used the plot seen in Fig. 61 to develop an equation to calculate the metabolic heat generation rate of a tumor. The equation, seen below, is used in our IRI-MRI study to calculate the metabolic heat generation rate using the tumor diameter to detect and localize tumor within the breast.

$$q_t = \frac{3.27 \cdot 10^6}{468.5 \ln(100d_t) + 50} \quad (12)$$

Additionally, following surgical resection of the tumors reported in Fig. 61, histologic examination was completed to determine lymphatic metastases. The graph denotes which cancers had spread to the surrounding lymphatic system, upgrading the stage of breast cancer. “Most cancers with rapid growth rate and high heat production exhibited signs of dissemination.” This indicates that the metabolic heat production is calculated to be higher in tumors at a more advanced stage.

6.1.3 Internal Rhythms

Similar to other authors, Gautherie mentions the concern surrounding the time when imaging takes place. The ovulation cycle can influence mammary blood flow, causing additional fluctuations in effective thermal conductivity. An additional study is carried out examining the cyclical rhythms on mammary skin temperature. Gautherie examined 26 patients with breast cancer ranging from 37-76 years old. The patient’s behavior and daily activities were heavily monitored and are reported in Table 23. The temperatures on the cancerous and healthy breast were measured chronologically.

Table 23. Structured regiment for patients in Gautherie’s study for circadian rhythm control.

Retired to Sleep	9:30 PM		
Awoke or Awakened	7:00 AM		
Meals	7:00 AM	12:30 PM	6:30 PM
Ambient Conditions	22 – 24 °C		

Two groups were examined. The first group had 15 cases and the second had 11 cases. Healthy breasts showed circadian, circaseptan, and circatrigintan rhythms are consistent over 24 hours, 7 days, and 29 days (approximate length of menstrual cycle).

Conclusions from the first group (15 cases):

- In the cancerous breast, the circadian rhythm was shortened, and significant changes were noted at 21 hours, 42 hours, and 84 hours.
- Circadian rhythm of skin temperature was desynchronized on cancerous breast.
- Rhythms on the cancerous breast replaced by additional periods that do not correspond to known cyclic patterns.
- These patients had a rapid growth rate ($DT < 100$ days) and high q^* (> 30 mW/cm³).
- Overall, more rapidly growing tumors are demonstrating extensive changes in normal cyclical patterns.

Conclusions from the second group (11 cases):

- Circadian rhythm of cancerous breast 24-hour synchronized.
- Rhythms are different from each other in cancerous and healthy breasts.
- These patients had relatively slow growth rate ($DT > 200$ days) and low q^* (< 15 mW/cm³).
- Pathology of tumors in second group are well differentiated.
- Overall, there are still differences between the cancerous and healthy rhythms however, the changes appear to be lesser comparably. This could be due to histology and growth rate of the tumors.

Additionally, he performed a series of thermograms recorded every hour between 8 AM and 9 PM on another group of patients at the hospital. The resulting changes in temperature from different

times during the day have led to a conclusion that morning is an ideal time for thermographic imaging. Gautherie discusses that there are potentially two distinct categories of human breast cancers: those that alter the circadian variations and therefore the breast skin temperature and those that do not.

Finally, Gautherie discusses the potential of abnormal thermograms as classifiers for high risk patients or early breast cancer. Primarily, adding thermal classifications when cancer is given a “stage”. The TNM (primary tumor, lymph nodes and distance metastasis) nomenclature discussed in Chapter 1 involves classification of cancer based on the presence of malignant cells in various regions of the body. Gautherie discusses the addition of a fourth classifier called “Q” dependent on intensity, extent, and pattern of hyperthermia on the resulting thermogram. However, prior to additional classification, further understanding on the complex relationships in the body is needed.

The work presented by Gautherie has great potential for the future of infrared imaging. Developing a better understanding of the heat transfer within the breast and how the body can influence tumor growth will further optimize the technology. Most notably, the effective thermal conductivity within the cancerous breast can help with numerical modeling. The models presented in Chapter 3 and 4 utilize Gautherie’s work to calculate tumor doubling time and metabolic heat generation. The thermal conductivity is also calculated to determine and verify breast density, but the *effective* thermal conductivity is not considered. This is primarily due to the complications associated with calculated perfusion rate within the breast. The current model utilizes a constant perfusion rate from literature as opposed to a variable rate. However, many tumors grow at different rates with some more aggressive than others. The perfusion rate into the tumor and within the breast will vary for each patient, cancer type, and tumor pathology. The following section discusses an additional solution to perfusion rate calculation within the breast for further model optimization.

6.2 Calculating Blood Perfusion

As referenced in Chapter 1, angiogenesis is an essential process in cancer growth. Tumors are seen to have a high amount of angiogenesis activity in order to grow and spread to other parts of the body. The process of angiogenesis is highly complex, and vascular endothelial growth factor (VEGF) produced by growing tumors plays a predominant role [132]. Garcia-Figuerias et al. [132] discuss the use of imaging techniques (MRI, CT, ultrasound and PET) to indirectly measure angiogenesis and continued growth. Computed tomography (CT) perfusion involves the use of x-rays to examine blood perfusion within the body, primarily to the brain [133]. A contrast material is used to enhance the tumor vasculature network in the CT. The authors discuss the potential of using CT, particular to characterize lesions within the body. Tumor vasculature structural abnormalities, particularly an increase in capillary permeability and tumor perfusion, are suggestive of malignancy.

Satoh et al. [134] utilized CT Perfusion to study the blood flow in gastric cancer. Approximately 50 patients were enrolled in the study with varying stages of gastric cancer. More advanced cases were seen to have lower blood flow, which is consistent with Gautherie's study. The authors were able to visualize decreasing tumor perfusion rate with increasing levels of malignancy. Additionally, they found a correlation between tumor blood flow and tumor depth. Despite the higher levels of cancer stage, none of the tumors presented in this study had necrotic tissue. They present P-CT (perfusion CT) as a potential imaging technique in inoperable cases, a marker for tumor perfusion, and potential to personalize treatment dependent on tumor characteristics.

Finally, a study presented by [135] measures the vascular networks in malignant breast tumors through diffuse correlation spectroscopy (DCS). DCS measures blood flow using the intensity fluctuations of near-infrared light intensity. Most notable is that DCS does not involve the injection

of a contrast agent. Satoh et al. mention in their study the possible impact contrast agent has on the microenvironment of the tumor. Removing this element may be important in determining perfusion rate and other correlations between blood flow and microenvironment. Thirty-two patients with biopsy-proven breast cancer were imaged in this study. Using this technique, they were able to differentiate breast cancer from surrounding normal tissue. This suggests that the blood flow in the tumor can be a useful marker, particularly when differentiating malignancy.

In our study, the perfusion rate for healthy tissue and tumor were assumed to be 0.00018 and 0.009 ml/s/ml, respectively [136]. However, little data is available on a general guideline for perfusion rate within the breast. In order to have a more optimized model, a perfusion rate range is proposed as a first step. To find this range, we propose the use of angiograms to study blood flow through the body, both in healthy tissue and in the presence of malignant cells. An angiogram utilizes x-rays to capture blood flow throughout the body for diagnostic purposes. A contrast agent is injected into the arteries to improve visibility on an x-ray. Angiograms are generally used to view blood flow but is occasionally used to examine blood supply to a tumor. Several examples of the techniques discussed above are seen in Fig. 62, 63, and 64.

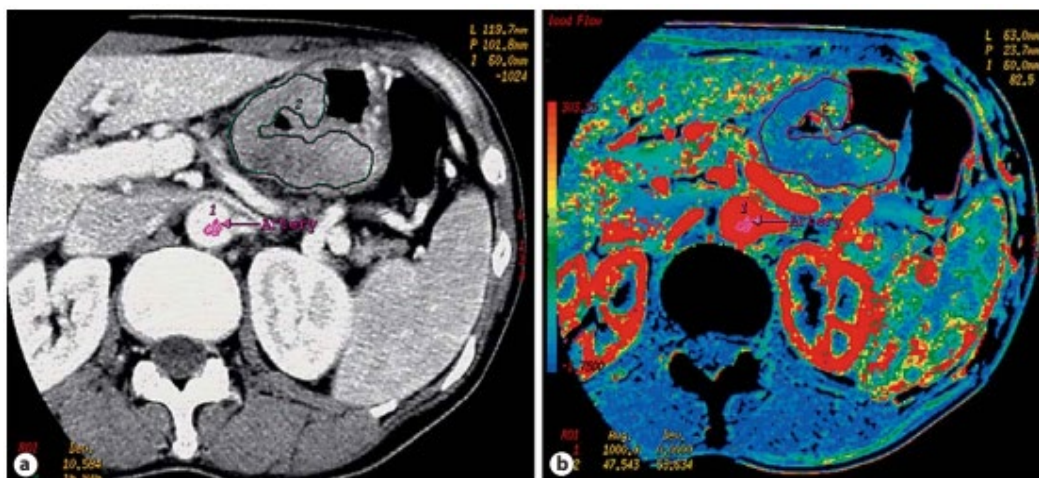


Figure 62. (a) P-CT image of gastric cancer with indication of tumor and (b) Perfusion map of blood flow. An average blood flow of 49.8 ml/min/100 g was calculated [134].

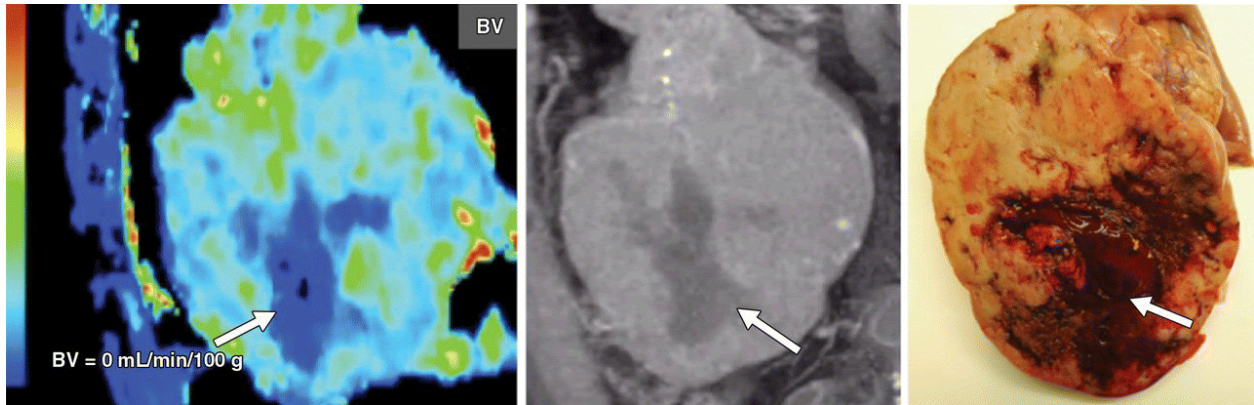


Figure 63. Malignant gastrointestinal stromal tumor. (left) Blood volume map, (center) maximum intensity projection image and (right) physical specimen. Authors believe that areas pointed out with arrows are suggestive of necrosis [132].

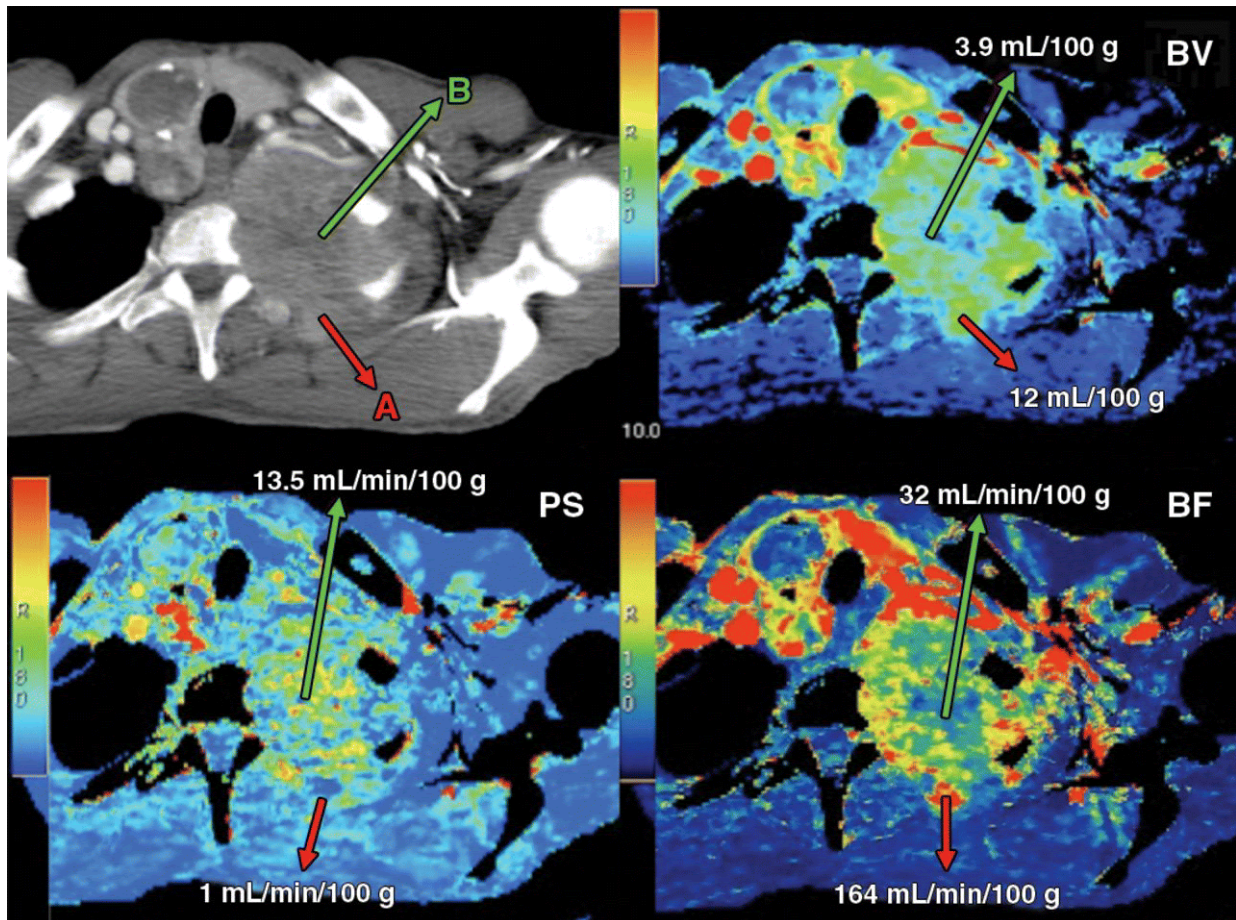


Figure 64. (top left) A conventional CT image, (top right) CT parametric map of blood volume or BV, (bottom left) CT parametric map of permeability-surface area product or PS and (bottom right) CT parametric map of blood flow or BS [132].

Determining blood perfusion rate in a patient can be difficult, especially with the random nature of tumor angiogenesis. Using CT or angiograms to measure the perfusion rate through breast tissue is not necessarily the future path of this study. However, using pre-existing angiograms with varying conditions, we can develop a range of blood perfusion rates to enhance the existing models. By varying blood perfusion within our numerical model, we can examine the subtle thermal variations and further optimize our detection process.

6.3 Thermal Biomarkers

Many tumors are classified in terms of their cellular structure or extent in the body. However, perhaps researchers should consider the addition of internal factors characteristic of tumor hyperthermia. Further classifications could assist in additional screening, interpretation, and eventual diagnosis.

Based on the above discussion, it is noted that there are thermal biomarkers indicative of breast cancer. We postulate that perfusion rate, metabolic activity and effective thermal conductivity are highly indicative of breast cancer. These are all values that, using computational methods and theoretical calculation, we can evaluate. The values used in our initial numerical methods (seen in Chapter 3 and repeated in Table 24 below) are derived from several different authors. These values come from different authors examining different portions of the breast and body.

Table 24. Values of the parameters used in the simulations.

Parameter	Value
Thermal conductivity (k), $\text{W m}^{-1} \text{ }^\circ\text{C}^{-1}$ [19]	0.25 – 0.8
Perfusion rate of healthy tissue (ω_h), s^{-1} [19]	1.8×10^{-4}
Perfusion rate of tumor (ω_t), s^{-1} [19]	9×10^{-3}
Metabolic activity of healthy tissue, W/m^3 (q_h) [19]	450
Metabolic activity of tumor (q_t), W/m^3 [19]	From (2)
Temperature of arteries (T_a), $^\circ\text{C}$ [137]	37
Specific heat of blood (c_b), $\text{J kg}^{-1} \text{ }^\circ\text{C}^{-1}$ [137]	3,840
Density of blood (ρ_b), kg m^{-3} [137]	1,060
Core temperature (T_c), $^\circ\text{C}$ [19]	37
Ambient temperature (T_∞), $^\circ\text{C}$ [138]	21
Heat transfer coefficient, $\text{W m}^{-2} \text{ K}^{-1}$ [139]	13.5

The modeling process utilized in the preliminary study utilizes the thermal characteristics of a thermal image and compares with a patient-specific digital breast model in order to find the position and size of a tumor. The process is primarily dependent on the understanding of bioheat through the body and the metabolic activity of the tumor. The metabolic activity, calculated using Gautherie's model, utilizes the diameter of the tumor and the volumetric doubling time. This model presents a fundamental understanding of the metabolic rate of growing tumors and is vital in advancing thermography technology. The model also discusses the changing thermal conductivity of the breast dependent on the density of vasculature within the tissue. An increase in thermal conductivity and subsequently vasculature can be indicative of a growing tumor within the region.

As seen in Figures 59 and 60, the presence of a tumor drastically alters the temperature within the breast. The presence of additional vasculature through angiogenesis increases the perfusion rate

and effective thermal conductivity of the tissue. The variables and constants in Table 24 consider both healthy and cancerous tissue values. However, to further update and optimize our modeling process, we must consider updated perfusion rate values.

The first step involves obtaining angiograms at RGH and determining the maximum and minimum observable blood perfusion rates. These angiograms do not necessarily need to be breast cancer related, but the vessel size involved should be comparable. Using these angiograms, the relative perfusion rate within the body will be determined. Due to the presence of disease and other maladies within the body, there will be a natural range of values. Next, a parametric study will be employed to examine the range of blood perfusion values in ANSYS with our previously tested models. The resulting images will validate Gautherie's theories with increased effective thermal conductivity dependent on the aggressivity, size, and metabolic rate of the tumor. Additionally, the range of perfusion rate values will provide insight on the skin temperatures seen in infrared imaging. Our previous model predicted the size and placement of tumor within the breast but there were cases where our model was 'off'. While uncertainty is to be expected in any complex model, it can be assumed that the addition of perfusion rate and effective thermal conductivity will provide a more comprehensive model. Finally, perfusion rate will be added into the model parameters as a variable instead of a constant. The variation in tumor angiogenesis could depend on the placement, size, or pathology of the mass. These are all suggested future correlations to further optimize the computational process.

6.4 Tumor Aggressivity

Classifying thermal biomarkers will not only assist with the development of IRI screening techniques but will also assist with determining tumor aggressivity. Differentiating between highly aggressive tumors and indolent masses is essential in reducing patient anxiety, medical cost, and

time for all parties involved. Overdiagnosis is the identification of a condition that would not result in any symptoms or affect one's lifespan [140]. By diagnosing indolent breast cancers through routine screening mammography that would not have otherwise significantly progressed, there is no overall clinical benefit. This closely relates to overtreatment, which refers to the management of a breast cancer through surgery, radiation, and chemotherapy and the adverse effects associated with them for no clinical gain. Overdiagnosis is difficult to definitively measure, but studies estimate that screening mammography results in 1-10% cases of overdiagnosis [141]. This can occur more frequently in aging women as overall mortality from other causes increases but can also happen in younger subjects that suffer from unrelated life-threatening conditions limiting their life expectancy.

The US Preventive Services Task Force (USPSTF) now recommends that women begin biennial screening mammography at age 50. This recommendation is based on the idea that there will be decreased incidence of overdiagnosis when compared to annual screening starting at age 40. The overdiagnosis and overtreatment of DCIS has increased recently with the increased utilization of screening mammography [142]. Prior to the institution of routine screening mammography, DCIS accounted for less than 5% of cancers [143], but now represents approximately 25%. Some diagnosed cases of DCIS will never progress to invasive cancer [144], [145] which is thought to be one of the risks of routine breast cancer screening. The natural progression of DCIS is not fully understood, but studies have shown that low and high-grade DCIS likely follow separate developmental pathways and low-grade DCIS tends to progress to low-grade invasive carcinoma that is well differentiated [146], [147]. Oftentimes low-grade DCIS may never actually progress to any meaningful invasive disease that would affect mortality [148]. Despite this, National

Comprehensive Cancer Network (NCCN) guidelines still recommend treating DCIS similar to an early invasive cancer.

Multiple trials are currently taking place to determine whether biopsy proven low-risk DCIS can be safely and actively observed without affecting invasive cancer-free survival. The Low-risk DCIS (LORD) trial from the Netherlands, the Low-risk DCIS (LORIS) trial and European Organization for Research and Treatment of Cancer (EORTC) from the UK are evaluating observation against surgical management of low-grade DCIS [149], [150]. There remains the possibility that surgical management and utilization of radiation therapy could qualify as overtreatment in these diagnosed low-grade DCIS lesions. With advancements in diagnostic methodology, the consequences of overtreatment can be tamped down with more appropriate individualized management or active observation. None of the current imaging technology in widespread use in breast imaging, i.e. mammography, ultrasound and MRI can reliably differentiate indolent from potentially aggressive DCIS. Grana-Lopez et al. [151] explored the utility of metabolic imaging with dedicated breast positron emission tomography (dbPET) to differentiate indolent from potentially aggressive DCIS. FDG-dbPET measures glucose metabolism reflecting the biological activity of cancer cells. They found that metabolic imaging with PET could potentially differentiate indolent from aggressive DCIS that can be managed by active monitoring. The sensitivity and specificity of dbPET to differentiate between indolent and potentially aggressive DCIS were 90% and 92%, respectively [151].

Developing correlations between tumor biology and thermal biomarkers is vitally important to determine the correlative nature of deadly vs non-deadly breast cancers. The metabolic activity, calculated using Gautherie's model, utilizes the diameter of the tumor and the volumetric doubling time. This model presents a fundamental understanding of the metabolic rate of growing tumors

and is vital in advancing thermography technology. The model also discusses the changing thermal conductivity of the breast dependent on the vascularity within the tissue (effective thermal conductivity). An increase in effectively thermal conductivity and subsequently vasculature can be indicative of a growing tumor within the region. Modifying the input parameters in future models while maintaining the detection and localization algorithm (and verified through subsequent mammograms) will help in determining tumor aggressivity. Specifically, the predicted thermal conductivity, perfusion rate and metabolic heat generation can be compared with normal tissue properties and properties of aggressive tumors as outlined in Gautherie's work [19] to determine whether the tumor is aggressive or indolent.

Chapter 7: Conclusions

7.1 Summary of Work Done

Breast cancer is a debilitating and widespread disease, affecting thousands around the world every year. The screening techniques currently available have many positive attributes. But unfortunately, the patient discomfort, added radiation or contrast material, and high cost can be problematic. There are several key populations with a higher need for more accessible, safer, and inexpensive screening.

- Low income populations – Early breast screening is less accessible. There is a need for a more portable, easy-to-use, and inexpensive breast cancer screening technique,
- Younger patients – The mammographic radiation has been known to have negative effects, particularly in younger patients. Mammography is not recommended for women younger than 40 years. Traditionally, ultrasound and physical examination are used for younger patients.
- High risk – Subjects are classified as high risk either due to a genetic predisposition or other biological/environmental factors. These subjects are strongly encouraged to begin annual breast cancer screening earlier than most women.
- Medical issues – Women with allergic reactions to contrast material or issues with claustrophobia are unable to receive an MRI. Additionally, women with pacemakers or other medical implants are not able to utilize an MRI for more advanced screening.
- General population – The lower cost of thermal imaging makes it a more cost effective adjunct to mammography particularly in a larger population of women at intermediate risk

or those with dense breast tissue (40%-50%) in whom mammography alone or in combination with ultrasound is inadequate.

This study focused on the use of steady-state infrared imaging to screen patients with biopsy-proven breast cancer. The following points present the work completed in this thesis.

- Patient population of IRI-MRI study involved patients with biopsy-proven breast cancer prior to surgical resection. The MRI and pathology data were utilized for scientific validation. MRI images were also used to help generate the patient-specific digital breast model for detection and localization process.
- The patient data of the IRI-MRI study is presented including temperature changes between the breasts. Details on tumor placement and thermal differences are presented. Additional pathology can be seen in the Appendix as well as an example patient report.
- For the second phase of the clinical study, the specificity of the technology is needed. A new patient population, IRI-Mammo, introduced patients with suspicious masses prior to biopsy. These patients were screened as suspicious on mammography but had yet to receive a biopsy. All of the patients screened up to this point are benign.
- The patient data of the IRI-Mammo study is currently limited due to limited patient numbers. The data presented here shows the BI-RADS classification and patient characteristics. The introduction of the global COVID-19 pandemic has limited the research study and patient recruitment at the hospital.
- Utilized steady-state infrared imaging without the use of cold stress. Ten minutes were allowed for the breast to acclimate to the ambient room conditions. The entire imaging process lasted approximately 25 minutes for acclimation and imaging of both breasts.

- The modeling portion performed by Gonzalez-Hernandez [60] utilized clinical images to create a digital model. Further iterations will require IRI images and depth sensor data.
- Using a combination of the collected IRI images and model, detected and localized tumor in seven patients from the IRI-MRI study.
- Design of a suggested large-scale clinical study including patient population, clinical changes, and modeling changes. Additional future recommendations towards the efficacy of this technology are presented.

7.2 Conclusions

Thermography or Infrared Imaging (IRI) is a cost-effective, portable, and noninvasive technique for breast cancer screening. However, previous studies have failed to convince the medical community of the merits of the technology. Previous thermography studies have included inconsistent screening protocol, lack of scientific validation, and empirical human interpretation. The clinical study discussed here attempts to address the negative qualities of previous approaches while also introducing new methods for more effective imaging. Additionally, human bias was removed from image interpretation through patient-specific digital breast model generation. The major works of Gautherie are introduced as a thermal classification system, pinpointing biomarkers in the breast associated with abnormal pathology. Finally, the modality presented has paved the way for a large-scale clinical study and suggestions on the design and implementation are discussed. The main conclusions of the approach are presented here.

- Designed a clinical study to determine the efficacy of infrared imaging for early breast cancer detection.

- Developed a screening protocol considering previous clinical studies, patient comfort, and full-breast views for more accurate infrared imaging.
- Validated clinical approach using corresponding images and patient reports (MRI, mammography, and ultrasound).
- Two studies were conducted: IRI-MRI where we screened 30 patients with biopsy-proven breast cancer and IRI-Mammo where we screened 6 patients with suspicious mammograms. Ultimately, the two populations are aimed at determining the sensitivity and specificity of our method.
- Acclimation of patients is vitally important, particularly in a steady-state test without the use of a cold stress. We observed significant temperature changes over a 10-minute time period, altering the thermal images. At least 10 minutes are required for proper acclimation to the room temperature although time of day and year may influence this. Acclimation time and ambient conditions will continue to be explored for further optimization.
- Focused on proper image analysis without bias human interpretation by developing a patient-specific digital breast model using MRI images and edge detection software. The breast model was created and used by Gonzalez-Hernandez [60], [125], [152] for the detection and localization process.
- The digital breast model developed here can be effectively utilized to provide an accurate representation of heat transfer within the breast.
- Gautherie's major works are considered significant as a blueprint for thermal activity within the breast. The key points are discussed including effective thermal conductivity, metabolic heat generation, natural body rhythms, and the thermal influence on the breast

and infrared imaging. A thermal classification system is presented to further optimize image interpretation and screening protocol.

Future recommendations are presented to improve the processes of IRI and modeling. A design is presented for a large-scale clinical study in Chapter 5 and additional recommendations are presented in Chapter 8. The major points are summarized here.

- The recommendations proposed in Chapter 5 discuss the design of a large-scale clinical study including changes to the screening setup (camera and imaging table), patient population and sample size, collected clinical data and patient protocol.
- Animal studies or experimental phantom models can be used to study IRI techniques and detection methods without the need for patients, especially considering the current global circumstances (novel coronavirus).
- Further image interpretation techniques and detection methods are discussed to differentiate between vasculature and tumor heat signatures.
- Additions to the modeling process primarily involve updates to the digital model generation and CFD process, allowing for standalone IRI without the need for MRI. The imaging setup and image interpretation could be upgraded to ensure more rapid screening and diagnosis while also improving patient comfort.

The results from this multidisciplinary study have shown great potential for this modality, especially with the combined imaging/digital model approach. Utilizing medical and engineering knowledge has led to a scientifically valid method with the patient at the center of development.

The future of thermography is bright and there are many different avenues for further study.

- Despite the bad reputation of thermography in previous studies, this novel work combining infrared imaging and computational methods has great potential to rapidly screen a wider subset of patients, leading to several major advancements in breast cancer imaging:
 - The potential for personalized medicine and reduction of overdiagnosis/overtreatment. Our method, once refined, can be used to determine whether a patient needs treatment (that could potentially negatively influence health further) or disease monitoring.
 - Access to a screening method that is inexpensive, nonradiative, no contact, and noninvasive.
 - Rapid screening and diagnosis for a larger subset of patients. Particularly for younger, high-risk, or rural populations that do not have sufficient access to screening.

Thermography holds great potential as an adjunctive modality for breast cancer screening, particularly for younger populations, high risk populations, or those in rural areas. The technique has been studied for over half a century, yet thermography is widely misunderstood by the medical community. Many studies in the past have utilized varying methods and protocols that may have skewed results or painted thermography in a bad light. Nevertheless, the positive attributes associated with the method potentially outweigh the negative results of the past. The method is inexpensive, nonradiative, and highly accessible, allowing for wider population screening. Taking the many attributes discussed above into consideration, further study into the use of thermography by the medical community is warranted.

7.3 Research Contributions

7.3.1 Technical Contributions

Major technical contributions involve the clinical imaging process and thermal biomarker classification. This work provided a novel clinical study aided by computerized digital image processing to detect breast cancer. The findings have been validated with MRI images for each patient. The following components were developed to ensure valid experimentation while considering ethical considerations: IRB documentation, patient protocols, an image acquisition system (camera setup and screening table), and the necessary tools needed for image analysis without human interpretation. Further, the developed method provided insight into infrared features corresponding to other biological images, pathology reports and patient history. The clinical work was done in collaboration with Dr. Phatak, Dr. Dabydeen, Dr. Medeiros, Dr. Godbole, and the Clinical Research Team at RGH and the image analysis was done at RIT. This work resulted in the following contributions in the field of breast cancer detection:

Major Contributions

- Designed a clinical study to determine the efficacy of infrared imaging for early breast cancer detection and developed an approach to evaluate the method. The novel method here combines steady-state infrared imaging in the prone position and computerized digital modeling for detection and localization.
- Identified patient populations for two studies: IRI-MRI and IRI-Mammo. The first population (IRI-MRI) provides patients with biopsy-proven breast cancer to determine the sensitivity of the method. The second population (IRI-Mammo) provides patients with

suspicious screening mammograms classified as BI-RADS 3, 4 or 5 to determine the specificity of the method. Both of these studies are actively ongoing.

- Obtained clinical IRI images of 35 patients from two different patient populations: (1) patients with biopsy-proven breast cancer (30 patients) and (2) patients with suspicious screenings (6 patients).
- IRI approach validated using clinical data from subsequent MRI images, mammograms, and pathology data.
- Developed the screening protocol and process including patient flow, patient questionnaire with internal and external influencers, patient protocols, patient consent forms, and IRB documentation.
- Determined an acclimation time of 10 minutes with a room temperature of approximately 21°C to reach proper steady state conditions. Identified that this period was sufficient to cool the breast down considerably for more accurate imaging.
- Identified the tumor in the breast of seven patients, localizing the tumor diameter within 2 mm and the tumor placement within 7 mm [60].
- Working with the RGH clinicians, introduced a thermal biomarker classification system to further optimize the computerized digital imaging process and identify tumor aggressivity. This work provides the basis for a larger study focusing on correlations between tumor pathology and thermal profiles on the breast surface.
- Identified key areas of improvement for further model development including patient specific digital model without MRI.
- Discussed future recommendations for a suggested large-scale clinical study. The recommendations presented include a statistically significant patient population, updates

to the screening setup for more optimized imaging, and a modeling process without the need for MRI images.

- Further clinical research needed for developing IRI as an adjunctive screening technique to mammographic screening is outlined.

Other Contributions

- Worked closely with RGH clinicians and research teams, participated in self-learning from cancer experts, and witnessed a surgical mastectomy and lumpectomy to develop a better understanding of breast anatomy, cancer metastasis, and tumor biology.
- Published several peer-reviewed journal and conference articles and a non-provisional patent application.
- Assisted in the writing and development of thirteen grant applications to various national, state, and local government entities.

7.3.2 Societal Contributions

Societal contributions primarily involve developing a technique that has great potential to help many people. I have thoroughly enjoyed working with patients and a disease that is so widespread across the world. When I finished my bachelor's degree, I promised to use my degree and my skills to help other people. Working in the hospital with breast cancer patients has been incredibly humbling. I have had family members and friends with cancer and have felt the impact of a loved one struggling against a terrible disease. But working on this study has shown me another side of cancer, a side filled with virtue and strength. Many of the women I have screened are in a whirlwind, about to get a tumor removed or their entire breast removed. It has been an incredibly

humbling experience working with these patients, all of whom are volunteers. I feel strongly that the goal of engineering is to contribute to the improvement of people's lives wherever they exist on this planet. While this technology is still in the early stages, it has immense potential. In the words of one of the powerful women I have screened, "This may not help me, but it could help my granddaughter."

Chapter 8: Recommendations for Future Study

Based on current trends, thermography research has increased greatly over the past few decades. The need for inexpensive and reliable breast cancer screening methods has been steadily growing, particularly in low-income countries where common diagnostic techniques are not accessible. Methods such as thermography are highly portable, more comfortable, and inexpensive compared to other commonly used techniques. Despite the innovation in newer screening methodology, several factors should be considered for future success. In addition to the suggestions for a large-scale clinical study presented in Chapter 5, the recommendations for future study are presented here including changes to clinical setup, image interpretation, and non-human study.

8.1 Adjunctive Technique

The BCDDP considered thermography as a replacement for mammography when they began their study. However, thermography, similar to other modalities, is not meant as a replacement but instead as an adjunctive technique. For future studies observing thermography as a screening technique for breast cancer, authors should approach their studies using thermography in adjunct to a scientifically validated technique, such as mammography. Additionally, combining techniques has proven an increase in sensitivity for screening. The decision for additional screening is often made on an individual basis by considering breast density and other risk factors. Women at high risk, such as women with >20% lifetime risk or known BRCA gene mutations, are screened using mammography and MRI annually. Combining screening methods or allowing for earlier screening (ultrasound and thermography are perfectly safe for women under the age of 50) may be key for earlier diagnosis.

8.2 Screening Setup

In addition to an added perforated cloth in between the two breasts, discussed in Chapter 5, adjustable holes could be added to fit the patient. The table and the imaging system are designed to accommodate different ranges in breast size, shoulder width, body contour, and weight. In order to have one table that matches all patients, it can be made adjustable. A top view and bottom view of the new table with modular design is seen in Fig. 65.

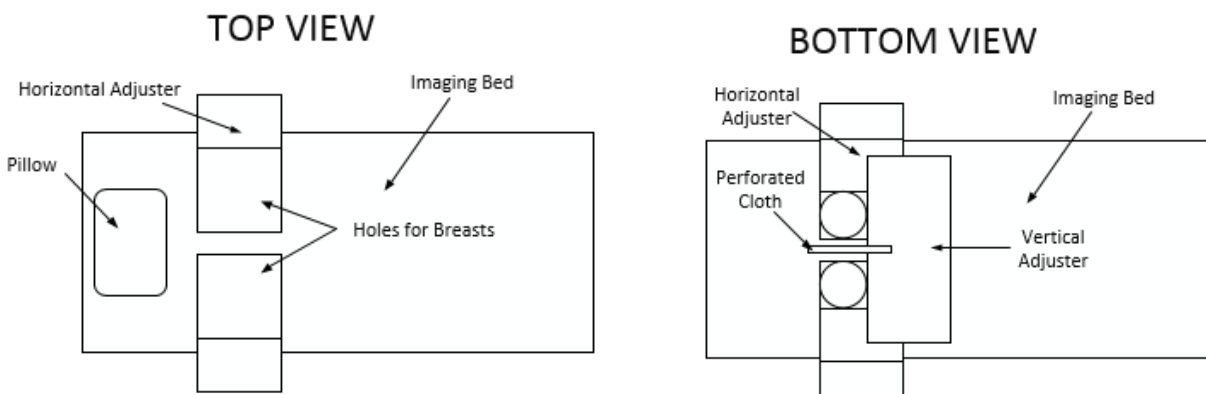


Figure 65. A top view (left) and bottom view (right) of a clinical bed with two holes and modular pieces to fit each subject.

There are modular pieces in the horizontal and vertical directions for each breast hole. When the subject lies on the table, the modular pieces will be adjusted to fit their breast size and weight. Once everything is adjusted accordingly, the perforated cloth will pull one breast to the side (Fig. 3C) and the acclimation period will begin. Extra padding will be added between the two modular holes to ensure subject comfort. The perforated cloth serves the function of pulling the non-imaged breast away so that clear access can be achieved for the IR camera. It needs to move the breast without causing significant thermal changes due to insulating effect. The perforations serve the purpose of providing air cooling while the breast is moved away. The perforated cloth may be replaced with a mesh, be made of different materials including wire, polyester, nylon, etc. Other

potential modular designs could include a specially made gown for each patient with holes where the breasts lie and a larger slot within the imaging table. This would significantly reduce the influence of the chest wall on the resulting thermal images and would provide more comfort for the patient. Instead of altering the gown, a softer, cloth-made modular design could be implemented for the same purpose. Altering the clinical imaging table as opposed to the subject gowns will provide much more control and help with cleanliness.

Breast cancer survival rates range widely throughout the world with 80% in North America, 60% in middle-income countries and below 40% in low-income countries. “The low survival rates in less developed countries can be explained mainly by the lack of early detection programs...” [153]. Breast cancer-related mortality rates in the United States have decreased due to advancements in screening and treatment [154]. The prevalence of breast cancer in the United States is higher than in the developing countries, but the mortality to incidence ratio in developing countries is higher [155]. Following successful scientific development, a sturdy and more portable imaging table and camera stand could be developed. Although the infrared cameras can be heavy and require special hardware, camera manufacturers have begun to develop smaller and lighter cameras. Different imaging strategies and table designs should be explored to determine the ideal prone position while still maintaining patient comfort. Ultimately, developing a compact system that can be easily transported will be essential for success. A packaging unit will be developed to ensure smooth transport from one location to the next.

8.3 Clinical Study

The topics associated with past thermography studies (screening positions, screening protocol, and image interpretation) all represent areas for growth. There are many paths to follow, involving changes in interpretation, when patients are screened, how they are screened, bodily or

environmental factors, etc. However, the variation in method is potentially problematic to furthering the advancement of this technology. Firstly, it is important to consider the environmental or internal conditions that can affect thermal imaging. There are specific environmental and internal factors that can be accounted for such as weather conditions, circadian rhythm, or screening room conditions. More effort should be given to determine the exact conditions into which a patient should be thermally screened. There are many studies disagreeing on exact time and temperature needed for proper acclimation. Determining these exact factors and their influence will ensure proper conditions prior to thermograms.

Next, the imaging position and number of images should be considered. In many current commercial and research setups, women sit upright with their arms over their head and few images are taken (front view and side views). However, imaging in this position has resulted in many potential issues including but not limited to thermal alterations in the inframammary fold, gravitational deformation of the breasts and limited optical access to the entire breast surface. Further inspections should be made for imaging in the prone position, particularly for obtaining a 360° view around the entirety of the breast. Screening positions and imaging bed/stand designs should consider optimal screening conditions as well as patient comfort. Certain positions may be uncomfortable, particularly for patients with other ailments such as joint inflammation, obesity, or back pain. Ergonomic screening setups should be designed with the patient in mind while also considering thermal abnormalities and imaging capacity of the breast.

Finally, researchers should consider the methods in which a thermogram is interpreted. Previous methods have been dependent on thermal patterns or empirical observation. However, as we have learned in many fields including thermography, the human eye is not a perfect interpreter. Advanced computational methods should be utilized to assist in image interpretation and

diagnosis. Tools such as artificial intelligence, machine learning, mathematical algorithms, computational fluid dynamics, etc. can all be utilized for automatic image analysis. The slight variations in temperature resulting from a tumor may not be detectable by the human eye but computational tools could easily pick up on smaller inconsistencies. Additionally, many authors use patterns, breast asymmetry, or temperature differentials to classify breast cancer. However, there is yet to be a comprehensive understanding of the influences of breast geometry, tumor pathology and natural circadian rhythm on resulting thermal images. Before exploring the efficacy of the technology itself, a better understanding of bioheat transfer and tumor pathology is needed.

8.4 Non-Human Studies

Testing on patients can be very problematic creating a need for non-subject experimentation. Animal studies could be conducted to examine additional situations within the body without the need for human subjects. Existing or implanted tumors within animal subjects could be used to examine pathology correlations and temperature changes associated with tumor aggressivity. Infrared imaging of animal subjects is potentially less problematic, leading to accurate imaging and deeper understanding of cellular relationships.

Experimental phantom models can help replicate a clinical situation of a breast to optimize screening setups prior to patient usage. Prior to the IRB approval of this clinical study, we considered agar-agar models to examine thermal situations without the need for patient recruitment. Examples of potential phantom model setups can be seen below. The setup in Fig. 66 is comprised of a breast model and an infrared camera. The cartridge heater used to simulate the tumor is a 15W, 0.5” long heater. The components used for experimentation consist of two main sections: (1) the breast model and (2) the camera setup.

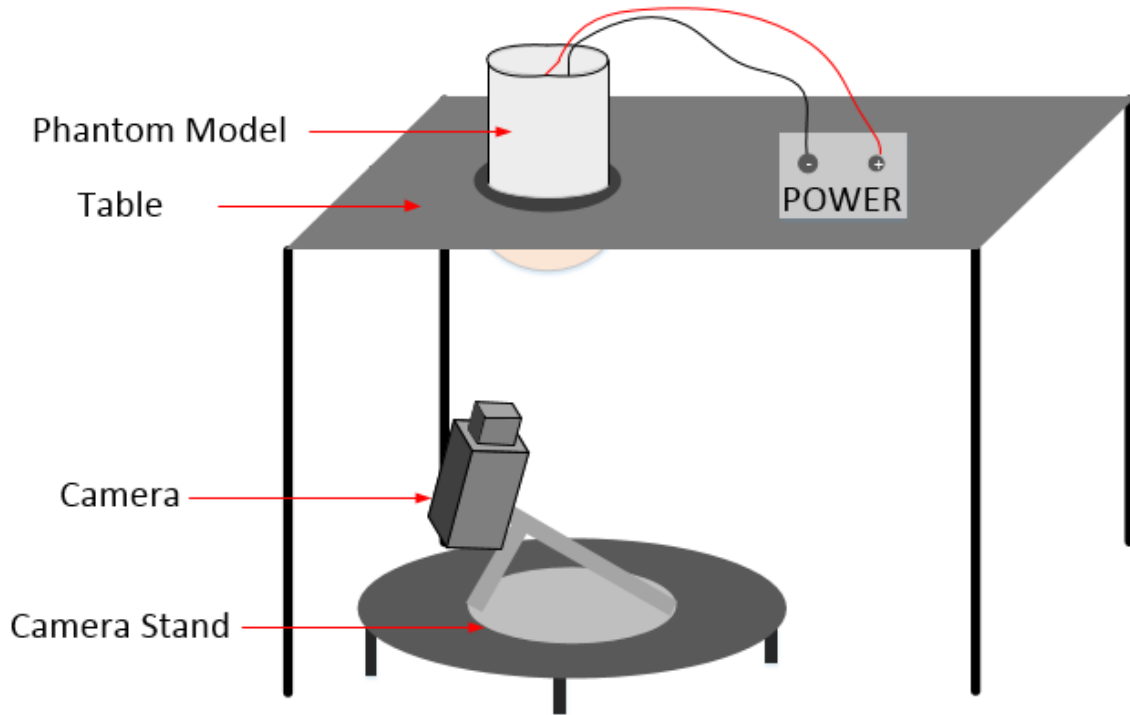


Figure 66. Entire experimental setup with rotating camera stand and breast model.

A hemisphere 6" in diameter and 3" deep can be used to simulate the breast. For a more accurate model, future studies can consider 3D printing a mold using the patient-specific modeling process described in Chapter 3. The intricate breast geometry will more accurately reflect the heat from a cartridge heater. Agar-agar is one possible substance to simulate the breast tissue with warm water as a stable chest wall temperature. Agar-agar originates in powder form and mixes with water in order to become gel-like with similar thermal properties to tissue within the breast. Before solidification, one or more cartridge heaters can simulate a tumor within the breast, depending on the desired observable aggressivity and metabolic rate. A piping system can simulate a simplistic vasculature structure within the breast with varying perfusion rate and temperature.

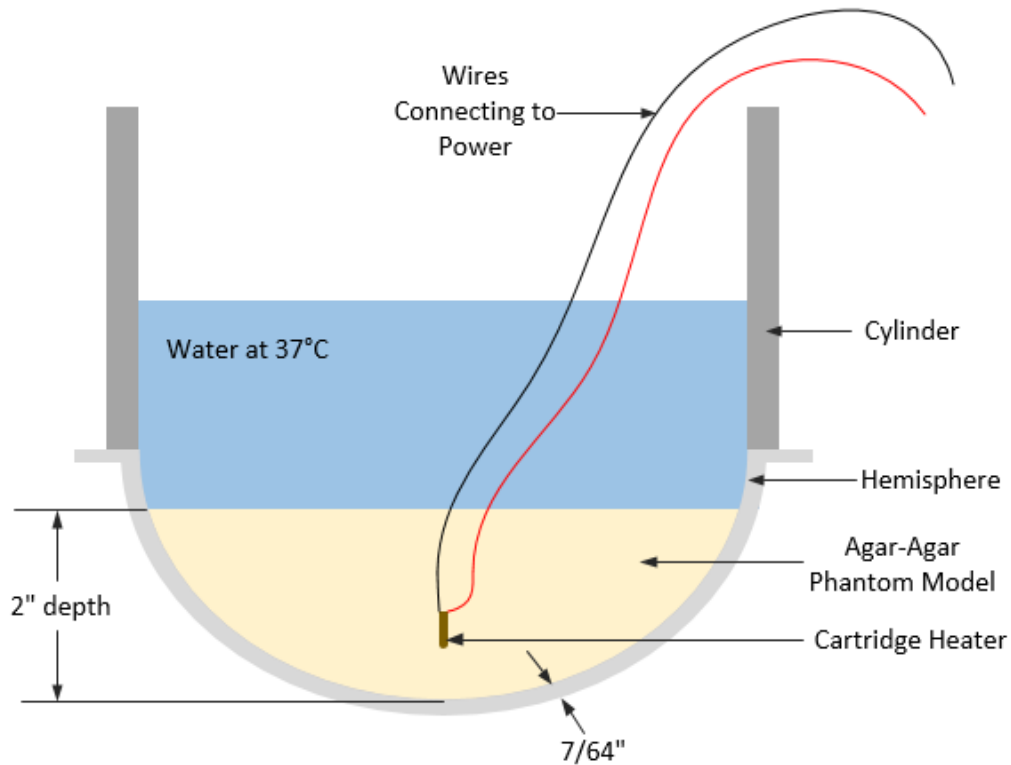


Figure 67. Breast model with imposed heaters to simulate chest wall temperature and tumor.

Finally, a parametric study is recommended to determine detectability limits of the technology. A cartridge heater can easily be placed at any depth or location within the model, allowing for a more accurate assessment of imaging limits.

8.5 Model Generation and Modeling

The IRI-MRI study utilized MRI images to create patient-specific digital breast models to use for the numerical simulation process. As discussed in Chapter 5, the digital model could be generated using different 2D clinical images. Creating a 3D model from 2D images, or 3D image reconstruction, has been a useful tool in different research areas where the physical object in the image is not readily available for constant tests or monitoring. Photogrammetry software, such as Autodesk Recap Photo, use multi-view 2D images of an object and create a 3D model by extracting

geometric information from the images. One additional future path could involve the development of a patient-specific digital breast model generated from the multi-view IRI images captured a combination of IRI images and a depth sensor. Additional depth sensors such as Intel RealSense Depth Cameras could be used to spatially map the breast during imaging for additional 3D details needed in generating the digital model. Combining more than one technique to generate a digital breast model will allow for a patient-specific model for detection and localization without the need for MRI images or additional imaging techniques.

As discussed in Chapter 6, thermal biomarkers are proposed as additional classifications in cancer diagnosis when using infrared imaging. The preliminary studies presented here have been used to further develop steady-state infrared imaging with a paired numerical modeling method. Additional modifications should be made to the numerical method to enhance the detection and localization process. Without the use of actual patients, a parametric study should be conducted to examine the effect of angiogenesis within the breast due to malignancy. If there are any potential variations due to tumor size, depth or pathology, these situations could be explored.

Finally, the current collected data has not been fully studied. There are many intricacies in the thermal images that have yet to be further explored. The subsequent pathology reports and additional images associated with each patient should be further examined. This can include more modeling, developing correlations between pathology reports and IRI images, or optimizing the screening process by learning from the collected images. The amount of data collected has great potential to lead to several larger research projects and should be explored.

8.6 Additional Detection Methods

For more rapid diagnosis or first level screening, additional detection methods could be considered. There are multiple methods that are used to detect hyperthermic regions of interest within tissue.

The methods proposed here involve gridlines, profile lines, and thermal contours. Additional mathematical, visual, or statistical parameters can be employed. A region of interest is identified as a region on the body part surface where further analysis is considered based on the value of its geometric and thermal identifiers. Tumors within tissue will have a greater amount of heat propagation throughout the tissue whereas vasculature or other thermally altering features will have a singular point or line of heat. After an image is taken, these methods are used on the images to identify regions of interest and analyze them for potential malignant suspicion. Care is taken to avoid thermal saturation in the image over the tissue so that accurate information on temperature profile and its variation is obtained. It may or may not represent the exact surface temperature due to emissivity correction needed in the image. However, assuming the surface emissivity is uniform, the temperatures indicated by the infrared image are representative of the temperature field which may be somewhat offset from the true value. Use of lotion and other creams, etc. may cause changes in emissivity and their use is discouraged prior to imaging. The following thermal features in an infrared image are used for further analysis.

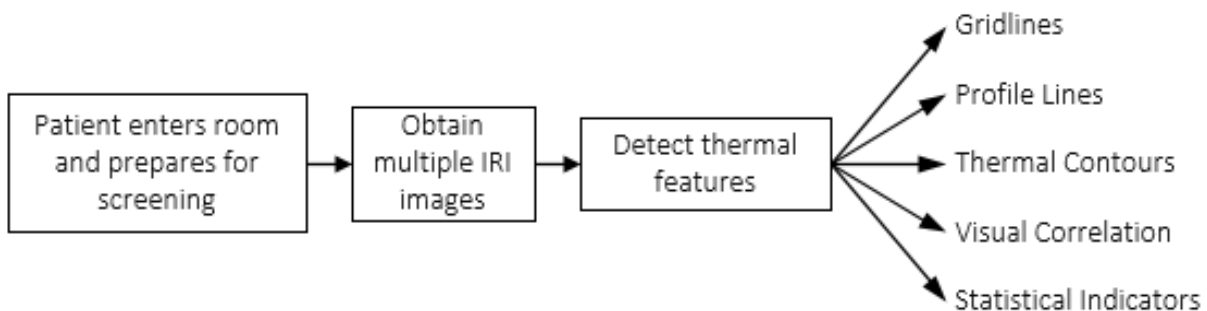


Figure 68. Potential pathways to detect thermal features within the breast.

Temperature Distribution in a Thermal Grid – One such system of analysis would be the implementation of a grid along the body part. This grid could be sketched in multiple ways including a longitude-latitude type pattern with the longitudinal and latitudinal lines matching the

contours of the body part. Other gridding systems could involve biased lines, changing line density based on features of focus or an alternate style of grid pattern. Although a few types of grids are described, any grid pattern that can be generated on the infrared image for further analysis or comparison will provide the needed information. The goal of implementing a grid is to enable defining the temperature variation in each segment of the body part. With an overall estimated average surface temperature, finding the variation in the mean temperature in each section of the body part can make it much easier to find abnormalities. Using a biased grid or a varying density grid can help for various purposes. It can also be used to single out various thermal abnormalities. Thermal abnormalities are defined as hot spots or regions of interest including but not limited to suspected malignancy, suspected benign masses, suspected vasculature, or suspected scar tissue. With fewer grid boxes, it will be easier to find the boundaries of the thermal abnormality in order to determine if malignancy is a concern or if stray vasculature is creating additional heat signatures. The grid temperatures may be obtained as an average of one or more pixels at known locations in a grid that is mapped over the infrared image of the skin surface. Additional features such as elimination of outliers or similar procedures used in image processing may be applied.

Another example gridding system, seen in Fig. 69, can show the importance of a finer mesh. The hot spot resulting from the tumor is on the left side of the breast and the hot spot resulting from a vein is on the right side of the breast. The grid system is drawn over the breast surface with horizontal (latitude) and vertical (longitude) lines. When a region of interest is identified, a finer meshing system is applied. The average temperature value in each square can be found to determine the significance of the hot spot. With a finer grid in specified regions of interest, the average temperature values will change. The temperatures at the hot spot will be significantly

hotter than the surrounding tissue. Using a grid system can help identify potential regions of concern as well as differentiate between a tumor and a vein.

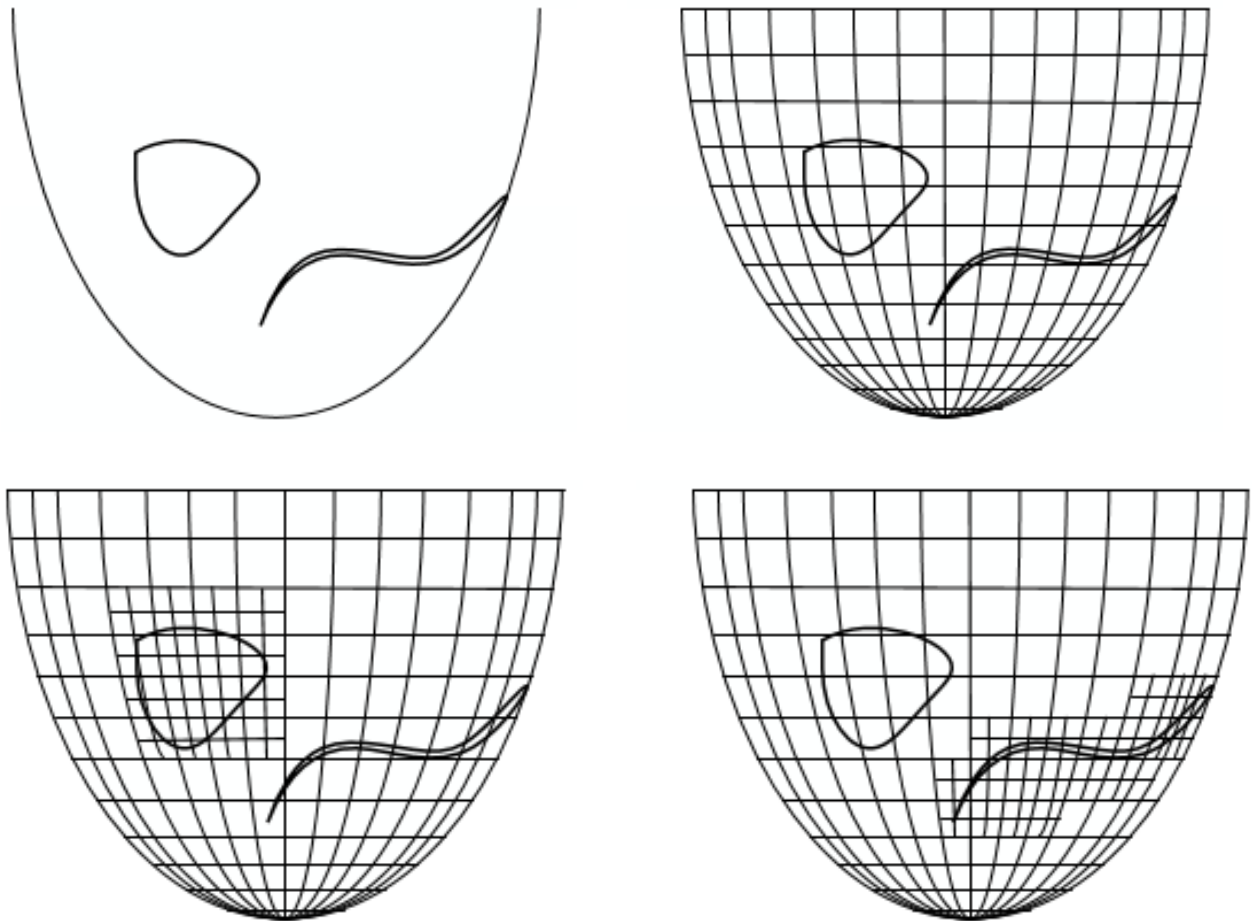
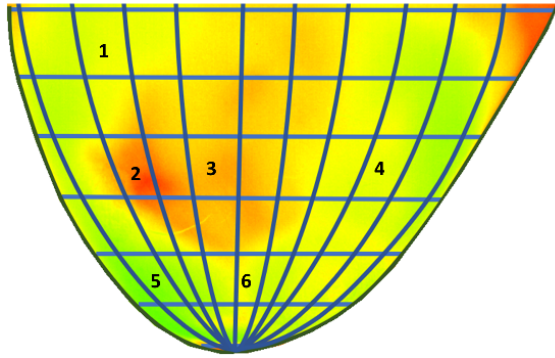


Figure 69. (a) Breast with tumor hot spot and vein hot spot, (b) gridding system on breast, (c) refined mesh highlighting tumor hot spot and (d) refined mesh highlighting vein hot spot.

Initially, a medium density of lines in each of the two directions is recommended, with 5 to 15 lines in each direction, the number of lines in each direction can be either equal or different. Figure 70 shows a thermal grid with latitudinal and longitudinal lines on a breast with a known tumor, with 12 latitudinal lines and 7 longitudinal lines.



Region	T_{mean} [°C]	T_{max} [°C]	T_{min} [°C]	SD [°C]
1	30.3	30.6	30.1	0.1033
2	32	33.3	30.6	0.5940
3	31.6	32	31	0.1827
4	30.5	30.8	30.1	0.1049
5	29.3	29.9	28.8	0.2040
6	30.2	30.6	29.8	0.1150

a)

b)

Figure 70. Images created by Gonzalez-Hernandez [52]. a) Thermal grid composed of latitudinal and longitudinal lines on a breast thermogram, b) Statistical indicators in selected regions of the grid.

Temperature profiles – Another method to identify thermal features is to obtain the surface temperature profile along lines drawn on the skin surface. These lines can be the same as described for the generation of the thermal grid. The temperature profile along these lines can be treated without processing or processed to mitigate small temperature variations. Such processing can be done through Median, Average, Gaussian, Moving Average, Savitzky-Golay, Regression, or any combination of these filters. If the sign of the temperature gradient along the distance from the chest wall changes from positive to negative, it may be used as a marker of the presence of cancer. The distance over which the gradient is obtained is an important consideration. If the slope changes in certain region, while it may not change the sign, it may also be indicative of the cancer. If the slope changes by more than 10 percent over the certain distance, it may be used as a threshold. In other cases, a change from 10-50 percent or higher may be used as a marker. The slope is calculated over a reasonable distance to avoid any image aberrations.

Thermal Contours – Using thermal contours with the hot spot in question as the central point is another method to hot spot differentiation and detection. Similar to a topographical map, thermal contours can be drawn around the hot spot and the diffusion through the tissue measured. Because

of the increase in blood perfusion, malignant tumors have a stronger heat presence that steadily warms the surrounding areas, dissimilar to vasculature. Using appropriate markers, it is possible to identify the thermal changes due to angiogenesis. This may be a result of observing specific vasculature patterns that are noted in angiogenesis that are different from the regular vasculature. A comparison may also be made with infrared images obtained from prior visit or visits of the same subject to observe the thermal artifacts.

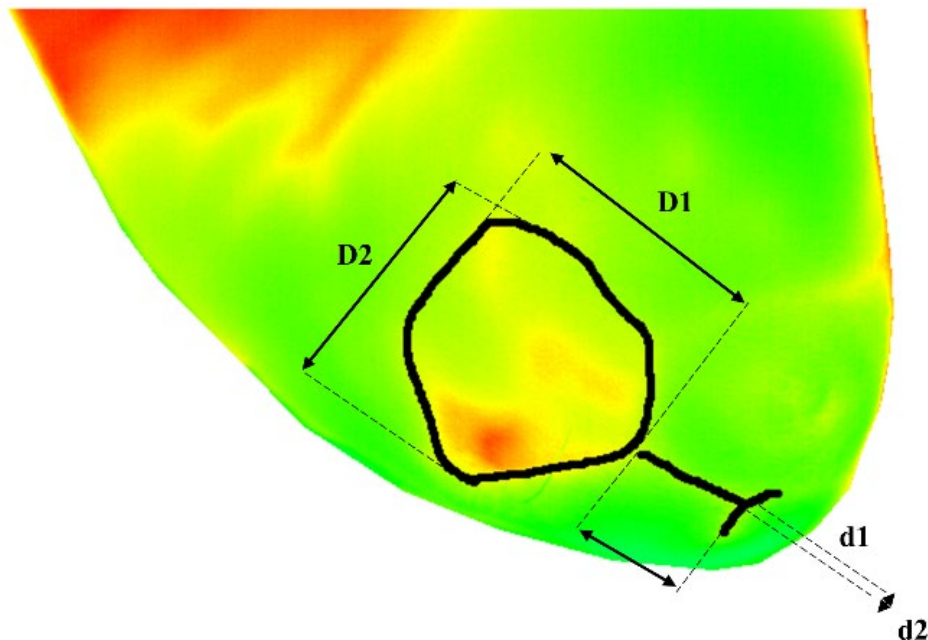


Figure 71. IR image of breast with tumor showing two regions of interest.

8.7 Additional Disease Detection

Breast cancer is an ideal candidate for IR imaging because the breasts lie in between the chest wall and the environment. There is no empty space in the body for other factors to block or alter the

resulting thermal images. IR imaging could be incredibly beneficial for other cancerous diseases with a similar ideal setting.

- *Thyroid Cancer* – Thyroid cancer is rarer in the United States compared to breast and colon. It is also highly treatable with a low mortality rate. Similar to breast cancer, it is often initially discovered through self-examination. A lump or nodule discovered in the thyroid leads to an ultrasound and biopsy before cancer is diagnosed. Detecting the early signs of thyroid cancer can be challenging. Although the prognosis of thyroid cancer is particularly good, early detection is always an issue. Because the thyroid is located close to the neck surface, surface thermal imaging would be simple.
- *Skin Cancer* – Although much of skin cancer can be visually assessed, rarer forms of skin cancer can be harder to diagnose. Skin cancer involves lesions, bumps, inflammation, or internal disease. Determining the extent of the cancer and later stage metastasis such as lymph node involvement is where imaging techniques are needed and where IR imaging could particularly come into play.
- *Testicular Cancer* – Testicular cancer is a rarer form of cancer with only approximately 20,000 cases in the United States per year. Similar to breast cancer, detection is similar by feeling a lump in either testicle. Due to the similar properties of the breast and breast cancer, IRI could easily be implemented to screen for testicular cancer.
- *Non-Cancerous Diseases* – The heat and increased blood perfusion associated with tumors provides a good environment for thermal imaging. Other diseases, such as inflammatory diseases, are also strong contenders for this diagnosis modality. Diseases such as neuropathy, joint inflammation and arthritis, and various bowel diseases have been imaged using IR imaging.

- *Chemotherapy and radiation* – Infrared Imaging can also be used to track the progress of cancer-related treatment. As chemotherapy drugs or radiation is induced into the growing tumor to shrink the mass, cancer patients can receive periodic infrared screening to observe the tumor's activity. As the drugs are added, the tumor should begin to shrink, and its metabolic activity should reduce. However, some chemotherapy is effective while others are not. Infrared imaging can be used to analyze the effectiveness of chemotherapy treatments for various patients to ensure treatment is progressing properly.

Chapter 9: References

- [1] “What Is Cancer?,” *National Cancer Institute*. <https://www.cancer.gov/about-cancer/understanding/what-is-cancer> (accessed Jan. 08, 2018).
- [2] “Worldwide cancer statistics,” *Cancer Research UK*, May 13, 2015. <http://www.cancerresearchuk.org/health-professional/cancer-statistics/worldwide-cancer> (accessed Jan. 08, 2018).
- [3] “Economic Impact of Cancer.” <https://www.cancer.org/cancer/cancer-basics/economic-impact-of-cancer.html> (accessed Jan. 17, 2018).
- [4] Elaine Marieb, Jon Mallatt, and Patricia Brady Wilhelm, *Human Anatomy*, Fourth. Pearson, 2005.
- [5] “Types of Breast Cancer.” <https://www.cancer.org/cancer/breast-cancer/understanding-a-breast-cancer-diagnosis/types-of-breast-cancer.html> (accessed Jan. 09, 2018).
- [6] “DCIS — Ductal Carcinoma In Situ,” *Breastcancer.org*. <http://www.breastcancer.org/symptoms/types/dcis> (accessed Jan. 09, 2018).
- [7] “NCI Dictionary of Cancer Terms,” *National Cancer Institute*. <https://www.cancer.gov/publications/dictionaries/cancer-terms> (accessed Jan. 09, 2018).
- [8] “LCIS — Lobular Carcinoma In Situ,” *Breastcancer.org*. <http://www.breastcancer.org/symptoms/types/lcis> (accessed Jan. 09, 2018).
- [9] “Clinical Negligence Solicitors for Breast Cancer Claims Oxford, Newcastle, Sheffield, Yorkshire, UK,” *Medical Solicitors*. <https://www.medical-solicitors.com/medical-claims/cancer-cases/breast-cancer-claims/> (accessed Jan. 25, 2018).
- [10] “Invasive Breast Cancer (IDC/ILC).” <https://www.cancer.org/cancer/breast-cancer/understanding-a-breast-cancer-diagnosis/types-of-breast-cancer/invasive-breast-cancer.html> (accessed Jan. 09, 2018).
- [11] “IDC — Invasive Ductal Carcinoma,” *Breastcancer.org*. <http://www.breastcancer.org/symptoms/types/idc> (accessed Jan. 09, 2018).
- [12] “ILC — Invasive Lobular Carcinoma,” *Breastcancer.org*. <http://www.breastcancer.org/symptoms/types/ilc> (accessed Jan. 09, 2018).
- [13] “Types of Breast Tumors - Types, Size, Grade | Susan G. Komen®.” <http://ww5.komen.org/AboutBreastCancer/DiagnosingBreastCancer/UnderstandingaDiagnosis/TumorTypesSizesGrades.html> (accessed Jan. 09, 2018).
- [14] D. Hanahan and R. A. Weinberg, “The Hallmarks of Cancer,” *Cell*, vol. 100, pp. 57–70, 2000.
- [15] D. Hanahan and R. A. Weinberg, “Hallmarks of Cancer: The Next Generation,” *Cell*, vol. 144, no. 5, pp. 646–674, Mar. 2011, doi: 10.1016/j.cell.2011.02.013.
- [16] O. Warburg, “On the origin of cancer cells,” *Science*, vol. 123, no. 3191, pp. 309–314, Feb. 1956.
- [17] “A Breakthrough Treatment for Lung Cancer Approved,” *The Tattler*, Nov. 07, 2015. <http://tattlerextra.org/wordpress1/2015/11/07/a-breakthrough-treatment-for-lung-cancer-approved/> (accessed Mar. 11, 2019).
- [18] “Necrosis,” *ScienceDaily*. <https://www.sciencedaily.com/terms/necrosis.htm> (accessed May 24, 2020).
- [19] M. Gautherie, “Thermopathology of breast cancer: measurement and analysis of in vivo temperature and blood flow,” *Ann. N. Y. Acad. Sci.*, vol. 335, pp. 383–415, 1980.

- [20] “Biological Rhythms: Types, Disorders, and Treatments,” *Healthline*. <https://www.healthline.com/health/biological-rhythms> (accessed May 24, 2020).
- [21] “Chances of Developing Breast Cancer by Age 70,” *National Cancer Institute*, Apr. 30, 2015. <https://www.cancer.gov/research/progress/discovery/breca-cancer-risk-infographic> (accessed Mar. 12, 2019).
- [22] “Staging,” *National Cancer Institute*, Mar. 09, 2015. <https://www.cancer.gov/about-cancer/diagnosis-staging/staging> (accessed Mar. 11, 2019).
- [23] “AJCC - Updated Breast Chapter for 8th Edition.” <https://cancerstaging.org/references-tools/deskreferences/Pages/Breast-Cancer-Staging.aspx> (accessed Feb. 07, 2019).
- [24] “Breast Cancer Hormone Receptor Status | Estrogen Receptor.” <https://www.cancer.org/cancer/breast-cancer/understanding-a-breast-cancer-diagnosis/breast-cancer-hormone-receptor-status.html> (accessed Mar. 13, 2019).
- [25] “Breast Cancer HER2 Status | HER2 Positive Breast Cancer.” <https://www.cancer.org/cancer/breast-cancer/understanding-a-breast-cancer-diagnosis/breast-cancer-her2-status.html> (accessed Mar. 13, 2019).
- [26] American Joint Committee on Cancer, “AJCC Cancer Staging Form Supplement,” AJCC, Staging Manual 8th Edition.
- [27] “WebPathology.” <http://webpathology.com> (accessed Mar. 13, 2019).
- [28] “The Electromagnetic Spectrum,” *Mini Physics*, Jul. 24, 2011. https://www.miniphysics.com/electromagnetic-spectrum_25.html (accessed Mar. 11, 2019).
- [29] H. D. Nelson *et al.*, *Screening for Breast Cancer: A Systematic Review to Update the 2009 U.S. Preventive Services Task Force Recommendation*. Rockville (MD): Agency for Healthcare Research and Quality (US), 2016.
- [30] “Mammography.” <https://medlineplus.gov/mammography.html> (accessed Jan. 10, 2018).
- [31] “Tomosynthesis: Cost and How It Compares to Mammograms,” *Healthline*. <https://www.healthline.com/health/breast-cancer/tomosynthesis> (accessed May 06, 2020).
- [32] R. S. of N. A. (RSNA) and A. C. of Radiology (ACR), “Breast Tomosynthesis.” <https://www.radiologyinfo.org/en/info.cfm?pg=tomosynthesis> (accessed Jan. 03, 2019).
- [33] K. Yamaguchi *et al.*, “Breast Cancer Detected on an Incident (Second or Subsequent) Round of Screening MRI: MRI Features of False-Negative Cases,” *Am. J. Roentgenol.*, vol. 201, no. 5, pp. 1155–1163, Nov. 2013, doi: 10.2214/AJR.12.9707.
- [34] P. A. Carney *et al.*, “Individual and combined effects of age, breast density, and hormone replacement therapy use on the accuracy of screening mammography,” *Ann. Intern. Med.*, vol. 138, no. 3, pp. 168–175, Feb. 2003, doi: 10.7326/0003-4819-138-3-200302040-00008.
- [35] “Mammogram Beverly Hills | Mammography Beverly Hills,” *Bedford Breast Center*. <https://www.bedfordbreastcenter.com/mammogram-los-angeles/> (accessed Jan. 22, 2018).
- [36] “Ultrasound,” *Breastcancer.org*. <http://www.breastcancer.org/symptoms/testing/types/ultrasound> (accessed Jan. 10, 2018).
- [37] “Breast ultrasound: Why it is done and what to expect,” *Medical News Today*. <https://www.medicalnewstoday.com/articles/319202.php> (accessed Mar. 12, 2019).
- [38] S. Gokhale, “Ultrasound characterization of breast masses,” *Indian J. Radiol. Imaging*, vol. 19, no. 3, pp. 242–247, Aug. 2009, doi: 10.4103/0971-3026.54878.
- [39] “Breast MRI - Mayo Clinic.” <https://www.mayoclinic.org/tests-procedures/breast-mri/about/pac-20384809> (accessed Mar. 12, 2019).

- [40] R. Lawson, “Implications of Surface Temperatures in the Diagnosis of Breast Cancer,” *Clin. Lab. Notes*, vol. 75, pp. 309–310, 1956.
- [41] R. N. Lawson and M. S. Chughtai, “Breast Cancer and Body Temperature,” *Can. Med. Assoc. J.*, vol. 88, no. 2, pp. 68–70, Jan. 1963.
- [42] J. W. Gorechlad *et al.*, “Screening for Recurrences in Patients Treated with Breast-Conserving Surgery: Is there a Role for MRI?,” *Ann. Surg. Oncol.*, vol. 15, no. 6, pp. 1703–1709, Jun. 2008, doi: 10.1245/s10434-008-9832-2.
- [43] L. R. Rechtman *et al.*, “Breast-Specific Gamma Imaging for the Detection of Breast Cancer in Dense Versus Nondense Breasts,” *Am. J. Roentgenol.*, vol. 202, no. 2, pp. 293–298, Jan. 2014, doi: 10.2214/AJR.13.11585.
- [44] D. J. Rhodes, C. B. Hruska, S. W. Phillips, D. H. Whaley, and M. K. O’Connor, “Dedicated Dual-Head Gamma Imaging for Breast Cancer Screening in Women with Mammographically Dense Breasts,” *Radiology*, vol. 258, no. 1, pp. 106–118, Jan. 2011, doi: 10.1148/radiol.10100625.
- [45] S. B. Glass and Z. A. Shah, “Clinical utility of positron emission mammography,” *Proc. Bayl. Univ. Med. Cent.*, vol. 26, no. 3, pp. 314–319, Jul. 2013.
- [46] “IR Cameras: An Overview for Inspectors - InterNACHI.” <https://www.nachi.org/ir-camera-overview-inspectors.htm> (accessed Jan. 10, 2018).
- [47] “FLIR T-Series Thermal Imaging Cameras | FLIR Systems.” <http://www.flir.com/instruments/content/?id=84344> (accessed Jan. 10, 2018).
- [48] “Remembering the meanings of sensitivity, specificity, and predictive values,” *J. Fam. Pract.*, vol. 53, no. 1, Jan. 2004, Accessed: May 07, 2020. [Online]. Available: <https://www.mdedge.com/familymedicine/article/65505/practice-management/remembering-meanings-sensitivity-specificity-and>.
- [49] E. Sharp·Statistics, “Statistics | Sensitivity, Specificity, PPV and NPV,” *Geeky Medics*, Jun. 30, 2018. <https://geekymedics.com/sensitivity-specificity-ppv-and-npv/> (accessed May 07, 2020).
- [50] R. Parikh, A. Mathai, S. Parikh, G. Chandra Sekhar, and R. Thomas, “Understanding and using sensitivity, specificity and predictive values,” *Indian J. Ophthalmol.*, vol. 56, no. 1, pp. 45–50, 2008.
- [51] S. Tenny and M. R. Hoffman, “Prevalence,” in *StatPearls*, Treasure Island (FL): StatPearls Publishing, 2020.
- [52] E. A. Morris *et al.*, “MRI of Occult Breast Carcinoma in a High-Risk Population,” *Am. J. Roentgenol.*, vol. 181, no. 3, pp. 619–626, Sep. 2003, doi: 10.2214/ajr.181.3.1810619.
- [53] W. A. Berg, “Combined Screening With Ultrasound and Mammography vs Mammography Alone in Women at Elevated Risk of Breast Cancer,” *JAMA*, vol. 299, no. 18, p. 2151, May 2008, doi: 10.1001/jama.299.18.2151.
- [54] E. Warner, “Surveillance of BRCA1 and BRCA2 Mutation Carriers With Magnetic Resonance Imaging, Ultrasound, Mammography, and Clinical Breast Examination,” *JAMA*, vol. 292, no. 11, p. 1317, Sep. 2004, doi: 10.1001/jama.292.11.1317.
- [55] D. Saslow *et al.*, “American Cancer Society Guidelines for Breast Screening with MRI as an Adjunct to Mammography,” *CA. Cancer J. Clin.*, vol. 57, no. 2, pp. 75–89, Mar. 2007, doi: 10.3322/canjclin.57.2.75.
- [56] J. G. Elmore, M. B. Barton, V. M. Mocerri, S. Polk, P. J. Arena, and S. W. Fletcher, “Ten-Year Risk of False Positive Screening Mammograms and Clinical Breast Examinations,” *N.*

- Engl. J. Med.*, vol. 338, no. 16, pp. 1089–1096, Apr. 1998, doi: 10.1056/NEJM199804163381601.
- [57] S. G. Kandlikar *et al.*, “Infrared imaging technology for breast cancer detection – Current status, protocols and new directions,” *Int. J. Heat Mass Transf.*, vol. 108, Part B, pp. 2303–2320, May 2017, doi: 10.1016/j.ijheatmasstransfer.2017.01.086.
- [58] “Learn About Clinical Studies - ClinicalTrials.gov.” <https://clinicaltrials.gov/ct2/about-studies/learn> (accessed May 11, 2020).
- [59] “How Common Is Breast Cancer?” <https://www.cancer.org/cancer/breast-cancer/about/how-common-is-breast-cancer.html> (accessed Dec. 05, 2018).
- [60] J. L. Gonzalez Hernandez, “A Patient-Specific Approach for Breast Cancer Detection and Tumor Localization Using Infrared Imaging,” *Theses*, Aug. 2019, [Online]. Available: <https://scholarworks.rit.edu/theses/10212>.
- [61] C. Bernard, *Leçons sur la chaleur animale, sur les effets de la chaleur et sur la fièvre*. J.-B. Baillière, 1876.
- [62] H. Pennes, “Analysis of Tissue and Arterial Blood Temperatures in the Resting Human Forearm.” *Journal of Applied Physiology*, 1948.
- [63] M. Gautherie, “Thermobiological assessment of benign and malignant breast diseases,” *Am. J. Obstet. Gynecol.*, vol. 147, no. 8, pp. 861–869, Dec. 1983, doi: 10.1016/0002-9378(83)90236-3.
- [64] The BCDDP Working Group, “DETAILED REPORT OF THE WORKING GROUP’S REVIEW OF BCDDP,” *JNCI J. Natl. Cancer Inst.*, vol. 62, no. 3, Mar. 1979.
- [65] The BCDDP Working Group, “REPORT OF THE WORKING GROUP,” *JNCI J. Natl. Cancer Inst.*, vol. 62, no. 3, Mar. 1979.
- [66] The BCDDP Working Group, “Section I. General Issues Related to Breast Cancer Screening,” *JNCI J. Natl. Cancer Inst.*, vol. 62, no. 3, pp. 655–662, Mar. 1979, doi: 10.1093/jnci/62.3.655.
- [67] The BCDDP Working Group, “Section II: Analysis of Screening in BCDDP,” *JNCI J. Natl. Cancer Inst.*, vol. 62, no. 3, 1979.
- [68] The BCDDP Working Group, “Section III. Pathology Review of Minimal Breast Cancers Detected in BCDDP,” *JNCI J. Natl. Cancer Inst.*, vol. 62, no. 3, pp. 673–684, Mar. 1979, doi: 10.1093/jnci/62.3.673.
- [69] The BCDDP Working Group, “Section IV. Assessment of the BCDDP’S Experience for the Measurement of Benefit from Screening,” *JNCI J. Natl. Cancer Inst.*, vol. 62, no. 3, pp. 685–690, Mar. 1979, doi: 10.1093/jnci/62.3.685.
- [70] The BCDDP Working Group, “Section V. Randomized Controlled Trials to Resolve Issues About the Efficacy of Periodic Breast Cancer Screening,” *JNCI J. Natl. Cancer Inst.*, vol. 62, no. 3, pp. 691–693, Mar. 1979, doi: 10.1093/jnci/62.3.691.
- [71] The BCDDP Working Group, “Appendix. Utility of Statistical Models for Assessment of the BCDDP’S Experience,” *JNCI J. Natl. Cancer Inst.*, vol. 62, no. 3, pp. 695–698, Mar. 1979, doi: 10.1093/jnci/62.3.695.
- [72] The BCDDP Working Group, “Supplemental and Concluding Report of the Working Group to Review the National Cancer Institute-American Cancer Society Breast Cancer Detection Demonstration Projects,” *JNCI J. Natl. Cancer Inst.*, vol. 62, no. 3, pp. 699–709, Mar. 1979, doi: 10.1093/jnci/62.3.699.

- [73] L. H. Baker, “Breast Cancer Detection Demonstration Project: Five-Year Summary Report,” *CA. Cancer J. Clin.*, vol. 32, no. 4, pp. 194–225, Jul. 1982, doi: 10.3322/canjclin.32.4.194.
- [74] A. Lilienfeld, J. Barnes, and R. Barnes, “An evaluation of thermography in the detection of breast cancer: A cooperative pilot study,” *Cancer*, vol. 24, pp. 1206–1211, 1969.
- [75] Medical News, “In the Hot Seat-Thermography for Breast Cancer Diagnosis,” *JAMA: The Journal of the American Medical Association*, vol. 251, no. 6, pp. 693–695, 1984.
- [76] C. R. Smart *et al.*, “Twenty-year follow-up of the breast cancers diagnosed during the Breast Cancer Detection Demonstration Project,” *CA. Cancer J. Clin.*, vol. 47, no. 3, pp. 134–149, May 1997, doi: 10.3322/canjclin.47.3.134.
- [77] M. P. Cunningham, “The Breast Cancer Detection Demonstration Project 25 years later,” *CA. Cancer J. Clin.*, vol. 47, no. 3, pp. 131–133, May 1997, doi: 10.3322/canjclin.47.3.131.
- [78] J.-L. Gonzalez-Hernandez, A. N. Recinella, S. G. Kandlikar, D. Dabydeen, L. Medeiros, and P. Phatak, “Technology, application and potential of dynamic breast thermography for the detection of breast cancer,” *Int. J. Heat Mass Transf.*, vol. 131, pp. 558–573, Mar. 2019, doi: 10.1016/j.ijheatmasstransfer.2018.11.089.
- [79] S. T. Kakileti, G. Manjunath, and H. M. and H. V. Ramprakash, “Advances in Breast Thermography,” *New Perspect. Breast Imaging*, Oct. 2017, doi: 10.5772/intechopen.69198.
- [80] “Our Technology.” <http://www.notouchbreastscan.com/thermography.html> (accessed Mar. 14, 2019).
- [81] L. Hu, A. Gupta, J. P. Gore, and L. X. Xu, “Effect of Forced Convection on the Skin Thermal Expression of Breast Cancer,” *J. Biomech. Eng.*, vol. 126, no. 2, p. 204, 2004, doi: 10.1115/1.1688779.
- [82] Y. Ohashi and I. Uchida, “Applying dynamic thermography in the diagnosis of breast cancer,” *IEEE Eng. Med. Biol. Mag.*, vol. 19, no. 3, pp. 42–51, May 2000, doi: 10.1109/51.844379.
- [83] G. C. Wishart *et al.*, “The Accuracy Of Digital Infrared Imaging For Breast Cancer Detection In Women Undergoing Breast Biopsy,” *EJSO - Eur. J. Surg. Oncol.*, vol. 36, no. 6, p. 535, Jun. 2010, doi: 10.1016/j.ejso.2010.04.003.
- [84] N. M. Sudharsan, E. Y. K. Ng, and S. L. Teh, “Surface Temperature Distribution of a Breast With and Without Tumour,” *Comput. Methods Biomech. Biomed. Engin.*, vol. 2, no. 3, pp. 187–199, Jan. 1999, doi: 10.1080/10255849908907987.
- [85] E. Y. K. Ng and N. M. Sudharsan, “An Improved 3D Direct Numerical Modeling and Thermal Analysis of a Female Breast with Tumor,” *Proc Instn Mech Engrs*, vol. 215, no. H, pp. 25–36.
- [86] Feasey, Davison, and James, “Effects of Natural and Forced Cooling on the Thermographic Patterns of Tumours,” *Phys. Med. Biol.*, vol. 16, no. 2, pp. 213–220, 1971.
- [87] S. Nilsson, “Skin Temperature over an Artificial Heat Source Implanted in Man,” *Phys. Med. Biol.*, vol. 20, no. 3, pp. 366–383, 1975.
- [88] S. Nilsson and S. Gustafsson, “Surface Temperature over an Implanted Artificial Heat Source,” *Phys. Med. Biol.*, vol. 19, no. 5, pp. 677–691, 1974.
- [89] M. Mital and E. P. Scott, “Thermal Detection of Embedded Tumors Using Infrared Imaging,” *J. Biomech. Eng.*, vol. 129, no. 1, p. 33, 2007, doi: 10.1115/1.2401181.
- [90] A. A. Wahab, M. I. M. Salim, and J. Yunus, “Thermal distribution analysis in multi-layers homogeneous phantom using Infrared Imaging Technique: A preliminary study,” in

- Biomedical Engineering and Sciences (IECBES), 2014 IEEE Conference on*, 2014, pp. 628–633.
- [91] J. F. Head, F. Wang, C. A. Lipari, and R. L. Elliott, “The important role of infrared imaging in breast cancer,” *IEEE Eng. Med. Biol. Mag.*, vol. 19, no. 3, pp. 52–57, May 2000, doi: 10.1109/51.844380.
- [92] A. M. Stark and S. Way, “The use of thermovision in the detection of early breast cancer,” *Cancer*, vol. 33, no. 6, pp. 1664–1670, Jun. 1974, doi: 10.1002/1097-0142(197406)33:6<1664::AID-CNCR2820330629>3.0.CO;2-7.
- [93] F. Gutierrez-Delgado and J. G. Vázquez-Luna, “Feasibility of New-generation Infrared Imaging Screening for Breast Cancer in Rural Communities,” *J. - Feasibility New-Gener. Infrared Imaging Screen. Breast Cancer Rural Communities*, Accessed: Mar. 04, 2019. [Online]. Available: <https://www.touchoncology.com/articles/feasibility-new-generation-infrared-imaging-screening-breast-cancer-rural-communities>.
- [94] Gautherie and Gros, “Breast thermography and cancer risk prediction,” *Cancer*, vol. 45, no. 1, pp. 51–56, 1980.
- [95] J. D. Haberman, T. J. Love, and J. E. Francis, “SCREENING A RURAL POPULATION FOR BREAST CANCER USING THERMOGRAPHY AND PHYSICAL EXAMINATION TECHNIQUES: METHODS AND RESULTS-A PRELIMINARY REPORT,” *Ann. N. Y. Acad. Sci.*, vol. 335, no. 1 Thermal Chara, pp. 492–500, Mar. 1980, doi: 10.1111/j.1749-6632.1980.tb50774.x.
- [96] S. V. Francis, M. Sasikala, G. Bhavani Bharathi, and S. D. Jaipurkar, “Breast cancer detection in rotational thermography images using texture features,” *Infrared Phys. Technol.*, vol. 67, no. Supplement C, pp. 490–496, Nov. 2014, doi: 10.1016/j.infrared.2014.08.019.
- [97] A. Lozano and F. Hassanipour, “Infrared imaging for breast cancer detection: An objective review of foundational studies and its proper role in breast cancer screening,” *Infrared Phys. Technol.*, vol. 97, pp. 244–257, Mar. 2019, doi: 10.1016/j.infrared.2018.12.017.
- [98] I. Fernández-Cuevas *et al.*, “Classification of factors influencing the use of infrared thermography in humans: A review,” *Infrared Phys. Technol.*, vol. 71, pp. 28–55, Jul. 2015, doi: 10.1016/j.infrared.2015.02.007.
- [99] K. L. Ewing, T. W. Davison, and J. L. Fergason, “EFFECTS OF ACTIVITY, ALCOHOL, SMOKING, AND THE MENSTRUAL CYCLE ON LIQUID CRYSTAL BREAST THERMOGRAPHY,” vol. 73, p. 5.
- [100] L. Jiang, W. Zhan, and M. H. Loew, “Modeling static and dynamic thermography of the human breast under elastic deformation,” *Phys. Med. Biol.*, vol. 56, no. 1, pp. 187–202, Jan. 2011, doi: 10.1088/0031-9155/56/1/012.
- [101] Keyserlingk, J. R., Ahlgren, P. D., Yu, E., and Belliveau, N., “Infrared Imaging of the Breast: Initial Reappraisal using High-Resolution Digital Technology in 100 Successive Cases of Stage I and II Breast Cancer,” *Breast J.*, vol. 4, no. 4, pp. 245–251, 1998.
- [102] S. V. Francis, M. Sasikala, G. Bhavani Bharathi, and S. D. Jaipurkar, “Breast cancer detection in rotational thermography images using texture features,” *Infrared Phys. Technol.*, vol. 67, pp. 490–496, Nov. 2014, doi: 10.1016/j.infrared.2014.08.019.
- [103] Y. R. Parisky *et al.*, “Efficacy of computerized infrared imaging analysis to evaluate mammographically suspicious lesions,” *AJR Am. J. Roentgenol.*, vol. 180, no. 1, pp. 263–269, Jan. 2003, doi: 10.2214/ajr.180.1.1800263.

- [104] A. E. Collett, C. Guilfoyle, E. J. Gracely, T. G. Frazier, and A. V. Barrio, “Infrared Imaging Does Not Predict the Presence of Malignancy in Patients with Suspicious Radiologic Breast Abnormalities,” *Breast J.*, vol. 20, no. 4, pp. 375–380, Jul. 2014, doi: 10.1111/tbj.12273.
- [105] M. Rassiwalla *et al.*, “Evaluation of digital infra–red thermal imaging as an adjunctive screening method for breast carcinoma: A pilot study,” *Int. J. Surg.*, vol. 12, no. 12, pp. 1439–1443, Dec. 2014, doi: 10.1016/j.ijisu.2014.10.010.
- [106] L.-A. Wu, W.-H. Kuo, C.-Y. Chen, Y.-S. Tsai, and J. Wang, “The association of infrared imaging findings of the breast with prognosis in breast cancer patients: an observational cohort study,” *BMC Cancer*, vol. 16, no. 1, p. 541, Dec. 2016, doi: 10.1186/s12885-016-2602-9.
- [107] J. Wang *et al.*, “Evaluation of the diagnostic performance of infrared imaging of the breast: a preliminary study,” *Biomed. Eng. OnLine*, vol. 9, no. 1, p. 3, 2010, doi: 10.1186/1475-925X-9-3.
- [108] J. D. Bronzino, *Medical Devices and Systems*. CRC Press, 2006.
- [109] E. Y. K. Ng and E. C. Kee, “Advanced integrated technique in breast cancer thermography,” *J. Med. Eng. Technol.*, vol. 32, no. 2, pp. 103–114, Jan. 2008, doi: 10.1080/03091900600562040.
- [110] M. EtehadTavakol, V. Chandran, E. Y. K. Ng, and R. Kafieh, “Breast cancer detection from thermal images using bispectral invariant features,” *Int. J. Therm. Sci.*, vol. 69, pp. 21–36, Jul. 2013, doi: 10.1016/j.ijthermalsci.2013.03.001.
- [111] C. for D. and R. Health, “Safety Communications - FDA Warns Thermography Should Not Be Used in Place of Mammography to Detect, Diagnose, or Screen for Breast Cancer: FDA Safety Communication.” https://www.fda.gov/MedicalDevices/Safety/AlertsandNotices/ucm631885.htm?utm_campaign=FDA%20MedWatch%20%20FDA%20Warns%20Thermography%20Should%20Not%20Be%20Used%20in%20Place%20of%20Mammography&utm_medium=email&utm_source=Eloqua (accessed Mar. 14, 2019).
- [112] “Breast Health - DITI.” American College of Clinical Thermology, 2019 2003, Accessed: Mar. 31, 2020. [Online]. Available: <https://www.thermologyonline.org/Breast/PDF/Breast%20Brochure.pdf>.
- [113] “Education and Training | Certification.” <https://www.iact-org.org/professionals/education-training.html> (accessed May 05, 2020).
- [114] “Thermography Guidelines. Standards and protocols.” <https://www.iact-org.org/professionals/thermog-guidelines.html> (accessed May 05, 2020).
- [115] “INTERPRETATIONS,” *Medical Thermology*. <https://medicalthermology.org/interpretations/> (accessed May 05, 2020).
- [116] E. Y.-K. Ng, “A review of thermography as promising non-invasive detection modality for breast tumor,” *Int. J. Therm. Sci.*, vol. 48, no. 5, pp. 849–859, May 2009, doi: 10.1016/j.ijthermalsci.2008.06.015.
- [117] J. r. Keyserlingk, P. d. Ahlgren, E. Yu, and N. Belliveau, “Infrared Imaging of the Breast: Initial Reappraisal Using High-Resolution Digital Technology in 100 Successive Cases of Stage I and II Breast Cancer,” *Breast J.*, vol. 4, no. 4, pp. 245–251, Jul. 1998, doi: 10.1046/j.1524-4741.1998.440245.x.

- [118] A. Zolfaghari and M. Maerefat, “A new simplified model for evaluating non-uniform thermal sensation caused by wearing clothing,” *Build. Environ.*, vol. 45, no. 3, pp. 776–783, Mar. 2010, doi: 10.1016/j.buildenv.2009.08.015.
- [119] K. L. EWING, T. W. DAVISON, and J. L. FERGASON, “EFFECTS OF ACTIVITY, ALCOHOL, SMOKING, AND THE MENSTRUAL CYCLE ON LIQUID CRYSTAL BREAST THERMOGRAPHY,” vol. 73, p. 5.
- [120] S. G. Kandlikar *et al.*, “Infrared imaging technology for breast cancer detection – Current status, protocols and new directions,” *Int. J. Heat Mass Transf.*, vol. 108, no. Part B, pp. 2303–2320, May 2017, doi: 10.1016/j.ijheatmasstransfer.2017.01.086.
- [121] A. Amri, A. J. Wilkinson, and S. H. Pulko, “Potentialities of Dynamic Breast Thermography,” in *Application of Infrared to Biomedical Sciences*, E. Y. Ng and M. Etehadtavakol, Eds. Singapore: Springer Singapore, 2017, pp. 79–107.
- [122] R. B. Barnes, “Thermography,” *Ann. N. Y. Acad. Sci.*, vol. 121, no. 1, pp. 34–48, Oct. 1964, doi: 10.1111/j.1749-6632.1964.tb13683.x.
- [123] J. C. B. Marins *et al.*, “Time required to stabilize thermographic images at rest,” *Infrared Phys. Technol.*, vol. 65, pp. 30–35, Jul. 2014, doi: 10.1016/j.infrared.2014.02.008.
- [124] J.-L. Gonzalez-Hernandez, S. G. Kandlikar, D. Dabydeen, L. Medeiros, and P. Phatak, “Generation and Thermal Simulation of a Digital Model of the Female Breast in Prone Position,” *J. Eng. Sci. Med. Diagn. Ther.*, vol. 1, no. 4, pp. 041006-041006–8, Oct. 2018, doi: 10.1115/1.4041421.
- [125] J.-L. Gonzalez-Hernandez, A. N. Recinella, S. G. Kandlikar, D. Dabydeen, L. Medeiros, and P. Phatak, “An inverse heat transfer approach for patient-specific breast cancer detection and tumor localization using surface thermal images in the prone position,” *Infrared Phys. Technol.*, vol. 105, p. 103202, Mar. 2020, doi: 10.1016/j.infrared.2020.103202.
- [126] A. N. Recinella, J.-L. Gonzalez-Hernandez, S. G. Kandlikar, D. Dabydeen, L. Medeiros, and P. Phatak, “Clinical Infrared Imaging in the Prone Position for Breast Cancer Screening—Initial Screening and Digital Model Validation,” *J. Eng. Sci. Med. Diagn. Ther.*, vol. 3, no. 1, Feb. 2020, doi: 10.1115/1.4045319.
- [127] M. A. Bujang and T. H. Adnan, “Requirements for Minimum Sample Size for Sensitivity and Specificity Analysis,” *J. Clin. Diagn. Res. JCDR*, vol. 10, no. 10, pp. YE01–YE06, Oct. 2016, doi: 10.7860/JCDR/2016/18129.8744.
- [128] N. M. F. Buderer, “Statistical Methodology: I. Incorporating the Prevalence of Disease into the Sample Size Calculation for Sensitivity and Specificity,” *Acad. Emerg. Med.*, vol. 3, no. 9, pp. 895–900, Sep. 1996, doi: 10.1111/j.1553-2712.1996.tb03538.x.
- [129] M. M. Eberl, C. H. Fox, S. B. Edge, C. A. Carter, and M. C. Mahoney, “BI-RADS Classification for Management of Abnormal Mammograms,” *J. Am. Board Fam. Med.*, vol. 19, no. 2, pp. 161–164, Mar. 2006, doi: 10.3122/jabfm.19.2.161.
- [130] S. P. Poplack, A. N. Tosteson, M. R. Grove, W. A. Wells, and P. A. Carney, “Mammography in 53,803 women from the New Hampshire mammography network,” *Radiology*, vol. 217, no. 3, pp. 832–840, Dec. 2000, doi: 10.1148/radiology.217.3.r00dc33832.
- [131] “NIMH » What is Prevalence?” <https://www.nimh.nih.gov/health/statistics/what-is-prevalence.shtml> (accessed May 14, 2020).
- [132] R. García-Figueiras *et al.*, “CT Perfusion in Oncologic Imaging: A Useful Tool?,” *Am. J. Roentgenol.*, vol. 200, no. 1, pp. 8–19, Jan. 2013, doi: 10.2214/AJR.11.8476.

- [133] R. S. of N. A. (RSNA) and A. C. of Radiology (ACR), “CT Perfusion of the Head.” <https://www.radiologyinfo.org/en/info.cfm?pg=perfusionheadct> (accessed May 21, 2020).
- [134] A. Satoh *et al.*, “Role of Perfusion CT in Assessing Tumor Blood Flow and Malignancy Level of Gastric Cancer,” *Dig. Surg.*, vol. 27, no. 4, pp. 253–260, 2010, doi: 10.1159/000288703.
- [135] R. Choe *et al.*, “Optically Measured Microvascular Blood Flow Contrast of Malignant Breast Tumors,” *PLoS ONE*, vol. 9, no. 6, p. e99683, Jun. 2014, doi: 10.1371/journal.pone.0099683.
- [136] F. J. González, “Thermal simulation of breast tumors,” *Rev. Mex. Física*, vol. 53, no. 4, pp. 323–326, 2007.
- [137] *Physical Properties of Tissue: A Comprehensive Reference Book*. IPEM, 2012.
- [138] E. Y.-K. Ng, “A review of thermography as promising non-invasive detection modality for breast tumor,” *Int. J. Therm. Sci.*, vol. 48, no. 5, pp. 849–859, May 2009, doi: 10.1016/j.ijthermalsci.2008.06.015.
- [139] M. M. Osman and E. M. Afify, “Thermal modeling of the normal woman’s breast,” *J. Biomech. Eng.*, vol. 106, no. 2, pp. 123–130, 1984.
- [140] H. G. Welch and W. C. Black, “Overdiagnosis in cancer,” *J. Natl. Cancer Inst.*, vol. 102, no. 9, pp. 605–613, May 2010, doi: 10.1093/jnci/djq099.
- [141] D. Puliti *et al.*, “Overdiagnosis in mammographic screening for breast cancer in Europe: a literature review,” *J. Med. Screen.*, vol. 19 Suppl 1, pp. 42–56, 2012, doi: 10.1258/jms.2012.012082.
- [142] P. A. van Luijt *et al.*, “The distribution of ductal carcinoma in situ (DCIS) grade in 4232 women and its impact on overdiagnosis in breast cancer screening,” *Breast Cancer Res. BCR*, vol. 18, 2016, doi: 10.1186/s13058-016-0705-5.
- [143] D. Rosner, R. N. Bedwani, J. Vana, H. W. Baker, and G. P. Murphy, “Noninvasive Breast Carcinoma: Results of a National Survey by the American College of Surgeons,” *Ann. Surg.*, vol. 192, no. 2, pp. 139–147, Aug. 1980.
- [144] M. Blichert-Toft, H. P. Graversen, J. Andersen, U. Dyreborg, and A. Green, “In situ breast carcinomas: A population-based study on frequency, growth pattern, and clinical aspects,” *World J. Surg.*, vol. 12, no. 6, pp. 845–850, Dec. 1988, doi: 10.1007/BF01655494.
- [145] B. A. Ward, C. F. McKhann, and T. S. Ravikumar, “Ten-Year Follow-up of Breast Carcinoma In Situ in Connecticut,” *Arch. Surg.*, vol. 127, no. 12, pp. 1392–1395, Dec. 1992, doi: 10.1001/archsurg.1992.01420120026004.
- [146] S. K. Mardekian, A. Bombonati, and J. P. Palazzo, “Ductal carcinoma in situ of the breast: the importance of morphologic and molecular interactions,” *Hum. Pathol.*, vol. 49, pp. 114–123, Mar. 2016, doi: 10.1016/j.humpath.2015.11.003.
- [147] M. A. Lopez-Garcia, F. C. Geyer, M. Lacroix-Triki, C. Marchió, and J. S. Reis-Filho, “Breast cancer precursors revisited: molecular features and progression pathways,” *Histopathology*, vol. 57, no. 2, pp. 171–192, Aug. 2010, doi: 10.1111/j.1365-2559.2010.03568.x.
- [148] P. C. Gøtzsche and O. Olsen, “Is screening for breast cancer with mammography justifiable?,” *Lancet Lond. Engl.*, vol. 355, no. 9198, pp. 129–134, Jan. 2000, doi: 10.1016/S0140-6736(99)06065-1.
- [149] A. Francis, L. Fallowfield, and D. Rea, “The LORIS Trial: Addressing overtreatment of ductal carcinoma in situ,” *Clin. Oncol. R. Coll. Radiol. G. B.*, vol. 27, no. 1, pp. 6–8, Jan. 2015, doi: 10.1016/j.clon.2014.09.015.

- [150] A. Hosseini, A. L. Khoury, and L. J. Esserman, “Precision surgery and avoiding over-treatment,” *Eur. J. Surg. Oncol. J. Eur. Soc. Surg. Oncol. Br. Assoc. Surg. Oncol.*, vol. 43, no. 5, pp. 938–943, May 2017, doi: 10.1016/j.ejso.2017.02.003.
- [151] L. Graña-López, M. Herranz, I. Domínguez-Prado, S. Argibay, Á. Villares, and M. Vázquez-Caruncho, “Can dedicated breast PET help to reduce overdiagnosis and overtreatment by differentiating between indolent and potentially aggressive ductal carcinoma in situ?,” *Eur. Radiol.*, vol. 30, no. 1, pp. 514–522, Jan. 2020, doi: 10.1007/s00330-019-06356-9.
- [152] J.-L. Gonzalez-Hernandez, S. G. Kandlikar, D. Dabydeen, L. Medeiros, and P. Phatak, “Generation and Thermal Simulation of a Digital Model of the Female Breast in Prone Position,” *J. Eng. Sci. Med. Diagn. Ther.*, vol. 1, no. 4, p. 041006, Nov. 2018, doi: 10.1115/1.4041421.
- [153] “WHO | Breast cancer: prevention and control,” *WHO*. <http://www.who.int/cancer/detection/breastcancer/en/> (accessed Apr. 30, 2019).
- [154] R. A. da Costa Vieira, G. Biller, G. Uemura, C. A. Ruiz, and M. P. Curado, “Breast cancer screening in developing countries,” *Clinics*, vol. 72, no. 4, pp. 244–253, Apr. 2017, doi: 10.6061/clinics/2017(04)09.
- [155] D. M. Parkin, F. Bray, J. Ferlay, and P. Pisani, “Global cancer statistics, 2002,” *CA. Cancer J. Clin.*, vol. 55, no. 2, pp. 74–108, Apr. 2005.

Appendix

IRI-MRI Data – 1

IRI-MRI Data – 2

IRI-MRI Data – 3

IRI-MRI Data – 4

IRI-MRI Patient Questionnaire

IRI-MRI Consent Form

IRI-MRI IRB Proposal

IRI-Mammo Patient Questionnaire

IRI-Mammo IRB Addendum

IRI-Mammo Data

IRI-MRI Pathology Report – Patient 029a (*identifying information removed*)

IRI-Mammo Pathology Report – Patient 002b (*identifying information removed*)

IRI-MRI Data – 1

Patient #	Test Date	Patient Information				Acclimation				Patient Questionnaire					
		Age	Breast Density	Bra Size	IC?	Right waiting	Right imaging	Left waiting	Left imaging	Sun-bathed	Lotion, etc.	Exercise	Smoked or drank	Tea or coffee	Tight-fitted clothing
001	12-Mar	60	HD	US	yes		Not collected						X		
002	12-Mar	70	SF	US	yes		Not collected				X	X			X
003	16-Mar	71	PF	US	yes		Not collected				X				
004	20-Mar	62	SF	US	yes		Not collected								
005	30-Mar	53	SF	US	yes		Not collected								
006	19-Apr	68	SF	US	yes		Not collected								
007	20-Apr	51	SF	US	yes		Not collected								
008	26-Apr	67	SF	US	yes		Not collected			X	X				
009	26-Apr	43	SF	US	yes		Not collected						X	X	
010	25-May	67	SF	34B	yes		Not collected				X	X		X	
011	4-Jun	46	HD	36D	yes		Not collected				X			X	
012	16-Jul	48	SF	46C	yes		Not collected				X			X	X
013	17-Jul	64	HD	50DD	yes	9m, 59s	3m, 34s	10m, 11s	3m, 39s					X	
014	19-Jul	68	HD	36DD	yes	13m, 20s	1m, 36s	7m	1m, 21s					X	
015	9-Aug	68	SF	40D	yes	9m, 25s	5m, 16s	7m, 18s	1m, 40s						

IC – Informed Consent Signed
HD – Heterogeneously Dense
SF – Scattered Fibroglandular
PF – Predominantly Fat
US – Unspecified or not collected

IRI-MRI Data – 2

Patient #	Test Date	Patient Information				Acclimation				Patient Questionnaire					
		Age	Breast Density	Bra Size	IC?	Right waiting	Right imaging	Left waiting	Left imaging	Sun-bathed	Lotion, etc.	Exercise	Smoked or drank	Tea or coffee	Tight-fitted clothing
016	10-Aug	56	SF	US	yes	7m, 53s	56s	9m, 34s	1m, 12s		X				
017	13-Aug	70	SF	38B	yes	8m, 11s	1m, 38s	9m, 19s	59s			X			
018	15-Aug	42	HD	40DD	yes	7m, 8s	46s	10m, 37s	1m, 2s		X			X	
019	20-Aug	49	US	SF	yes	7m, 41s	1m, 11s	9m, 15s	1m, 17s						
020	13-Sep	70	SF	US	yes	7m, 24s	1m, 54s	9m, 2s	1m, 41s						
021	1-Oct	65	HD	US	yes	8m, 55s	55s	9m, 25s	1m, 4s						
022	19-Nov	67	ED	36B	yes	10m, 3s	1m, 32s	10m, 3s	1m, 51s		X			X	X
023	3-Dec	72	SF	38C	yes	12m, 5s	1m, 42s	9m, 4s	1m, 20s		X				
024	17-Jan	72	SF	36B	yes	10m, 9s	1m, 57s	10m, 3s	1m, 57s						
025	19-Mar	64	SF	38C	yes	10m, 4s	3m, 15s	10m, 10s	3m, 2s					X	
026	30-May	63	HD	38B	yes	10m, 5s	1m, 35s	10m, 4s	2m, 3s					X	
027	7-Aug	75	SF	38B	yes	7m, 59s	2m, 4s	8m, 0s	1m, 58s					X	
028	13-Aug	57	SF	38C	yes	9m, 7s	1m, 40s	9m, 3s	1m, 38s		X				
029	26-Aug	76	US	42DD	yes	9m, 56s	2m, 12s	9m, 59s	2m, 15s						
030	18-Sep	69	HD	1X	yes	10m, 3s	2m, 43s	10m, 5s	1m, 43s		X		X	X	

IC – Informed Consent Signed
 ED – Extremely Dense
 HD – Heterogeneously Dense
 SF – Scattered Fibroglandular
 PF – Predominantly Fat
 US – Unspecified or not collected

IRI-MRI Data – 3

Patient #	Tumor Details					Pathology							
	Affected Breast	Size	Quad/ Pos	Distance from nipple	Depth	Type of Cancer	ER+?	PR+?	HER2?	MR	TD	NP	Overall Histologic Grade
001	Right	(1.6 x 1.0 x 1.1) cm	LOQ	US	Posterior	DCIS	+	+	US	US	US	US	2
002	Right	1.4 cm	UOQ	US	Middle	IDC	+	+	-	2	3	2	2
003	Right	9.4 mm	12:00	3 cm	Anterior	IDC	+	+	-	1	1	2	1
004	Left	(2.0 x 1.1 x 1.4) cm	LOQ	5 cm	Middle	ILC	+	+	-	3	3	2	3
005	Right	(2.9 x 1.3) cm	UOQ	US	Posterior	IDC	-	-	-	2	3	3	3
006	Right	(3.5 x 2.4 x 2.3) cm	12:00	2 cm	Middle	IDC	+	+	-	3	3	3	3
	Left	(0.8 x 0.6 x 0.4) cm	2:00	3 cm	Middle	ILC	+	+	-	1	3	1	1
007	Left	(1.3 x 1.0 x 0.9) cm	2:00	7 cm	Anterior	IDC	+	+	-	1	2	3	2
008	Left	(1.8 x 1.2 x 1.3) cm	10:00	5 cm	Posterior	IDC	+	+	-	1	2	2	1
009	Right	(1.2 x 0.8 x 0.8) cm	12:00	1 cm	Middle	IDC	+	+	-	1	3	2	2
010	Left	(1.4 x 1.1 x 1.3) cm	12:00	2 cm	Anterior	IDC	+	+	-	1	3	1	1
	011	Right	(1.1 x 0.8 x 1.0) cm	5:00	4 cm	Middle	IDC	+	+	-	1	3	2
		(1.0 x 0.8 x 0.7) cm	5:00	1 cm	Posterior	IDC	+	+	-	2	2	2	2
012	Right	(1.1 x 0.8) cm	10:00	8 cm	Posterior	IDC	+	+	-	1	1	2	1
013	Right	(1.5 x 0.9 x 1.2) cm	11:00	US	Middle	IDC	+	+	-	1	2	2	1
014	Left	MCs	3:00	4 cm	Middle	ADH, DCIS	US	US	US	US	US	US	US
015	Left	(1.7 x 1.1 x 1.3)	3:00	US	Posterior	IDC	-	-	-	3	3	3	3

US – Unspecified, MCs – Microcalcifications

LOQ – Left Outer Quadrant, UOQ – Upper Outer Quadrant

IDC – Invasive Ductal Carcinoma, ILC – Invasive Lobular Carcinoma, DCIS – Ductal Carcinoma In Situ, ADH – Atypical Ductal Hyperplasia

ER – Estrogen Receptor, PR – Progesterone Receptor, HER2 – Human Epidermal Growth Factor Receptor 2

MR – Mitotic Rate, TD – Tubular Differentiation, NP – Nuclear Pleomorphism

IRI-MRI Data – 4

Patient #	Tumor Details					Pathology							
	Affected Breast	Size	Quad/Pos	Distance from nipple	Depth	Type of Cancer	ER+?	PR+?	HER2?	MR	TD	NP	Overall Histologic Grade
016	Left	(0.9 x 1.1) cm	1:00	US	Middle	IDC	+	+	-	1	2	2	1
017	Right	(0.5 x 0.5 x 0.6) cm	5:00	3 cm	Posterior	IDC	-	-	-	3	3	3	3
018	Right	5 mm	10:00	8 cm	Posterior	IDC	-	-	-	3	3	3	3
019	Right	(2.6 x 2.3 x 2) cm	6:30	6 cm	Middle	IDC	-	-	-	3	3	3	3
020	Right	(0.8 x 1.0 x 0.7) cm	12:00	2 cm	Posterior	LCIS	+	+	-	1	3	1	1
	Left	(2.1 x 1.3 x 1.8) cm	12:00	2 cm	Anterior	ILC	+	+	-	2	3	2	2
021	Left	(1.7 x 1.4 x 1.3) cm	12:00	3 cm	Middle	IDC	+	+	-	1	3	1	1
022	Left	MCs	11:00	US	Middle	LCIS	US	US	US	US	US	US	US
023	Right	(1.8 x 1.1 x 1.3) cm	10:00	US	Middle	IDC	+	+	-	1	3	2	2
024	Left	(0.7 x 0.7 x 0.9) cm	11:00	US	Anterior	IDC	-	-	-	3	3	3	3
025	Left	(1.9 x 1.7 x 2.4) cm	2:00	3 cm	Middle	IDC	+	+	-	1	3	1	1
026	Left	MCs	11:30	US	Posterior	IDC	+	+	-	1	3	1	1
027	Right	(1.0 x 0.8 x 0.7) cm	10:00	4 cm	Middle	IDC	+	+	-	1	2	1	1
028	Left	(1.4 x 1.0 x 0.7) cm	10:00	4 cm	Middle	IDC	+	+	-	1	3	2	2
029	Left	(2.4 x 1.7 x 1.8) cm	1:00	US	Anterior	IDC	+	+	-	1	1	1	1
030	Left	(0.7 x 0.6 x 0.3) cm	2:00	5 cm	Posterior	ILC	+	+	-	1	US	1	3

US – Unspecified, MCs – Microcalcifications

IDC – Invasive Ductal Carcinoma, ILC – Invasive Lobular Carcinoma, DCIS – Ductal Carcinoma In Situ, LCIS – Lobular Carcinoma In Situ

ER – Estrogen Receptor, PR – Progesterone Receptor, HER2 - Human Epidermal Growth Factor Receptor 2

MR – Mitotic Rate, TD – Tubular Differentiation, NP – Nuclear Pleomorphism

IRI-MRI Patient Questionnaire

Subject #: _____ Initials: _____ DOB: _____

Name of Medical Professional:

Date: _____

Consent Form signed? **Yes** **No**

Please check off the following if they apply:

- Patient has sunbathed within five days prior to the exam.
- Patient has used lotion, cream, powder, makeup, deodorant/antiperspirants on the breasts on the day of the exam.
- Patient exercised the day of the exam.
- Patient has smoked or drank alcohol the day of the exam.
- Patient has had coffee or tea to the exam.
- Patient is wearing tight-fitted clothing the day of the exam.

Patient Info

Age of patient: _____

Breast Density: _____
(classified as fatty or extremely dense)

Pathology of Tumor

Tumor type: _____

Tumor location (interior, mid or posterior): _____

Tumor size: _____

Tumor stage: _____

Type of cancer: _____

IRI-MRI Consent Form



ROCHESTER GENERAL HOSPITAL
1425 Portland Avenue
Rochester, NY 14621

Center for Clinical Research

RESEARCH SUBJECT INFORMED CONSENT DOCUMENT

Title: A Thermal Imaging Technique for the Detection of Breast Cancer Based on Computational Simulations

Protocol: NSF CBT-1511314

Sponsor: National Science Foundation

Investigator/Study Doctor: Donnette Dabydeen, MD
Rochester General Hospital
1425 Portland Avenue Rochester, NY 14621
[REDACTED]

Sub-Investigators: Satish G. Kandlikar, PhD
Lori Medeiros, MD
Pradyumna Phatak, MD

Study Staff: Tia Albro, NP
Kayla Malchoff, CRA
Alyssa Recinella, RIT PhD student
Jose Luis Gonzalez Hernandez, RIT PhD student

Summary

You are being asked to participate in this research study and your participation is entirely voluntary. The purpose of this consent form is to explain to you the purpose of the study and explain what will be required of you if you choose to participate.

Breast cancer remains the second largest cause of death in women; despite major advances in treatment, over 40,000 women died of breast cancer in 2016 alone. Early detection of breast cancer increases the chance of survival, increases the options for treatment, and decreases the possibility of spreading to other parts of the body. Mammography is the use of low-energy x-rays to detect tumors and malformations in the breasts by pressing on the breasts to get an image. This technique is currently the gold standard for detection of breast cancer, but there are limitations to mammography. Patients with dense breasts (breasts that contain more muscle tissue rather than fat tissue) experience a decrease in sensitivity with mammography screening by approximately

10-20%. Promising supplemental tools for breast cancer screening are also not without limitations and risks, such as increased cost, increased radiation, operator dependence, and increased false-positive rate. There is therefore a continued need to develop better tools for breast cancer detection. Thermography is the observation of temperature changes throughout an object. Breast thermography has the potential to detect temperature patterns associated with early stages of breast cancer.

Purpose of the Study

The purpose of this study is to take thermal images (images that use color to show difference in temperature) of the breasts using an infrared (IR) camera to determine the accuracy of thermography in the early detection of breast cancer. An IR camera is a device that is used to take the thermal images mentioned above. The thermal images and your magnetic resonance imaging (MRI) (device that uses magnets and energy to make images of your body) or mammogram (device that uses x-rays and compression to take images of the breast) will then be sent to the Rochester Institute of Technology (with no personal identifiers) to be compiled and analyzed. Thermography is a non-invasive (not requiring the introduction of instruments into the body), rapid, and cost-effective test that we hope will help in improving and enhancing current screening practices, especially for dense breast tissues.

Procedures

The study will include up to 100 participants at RGH. If you agree to be in the study it will require approximately an hour of your time. There are no follow-up visits.

If you have a tumor or diagnosed breast cancer, your participation in this study will either occur **on the same day of your MRI** or **within two weeks of your MRI**. If you do not have breast cancer, your participation in this study will either occur **on the same day of your mammogram** or **within three weeks of your mammogram**.

If you choose to participate in the study you must follow the instructions below prior to the clinical examination:

- No sunbathing on the breasts within five days prior to examination.
- Avoid the use of lotion, cream, powder, makeup, deodorant, and antiperspirants on the breasts the day of the examination.
- Avoid physical stimulation of the breasts 24 hours prior to the examination.
- No exercise 4 hours before the examination.
- If bathing, it must be at least one hour before examination.
- No smoking or alcohol intake before the examination.
- Avoid large meals and excessive intake of coffee or tea prior to examination.
- Avoid tight fitted clothing the day of the examination.

If you choose to participate, the following things will be required of you in the **Department of Radiology at RGH**

- (1) You will enter the clinical room and disrobe from the waist up and wear a gown. You will remain for at least 15 minutes in the prone position (face down) with the breasts placed inside a hole and hanging freely. This step is necessary to acclimate the breasts to the temperature of the clinical room.
- (2) Eight different thermograms (temperature images) will be obtained using an infrared camera that is mounted on a mechanism that allows the camera to cover the entire surface of the breasts. You are required to lie in a prone position (face down) while the thermal images are obtained from below using an infrared (IR) camera.

For participants with a tumor or diagnosed breast cancer: The following steps will be conducted at the **Rochester Institute of Technology** with your images, which do not contain any identifying information.

- (1) Your MRI study will be used to generate a digital model of your breasts.
- (2) The digital model of the breasts will be used to perform a computer analysis to predict the temperature of your breasts.
- (3) The predicted temperature will be compared with the temperature observed in the clinical study to verify the accuracy of the predictions from the three-dimensional digital model.

For participants without a tumor or diagnosed breast cancer: The following steps will be conducted at the **Rochester Institute of Technology** with your images, which do not contain any identifying information.

- (1) Your mammogram study will be used to observe breast density and vasculature.
- (2) The collected temperature images observed in the clinical study will be observed for changing temperature profiles based on procedure, acclimation period, or anatomical properties.
 - a. Example: Will breast density or size produce a different profile? Will the procedure or acclimation time produce a different profile?

Risks and Discomforts

The thermographic examination is noninvasive and therefore does not pose any risk to you. There is no radiation risk. There are no side effects associated with the examination.

New Study Findings

New findings developed during the course of research may change and may affect your decision about wanting to participate. In that event, the findings will be told to you and a new consent form may be necessary.

Benefits

Although you will help in the development of this technology, you will not receive any direct benefit from this technology at this time. Participation in this study will assist in further research of non-invasive imaging techniques. Infrared imaging has the potential to provide earlier detection of cancerous tumors in a non-invasive, comfortable fashion.

Costs

There is no cost to you to participate in this research study.

Compensation

There are no incentive payments for you in this research study.

Compensation for injury

This study has minimal risks of injury. Rochester Regional Health, in fulfilling its public responsibilities, has provided professional liability insurance coverage and will be responsible for any injury only in the event such injury is caused by the negligence of Rochester Regional Health.

Confidentiality of Records and HIPAA Authorization

A federal government rule has been issued to protect the privacy rights of patients. This rule was issued under a law called the Health Insurance Portability and Accountability Act of 1996 (HIPAA). This rule is designed to protect the confidentiality of your personal health information. Your personal health information is information about you that could be used to find out who you are. For this research study, this includes information in your existing medical records needed for this study and new information created or collected during the study.

This Data Privacy Statement explains how your personal health information will be used and who it will be given to (“disclosed”) for this research study. It also describes your privacy rights, including your right to see your personal health information.

By signing the consent document for this study, you will give permission (“authorization”) for the uses and disclosures of your personal health information that are described in this Data Privacy Statement. If you do not want to allow these uses, you should not participate in this study.

If you agree to participate in the research study, your personal health information will be used and disclosed in the following ways:

- The study doctor/investigator and staff will use your medical records and information created or collected during the study to conduct the study.

- The study doctor/investigator and staff will send your study-related health information (“study data”) to the sponsor (if applicable) of the study and its representatives (“sponsor”). Because the sponsor conducts business related to clinical research in many countries around the world, this may involve sending your study data outside of the United States. Other countries may have privacy laws that do not provide the same protections as the laws in this country. However, the sponsor will represent the terms of this Data Privacy Statement in all countries.
- The study data sent by the study doctor/investigator to the sponsor does not include your name, address, social security number, or other information that directly identifies you. Instead, the study doctor/investigator assigns a code number to the study data and may use your initials. Some study data sent to the sponsor may contain information that could be used (perhaps in combination with other information) to identify you (e.g. date of birth). If you have questions about the specific health information that will be sent to the sponsor, you should ask the study doctor/investigator.
- The sponsor will use the study data for research purposes to support the scientific objectives described in the consent document and the process of getting regulatory approvals for its drugs.
- The sponsor may add your study data to data from other studies in research databases so that it can study better measures of safety and effectiveness, study other therapies for patients, develop a better understanding of diseases, or improve the design of future clinical trials.
- Your study data, either alone or combined with data from other studies, may be shared with regulatory authorities in the United States and other countries, doctors at other institutions participating in the study, and the Rochester Regional Health Clinical Investigations Committee overseeing this study at Rochester Regional Health.
- Study data that does not directly identify you may be published in medical journals or shared with others as part of scientific discussions.
- Your original medical records, which may contain information that directly identifies you, may be reviewed by the sponsor, the Rochester Regional Health Clinical Investigations Committee overseeing this study at Rochester Regional Health, and regulatory authorities in the United States and other countries. The purpose of these reviews is to assure the quality of the study conduct and the study data, or for other uses authorized by law.
- The sponsor works with business partners in drug development. The sponsor may share your study data with these business partners, but only if the business partners need the information as a part of this work with the sponsor, and only if the business partners signs a contract that requires it to protect your study data in the same way as the sponsor.

- The sponsor will not disclose personal health information to insurance companies unless required to do so by the law, or unless you provide separate written consent to do so.
- Your medical records and study data may be held and processed on computers.
- If research related procedures are performed within the Rochester Regional Health (RRH) (i.e. laboratory tests, imaging studies and clinical procedures), the results will be placed in your Electronic Medical Record (EMR). Once placed in your EMR, results are accessible to appropriate RRH staff who are not part of the research team.

Your personal health information may no longer be protected by HIPAA privacy rule once it is disclosed by your study doctor/investigator to these other parties.

You have the right to see and copy your personal health information related to the research study for as long as this information is held by the study doctor/investigator or Rochester Regional Health. However, to ensure the scientific integrity of the study, you will not be able to review some of the study information until after the study has been completed.

You may cancel your authorization at any time by providing written notice to the study doctor/investigator. If you cancel your authorization, the study doctor/investigator and staff will no longer use or disclose your personal health information in connection with this study, unless the study doctor/investigator or staff needs to use or disclose some of your personal health information to preserve the scientific integrity of the study. The sponsor will still use study data that was collected before you cancelled your authorization. If you cancel your authorization, you will no longer be able to participate in the study. However, if you decide to cancel your authorization and withdraw from the study, you will not be penalized or lose any benefits to which you are otherwise entitled.

Your authorization for the use and disclosures described in this Data Privacy Statement (DPS) does not have an expiration date.

Note: If there is not a sponsor for the protocol, remove such reference in the HIPAA statement. Additionally, if the HIPAA statement is altered (either by the request of the sponsor or other regulatory site, the DPS must be reviewed and approved by the CIC prior to use in the consent form.

Voluntary Participation and Withdrawal

Your participation in this study is voluntary. You may decide not to participate or you may leave the study at any time. Your participation may be stopped at any time by the study doctor or the sponsor without your consent for any reason. Specific reasons are as follows:

- If you do not come to the clinical examination
- If you do not sign or complete the consent form
- If you do not follow the recommendations prior to the examination that you are given.

A Thermal Imaging Technique for the Detection of Breast Cancer Based on Computational Simulations

Satish G. Kandlikar, PhD [REDACTED]

Donnette Dabydeen, MD

Lori Medeiros, MD

Phatak Pradyumna, MD

Introduction

Mammography is currently the gold standard for breast cancer screening and is the only screening tool that has been demonstrated through large randomized clinical trials to decrease breast cancer mortality. Nevertheless, there are limitations of mammography, particularly in patients with dense breasts, where sensitivity is decreased by approximately 10-20%. While ultrasound, MRI, and tomosynthesis have shown promise as supplemental tools for breast cancer screening, the use of these modalities are not without limitations and risks, such as increased cost, increased radiation, operator dependence, and increased false positive rate. There is therefore a continued need to develop better tools for breast cancer detection. Thermography for breast screening was introduced in 1956 and was approved by the FDA in 1982. Infrared thermography fell out of favor due to poor sensitivity. With advances in infrared camera technology, there has been renewed interests on the use of infrared thermography as an adjunct to mammography for breast cancer screening with advantages such as lack of ionizing radiation, patient comfort (touchless and does not require compressing the breast), and portability. In this research study, a methodology for the early detection of breast cancer will be explored using infrared thermography. First, the typical temperature patterns of both healthy individuals and patients with cancer will be identified. Second, computer models will be developed to predict the temperature observed during the clinical study

Purpose of Study

The aim of this study is to determine the feasibility of infrared thermography to detect breast cancer. This research study consists of two parts. First, a clinical study that will be conducted at the Rochester General Hospital in the Department of Radiology. Second, a computational study that will be conducted at the Rochester Institute of Technology in the Thermal Analysis Laboratory. Success in these parts will enable a novel, non-invasive technique based on computer simulations for the detection of early breast cancer using breast thermography. Early, inexpensive, and accurate breast cancer detection can dramatically improve the quality of life of patients and reduce costs for cancer treatment.

The aim of the first part is to identify the temperature patterns on the breasts of both healthy individuals and patients with cancer. Participants will lie in the prone position (face down) while the temperature of the breasts will be obtained from below using an infrared (IR) camera. Previous thermographic studies of the breasts have been conducted while patients are seated in front of the IR camera; this position induces deformation of the breasts due to gravity and creates temperature artifacts due to the contact of the breasts with the chest. The prone position that will be adopted in this study is expected to eliminate these two drawbacks. We hypothesize that thermal images of the breasts in the prone position will aid to enhance and identify the temperature patterns in breasts with and without a tumor.

For the second part, participants are required to have a Magnetic Resonance Imaging (MRI) study of the breasts within two weeks prior to the participation in the IR research study. The images from the MRI study will be used to generate a three dimensional model of the breasts. The digital model of the breasts will be used to predict the temperature through computer simulations. The predicted temperature will be compared with the clinical temperature images to determine the validity of the numerical model of the breasts.

Method

This is a prospective, single center non-invasive study that poses no risk to the enrolled subjects. Subjects who have provided informed consent will obtain imaging with infrared camera. The patients will be recruited by Lori Medeiros, MD, from the department of surgery, at the time of their surgical consultation. A RIT PhD student and a Rochester General Hospital Research coordinator will be consenting the patients and will both be involved in obtaining the images.

Participants in the study should follow the next recommendations prior to the clinical examination:

- No sunbathing on the breasts within five days prior to examination.
- Avoid the use of lotion, cream, powder, makeup, deodorant, and antiperspirants on the breasts the day of the examination.
- Avoid physical stimulation of the breasts 24 hours prior to the examination.
- No exercise 4 hours before the examination.
- If bathing, it must be at least one hour before examination.
- No smoking or alcohol intake before the examination.
- Avoid large meals and excessive intake of coffee or tea prior to examination.
- Avoid tight fitted clothing the day of the examination.

The following list of steps of the study will be conducted at the Rochester General Hospital in the Department of Radiology

- (1) When Participants enter the clinical room, Participants will be asked to disrobe from the waist up and wear a gown.
- (2) Participants should remain for at least 15 (fifteen) minutes in the prone position (face down) with the breasts with the breasts placed inside a hole and hanging freely. This step is necessary to acclimate the breasts to the temperature of the clinical room.
- (3) Eight different temperature images (thermograms) will be obtained using an infrared camera mounted on a mechanism that allows the camera to cover the entire surface of the breasts.

The following steps will be conducted at the Rochester Institute of Technology with images that do not contain personal information of the participants:

- (4) The MRI study of the participants will be used to generate a digital model of the breasts.
- (5) The digital model of the breasts will be used to perform computer simulations to predict the temperature of the breasts.
- (6) The predicted temperature will be compared with the temperature observed in the clinical study to verify the validity of the predictions.

Risks of Participation

The thermographic examination is noninvasive, does not involve contact with the patient, and therefore does not pose any risk to participants. There is no radiation risk. There are no study-

related treatments or interventions. Adverse events and serious adverse events reporting are not required. The definitive treatment for enrolled patients, i.e. surgery/radiation/chemotherapy will not be delayed for the purposes of the study.

Benefit of Participation

Although participants will help in the development of this technology, they will not receive any direct benefit from this experimental examination. Participation in this study will assist in further research of non-invasive imaging techniques. IR imaging has the potential to provide earlier detection of cancerous tumors in a non-invasive, comfortable fashion.

Study Duration

Study recruitment will continue until up to approximately 100 subjects have been enrolled.

Study Population

Participants in the study will be selected according with the following inclusion criteria:

Table 1. Breast and tumor parameters for selection of prospective Participants

Breast Density	Tumor size	Tumor position	Tumor depth
Fatty	< 1.5 cm	Center	Anterior
Extremely dense	> 3 cm	Two quadrants	Posterior

1. Signed written informed consent
2. Women 21 years or older who have a recent diagnosis of breast cancer and have not yet had treatment.
3. Women 21 years or older with no diagnosis of breast cancer
4. All participants have had a recent MRI.

Data collection

The following data will be collected during the study

1. Age
2. Histopathology
3. Breast density
4. Size and location of the tumor
5. De-identified copies of the IR images and MRI will be sent to RIT for data analysis.

Study Information and Consent

The Investigator will explain the benefits and risks of participation in the study to each subject and obtain written informed consent using an informed consent form approved by an IRB/Ethics Committee. This must be obtained before the subject enters the study and before any study procedure is performed.

IRI-Mammo Patient Questionnaire

Subject #: _____ Initials: _____ DOB: _____

Date of exam: _____

Name of Medical Professional: _____

Consent Form signed? Yes No

Please check off the following if they apply:

- Patient has sunbathed within five days prior to exam
- Patient has used lotion, cream, powder, makeup, deodorant/antiperspirants on the breasts on the day of the exam
- Patient exercised the day of the exam
- Patient has smoked or drank alcohol the day of the exam
- Patient has had coffee or tea prior to exam
- Patient is wearing tight-fitted clothing the day of the exam

Is the patient menstruating or menopausal?

- Menopausal Menstruating

Is the patient on any type of hormonal birth control?

- Yes No

Has the patient has breast cancer before?

- Yes No

Has the patient had breast surgery before?

- Yes No

If yes, circle the type: Lumpectomy Mastectomy Breast Reduction
 Breast Implant Other

Age of patient: _____

Breast Size: _____

IRI-Mammo IRB Addendum

This IRB has been altered to add an additional depth sensor which will aid in creating a patient-specific 3D model of the breast. Using this model, we are able to localize the tumor and analyze additional parameters without the need of MRI.

The above changes are being made in order to capture the actual shape of the breast without the need for other imaging modalities such as MRI. Throughout the past year and a half, we have been collecting both patient data and MRI data. The MRI data has been used to find the outline of the breast in order to create a 3D model. With the use of a depth sensor, the sensor can detect the shape in front of it and map the breast to create a 3D model, without the need for MRI. For the future of this study, we would like to see the efficacy of using a depth sensor to eliminate the need for MRI.

IRI-Mammo Data – 1

Test Date	Patient Information				Acclimation				Positive Mammo?	BI-RADS
	Classification	Age	Breast Density	Consent?	Right waiting	Right imaging	Left waiting	Left imaging		
21-Nov	001b	70	SF	yes	8m, 0s	2m, 41s	8m, 2s	2m, 49s	benign	3
19-Dec	002b	31	SF	yes	10m, 7s	3m, 8s	10m, 0s	2m, 51s	negative	1
2-Jan-20	003b	43	HD	yes	9m, 59s	3m, 14s	10m, 0s	3m, 6s	negative	0
9-Jan-20	004b	64	SF	yes	10m, 29s	2m, 49s	9m, 56s	2m, 16s	benign	3
17-Feb-20	005b	54	HD	yes	10m, 0s	2m, 19s	10m, 4s	2m, 34s	malignant	6
18-Feb-20	006b	78	SF	yes	9m, 2s	2m, 43s	9m, 47s	2m, 9s	malignant	4

Classification	Patient Questionnaire - Environmental Factors					Patient Questionnaire - Hormonal Factors						
	Sun-bathed	Lotion, etc.	Exercised	Smoked or drank	Tea or coffee	Tight-fitted clothing	Menstruating or Menopausal?	Birth control?	If so, what type?	History of BC?	Breast surgery?	If so, what type?
001b							US	US	US	Yes	Yes	lumpectomy
002b							US	US	US	No	No	N/A
003b	X				X	X	Menopausal	Yes	Mirena	No	No	N/A
004b					X	X	N/A	No	N/A	No	No	N/A
005b					X	X	Menopausal	No	N/A	No	No	N/A
006b	X						Menopausal	No	N/A	No	Yes	lumpectomy

BI-RADS – Breast Imaging-Reporting and Data System

US – Unspecified, BC – Breast Cancer

IRI-Mammo Data – 2

Patient #	Tumor Details					Pathology							
	Affected Breast	Size	Quad/Pos	Distance from nipple	Depth	Cancer	ER+?	PR+?	HER2?	MR	TD	NP	Histologic Grade
005b	Left	US	7:00	US	Middle	IDC	+	-	-	1	3	2	1
006b	Left	1.7 x 1.6 x 1.6 cm	1:00	US									

US – Unspecified

IDC – Invasive Ductal Carcinoma, ILC – Invasive Lobular Carcinoma, DCIS – Ductal Carcinoma In Situ, ADH – Atypical Ductal Hyperplasia

ER – Estrogen Receptor, PR – Progesterone Receptor, HER2 - Human Epidermal Growth Factor Receptor 2

MR – Mitotic Rate, TD – Tubular Differentiation, NP – Nuclear Pleomorphism

IRI-MRI Pathology Report – Patient 029a (identifying information removed)

MRI breast bilateral w wo contrast

Order # [REDACTED] Session # [REDACTED]

Patient Information

Patient Name [REDACTED]	Sex Female	DOB 4/22/1944	SSN [REDACTED]
Check In Date/Time: 08/26/2019 1:21 PM	Begin Date/Time: 08/26/2019 1:37 PM	End Date/Time: 08/26/2019 2:10 PM	

PACS Images

➤ Show images for MRI breast bilateral w wo contrast

Study Result

Clinical history: Infiltrating ductal carcinoma of left breast [C50.912 (ICD-10-CM)]

Technique: MRI sequences at 3 Tesla utilizing dedicated bilateral breast coil include: Axial locator, axial sequences of both breasts before and during dynamic imaging (13 ml of MultiHance), delayed sagittal vibrant series.

Further 3-D and dynamic enhancement analysis was performed on an independent Invivo DynaCAD system.

Comparison:

Findings:

Left breast: There is normal distribution of fibroglandular tissue. There are 2 stereotactic clips identified in the upper outer quadrant, corresponding to recent biopsy proven malignancies. These are associated with a 2.4 x 1.7 x 1.8 cm mass of intermediate signal intensity in the anterior breast, and a 6 mm in diameter mass of intermediate signal intensity at middle depth. There are additional rounded satellite lesions extending between these 2 anchor lesions as well as satellite lesions that extend at least 2 cm posterior to the deeper lesion. Lesions demonstrate brisk enhancement with either plateau or typical washout curves that are consistent with malignancy.

Right breast: Normal distribution of fibroglandular tissue is identified with no focus of abnormal signal intensity or architectural distortion. There is no focus of abnormal enhancement to suggest underlying malignancy.

Impression:

Left breast: Multifocal malignancy within at least one segment of the breast in the upper outer quadrant. This extends from the larger biopsy-proven malignancy in the anterior breast to approximately 2 cm posterior to the deeper lesion.

Right breast: No evidence of contralateral malignancy.

Signed by Attending: [REDACTED] on 8/28/2019 2:32 PM

Result History

MRI breast bilateral w wo contrast (Order # [REDACTED]) on 8/28/2019 - Order Result History Report

Signed by

Signed	Date/Time	Phone	Pager
[REDACTED]	8/28/2019 14:32	[REDACTED]	[REDACTED]

There is no interpretation history.

Result Notes for MRI breast bilateral w wo contrast

Notes recorded by [redacted] on 8/28/2019 at 4:37 PM EDT
Please being in to speak to me re finalizing surgery Friday or Tuesday

Reviewed by

[redacted]

9/10/2019 15:49

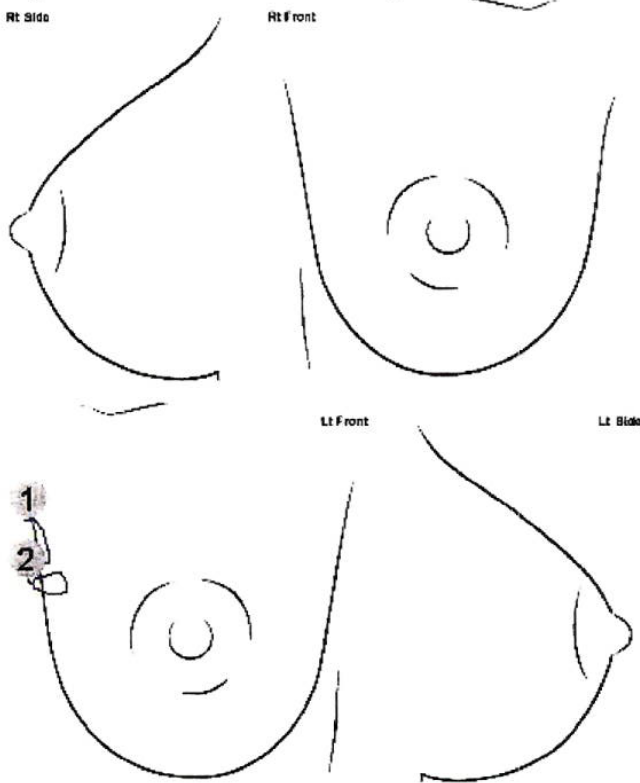
9/5/2019 13:20

Encounter

View Encounter

MRI breast bilateral w wo contrast (Accession [redacted], Order [redacted])

Image Documentation: Technologist



1. Mole - Noted on 11/03/2017

2. Mole - Noted on 11/03/2017

Documented by [redacted] on 08/26/2019

Begin Exam Questions

	Answer	Comment
Who verified the patient's identity?	[redacted]	
Do you have any history of allergic reaction during injection of IV contrast?	No	

	Answer	Comment
Has the MRI screening form been completed?	Yes	

End Exam Questions

	Answer	Comment
# of images?	1718	

Radiation Exposure Data

MRI breast bilateral w wo contrast
No radiation information documented for this order

Accession # [REDACTED]

Screening Form Questions

No questions have been answered for this form.

Form History

Status	User	Time
Created	N/A	08/08/2019 11:13 AM EDT

No previous implant documentation available.

External Results Report

[Open External Results Report](#)

Quality Tracking

Element	Status	Comment	User	Date/Time	Priority
---------	--------	---------	------	-----------	----------

Reprint Requisition

MRI breast bilateral w wo contrast (Order # [REDACTED]) on 8/26/19

[Show result history](#)

Result Comparison

Newer Version	MRI breast bilateral w wo contrast (Order # [REDACTED])
Final result	Older Version
8/28/2019 2:33 PM	
Edi, Rad Results In	

This is the newest version

No older versions exist

Narrative

Clinical history: Infiltrating ductal carcinoma of left breast [C50.912 (ICD-10-CM)]

Technique: MRI sequences at 3 Tesla utilizing dedicated bilateral breast coil include: Axial locator, axial sequences of both breasts before and during dynamic imaging (13 ml of MultiHance), delayed sagittal vibrant series.

Further 3-D and dynamic enhancement analysis was performed on an independent Invivo DynaCAD system.

Comparison:

Findings:

Left breast: There is normal distribution of fibroglandular tissue. There are 2 stereotactic clips identified in the upper outer quadrant, corresponding to recent biopsy proven malignancies. These are associated with a 2.4 x 1.7 x 1.8 cm mass of intermediate signal intensity in the anterior breast, and a 6 mm in diameter mass of intermediate signal intensity at middle depth. There are additional rounded satellite lesions extending between these 2 anchor lesions as well as satellite lesions that extend at least 2 cm posterior to the deeper lesion. Lesions demonstrate brisk enhancement with either plateau or typical washout curves that are consistent with malignancy.

Right breast: Normal distribution of fibroglandular tissue is identified with no focus of abnormal signal intensity or architectural distortion. There is no focus of abnormal enhancement to suggest underlying malignancy.

Impression:

Left breast: Multifocal malignancy within at least one segment of the breast in the upper outer quadrant. This extends from the larger biopsy-proven malignancy in the anterior breast to approximately 2 cm posterior to the deeper lesion.

Right breast: No evidence of contralateral malignancy.

Signed by Attending: [REDACTED] on 8/28/2019 2:32 PM

Results

Surgical Pathology Specimen (Order: [REDACTED])

Result Information

Status	Priority	Source
Edited Result - FINAL (10/14/2019 1048)	Routine	Lymph Node, Sentinel, Left Axilla

10/14/2019 10:48 AM - Edi, Lab In Hlseven

Surgical Pathology Specimen

Order: [REDACTED]

Status: Edited Result - FINAL Visible to patient: No (not released) Next appt: 06/02/2020 at 08:30 AM
in Geriatric Medicine ([REDACTED])

Narrative

Performed by: Path

**** THIS IS AN ADDENDUM REPORT ****

ROCHESTER GENERAL HOSPITAL

1425 Portland Avenue

ROCHESTER, NY 14621

Corporate MRN: [REDACTED]

Location: Rochester General Health System

Facility MRN: [REDACTED]

Account number: [REDACTED]

Patient: [REDACTED]

Birth date: [REDACTED]

Age; Sex: 75; F

Procedure date: 9/18/2019

Ordering physician: [REDACTED] [REDACTED]

CASE: [REDACTED]

*****Addendum*****

DIAGNOSIS:

- A. SENTINEL LYMPH NODE #1, LEFT AXILLARY, EXCISION:
 - 1 LYMPH NODE, NEGATIVE FOR MALIGNANCY (0/1)

- B. SENTINEL LYMPH NODE #2, LEFT AXILLARY, EXCISION:
 - 1 LYMPH NODE, NEGATIVE FOR MALIGNANCY (0/1)

- C. LEFT BREAST, TOTAL MASTECTOMY:
 - INVASIVE DUCTAL CARCINOMA, WITH NECROSIS, 24 MM, HISTOLOGIC GRADE 1
 - MULTIPLE SATELLITE FOCI OF INVASIVE DUCTAL CARCINOMA, FROM 1 TO 4 MM, IN UPPER OUTER QUADRANT
 - FOCI OF DUCTAL CARCINOMA IN SITU, NUCLEAR GRADE 1, SOLID AND PAPILLARY TYPE
 - ALL MARGINS ARE UNINVOLVED BY CARCINOMA
 - SEE SURGICAL PATHOLOGY CASE SUMMARY AND COMMENT

D. LEFT BREAST, INFERIOR ANTERIOR MARGIN:

- MAMMARY TISSUE WITH NO SIGNIFICANT PATHOLOGIC FINDINGS

E. SKIN, LEFT BREAST, EXCISION:

- SKIN WITH NO SIGNIFICANT PATHOLOGIC FINDINGS

Comment: The main tumor is 24 mm in greatest dimension with a 10 mm central necrotic area. Multiple satellite tumor foci, at least 8, are identified extending from the main tumor posteriorly in the upper outer quadrant, and range from 1 to 4 mm. The satellite tumor foci all appear similar to the main tumor. Immunostains for p63 and calponin were evaluated on the main tumor and on one block from satellite foci, and demonstrate negative staining for myoepithelial markers in the majority of foci, supporting invasive ductal carcinoma and focal DCIS.

SURGICAL PATHOLOGY CASE SUMMARY

MACROSCOPIC SUMMARY

Procedure: Total mastectomy (including nipple-sparing and skin-sparing mastectomy)

Specimen Laterality: Left

Tumor Site(s): 1 o'clock

Tumor Size: Greatest dimension of largest invasive focus 24mm

Tumor Focality: at least 8 satellite foci of invasive carcinoma, up to 4 mm

MICROSCOPIC SUMMARY

Histologic Type: Invasive carcinoma of no special type (ductal, not otherwise specified)

Histologic Grade (Nottingham Score): Tubular Differentiation: Score 1

Nuclear Pleomorphism: Score 1

Mitotic Rate: Score 1

Overall Grade: Grade 1 (Score 3-5)

Ductal carcinoma in situ (DCIS): DCIS present in specimen; negative for extensive intraductal component (EIC)

Grade I (low)

Necrosis not identified

Lobular Carcinoma In Situ (LCIS): No LCIS in specimen

Margins: Final assessment based on all submitted specimens

All margins uninvolved by invasive carcinoma (no invasive carcinoma on ink) ; distance from the closest margin 9 mm

All margins uninvolved by DCIS (no DCIS on ink) ; distance from the closest margin: 9 mm

Lymph Nodes: No lymph node involvement identified

Sentinel lymph nodes examined = 2 ; non-sentinel lymph nodes examined = 0 ; total lymph nodes examined = 2

Treatment Effect: No known presurgical therapy

Lymphovascular Invasion: Not identified

Dermal Lymphovascular Invasion: Not identified

Microcalcifications: Not identified

CLINICAL- PATHOLOGIC STAGING (TNM, AJCC 8th Edition)

TNM Descriptors: m (multiple foci of invasive carcinoma)

Primary Tumor: pT2 (Tumor >20 mm but <or equal to 50 mm in greatest dimension)

Regional Lymph Nodes: Modifier (sn): sentinel node(s) evaluated

pN0 (No regional lymph node metastasis identified or ITC's only)

Distant Metastasis: cM0 (per clinical history provided by surgeon)

BREAST BIOMARKERS

Estrogen Receptor: POSITIVE (67-100% of invasive tumor nuclei stain)

Performed on [REDACTED]; strong staining intensity; Allred Score 8

Formalin fixation; FDA-cleared Ventana Clone SP1 ; external control stains as expected; internal control stains as expected ; ASCO/CAP cold ischemic time fixation guidelines met

Progesterone Receptor: POSITIVE (67-100% of invasive tumor nuclei stain)

Performed on [REDACTED]; moderate staining intensity; Allred Score 7

Formalin fixation; FDA-cleared Ventana Clone 1E2 ; external control stains as expected; internal control stains as expected ; ASCO/CAP cold ischemic time fixation guidelines met

HER2 (by IHC): EQUIVOCAL (Score 2+); percent cells with uniform intense complete membrane staining 0

Performed on [REDACTED]; formalin fixation; FDA-cleared Ventana Clone 4B5; controls appropriate; ASCO/CAP cold ischemic time fixation guidelines met

HER2 (by FISH): NEGATIVE (Not Amplified) ; HER2/CEP17 ratio = 1.1

Average number HER2 signals/cell : 2.0 ; average number CEP17 signals/cell: 1.9

Performed on [REDACTED]; dual probe assay performed and interpreted by Integrated Oncology, Irvine, CA; cells counted = 30 ;number of observers = 2

Clinical Diagnosis and History:

Invasive ductal carcinoma left breast 1 o'clock position 2 cm from the nipple with additional satellite lesion in the 5 cm from the nipple position; both in the upper outer quadrant and along the same duct system; mention is made of the other nodules seen on imaging; a firm mass was seen in the upper outer quadrant of the left breast measuring 2 cm with ecchymosis related to recent biopsy; MRI of the breast on 8/26/19 demonstrates 2 stereotactic clips in the upper outer quadrant of the left breast associated with 2.4 cm mass with additional satellite lesions extending between these 2 acre lesions as well as satellite lesions extending at least 2 cm posterior to deepest; T2 N0 M) Stage II

Tissue(s) Submitted:

A. Left axillary sentinel lymph node

- B. Left axillary sentinel lymph node #2
- C. Left breast
- D. Left breast inferior anterior margin
- E. Left breast skin

Gross Description:

A. Received fresh for intraoperative consultation, labeled [REDACTED] - left axillary sentinel node #1," is a portion of fat containing a 1.3 cm blue dyed lymph node with no gross tumor. A scrape prep is done. The lymph node is entirely submitted in one cassette.

INTRAOPERATIVE SCRAPE PREP DIAGNOSIS: Negative for metastatic carcinoma, representative scrape preparation from one lymph node examined. ([REDACTED]; reported 9/18/19 at 7:25 p.m.)

B. Received fresh for intraoperative consultation, labeled [REDACTED] - left axillary sentinel node #2," is a portion of fat containing a 1.4 cm tan-red lymph node with no blue dye or gross tumor. A scrape prep is done. The lymph node is entirely submitted in one cassette.

INTRAOPERATIVE SCRAPE PREP DIAGNOSIS: Negative for metastatic carcinoma, representative scrape preparation of one lymph node. [REDACTED] reported 9/18/19 at 7:25 p.m.)

C. Received fresh, container labeled [REDACTED] left breast," is a 21.0 x 17.0 x 5.0 cm breast with an overlying coarsely wrinkled 12.0 x 4.0 cm blue stained ellipse of skin. There is a soft erect nipple. A short stitch marks superior and a long stitch marks lateral. The deep margin is delineated by a thin fascial plane with scant muscle. The margins are inked as follows: anterior (superior aspect), blue; anterior (inferior aspect), green; and posterior (deep), black. The specimen is sectioned showing approximately 2 cm beneath the nipple, is an indurated 24 x 19 x 14 mm markedly blue stained tumor with borders which grossly extend to within 9 mm from the anterior inferior margin, 35 mm from the deep margin of resection. Extending off of the main tumor towards the posterior part of the specimen, over an approximately 5 cm area, are multiple additional smaller tan-white nodules, 1 to 4 mm in greatest dimension. These nodules extend to within 25 mm from the deep margin and 15 mm from the anterior inferior margin of resection. The rest of the breast is composed of soft blue stained fat intermixed with delicate islands of parenchyma throughout. Sectioning at the lateral edge shows no lymph nodes. Representative sections are submitted as per labeled diagram in 16 cassettes. Time removed from patient: 19:18. Time placed in formalin: 19:40. Duration of formalin fixation 25.5 hours.

Slide Key:
C1 = nipple

[REDACTED]

C2-C5 = large tumor
C6-C9 = sequential sections extending off of large tumor, possible satellite nodules
C10, C11 = inferior anterior margin near large tumor
C12 = deep margin near large tumor
C13 = upper inner quadrant
C14 = lower inner quadrant
C15 = lower outer quadrant
C16 = upper outer quadrant

D. Received fresh, container labeled [REDACTED] - left inferior anterior margin, " is a markedly irregular tan-red lobulated fatty tissue piece measuring 22.0 x 4.5 x 1.5 cm. There is a stitch marking the new true margin which is inked black. Sectioning shows predominantly yellow-tan soft lobulated fat without gross lesions. Representative sections are submitted in three cassettes.

E. Received in formalin, container labeled "[REDACTED] - left breast skin," is a roughly triangular, tan-white, coarsely wrinkled, 19.0 x 5.5 cm piece of skin excised to a depth of 1.0 cm. The skin surface shows no pigmented or ulcerated areas. Sectioning shows no gross lesions. Representative sections are submitted in one cassette. (ejc/all)

Final Diagnosis performed by [REDACTED] Electronically Signed and Reported 9/24/2019 2:10:36PM Results reported at ROCHESTER GENERAL HOSPITAL 1425 Portland Avenue ROCHESTER, NY, 14621

ADDENDUM TO PATHOLOGY REPORT:
#1

At the request of [REDACTED] this case was submitted for Oncotype DX Breast Cancer Assay. The assay was performed at Genomic Health, Inc, 301 Penobscot Drive, Redwood City, CA, 94063. As reported on 10/11/2019, the patient's recurrence score is: 6 (Oncotype DX recurrence score range is 0-100). Please see the Genomic Health report for complete details, including methodology, assay description, results, and algorithms for prognosis and chemotherapy benefit.

Addendum #1 Final performed by [REDACTED] Electronically Signed and Reported 10/14/2019 10:38:05AM Results reported at



ROCHESTER GENERAL HOSPITAL 1425 Portland Avenue ROCHESTER, NY, 14621

FDA Testing Disclaimer (applicable only if flow cytometry and/or immunohistochemical results are included in this report). These tests were developed and their performance characteristics determined by Rochester General Hospital and/or Unity Hospital. They have not been cleared or approved by the U.S. Food Drug Administration (FDA). The FDA has determined that such clearance or approval is not necessary. These tests are used for clinical purposes and should not be regarded as investigational or for research. This laboratory is regulated under the Clinical Laboratory Improvement Amendments of 1988 (CLIA) as qualified to perform high complexity clinical testing.

Specimen Collected: 09/18/19 00:00 Last Resulted: 10/14/19 10:48 Order Details View Encounter Lab and Collection Details Routing Result History - Result Edited

Authorizing Provider Information

Name: [REDACTED] Fax: [REDACTED]
Phone: [REDACTED] Pager: [REDACTED]

Reprint Requisition

Surgical Pathology Specimen (Order # [REDACTED]) on 9/18/19

All Reviewers List

[REDACTED] on 10/15/2019 16:01
[REDACTED] on 9/25/2019 08:52

Cervical Cancer Screening History - Results and Follow-ups

Results from last 3 years

No results or procedures during the timeframe



ROCHESTER GENERAL HOSPITAL 1425 Portland Avenue ROCHESTER, NY, 14621

FDA Testing Disclaimer (applicable only if flow cytometry and/or immunohistochemical results are included in this report). These tests were developed and their performance characteristics determined by Rochester General Hospital and/or Unity Hospital. They have not been cleared or approved by the U.S. Food Drug Administration (FDA). The FDA has determined that such clearance or approval is not necessary. These tests are used for clinical purposes and should not be regarded as investigational or for research. This laboratory is regulated under the Clinical Laboratory Improvement Amendments of 1988 (CLIA) as qualified to perform high complexity clinical testing.

Specimen Collected: 09/18/19 00:00

Last Resulted: 10/14/19 10:48

Order Details View Encounter Lab and Collection Details Routing Result History - Result Edited

Authorizing Provider Information

Name: [Redacted] Fax: [Redacted]
Phone: [Redacted] Pager: [Redacted]

Reprint Requisition

Surgical Pathology Specimen (Order # [Redacted]) on 9/18/19

All Reviewers List

[Redacted] on 10/15/2019 16:01
[Redacted] on 9/25/2019 08:52

Cervical Cancer Screening History - Results and Follow-ups

No results or procedures during the timeframe

Results from last 3 years

Ultrasound breast left



Patient Information

Patient Name

[Redacted]

Sex

Female

DOB

[Redacted]

SSN

[Redacted]

Check In Date/Time: 12/19/2019 1:44 PM	Begin Date/Time: 12/19/2019 1:48 PM	End Date/Time: 12/19/2019 2:06 PM
---	--	--------------------------------------

PACS Images

Show images for Ultrasound breast left

Study Result

Indication: Lump or mass in breast. Pain.

Technique: Grayscale and Doppler interrogation of the 3 o'clock region 1 to 4 cm from the nipple of the left breast.

Comparison: None

Findings: The breast tissue is sonographically normal. There is dense normal fibroglandular tissue at the site of palpable concern. There is no mass or architectural distortion. Visualized underlying pectoralis major muscle ribs and pleura appear normal. The skin appears normal.

Results discussed with the patient at the time of the examination.

Impression: Sonographically normal breast tissue.

Corrected by: [Redacted] on 12/19/2019 2:23 PM

Signed by Attending: [Redacted] on 12/19/2019 4:10 PM

Result History

Ultrasound breast left (Order # [Redacted] on 12/19/2019 - Order Result History Report - Result Edited

Signed by

Signed

[Redacted]

Date/Time

12/19/2019 16:10

Phone

[Redacted]

Pager

There is no interpretation history.

Result Notes for Ultrasound breast left

Notes recorded by [Redacted] 12/20/2019 at 8:55 AM EST

Normal Lab result. Patient is to continue with regular follow-up.

Impression: Sonographically normal breast tissue.

Reviewed by

[Redacted]

12/20/2019 08:55

Encounter

View Encounter

MAMMO DIAGNOSTIC BILATERAL W/TOMO



Patient Information

Patient Name [REDACTED]	Sex Female	DOB [REDACTED]	SSN [REDACTED]
Check In Date/Time: 12/19/2019 1:46 PM	Begin Date/Time: 12/19/2019 2:25 PM	End Date/Time: 12/19/2019 2:38 PM	

PACS Images

Show images for MAMMO DIAGNOSTIC BILATERAL W/TOMO

Study Result

Procedure(s): Digital Mammography CAD Diagnostic

Indication: High risk breast cancer screening in a patient who received chest radiotherapy for lymphoma

Technique: Bilateral CC and MLO with tomosynthesis views.

Comparison: Today's ultrasound

Clinical History: History of lymphoma and thyroid cancer

Last clinical breast exam: Less than 12 months

Findings:

The breasts are composed of heterogeneously dense tissue, which may obscure underlying lesions at mammography..

Right breast: There is no mass, suspicious microcalcification, or architectural distortion in the breast

Left breast: There is no mass, suspicious microcalcification, or architectural distortion in the breast.

OVERALL ASSESSMENT:BI-RADS 1 Negative

Recommended follow-up: High-risk annual screening mammography.

This examination was interpreted by an ACR accredited radiologist and screened by a Computer Aided Detection System.

Results were given to the patient today at the time of her appointment.
The patient will also receive a letter in lay terms.

Signed by Attending: [REDACTED] on 12/19/2019 2:51 PM

Result History

MAMMO DIAGNOSTIC BILATERAL W/TOMO (Order # [REDACTED]) on 12/19/2019 - Order Result History Report

Signed by

Signed [REDACTED]	Date/Time 12/19/2019 14:51	Phone [REDACTED]	Pager [REDACTED]
----------------------	-------------------------------	---------------------	---------------------

There is no interpretation history.

Result Notes for MAMMO DIAGNOSTIC BILATERAL W/TOMO

Notes recorded by [REDACTED] 12/20/2019 at 8:55 AM EST
Normal mammo result. Patient is to continue with regular follow-up.

Reviewed by

[REDACTED]

12/20/2019 08:55

🔗 Encounter

[View Encounter](#)

Begin Exam Questions

	Answer	Comment
Have you ever had a previous Mammogram?	No	Baseline
Date of last clinical breast exam:	Less than 12 months	
Does the patient have any clinical complaints?	Yes	left breast lump
Is the patient currently taking hormones?	Yes	kurvelo, nexplanon implant
Who verified the patient's identity?	[REDACTED]	
Mobile mammogram?	No	

End Exam Questions

	Answer	Comment
# of images?	4	
Send to Radiologist? (If not ready to send study to Radiologist, indicate No)	Yes	

Radiation Exposure Data

MAMMO DIAGNOSTIC BILATERAL W/TOMO
No radiation information documented for this order

Accession #: [REDACTED]

External Results Report

[Open External Results Report](#)

Quality Tracking

Element	Status	Comment	User	Date/Time	Priority
---------	--------	---------	------	-----------	----------

Reprint Requisition

MAMMO DIAGNOSTIC BILATERAL W/TOMO (Order # [REDACTED]) on 12/19/19

[Show result history](#)

Result Comparison

Newer Version
Final result
12/19/2019 2:52 PM

MAMMO DIAGNOSTIC BILATERAL W/TOMO (Order # [REDACTED])
Older Version

Newer Version
Edi, Rad Results In

Older Version

This is the newest version

No older versions exist

Narrative

Procedure(s): Digital Mammography CAD Diagnostic

Indication: High risk breast cancer screening in a patient who received chest radiotherapy for lymphoma

Technique: Bilateral CC and MLO with tomosynthesis views.

Comparison: Today's ultrasound

Clinical History: History of lymphoma and thyroid cancer

Last clinical breast exam: Less than 12 months

Findings:

The breasts are composed of heterogeneously dense tissue, which may obscure underlying lesions at mammography..

Right breast: There is no mass, suspicious microcalcification, or architectural distortion in the breast

Left breast: There is no mass, suspicious microcalcification, or architectural distortion in the breast.

OVERALL ASSESSMENT:BI-RADS 1 Negative

Recommended follow-up: High-risk annual screening mammography.

This examination was interpreted by an ACR accredited radiologist and screened by a Computer Aided Detection System.

Results were given to the patient today at the time of her appointment.
The patient will also receive a letter in lay terms.

Signed by Attending: [REDACTED]

MRI breast bilateral with & without IV contrast



Patient Information

Patient Name	Sex	DOB	SSN
[REDACTED]	Female	[REDACTED]	[REDACTED]
Check In Date/Time:	Begin Date/Time:	End Date/Time:	
02/06/2020 9:40 AM	02/06/2020 9:49 AM	02/06/2020 10:35 AM	

PACS Images

Show images for MRI breast bilateral with & without IV contrast

Study Result

Indication: Breast cancer, surveillance. History of Hodgkin's lymphoma status post chest radiation. Reported palpable left breast abnormality.

Technique: 3 plane localizer, T2 fat sat axial, axial VIBRANT nonfat sat, T1 axial dynamic, post contrast injection 10 mL of Multihance, T1 fat sat axial subtraction, axial VIBRANT water suppression and sagittal VIBRANT postcontrast, using a dedicated breast coil on a 3.0 Tesla magnet, and evaluation with Invivo DynaCAD breast MRI CAD software.

Comparison: Prior mammograms

Findings: There is slight background parenchymal enhancement in both breasts.

Left breast: There is no mass, architectural distortion, or focus of abnormal enhancement in the breast. The visualized axillary lymph nodes appear normal.

Right breast: There is no mass, architectural distortion, or focus of abnormal enhancement in the breast. The visualized axillary lymph nodes appear normal.

Incidental findings: The left ventricle appears dilated. Correlate with echocardiography.

Impression: BI-RADS 1: Negative.

Given history of chest radiation for lymphoma, mammograms and ultrasounds should be performed annually for breast cancer screening. Breast MRI should also be performed annually but 6 months after the mammograms and ultrasound.

Approved by: [REDACTED]

The undersigned attending radiologist has personally reviewed the examination and the resident's interpretation thereof, and agrees with the findings. [REDACTED]

Signed by Attending: [REDACTED]

Result History

MRI breast bilateral with & without IV contrast (Order # [REDACTED]) on 2/6/2020 - Order Result History Report

Signed by

Signed	Date/Time	Phone	Pager
[REDACTED]	2/06/2020 15:00	[REDACTED]	[REDACTED]

There is no interpretation history.

Reviewed by



3/3/2020 15:12

Encounter

[View Encounter](#)

Begin Exam Questions

	Answer	Comment
Who verified the patient's identity?		
Are you pregnant?	No	
Do you have any history of allergic reaction during injection of IV contrast?	Yes	
Please describe:	hives	patient premedicated

End Exam Questions

	Answer	Comment
# of images?	1329	

Radiation Exposure Data

MRI breast bilateral with & without IV contrast
 No radiation information documented for this order



Screening Form Questions

	Answer	Comment
Patient cleared through imaging. See comments.		
Are you pregnant?	No	
How Many Weeks? LMP		
Do you have an IUD or pessary?	No	
Are you breast feeding?	No	
Are you claustrophobic?	Yes	
Do you have anything in your body that you were not born with?	Yes	
Please explain	nexplanon in arm	
Have you had any surgeries?	Yes	
Please describe specific surgeries along with dates	thyroid, tubal ligation, stomach orthoscopic, leap procedure	
Do you have an allergy to any of the following contrasts?	CT Contrast	
Please describe the reaction you had	hives in face	
Do you have a PACEMAKER, DEFIBRILLATOR, or NEUROSTIMULATOR?	No	
Have you had a heart valve replacement?	No	

	Answer	Comment
Do you have any metallic coils, filters or stents?	No	
Do you have an aneurysm clip or brain surgery clip?	No	
Do you have a shunt or catheter?	No	
Do you have cochlear implants (not tubes) ?	No	
Do you have an insulin pump or pain pump?	No	
Do you have a cardiac monitor or loop recorder?	No	
Do you have any surgical clips, wires, staples, mesh or tissue expanders?	No	
Do you have any orthopedic hardware such as pins, screws, plates or a joint replacement?	No	
Do you have any prosthetic implants (eye, penile, limb, etc.)?	No	
Do you have any gunshot wounds or possible shrapnel or BB's?	No	
Do you have any metal in your eyes or have you previously worked with metal?	No	
What is the date of your last eye exam?		
Are you currently wearing a medication patch?	No	
Have you had any tattoos or body piercings within 2 weeks?	No	
Do you have hearing aids, dentures or braces?	No	
Do you have in any hair pins/extensions/hair pieces or a wig?	No	
Are you on dialysis?	No	
Do any of these apply to you: kidney surgery/kidney transplant/single kidney	No	
Do you have kidney disease?	No	
Do you have severe liver disease or have you had a liver transplant?	No	
Have you ever been diagnosed with diabetes?	No	
Have you ever been diagnosed with high blood pressure requiring medication?	No	
Have you ever been diagnosed with cancer?	Yes	
What type of Cancer?	lymphoma, carcinoma	

Answer Comment

If the patient is unable to answer these questions, who is filling out the form on their behalf?

Form History

Status	User	Time
Created	N/A	01/27/2020 01:51 PM EST
Accessed	[REDACTED]	01/31/2020 01:02 PM EST
Accessed	[REDACTED]	02/05/2020 07:07 PM EST
Accessed	[REDACTED]	02/05/2020 07:07 PM EST

No previous implant documentation available.

External Results Report

[Open External Results Report](#)

Quality Tracking

Element	Status	Comment	User	Date/Time	Priority
---------	--------	---------	------	-----------	----------

Reprint Requisition

MRI breast bilateral with & without IV contrast (Order [REDACTED]) on 2/6/20

[Show result history](#)

Result Comparison

MRI breast bilateral with & without IV contrast (Order [REDACTED])

Newer Version	Older Version
Final result 2/6/2020 3:01 PM Edi, Rad Results In	

This is the newest version

No older versions exist

Narrative

Indication: Breast cancer, surveillance. History of Hodgkin's lymphoma status post chest radiation. Reported palpable left breast abnormality.

Technique:3 plane localizer, T2 fat sat axial, axial VIBRANT nonfat sat, T1 axial dynamic, post contrast injection 10 mL of Multihance, T1 fat sat axial subtraction, axial VIBRANT water suppression and sagittal VIBRANT postcontrast, using a dedicated breast coil on a 3.0 Tesla magnet, and evaluation with Invivo DynaCAD breast MRI CAD software.

Comparison:Prior mammograms

Findings: There is slight background parenchymal enhancement in both breasts.

Left breast:There is no mass, architectural distortion, or focus of abnormal enhancement in the breast. The visualized axillary lymph nodes appear normal.

Right breast:There is no mass, architectural distortion, or focus of abnormal enhancement in the breast. The visualized axillary lymph nodes appear normal.

Incidental findings: The left ventricle appears dilated. Correlate with echocardiography.

Impression: BI-RADS 1: Negative.

Given history of chest radiation for lymphoma, mammograms and ultrasounds should be performed annually for breast cancer screening. Breast MRI should also be performed annually but 6 months after the mammograms and ultrasound.

Approved by: [REDACTED]

The undersigned attending radiologist has personally reviewed the examination and the resident's interpretation thereof, and agrees with the findings. [REDACTED]

Signed by Attending: [REDACTED]